Lower Energy Recovery of Dilute Organics from Fermentation Broths

Davey, Chris

Award date:
2017

Awarding institution:
University of Bath

Lower Energy Recovery of Dilute Organics from Fermentation Broths

Christopher John Davey

A thesis submitted for the degree of Doctor of Philosophy

University of Bath

Department of Chemical Engineering

November 2016

Abstract

For sustainably produced fuels and chemicals to become viable resources they need to be cost comparable with crude oil based products. Microbial fermentation is a promising alternative route to a variety of sustainable fuels and chemicals; however, due to increased production costs, it is not currently as economical as crude oil extraction and refining. The recovery of the dilute fermentation products from the broth can be incredibly energy intensive due to distillation still being the main separation process utilised. For high boiling organics, such as 2,3-butanediol, purification from the fermentation broth can contribute to over half of the cost of production. Therefore, there is a clear need for lower energy technologies for the separation and purification of fermentation products. This thesis presents an investigation into the application of membrane processes for the lower energy recovery of a number of different fermentation products:

Nanofiltration (NF) and Reverse Osmosis (RO) membranes have been investigated for the purification and concentration of 2,3-butanediol and acetate within the broth of a gas fermentation process, developed and commercialised by LanzaTech, USA. A number of commercial NF and RO membranes were screened for their separation properties of 2,3-butanediol and acetate with BW30 identified as the highest performing membrane with a rejection of 2,3-butanediol and acetate of 96.1 % and 94.6 % respectively at pH 6.5 within the gas fermentation broth. A membrane series was then developed to purify the broth before concentration to limit the reduction in permeability due to fouling. The membrane series was studied at LanzaTech, USA and consisted of a microfiltration membrane for retention of cells, nanofiltration for the retention of salts and macromolecules and NF / RO for the concentration of 2,3-butanediol and acetate within the broth. 2,3-butanediol and acetate were successfully concentrated to > 5 times that of the fermentation broth.

The effect of 2,3-butanediol and acetate on the pervaporative recovery of ethanol from a gas fermentation broth using a MMM of ZIF-8 and PDMS has been investigated. ZIF-8 was shown to increase the uptake of 2,3-butanediol by the MMM. The as-synthesised membranes were also shown to be sensitive to the pH of an acetate solution. Increasing 2,3-butanediol concentration was shown to increase the total flux and decrease the separation factor and has been attributed to the increased uptake. When pervaporation of a fermentation broth was conducted, an increase in total flux with only a small decrease in separation factor was observed. This led to an increased average PSI of 1281 compared to the model solution of 805. This has been attributed to some beneficial effects of components of the fermentation broth.

An investigation into MMMs of two analogous MOFs composed of copper, glutarate and a bipyridine was undertaken. The two MOFs exhibit similar pore environments but different crystal morphologies depending on the solvent used in the synthesis and have been related to the overall

performance of these novel MMMs. The Cu-MOFs of larger plate-like crystals blocked permeation through the membrane. This has been shown to be due to the non-ideal orientation of the 1-dimensional pores of the Cu-MOF within these membranes. However, the smaller crystals exhibited better performance as inorganic filler and exhibited increased performance with a maximum at a 15 wt% loading for pervaporation of acetone from water. A total flux of 0.061 kg m^{-2} h^{-1} and separation factor of 10.3 were observed for a 5 wt% acetone solution at 30 ºC.

Finally a novel method for the determination of the molecular weight cut-off (MWCO) of organic solvent nanofiltration (OSN) membranes utilising polypropylene glycols has been developed. The method overcomes the limitations of previous methods that utilise polystyrene or polyethylene glycols. Advantages include low cost of polypropylene glycol, high resolution of oligomers (58 g mol^{-1}) and being suitable for use within polar, non-polar and polar aprotic solvents.

Overall this thesis presents investigations into a number of different membrane separation processes relevant to the recovery of dilute organics from fermentation broths. Specifically:

1. NF and RO have been identified as suitable for the partial purification and concentration of 2,3-butanediol and acetate within a gas fermentation broth.
2. The effect of 2,3-butanediol and acetate on the pervaporation of ethanol using a ZIF-8-PDMS MMM has been investigated.
3. Two novel MMMs of PDMS and Cu-MOFs have been developed for the removal of acetone from an aqueous feed and the relationship between structure and performance studied.
4. Finally a novel method for characterising the MWCO of OSN membranes has also been developed utilising polypropylene glycols.

Acknowledgements

First and foremost, I would like to thank my supervisor Dr. Darrell Patterson for his support and guidance throughout this project. I am grateful for the many meetings and discussions we have had and for providing the experience and resources required for me to complete this thesis.

I would also like to thank Prof. David Leak whose insight into the biological aspects of this project have been invaluable, along with his general guidance and support.

I am grateful to Alice Havill for her input into this project and organising for me to visit LanzaTech to perform experiments and learn more about the gas fermentation process. Also my thanks go to the rest of the team at LanzaTech for their help during my visit.

I would like to thank Prof. Len Barbour and Dr. Percy van der Gryp for allowing me to visit their labs at the University of Stellenbosch. I am grateful to all the researchers there who helped me during my visit specifically; Waylin Peddie, Charl Bezuidenhout, Prem Lama, Eleonora Macedi and Vincent Smith, who I think will agree that I should also thank Java Café for their catering services.

Many thanks to the technical staff in Chemical Engineering especially Fernando Acosta for always being willing to teach me the ins and outs of the different analytical equipment and Alex Ciupa for always being happy to help fix the HPLC and the many trips to and from the gas stores. I am also grateful to the many other technical staff, post docs and students at the University who have helped me during my PhD.

I would like to thank the Patterson Group for their company in the lab, Marcus and Jo for their company in the office, Paul McKeown for his hijinks, and the rest of the 2012 CSCT cohort for the Friday drinks.

Finally, Anneke, thanks for the lifts. ☺

Declaration of Authorship

The work presented within this thesis is my own, in the exception of where clear acknowledgement is made within the text. Experimental work performed in collaboration with other researchers is as follows:

Chapter 5:

The use of the Cu-MOFs within Chapter 5 was a result of discussions and collaboration with Dr. Vincent Smith and Charl Bezuidenhout at the University of Stellenbosch. There initial studies into the synthesis and characterisation of the MOFs were conducted as a collaboration. The work presented in Chapter 5 is from repeated scaled-up synthesis and characterisation at the University of Bath.

Chapter 6:

Z. Low performed the filtration of PPG within toluene for Puramem 280. R. H. Wirawan and Z. Low were both consulted during the development of the HPLC method.

Contents

List of Figures

List of Tables

List of Abbreviations

ABE	Acetone-butanol-ethanol (in reference to the fermentation process)
ASR	Apparent salt rejection
ATR	Attenuated total reflectance
bdc	Benzene-1,4-dicarboxylic acid / terephthalic acid
BET	Brunauer–Emmett–Teller theory
BFDH	Bravais, Friedel, Donnay and Harker (crystal morphology)
BOD	Biological oxygen demand
Bpp	4,4'-Trimethylenedipyridine
bza	Benzoate
CNT	Carbon nanotube
COD	Chemical oxygen demand
CuGluBpp-MeOH	$[Cu_2(glu)_2(bpp)]$ synthesised from a solution containing methanol
CuGluBpp-Acetone	$[Cu_2(glu)_2(bpp)]$ synthesised from a solution containing acetone
CVD	Chemical vapour deposition
DBDTL	Dibutylin dilaurate
DFT	Density functional theory
DI	Deionised
DMF	Dimethylformamide
DOS	Degree of solvent uptake
DSC	Differential scanning calorimetry
EDX	Energy-dispersive X-ray spectroscopy
ELSD	Evaporative light scattering detector
FGS	Functionalised graphene sheets

FO	Forward osmosis
FTIR	Fourier-transform infrared spectroscopy
Glu	Glutarate
HPA	Heteropolyacid
HPLC	High-performance liquid chromatography
IR	Infrared
LLE	Liquid-liquid extraction
MD	Membrane distillation
MF	Microfiltration
MMM	Mixed-matrix membrane
MMT	Montmorillonite
MOF	Metal-organic framework
MW	Molecular weight
MWCO	Molecular weight cut-off
MWCNT	Multi-walled carbon nanotube
MWidth	Molecular width
NF	Nanofiltration
NMP	N-Methyl-2-pyrrolidone
OSN	Organic solvent nanofiltration
PAH	poly(alylamine hydrochloride)
PBG	Poly(butylene) glycol
PBI	Polybenzimidazole
PDMS	Polydimethylsiloxane
PE	Polyethylene
PEBA	Polyether-block amide
PEG	Poly(ethylene) glycol

PI	Polyimide
PIM	Polymer of intrinsic microporosity
PMPS	Polymethylphenylsiloxane
POSS	Polyhedral oligomeric silesquioxanes
PP	Polypropylene
PPG	Poly(propylene) glycol
PS	Polystyrene
PSI	Pervaporation separation Index
PTFE	Polytetrafluoroethylene
PTMSP	Poly(1-trimehtylsilyl-1-propyne)
PV	Pervaporation
PVA	Polyvinylalcohol
PVDF	Polyvinylidene fluoride
PXRD	Powder X-ray diffraction
pyz	Pyrazine
PZNTs	Polyphosphazene nanotubes
RO	Reverse osmosis
RT	Room temperature
SAM	Self-assembled monolayer
SBU	Secondary building unit
SD	Standard deviation
SEM	Scanning electron microscopy
SLM	Standard litres per minute
SPES	Sulfonated poly(ether sulfone)
SRNF	Solvent resistant nanofiltration
STP	Standard temperature and pressure

SWCNT	Single-walled carbon nanotube
TDS	Total dissolved solids
TED	1,4-diazabicyclo[2.2.2]octane
TEOS	Tetraethyl orthosilicate
TFC	Thin film composite
TGA	Thermal gravimetric analysis
TN	Total nitrogen
TP	Total phosphorous
TSS	Total suspended solids
UF	Ultrafiltration
VMD	Vacuum membrane distillation
VP	Vapour permeation
VTES	Vinyltriethoxysilane
VTMS	Vinyltrimethoxysilane
ZIF	Zeolitic imidazolate framework

Chapter 1

Introduction and Motivation for Thesis

1.1 Motivation

Current levels of crude oil consumption are estimated at 90 million barrels worldwide per day,[1] and at this rate known reserves will be exhausted within 40 years.[2] Burning of these fossil fuels releases greenhouse gases and has led to rises in global temperatures and will continue to create serious environmental, economic and social problems.[3, 4] Although some industries that consume crude oil are transitioning towards alternative energy sources, there is still a large future need for liquid fuels, and there will always be a requirement for commodity chemicals within industries such as manufacturing, agriculture, and pharmaceuticals. Therefore, it is evident that there is a need for sustainable sources of fuels and chemicals.

Although a number of technologies exist to access sustainable liquid fuels and chemicals, a plethora of products can be produced biologically via fermentation from a range of waste and renewable sources of carbon. When managed effectively this overcomes the problems of resource depletion and environmental pollution from greenhouse gases (Figure 1-1). So called first generation biofuels are produced from potential food sources such as sugar, starch, animal fats, and vegetable oils. This can create competition between the use of land and resources for the production of fuel or food. Therefore, there has been a more recent drive into research for the use of feedstocks that will not compete with food supplies such as lignocellulosic biomass (e.g. wood) or syngas (CO and H_2, e.g. from steel mill flue gas or gasification of biomass).[5]

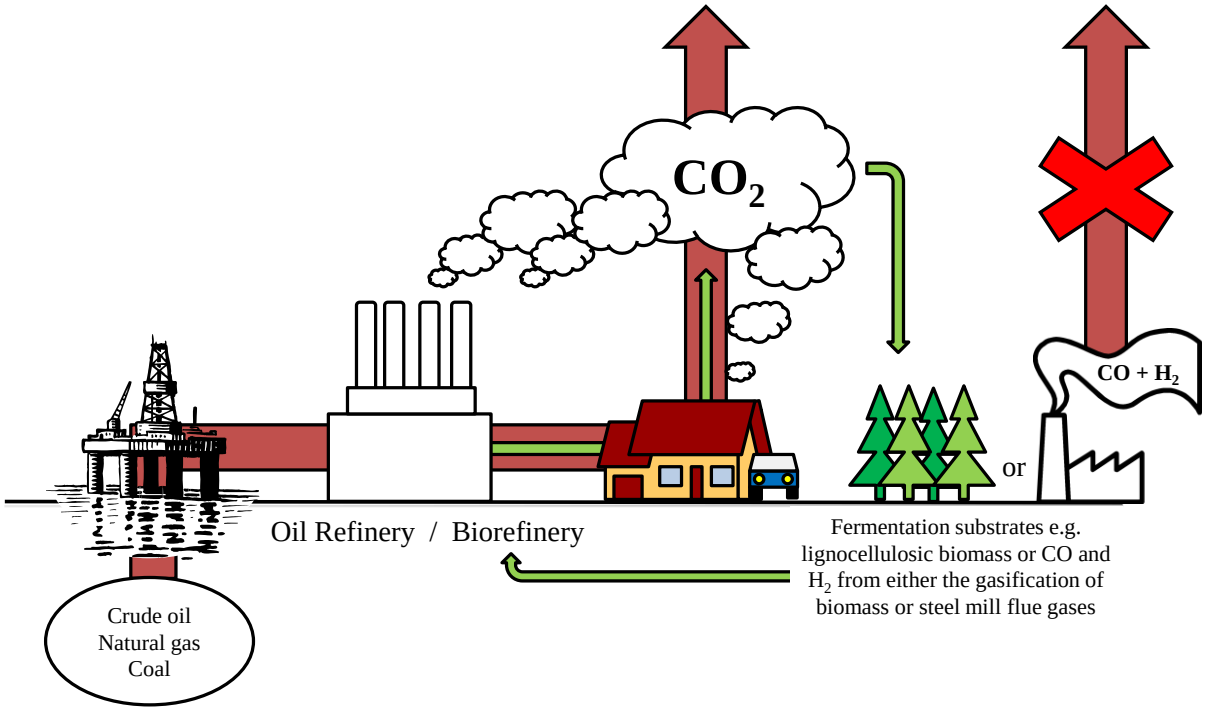

Figure 1-1. Crude oil industry vs. biorefinery with renewable and waste feeds.

The gas fermentation process, such as that commercialised by LanzaTech (USA) (Figure 1-2) uses CO rich feeds as the carbon and energy source for fermentation to produce various chemical products. It is advantageous over similar thermochemical processes such as the Fisher-Tropsch process due to the lower temperatures and pressures required as well as the ability to overcome impurities and varying compositions of CO, H_2 and CO_2 in the gas feed stream.[6]

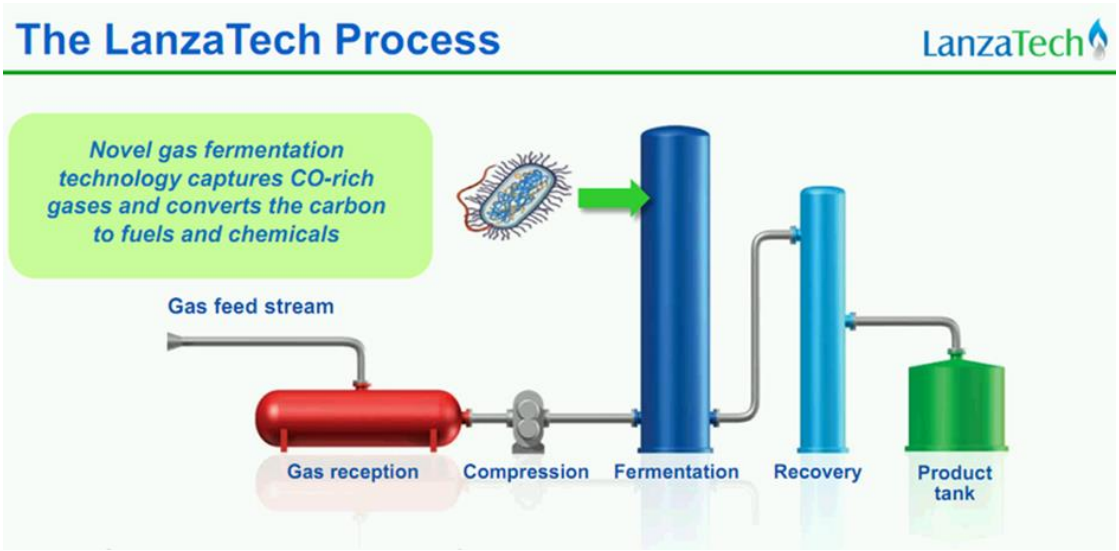

Figure 1-2. Overview of the LanzaTech process.[6, 7]

A number of different fermentation products can be produced from the gas fermentation process through the use of different acetogenic bacteria. One of the main fermentations conducted by LanzaTech produces ethanol, 2,3-butanediol and acetic acid as fermentation products (Table 1-1). There are huge markets for these fermentation products of 60,[8] 32[9] and 9 million[8] tons per year for ethanol, 2,3-butanediol and acetate respectively.

Table 1-1. Properties of water and LanzaTech's main fermentation products from 2,3-butanediol production: ethanol, 2,3-butanediol, and acetic acid.

Chemical Name	**Chemical Formula**	**Molecular Weight (g mol^{-1})**	**Density (g cm^{-3})**	**Boiling Point (ºC)**	**Vapour Pressure at 20 ºC (mmHg)**	**Azeotrope with water (wt% water)**	**Solubility in water at 25 ºC (g L^{-1})**	**Typical Concentration in LanzaTech Broth (g L^{-1})**
Water	H_2O	18.0	1.00	100	17.5	-	-	-
Ethanol	C_2H_6O	46.1	0.790	78.4	41.3	4	miscible	8 - 9
2,3-Butanediol	$C_4H_{10}O_2$	90.1	0.987	183	0.175	-	miscible	3 – 5
Acetic Acid	$C_2H_4O_2$	60.1	1.05	118	11.9	-	miscible	4 - 6

As with all fermentations though, the desired products are produced at a dilute concentration within the fermentation broth. Product recovery from the fermentation broth is therefore one of the most important steps for the downstream processing of these fermentation products into useable fuels and chemicals (Figure 1-3). Generally the product must be recovered from a < 6 % w/v culture broth. This fermentation broth is a complex aqueous mixture of metabolites, proteins, salts, sugars, vitamins and various other nutrients used as the growth media for the micro-organisms. The most common method currently adopted for product recovery is distillation. This can be an incredibly energy intensive process due to it requiring the heating of large volumes of broth. This can be exacerbated when recovering organics which are high boiling. For example, when 2,3-butanediol is recovered via distillation it must be recovered from the bottom of the distillation column and this can contribute to over half the cost of its overall microbial production.[10]

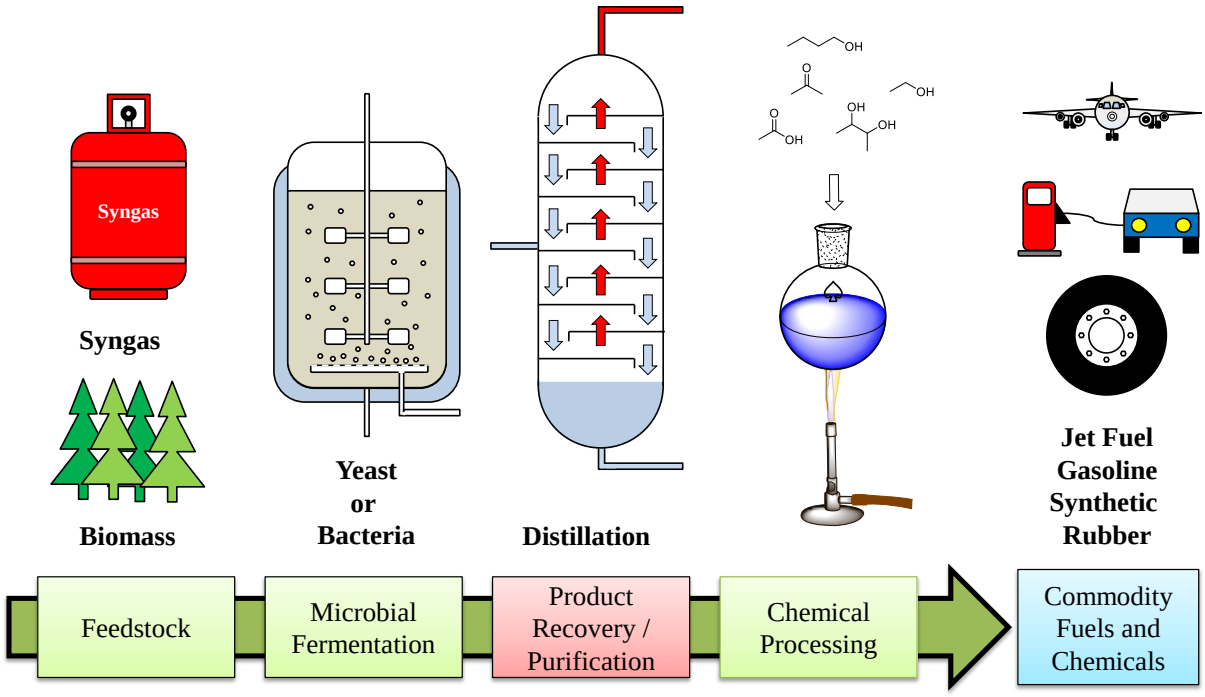

Figure 1-3. General steps involved in the microbial production of fuels and chemicals.[11]

Therefore, it is evident that low energy product recovery technologies can play a crucial role in the commercialisation of these biologically produced fuels and chemicals, and aid their implementation into a sustainable and circular economy. This thesis sets out work conducted within this area of low energy product recovery for biologically produced fuels and chemicals with specific regard to membrane technologies.

1.2 Overview of Low Energy Product Recovery Technologies for Fermentations

The downstream product recovery and purification of fermentation broths is an important part of the production process, often described as a bottleneck to commercialisation due to the associated cost and complexity involved. There are many different separation techniques available; however, distillation is the dominant technology in this area. Although distillation of volatile fermentation products can be cost effective at large scale (e.g. ethanol at > 4 wt%), it becomes increasingly less so for fermentation products that are produced at lower concentrations, are less volatile, and when produced on a small scale (e.g. when produced at small facilities close to the substrate source).[12] A number of alternative technologies have therefore been developed for the recovery and purification of fermentation products in these circumstances, but few of these have proven to be efficient

enough to allow biological products to compete with petrochemicals.[13] A number of the most common technologies for the recovery of dilute organics are discussed below with specific reference to 2,3-butanediol; however, many examples have also been reported for ethanol[12, 14, 15] and acetic acid.[16, 17]

- Adsorption

Adsorption involves the preferential binding of molecules from the bulk liquid broth to a solid surface through either physical intermolecular van der Waals / electrostatic forces (physisorption) or chemical bonding (chemisorption). Once adsorbed, the desired product must be desorbed from the surface to isolate the product and regenerate the adsorbent. Difficulty in applying this process arises from finding suitable materials with high affinities towards the desired fermentation product whilst also being able to undergo a suitable desorption process. The adsorbents are also required to exhibit similar performance over many regeneration cycles i.e. they do not degrade nor decompose. Adsorbents can also be susceptible to irreversible fouling from the numerous components within a fermentation broth.[18] Adsorption of 2,3-butanediol onto hydrophobic zeolites for recovery from a fermentation broth has been patented.[19] High purity 2,3-butanediol was recovered (> 90 %); however, no information on the regeneration or reuse of adsorbents has been reported.

- Liquid-Liquid Extraction

Liquid-liquid extraction (LLE), also known as solvent extraction, is where the desirable components of a liquid feed are extracted into an immiscible solvent or mixture of solvents. The separation is based on the solubility of the desired chemical in each of the solvents and it is important to utilise non-toxic solvents that will not inhibit the fermenting organism. There are many examples of LLE for the recovery of dilute fermentation products.[20] Once extracted from the broth, the compound / s must then be removed from the extractant liquid which can then be reused. This separation process must be low in energy consumption to offset the additional costs of the LLE. Alcohols and esters have been shown to be effective solvents for the extraction of 2,3-butanediol from a fermentation broth[21] and the extraction of 2,3-butanediol with oleyl alcohol has been demonstrated due to the relative non-toxicity of the solvent.[22] However, the toxicity of most organic solvents towards microorganisms and the affinity of 2,3-butanediol for water limits the use of this type of extraction.

- Reactive Extraction

Reactive extraction involves a reaction between an extractant and a solute to enable the separation of the solute into an immiscible solvent as in LLE. A reversible reaction is generally used so that the solute can be regenerated after extraction. Separation of 2,3-butanediol from a fermentation broth has been investigated by reactive extraction with aldehydes. The acid catalysed reaction of formaldehyde and 2,3-butanediol to form a dioxolane has been investigated by Senkus *et al.* (Figure 1-4).[23] However, the harsh acidic conditions required, caused by the use of sulphuric acid as a catalyst, prevents the application of this method on a large scale due to corrosion of the reaction vessels. A similar system was developed by Li *et al.* using an acetaldehyde-cyclohexane system.[24] Acetaldehyde was reacted with 2,3-butanediol under acidic conditions to form 2,3,5-trimethyl-1,3-dioxolane (Figure 1-4). Extraction into cyclohexane successfully separated the dioxolane from the fermentation broth where it was subsequently hydrolysed back to 2,3-butanediol and purified by vacuum distillation. A total rate yield of 90 % was observed. To overcome the effect of the acidic conditions on the reaction vessels, an ion-exchange resin was used as catalyst. The presence of proteins and salts in the fermentation broth dramatically decreases the catalytic activity of the resin with reuse; therefore, requiring thorough cleaning of the broth before reactive extraction.[24]

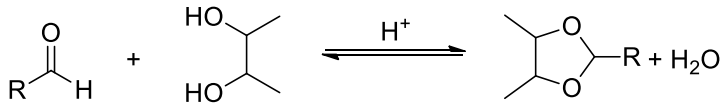

Senkus *et. al.* R = H
Li *et. al.* R = CH_3

Figure 1-4. Formation of 2,3,5-trimethyl-1,3-dioxolane and water under acidic conditions.

- Salting Out

Salting out involves the addition of salt to precipitate the desired product from the fermentation broth. Separation of 2,3-butanediol from the fermentation broth can be achieved via a salting out process.[25] Addition of potassium carbonate to an aqueous medium of the fermentation broth can be used to recover 97 % w/w 2,3-butanediol. However, large amounts of salt are required for an untreated bioprocess medium (1.16 g K_2CO_3 / 1 g 2,3-butanediol). Pre-cleaning of the media does reduce this (0.576 g K_2CO_3 / 1 g 2,3-butanediol) as well as increase the salt recycling lifetime; however, evaporation of water must therefore still be undertaken in the recovery of the salt.[25]

- Gas Stripping

Gas stripping involves the removal of a desired product from a liquid mixture through it transferring into a gas stream bubbled through the liquid mixture. Gas stripping has been studied for the removal of volatile alcohols from fermentations and is an attractive process as CO_2 produced during fermentation could be used. The relative concentrations of alcohol to water within the gas phase is governed by their gas-liquid partitioning behaviour and their ratios to the inert gas are a function of the temperature, arising from the partial pressures of water and the alcohol respectively. The stripped components are recovered through their condensation from the gas stream used, and multi-step condensation is normally required to achieve a high-purity alcohol.[12] Gas stripping is a common recovery technology in fermentations and has potential for the recovery of 2,3-butanediol.[26] The technology has been demonstrated at pilot scale; however, the concentration of 2,3-butanediol in the fermentation liquor is still concentrated to only ~ 14 wt% before introduction to the stripping column and a large amount of energy is required for the process which prevents its current application.[10, 27]

The discussed separation processes are compared in Table 1-2. The advantages and disadvantages have been presented generally for the different technologies. For recovery of a specific fermentation product, the characteristics of that product (e.g. volatility, solubility, chemical structure, etc.) will be the main factors in determining the most appropriate separation technology. Therefore, there is not one single product recovery technology that could be applied to all separations and in practice separation will invoke the use of several different technologies to achieve a high purity product. One of the most prominent low energy separation technologies not mentioned above is membrane separations. Membrane separations have a wide number of possible applications, potentially the most of all the described low-energy separation processes. This is due to the vast number of different membrane processes and the ability of these processes to easily separate mixtures based on a number of different factors such as molecular size, charge, hydrophilicity / hydrophobicity. Membrane separations could also be integrated into any of the technologies discussed above to improve their performance; or, standalone to achieve a number of fermentative separations. Therefore, membrane separations have been the focus of this PhD due to their broad applicability and diverse separation potential. The case for the use of membrane separations has been put forward in greater detail within Chapter 2.

Table 1-2. Comparison of various product recovery technologies for fermentations.

Product Recovery Technology	Advantages	Disadvantages
Distillation [12]	High Recovery. Good efficiency at moderate feed concentrations e.g. 4 wt% Ethanol. Easily scales up.	Azeotropes cannot be overcome without additional separation steps. Energy Requirement gets significantly higher at lower alcohol concentrations (< 4 wt%). High Temperatures required. Does not scale down easily.
Adsorption [18]	Low energy requirements. Easy to operate.	Fouling of adsorbents can limit adsorbent regeneration. Requires cyclic adsorption / desorption process (not continuous). High temperatures and low pressures required for adsorbent regeneration.
Liquid-Liquid Extraction [20]	High separation factors can be achieved. Separation generally not temperature dependent i.e. extraction can be conducted at fermentor temperature.	Extractant solvent can be inhibiting to microorganisms. High cost of extractant solvent. Only a limited number of solvents have been shown to be effective.
Reactive Extraction [28]	Can increases extraction efficiency of liquid-liquid extraction. Can convert fermentation product into a more valuable product.	Adds increasing complexity to liquid-liquid extraction. Large development costs. Recovery of reactants for reuse in subsequent reactive extractions.
Salting Out [29]	Can be conducted at ambient temperature.	Recovery of the salt used. Large amounts of salt can be required especially for dilute products.

Gas Stripping [12]	Can be conducted at fermentor temperature dependent on liquid-vapour equilibrium of products. Can be conducted in-situ. Can use CO_2 produced during fermentation process	Requires complex mass and energy integration systems. Low selectivity between volatile compounds.

1.3 Aims and Scope of this Thesis

This chapter has briefly introduced the importance of accessing sustainable sources of fuels and chemicals and the ability of fermentation processes to achieve this. Gas fermentation such as that conducted by LanzaTech can be used to access a number of commodity chemicals from waste or sustainably sourced syngas. The main limitation of these processes has been highlighted to be the downstream separation and purification of the fermentation products. This is due to a combination of the low concentration of the products within the fermentation broths and the use of energy intensive distillation to achieve separation. A number of low energy alternative separation processes have been introduced (adsorption, liquid-liquid extraction, reactive extraction, salting-out, and gas stripping); however, membrane separations have been presented as one of the most widely applicable and important low energy separation processes.

The overall aim of this thesis; therefore, is to investigate lower energy solutions for the recovery of products from a fermentation broth. The thesis focuses on the use of membrane based separations for recovery of 2,3-butanediol, acetic acid, ethanol, and other valuable products from LanzaTech's gas fermentation process. A number of investigations have been undertaken to improve the knowledge and application of membrane separations within these areas.

To achieve this aim, the specific objectives of the thesis have been summarised as:

- To identify suitable membrane separation processes for the low energy separation of products from a gas fermentation broth.
- To investigate the feasibility of current commercial membranes for the recovery of gas fermentation products, mainly 2,3-butanediol, acetate and ethanol.
- To identify ways to improve recovery of products from a gas fermentation process, this took the form of development of new membrane materials.
- To develop methods to improve the characterisation and understanding of membrane separation processes.

1.4 Thesis Outline

This thesis has been divided into 7 chapters:

Chapter 1 – Introduction and Motivation for Thesis:

This chapter has set out the motivation for this thesis. The chapter has outlined the requirement for sustainable sources of fuels and chemicals. Gas fermentation such as the LanzaTech process has been identified as a potential solution; however, the difficulty in recovery of the fermentation products and associated high energy requirements to achieve this has been identified as a pitfall to this method. Membrane separations have been identified as a suitable low energy recovery technology to ameliorate the product recovery process.

Chapter 2 - Literature Review:

This gives an introduction into the theory of membrane processes and gives specific examples from the literature of where membranes have been applied for the lower energy recovery of fermentation products. The literature review also covers the development of novel membrane materials for improving the separation of pervaporation membranes for the recovery of fermentation products.

Chapter 3 - Concentration and Purification of a Gas Fermentation Broth with Nanofiltration and Reverse Osmosis:

Chapter 3 gives an overview of the work conducted into identifying suitable nanofiltration and reverse osmosis membranes for the purification and concentration of 2,3-butanediol and acetate within a gas fermentation broth.

Chapter 4 – ZIF-8 PDMS MMMs for Ethanol Pervaporation: Effect of 2,3-Butanediol and Acetate

This chapter investigates the effect that the co-fermentation products of the LanzaTech process, 2,3-butanediol and acetate, have on the pervaporation of ethanol by a mixed-matrix membrane of ZIF-8 and PDMS.

Chapter 5 – Cu-MOF based PDMS mixed-matrix membranes for Acetone Pervaporation: Impact of Glutarate and Bipyridyl ligands on the MOF morphology

Two structurally similar metal-organic frameworks have been included within mixed-matrix membranes and the effect of the morphology of the MOFs investigated. The two classes of membranes were tested for their pervaporation performance for removal of acetone from an aqueous solution to simulate the removal of acetone from a fermentation broth.

Chapter 6 – Poly(propylene) glycols as probes for MWCO determination in Organic Solvent Nanofiltration

Once the dilute fermentation products have been concentrated, the purification changes to the removal of small quantities of impurities from the concentrated solvent. This falls into the realm of organic solvent nanofiltration (OSN) which can be used for the removal of impurities from organic solvents in the same manner that traditional NF can from an aqueous feed. The further application of OSN within this area will require greater understanding of the separation abilities of OSN membranes. Due to the pitfalls of current methods for determining the molecular weight cut off (MWCO) within OSN, a new method has been developed utilising poly(propylene) glycols. The method aids the understanding of rejection within OSN and can be used to complement existing methods.

Chapter 7 – Concluding Remarks and Future Work:

The results generated by this thesis are concluded and suggestions for future investigations within the scope of this work have been identified.

Chapter 2

Literature Review

Some of the concepts and literature discussed in this chapter have been published in part as a book chapter:

"D. A. Patterson, C. J. Davey, R. Rohani, Membrane Separations: from Purifications, Minimisation, Reuse and Recycling to Process Intensification, in: T. Letcher, J. Scott, D. Patterson (Eds.) Chemical Processes for a Sustainable Future, RSC, 2014, pp. 469 - 504."

And a review article:

"C. J. Davey, D. Leak, D. A. Patterson, Hybrid and Mixed Matrix Membranes for Separations from Fermentations, *Membranes*, 2016, **6**, 17."

2.1 Membrane Separations – General Overview

The following sections give an overview of what membrane separations are, the different types of membrane separations, process considerations for membrane separations; and finally, relevant membrane processes that have been applied to the recovery of fermentation products within the scope of this thesis.

2.1.1 General Description of Membrane Separations

Membranes are an important technology that can offer substantial energy savings over conventional thermal separation processes.[30] The ability to control the permeation rate of chemical species allows membranes to act as selective barriers. Therefore, membranes can retain one chemical species whilst allowing another to permeate freely (Figure 2-1). The main performance characteristics of a membrane are defined as the membranes flux and separation. Membrane flux relates to the flow rate of permeate through the membrane. Separation is defined differently for different techniques but gives a quantitative indication of the separation performance of the membrane. These factors are discussed in further detail for microfiltration (MF), ultrafiltration (UF), nanofiltration (NF) and reverse osmosis (RO) below (Section 2.1.3) and in Section 2.3 for pervaporation.

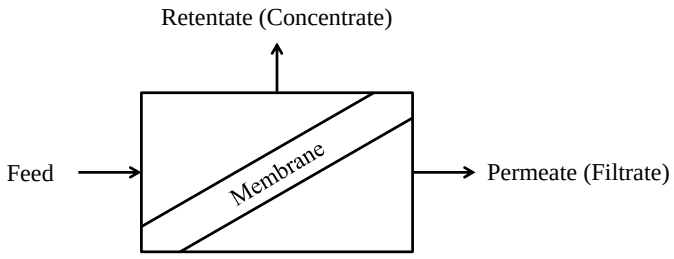

Figure 2-1. Schematic of a membrane indicating the permeate (filtrate) that passes through the membrane and the retentate (concentrate) blocked by the membrane.

Synthetic membranes used for industrial separations are generally made of either polymers or inorganic materials, as well as a combination of the two. Two main modes of membrane filtration are utilised; dead-end and cross-flow. Dead-end filtration (or frontal filtration) is where the feed flow is perpendicular to the membrane (Figure 2-2). No retentate flow is present in dead-end filtration so retentate builds up against the surface of the membrane until no more permeate can be collected. Dead-end systems therefore require regular cleaning and / or replacement of membranes to overcome this fouling. Dead-end systems; however, can better guarantee complete rejection of molecules from the feed stream as all the flow must pass through the membrane. They are commonly used in many industrial processes where rejection of key species must be guaranteed.[31]

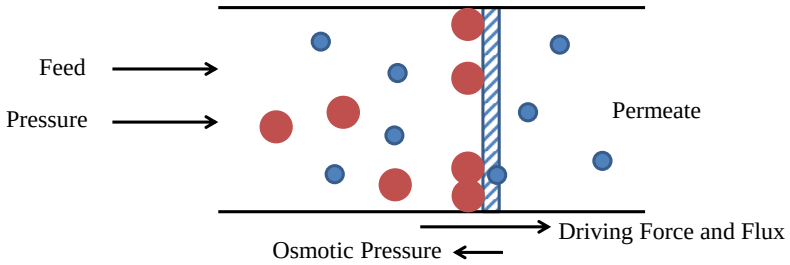

Figure 2-2. Schematic of a dead-end membrane filtration process.

Cross-flow filtration is where the membrane lies parallel to the flow of the feed and the transport across the membrane (Figure 2-3). In contrast to dead-end filtration, this allows a flow of the retentate stream. This reduces fouling of the membrane, but means that not all solvent passes through the membrane. The majority of industrial processes apply cross-flow filtration, since it minimises fouling on the membrane surface due to the retentate flow.[31]

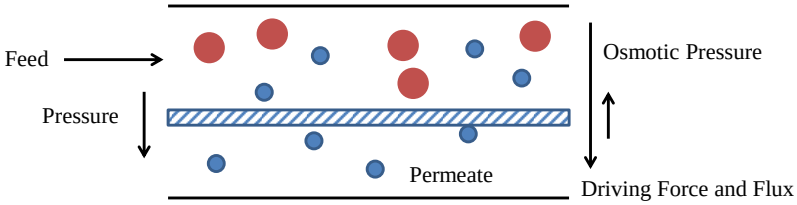

Figure 2-3. Schematic of a cross-flow membrane pressure driven filtration process.

The ability of a membrane to control the rate of permeation of different chemical species is their enabling property for separations. This transport through the membrane can be described by three models: pore flow, solution diffusion, and Donnan exclusion. In the pore flow model, permeants (solutes and solvent) are transported through the pores of the membrane by pressure driven convective flow. Separation occurs by solutes being excluded from pores of the membrane which other permeants can move through i.e. size exclusion (Figure 2-4).

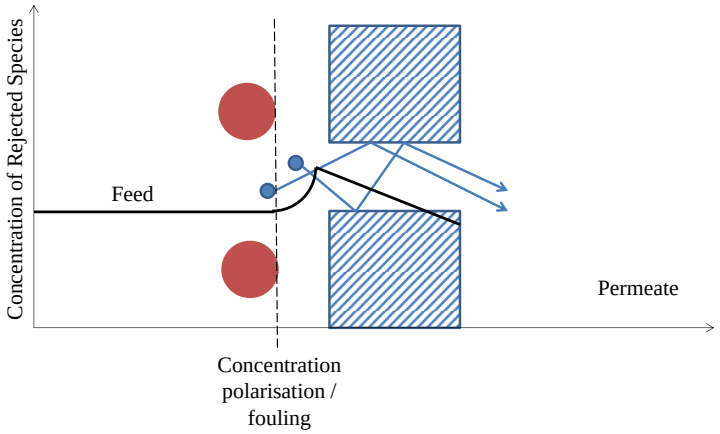

Figure 2-4. Schematic of the pore flow model; separation occurs by molecular filtration, the effect of concentration polarisation due to rejection is also shown.[32]

In the solution diffusion model, permeants dissolve and adsorb into the material of the membrane and subsequently diffuse through it (Figure 2-5). Separation of permeants occurs from their differing solubilities in the membrane material and subsequent rates of diffusion through it.

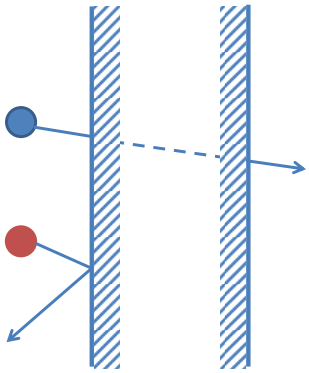

Figure 2-5. Schematic of the solution diffusion model; separation occurs due to solubility and mobility differences of permeates dissolved in the material of the membrane.[32]

2.1.2 Membrane Processes

A number of membrane technologies are described by the transport models presented in the previous section. These different techniques are generally characterised by the relative size of the pores of the membrane materials (Figure 2-6). The pore flow model describes those membranes with relatively large, fixed size pores, whereas dense membranes are best described by the solution

diffusion model where the pores are defined as spaces between the polymer chains caused by their thermal motion.[32]

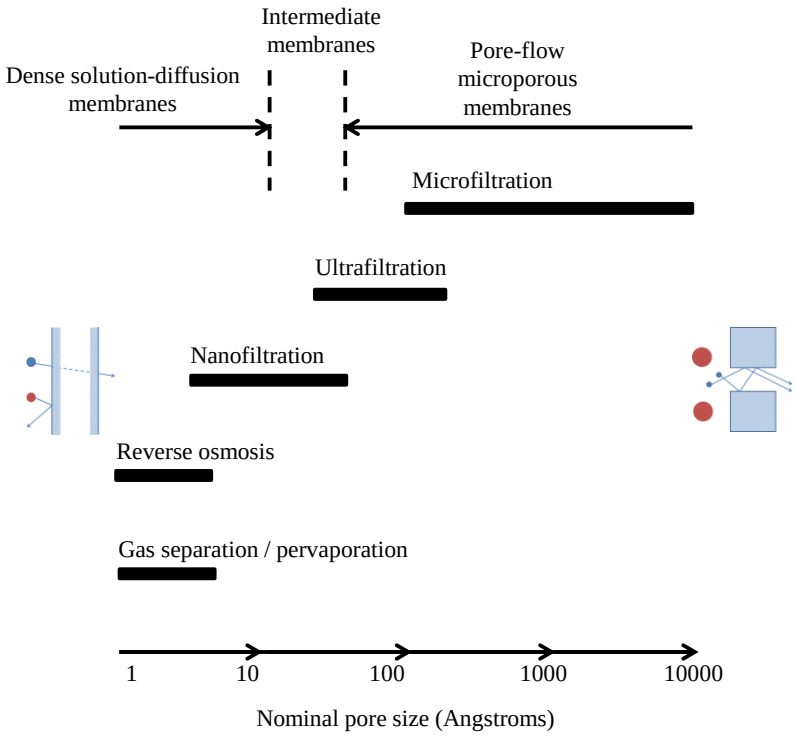

Figure 2-6. Schematic of the relationship between nominal pore size and theoretical models for different membrane processes (adapted from).[32]

The type of process and the driving force used to drive transport across the membrane are also related. The majority of membrane processes rely on either a pressure or vapour pressure driving force; however, other driving forces can also be used for membrane processes (Table 2-1). As can be seen, there are many different types of membrane processes and only those applicable to the separation of fermentation mixtures will be described herein.

Table 2-1. Membrane processes and associated driving forces for membrane transport.

Driving Force	Membrane Process
Pressure	Microfiltration (MF), Ultrafiltration (UF), Nanofiltration (NF), Reverse Osmosis (RO)
Vapour Pressure	Pervaporation (PV), Vapour Permeation (VP), Vacuum Membrane Distillation (VMD)
Temperature	Membrane Distillation (MD), Thermopervaporation (TPV)
Electrical Potential	Electro-dialysis / Electro Osmosis
Concentration	Dialysis / Forward Osmosis

- Microfiltration

Microfiltration (MF) is a pressure driven process (~ 1 – 4 bar) that can generally be defined by the pore-flow model and uses a porous membrane to separate particles of between 0.1 and 10 μm in size. MF membranes mainly exhibit rejection based on size exclusion (pore flow model) and can be used to retain solid particles such as yeast and bacteria. In fermentation processes MF is generally used in cell recycle systems.[33]

- Ultrafiltration

Ultrafiltration (UF) uses membranes with average pore sizes of between 10 – 1000 Å. The pressure driven process (~ 2 – 7 bar) also mainly separates based on size exclusion (pore flow model) and can be used for retaining proteins, cells, starch and enzymes with molecular weights of greater than ~ 500 g mol^{-1}.[34, 35]

- Nanofiltration

Nanofiltration (NF) again is a pressure driven process (~ 6 – 30 bar) with pore sizes between 1 and 10 nm. Separation is described using a mixture of the pore flow and solution diffusion models. NF is generally used for the separation of low molecular weight organics / multivalent salts from water or organic solvents. NF membranes are generally used to reject species with MW of between 150 – 1000 g mol^{-1}.

- Reverse Osmosis

Reverse Osmosis (RO) is a pressure driven process (~ 30 – 50 bar) utilising a membrane that will allow water to permeate freely whilst rejecting almost all other dissolved salts and small solutes. Rejection is best described by the solution-diffusion model and typically rejection of solutes ~ 150 g mol^{-1} is observed. RO is mainly used for wastewater treatment or producing drinking water by desalination of sea or brackish water.

- Pervaporation / Vapour Permeation

Pervaporation is a combination of evaporation and membrane permeation. A heated liquid feed is in contact with one side of a membrane and permeate vapour is removed from the other. The transport through the membrane is induced by the pressure difference maintained by either a vacuum or a sweep gas. The separation of the membrane is based on its interaction with the solvent / solute and best described by solution diffusion.[36] Vapour permeation differs solely in that the feed is a vapour rather than a liquid. Pervaporation is discussed in greater detail in Sections 2.3 – 2.6.

- Membrane distillation

Membrane distillation uses a microporous membrane with a liquid feed on one side and separation is dictated by the relative volatilities of the feed components. The driving force is a difference in partial vapour pressures induced by either temperature and / or a vacuum (in the case of VMD) but in contrast to PV the membrane has no influence on the separation of vapours.

- Forward Osmosis (FO)

Forward Osmosis (FO) uses an osmotic pressure gradient and a membrane that allows only permeation of water. Water diffuses from the feed to a "draw" solution with a higher osmotic pressure, resulting in a feed that has an increased concentration and a draw solution that is diluted. The osmotic pressure gradients that can be generated by FO are much greater than the pressure gradients possible using mechanical pumps (e.g. in RO).[37]

2.1.3 Membrane Performance Parameters

For a membrane to be effective it must exhibit suitable selectivity for the separation required whilst maintaining a suitably high permeation rate through the membrane (flux). How these performance factors are reported can differ slightly between the different membrane processes. Herein, the factors relate to pressure driven membrane processes (e.g. MF, UF, NF, RO) and the factors relevant for pervaporation processes are discussed in detail later (see Section 2.3). Flux (J) is defined as the flow rate of permeate per unit area (generally reported as volume L m^{-2} h^{-1} or mass kg m^{-2} h^{-1}). The main parameter to describe selectivity of a pressure driven-membrane is the observed rejection (Equation 2-1):

$$R_{obs} = \left(1 - \frac{C_p}{C_f}\right) \times 100\ \% \qquad 2\text{-}1$$

Where: C_p = Concentration of solute in permeate

C_f = Concentration of solute in feed

So when R_{obs} = 100 % a complete rejection is observed and when R_{obs} = 0 % no separation has been achieved.

The observed rejection is therefore specific to a particular separation by a certain membrane. It is used to determine the performance characteristics of a membrane for that particular separation and not the more general separation capacity of the membrane. A more general definition for the separation capability of a membrane is the molecular weight cut-off (MWCO). This is defined as the molecular weight (MW) where 90 % of the solute is rejected by the membrane. In theory a molecule that possesses a MW greater than the MWCO of the membrane should exhibit a high rejection. The MWCO curve should therefore ideally be sharp, exhibiting high rejections of compounds with MWs marginally greater than the MWCO and low rejections of solutes with MWs marginally less than the MWCO. In practice though this is rarely the case and it is important to note that a number of other properties affect the rejection of a solute such as molecular shape, charge, pK_a, solubility, concentration polarisation and fouling. Due to the non-ideal nature of separation the MWCO curve is typically blunt meaning that separation of molecules of similar MWs cannot be achieved. The MWCO gives an understanding of the separation behaviour of a membrane but prediction of rejection of a solute by MWCO alone can be misleading.

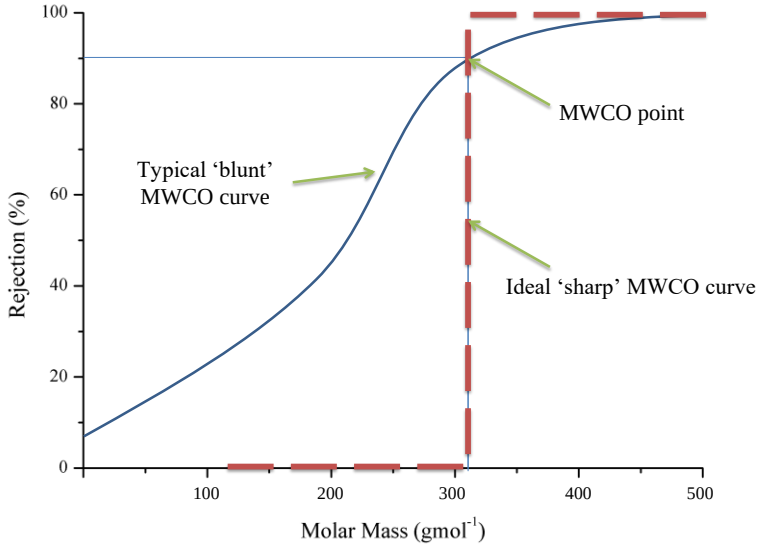

Figure 2-7. Ideal (sharp) and typical (blunt) MWCO curves for a NF membrane.

The importance of different solute properties on whether it will be retained by a NF or RO membrane has been reviewed by Bellona *et al.*[38] Other factors that govern rejection include the pK_a, hydrophobicity / hydrophilicity (log K_{ow}) and the molecular width (MWidth) of the solute. This gives a much clearer picture to be able to predict the retention of a solute (Figure 2-8). The only way to truly determine the rejection of a certain organic solute by a NF or RO membrane; however, is to measure it experimentally.

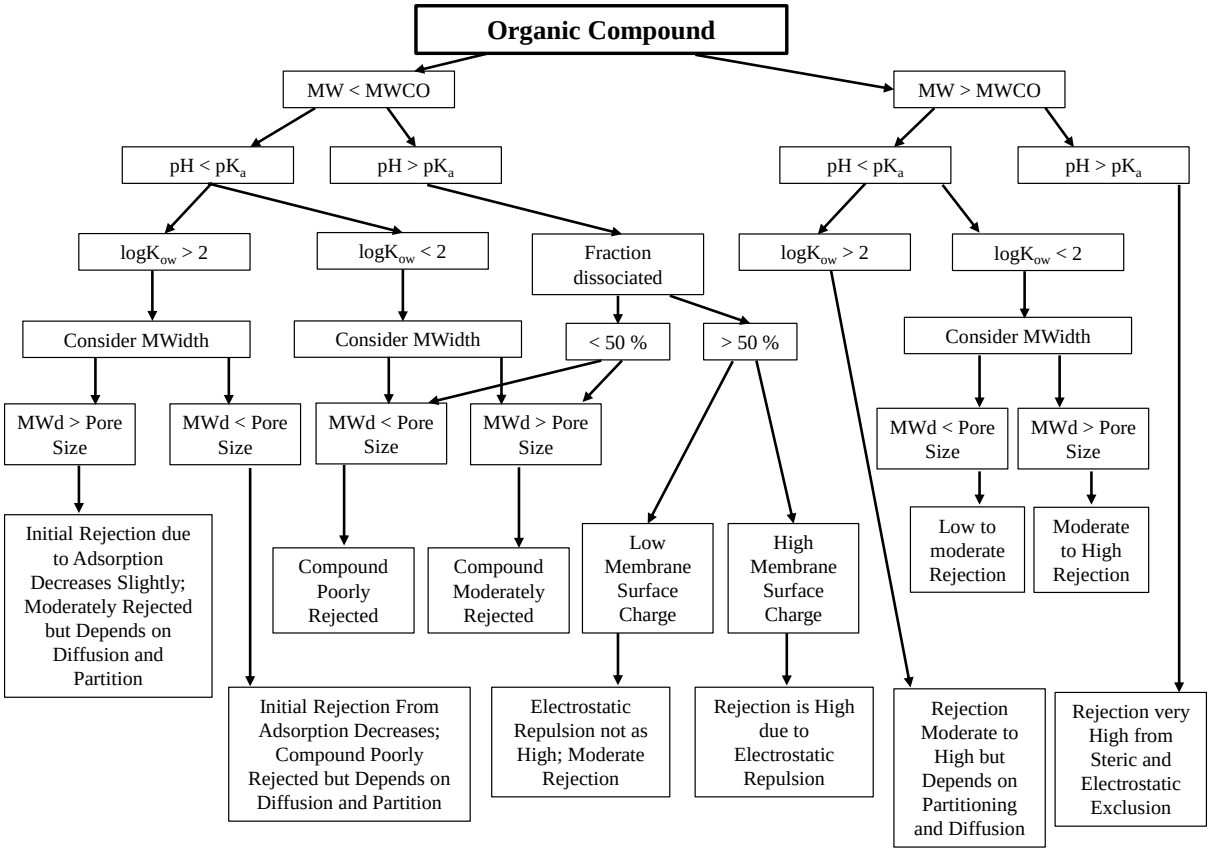

Figure 2-8. Flow diagram to determine an organic solutes rejection by an NF or RO membrane (reproduced from Bellona et al.).[38]

2.1.4 Membrane Materials and Modules

The majority of membranes are polymeric, due to their competitive separation performance, ease of production and low cost. Polymeric membranes can be produced as either flat sheets, or cylinders denoted tubular, capillaries, or hollow fibres, dependent on the dimensions of the tube diameter.[39] A vast number of polymers have been applied to different membrane processes and the choice of polymer is based on specific structural and chemical properties of the material which govern its intrinsic separation properties. Ceramic and inorganic membranes can also be produced in these fashions but are generally more difficult to produce and are often very brittle. They can; however, offer improved separation performance over polymeric membranes and can generally withstand much harsher operating conditions e.g. high temperatures. These polymeric and inorganic membranes can then be fabricated into the various membrane modules outlined below.

The active surface area of a membrane is a limiting factor in the total flux. For industrial application of membranes it is important to be able to have the largest membrane surface area in the smallest possible volume and a number of membrane modules have been designed to achieve

this. The design of the membrane module is also important for enhancing the throughput, flow dynamics, fouling and total cost of the membrane process. Currently the most common membrane modules are:

- Plate and Frame

Plate and frame modules are the simplest form of membrane module and generally consist of flat membranes with the feed / permeate sides facing together (Figure 2-9). Spacers are placed between the feed and permeate to allow for suitable solution flow. These modules can then be numbered up to create a plate-and-frame stack and can achieve membrane surface areas per module volumes of between 100 - 400 m^2 m^{-3}.[40]

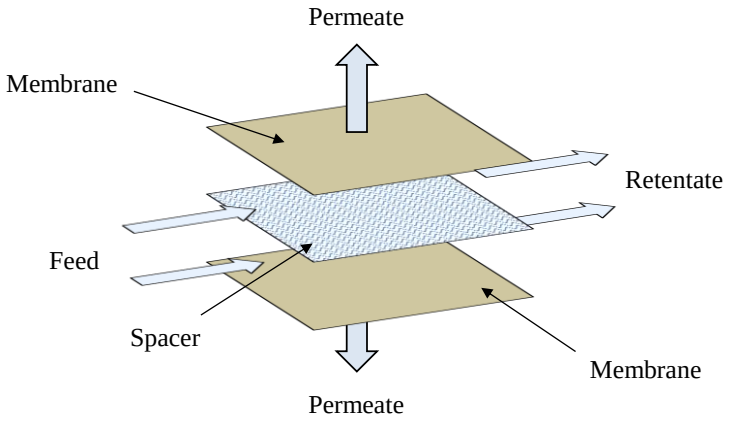

Figure 2-9. General schematic of a plate and frame membrane module.[40]

- Tubular

Tubular membranes and the following hollow-fibre / capillary membranes are similar in structure; however, tubular membranes are not self-supporting. They are placed inside porous stainless steel, plastic or ceramic tubes with diameters in excess of 10 mm and then a number of these tubules are put together to form a module (Figure 2-10.a). Tubular membranes always operate from the inside out, with the feed flowing through the middle of the membrane and the permeate permeating through the walls of the tubular membrane. These type of modules typically have packing densities of lower than 300 m^2 m^{-3}.[40] Monolithic tubular membranes (Figure 2-10.b) are a specific type of tubular membrane where a single porous block, typically ceramic, has many cylindrical cavities that have been coated with the selective membrane layer.

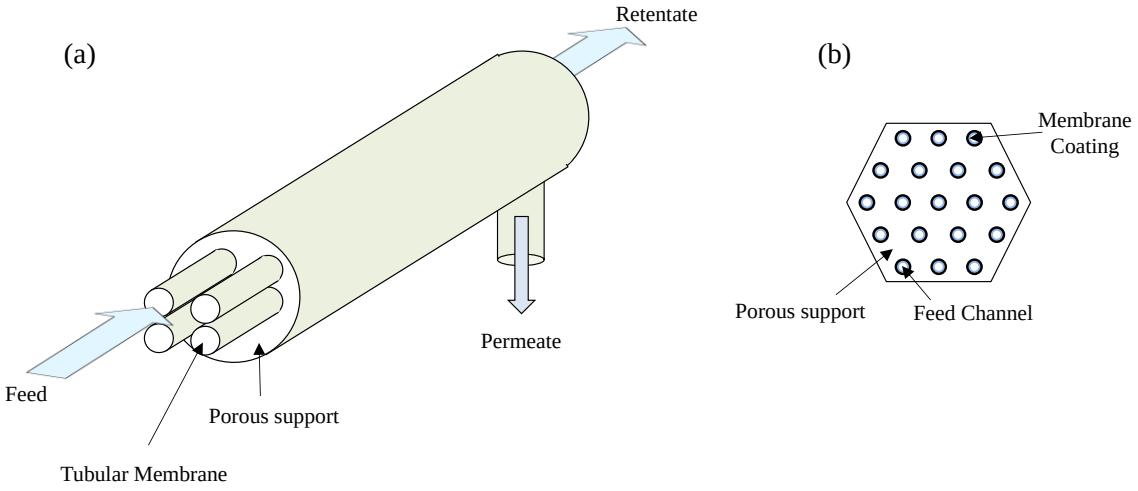

Figure 2-10. (a) Schematic of a tubular membrane module and (b) cross-section of a monolithic tubular membrane module.[40]

- Hollow Fibre / Capillary

Hollow fibre and capillary modules are analogous in configuration (and also similar to tubular membranes) but differ in the dimensions of the self-supporting tubules used. Capillaries are generally 0.5 – 5 mm in diameter and hollow fibres generally regarded as below 0.1 μm in diameter. The capillaries or hollow fibres are placed together and the ends potted together with either an epoxy resin, polyurethane, or silicone rubber. There are two modes of operation for these classes of membrane module as either inside-out (Figure 2-11.a) or outside-in (Figure 2-11.b) and depends on the separation, type of membrane, and the associated process parameters. As the internal diameters are small capillary and hollow fibre modules can only be used with relatively clean feed streams (hollow fibres more so than capillary). Packing densities of 600 - 1200 m^2 m^{-3} and up to 30 000 m^2 m^{-3} are common for capillary and hollow fibre modules respectively.[40]

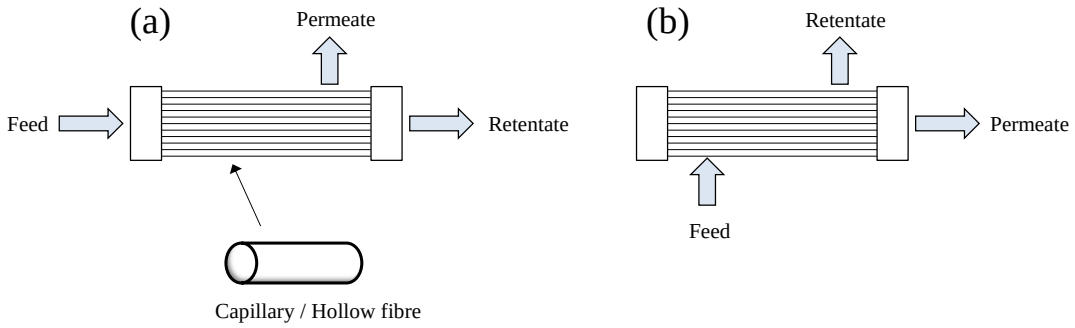

Figure 2-11. Schematic of a capillary / hollow fibre module showing the two possible operational modes of either: (a) inside-out and (b) outside-in.[40]

- Spiral Wound

Spiral wound membranes consist of flat-sheets of polymeric membrane rolled into a spiral fashion around a central permeate pipe (Figure 2-12.a). The cross section of this module (Figure 2-12.b) shows the similarities to the plate and frame module. The feed flows parallel to the central pipe through the feed spacer which creates turbulent flow and the permeate flows radially towards the centre of the module before flowing along the permeate tube. Packing densities can be anywhere between 300 – 1000 m^2 m^{-3}.[40]

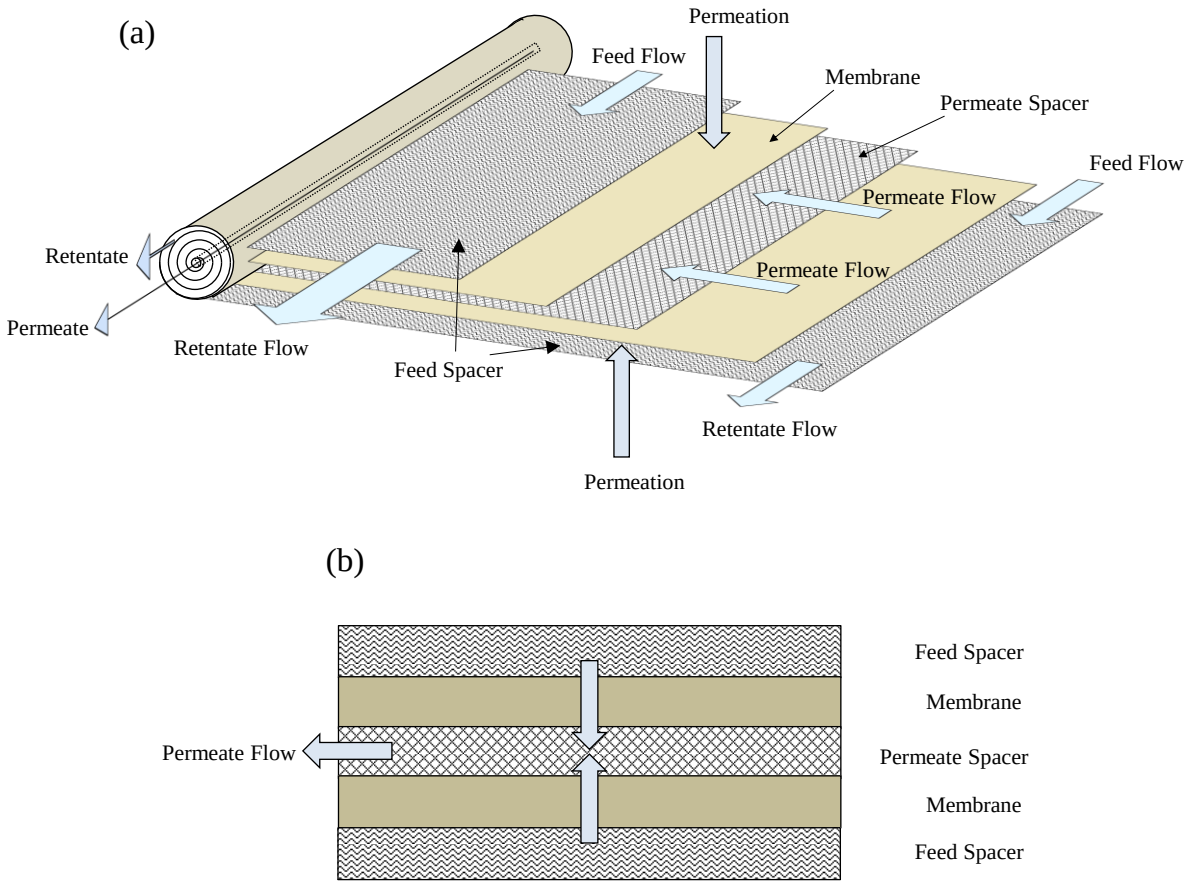

Figure 2-12. Schematic of a spiral wound module showing the unwound structure (a) and the cross-sectional view (b). The flat sheet membranes are separated by feed and permeate spacers and rolled up to form the module.[40]

The work presented in this thesis deals solely with flat-sheet membranes, which have been applied in laboratory scale plate and frame type modules with low laboratory scale surface areas (~ 14.6 cm^2). The design of membrane modules is not discussed in great detail herein; however, for the application of some of the novel membranes or commercial membranes tested, considerations of module design and process parameters will be of utmost importance.

2.2 Membrane Processes for Recovery of Organic Products from Fermentation Broths

Membranes can provide energy savings in recovering organics from fermentation broths by:

- Removing large biomolecules from the broth e.g. cells or proteins with permeation of a purified permeate.
- Concentrating the fermentation products within the broth / purified broth through the selective removal of water leading to a concentrated product in the retentate.
- Selectively removing fermentation products from the broth / purified broth providing a concentrated permeate.

It is envisaged that these membrane processes could provide energy savings as part of a larger separation process. Due to the complexity of fermentation broths, an array of different product recovery technologies are required due to the number of different components of the broth and effects these can have on different separation processes. The main processes that have been applied to the purification of a fermentation broth and recovery of the fermentation products are MF, UF, NF, RO, membrane distillation, and pervaporation (Table 2-2). This section will discuss important examples of these processes generally where they apply to the research in this thesis. Examples will focus on the production of 2,3-butanediol, acetate, and ethanol as these are the main fermentation products produced within the LanzaTech process, and the main fermentation process studied within this thesis.

Table 2-2. Description of different membrane filtration processes applied to separations of fermentation broths.

Filtration:	**Pore size / MWCO:**	**Retention of:**	**Literature:**
Microfiltration (MF)	0.1 – 10 μm	Yeast, Bacteria	41-43
Ultrafiltration (UF)	1 - 100 nm > 2000 $gmol^{-1}$	Proteins, DNA	44
Nanofiltration (NF)	200 – 2000 $gmol^{-1}$	Sugars, Acids	45-47
Reverse Osmosis (RO)	> 100 $gmol^{-1}$	Alcohols, Acids, Salts	48, 49
Pervaporation (PV)	Hydrophobic or Hydrophilic dense membrane	Water or Organic Solvent	11, 50
Membrane Distillation (MD)	~ 0.2 μm (separation based on VLE not membrane)	Permeation of water / product	51

Microfiltration has been successfully applied for the recycling of cells in many different fermentation processes. It is generally used to return the microbial cells back to the fermentor and can therefore be used in a continuous fermentation to protect cells from elevated temperatures used in downstream product recovery processes such as distillation.[42] Advantages of utilising MF for these separations include the operation at ambient temperature, good separation efficiency, and the use of compact simple and reliable equipment.[42] There are a vast number of examples of the use of MF in this manner; however, one specific example is where MF has been investigated for cell recovery in a 2,3-butanediol fermentation from blackstrap molasses where gas sparging was used to overcome membrane fouling.[41]

As discussed earlier NF and RO membranes exhibit MWCOs of $150 - 1000$ g mol^{-1} and < 100 g mol^{-1} respectively; and therefore, provide the correct rejections for separating organic solutes from water. It has been shown that RO membranes can remove low concentrations of organics from distillery condensates.[52-55] As 2,3-butanediol is present at low levels in these wastewater streams (~ 0.5 g L^{-1}), it has been shown to be rejected at low levels by a series of RO membranes.[52] No studies have been undertaken at higher concentrations, or where 2,3-butanediol is the desired fermentation product. Concentration of ethanol by reverse osmosis membranes has been reported; however, extremely high transmembrane pressures of almost 100 bar were required and fluxes were below 3 L m^{-2} h^{-1} with rejections between $80 - 90$ %.[56, 57] In a similar way butanol has been investigated, but again extremely low fluxes were exhibited at high pressures.[58]

NF and RO have also been used for concentrating organic acids from fermentation broths. Examples include the recovery of lactic acid[48, 49] and acetate.[45, 46] For the recovery of acetate, suitable commercial polymeric NF and RO membranes were identified by quantifying their flux and rejection parameters with model solutions.[45] The recovery process for sodium acetate in Figure 2-13 has since been proposed from this data.[46] It consists of a microfiltration membrane for returning cells to the fermenter, a low rejecting NF membrane for returning nutrients and sugars, and a high rejecting NF membrane for the concentration of a purified aqueous sodium acetate stream. The stream is then concentrated further using a series of lower rejecting NF membranes which overcomes a large increase in osmotic pressure that a high rejecting membrane would create. Finally, an evaporator concentrates the aqueous acetate stream further to the desired concentration of 300 g L^{-1}.[46]

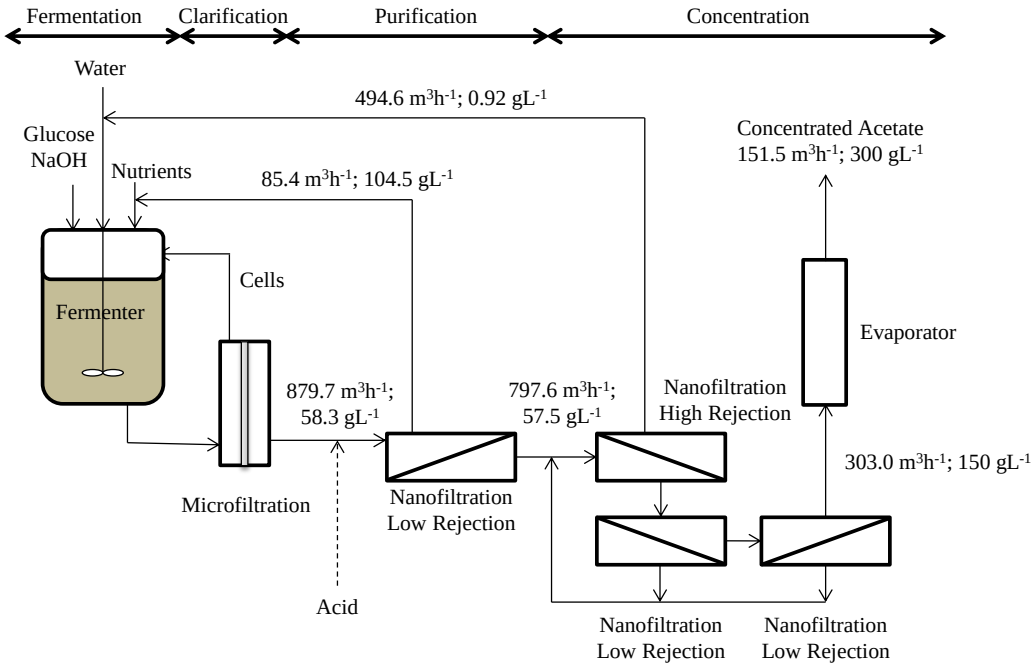

Figure 2-13. Proposed process for the recovery of acetate from a fermentation broth. Data refers to volumetric flow rate and concentration of sodium acetate (reproduced from Han et al.).[46]

Vacuum membrane distillation (VMD) can also be employed to concentrate a fermentation broth. Qureshi *et al*. reported an integrated fermentation and VMD process for the concentration of a 2,3-butanediol fermentation broth. This process utilised a hydrophilic 0.22 μm polytetrafluoroethylene (PTFE) membrane which selectively permeated water. The process allowed the concentration of model solutions of 2,3-butanediol from 4 wt% to 65 wt% and when utilised with a fermentation broth concentrations of up to 43 wt% diol were achieved.[51]

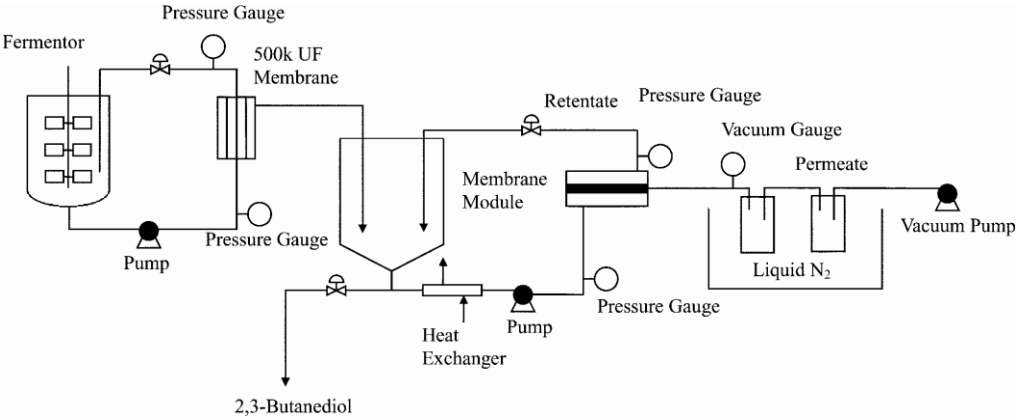

Figure 2-14. Integrated production and recovery of 2,3-butanediol in a fed batch reactor by VMD.[51]

For the selective removal of a fermentation product by a membrane process, pervaporation is generally utilised. The most important example of this is in the recovery of ethanol from a fermentation broth. Generally a microfiltration membrane is used to recycle cells back to the fermenter to protect them from the elevated temperatures required in pervaporation. Then an organophilic membrane removes ethanol from a dilute aqueous stream giving a permeate enriched in ethanol. A hydrophilic pervaporation process is subsequently utilised to remove the remaining water from the concentrated ethanol stream (Figure 2-15).[59]

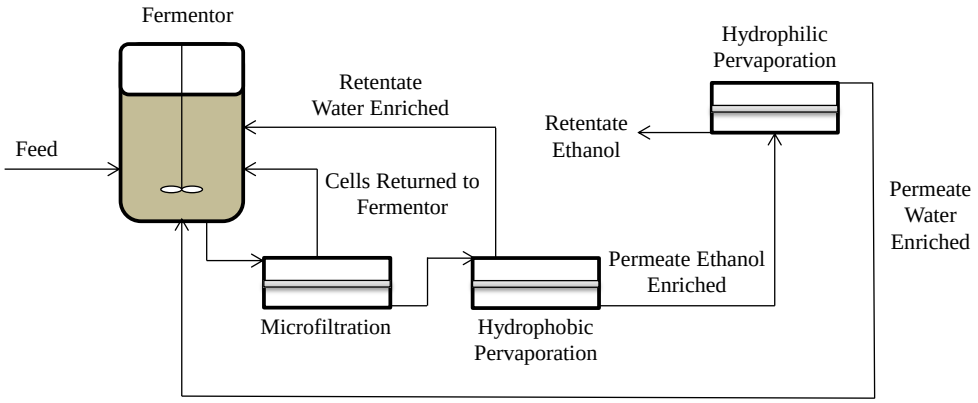

Figure 2-15. Schematic of the pervaporative recovery of ethanol from a dilute fermentation broth.[59]

The pervaporative removal of acetic acid from water and fermentation broths has also been investigated.[16] Many traditional polymers used for pervaporation such as silicone rubber exhibit poor selectivities towards acetic acid over water,[60] silicalite has been used in an attempt to improve this selectivity[61] and as a standalone membrane.[62] The selectivity of pervaporation membranes towards acetic acid is also dependent on the pH of the feed due to the level of deprotonation of the carboxylic acid; despite this, pH is often not reported, controlled, or ignored as a process parameter.[50]

Integrated production with pervaporative recovery of 2,3-butanediol has been modelled[63] but determining a membrane material exhibiting selectivity towards 2,3-butanediol over water is difficult, as Shao *et al.* have shown.[64] This is due to the two hydroxyl groups making 2,3-butanediol strongly hydrophilic and determining a membrane material which exhibits an increased affinity towards it over water is difficult when also combined with its low volatility and high boiling point. Therefore, an integrated solvent extraction and pervaporation process was developed by Shao, utilising 1-butanol as extracting solvent and a polydimethylsiloxane (PDMS) membrane.[65] Selectivity of 1-butanol over 2,3-butanediol was further increased by dispersing ZSM-5 zeolite within the matrix of the membrane.[66] This shows the importance of the membrane

material to achieve separation. Pervaporative recovery of fermentation products and the development of new materials to achieve superior separations is discussed further in the next sections.

2.3 Basics of Pervaporation

Pervaporation is a membrane process where a difference in partial vapour pressure, induced by either a vacuum or sweep gas, creates the driving force for a concentration gradient across the membrane. Pervaporation combines both evaporation and membrane permeation and is unique amongst membrane processes in that it involves a liquid-vapour phase change.[67] The upstream side is contacted with the liquid feed and vapour is withdrawn from the downstream side creating a concentration gradient (Figure 2-16). The transport across a pervaporation membrane is described as a three-step solution-diffusion-evaporation process and there are a number of transport mechanisms of which to describe diffusion across a pervaporation membrane.[67] The main factors affecting the permeability and selectivity performance of a membrane will be the solubility and diffusivity through the membrane and the relative volatility of the permeating species.[68] The relative volatility is an intrinsic property of the permeants but the solubility and diffusivity are determined by the membrane material. They are generally considered the rate-limiting steps of the process so long as the concentration of the solutes on the downstream side of the membrane is kept at zero through vaporization using a sufficient vacuum or sweep gas driving force. Therefore, the selection of an appropriate membrane material is paramount to achieving an optimum separation and flux in a specific pervaporation process.

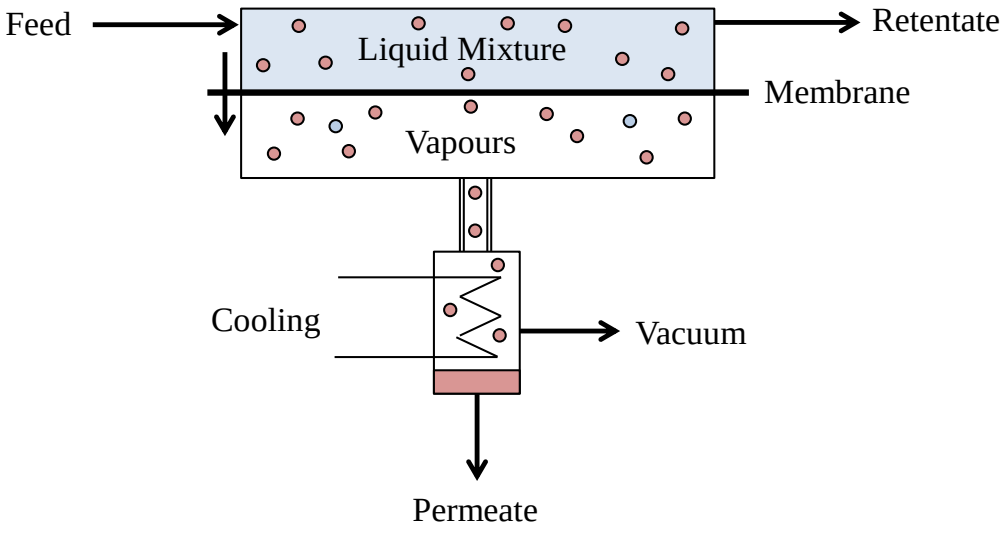

Figure 2-16. Schematic of a typical pervaporation process.

As with all pervaporation processes the key factors involved in quantifying the performance are the flux and selectivity. In pervaporation, flux is defined as the amount of permeant per unit time per unit area of the membrane. To quantify the selectivity of a pervaporation process this is defined by the separation factor or less commonly enrichment factor as outlined below.

- Separation Factor (Equation *2-2*):

$$\propto = \frac{A_P/(1-A_P)}{A_F/(1-A_F)} \qquad 2\text{-}2$$

- Enrichment Factor (Equation 2-3):

$$\beta = \frac{A_P}{A_F} \qquad 2\text{-}3$$

where:

- A_P = Weight fraction of permeating species A in the permeate
- A_F = Weight fraction of permeating species A in the feed
- $A_F + B_F = 1$ and $A_P + B_P$ where B_F and B_P are weight fractions of species B in feed and permeate respectively

To combine the factors of flux and separation factor into a single comparable parameter the pervaporation separation index (PSI) has been developed. This allows for cross comparison between membranes that may exhibit a high flux but low selectivity, and those that exhibit a low flux but high selectivity. Initially defined as the product of flux and separation factor[69, 70] this was found to be problematic as a membrane with high flux and no selectivity ($\alpha = 1$) could still have a large PSI value. Therefore, the PSI was redefined[71] as Equation 2-4:

$$PSI = J(\propto -1) \qquad 2\text{-}4$$

where J is the total flux and α the separation factor as defined above.

For the recovery of organics from aqueous streams, such as for recovery of fermentation products, pervaporation can be split into two main processes: hydrophilic pervaporation and organophilic / hydrophobic pervaporation (Figure 2-17).

- Hydrophilic pervaporation is used for the dehydration of highly concentrated organic solutions via preferentially permeating water across the membrane (Figure 2-17.a).
- Organophilic or hydrophobic pervaporation is used to recover small quantities of dilute organics from water through their preferential permeation across the membrane (Figure 2-17.b).

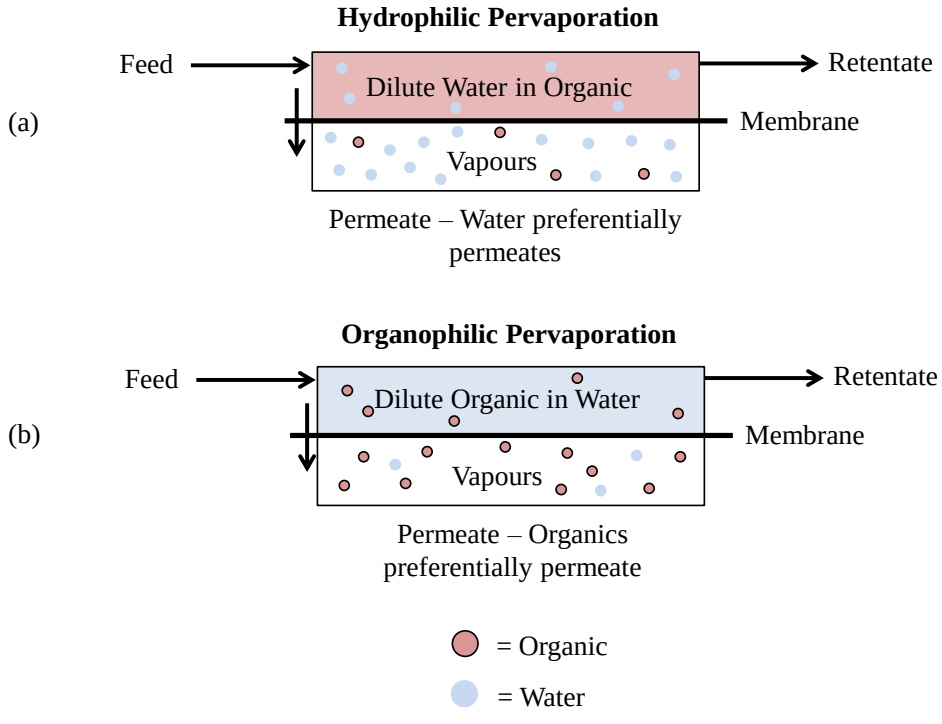

Figure 2-17. Schematic of (a) hydrophilic and (b) organophilic pervaporation processes.

As shown in Figure 2-15 both hydrophilic and organophilic pervaporation can be used in the recovery of fermentation products. As also briefly discussed at the end of Section 2.2, the membrane material has a large effect on the separation performance. As improved performance is required within pervaporation processes to apply them to product recovery from fermentations, a number of different and novel materials used for pervaporation membranes are discussed in the following section. The examples focus on mixed-matrix membranes (MMMs) and give an overview of this area that is relevant to the work conducted in Chapters 4 and 5 of this thesis.

2.4 Membrane Materials for Pervaporation

Pervaporation membranes can be defined by the material they are composed of. These generally fall into three categories: polymeric, inorganic or mixed-matrix. Each of these classes of pervaporation membrane will be discussed in the following sections.

2.4.1 Polymeric Pervaporation Membranes

Polymers are the most common material for pervaporation membranes due to their reasonable separation performance, low-cost, and ease of processing. When choosing a polymer for a pervaporation process it is important to find one that will have a high affinity towards the chosen permeant as well as being stable under the conditions of the pervaporation process. The compaction of polymer membranes by high pressure (which can be problematic in gas separations) is avoided with pervaporation due to no feed pressure being applied.[68] Other considerations such as cost and ageing of the polymer must be taken into account for producing a membrane that could be successfully applied in an industrial setting.

For the dehydration of organics via pervaporation, hydrophilic polymers should be used. The hydrophilicity of the polymers arises from the presence of many polar functional groups within the polymer chain (e.g., (-OH, -NH, -C=O, -C-O-, -CN) that will interact with water. Examples of these types of polymers used for hydrophilic pervaporation are given in Figure 2-18. Polymers which are ionic and neutralized by counter ions (such as sodium alginate) are generally water selective due to exhibiting high affinities towards it.[60]

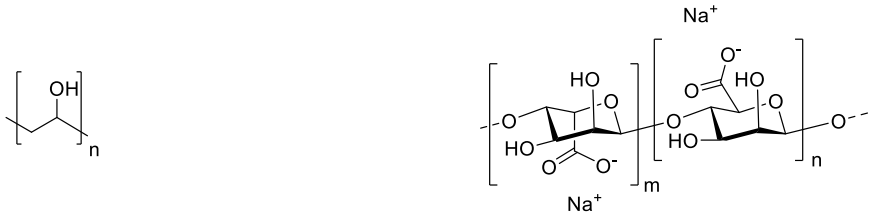

Polyvinylalcohol (PVA) Sodium Alginate

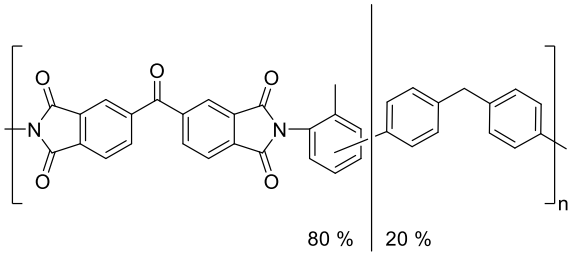

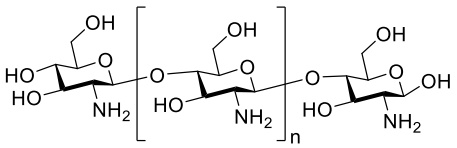

Polyimide P84 Chitosan

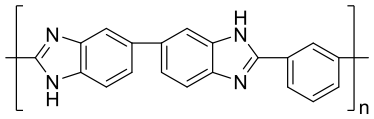

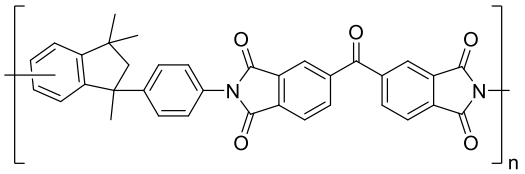

Polybenzimidazole (PBI) Matrimid 5218

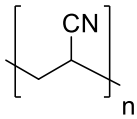

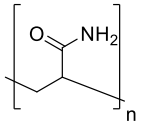

Polyacrylonitrile Polyacrylamide

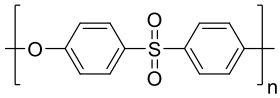

Polyethersulfone

Figure 2-18. Examples of polymers for hydrophilic pervaporation membranes.

Table 2-3 presents a comparison of polymers tested for the removal of water from concentrated ethanol solutions. It is evident that the choice of polymer used has a large impact on the performance characteristics of the membrane with the separation factor varying from 12,500 for a polyacrylonitrile membrane down to 52 for a polyethersulfone membrane with the total flux varying from 0.03 kg m^{-2} h^{-1} to 0.72 kg m^{-2} h^{-1} respectively. Table 2-3 also presents an example of the effect inclusion of an inorganic filler amongst the polymer matrix will have on the membrane performance. For the polyvinylalcohol membrane presented in[72], inclusion of Zeolite NaX at 11 wt% increased the flux to 0.21 kg m^{-2} h^{-1} but reduced the separation factor to 19.4. This

demonstrates the ability to modify a suitable polymer further through the creation of a mixed-matrix membrane, which is discussed further in section 2.2.3.

Table 2-3 Hydrophilic pervaporation of ethanol-water mixtures by various polymer membranes.

Dehydration of: Alcohol/Water (wt% / wt%)	**Polymer**	**Inorganic Filler**	**Membrane Performance**		**Temp (°C)**	**Membrane Thickness (μm)**	**Ref:**
			Total Flux ($kg \cdot m^{-2} \cdot h^{-1}$)	**Separation Factor (α)**			
Ethanol/Water (90/10)	Polyacrylonitrile	-	0.03	12500	70	50	[67]
Ethanol/Water (90/10)	Polyacrylamide	-	0.42	2200	70	50	[67]
Ethanol/Water (90/10)	Polyvinylalcohol	-	0.38	140	70	50	[67]
Ethanol/Water (90/10)	Polyethersulfone	-	0.72	52	70	50	[67]
Ethanol/Water (80/20)	Polyvinylalcohol	-	0.14	40	50	70–80	[72]
Ethanol/Water (80/20)	Polyvinylalcohol	Zeolite NaX (11 wt%)	0.21	19.4	50	70–80	[72]

For organophilic pervaporation, hydrophobic polymers are utilized. These polymers possess few or no polar functional groups that exhibit an affinity for water. Examples of polymers utilized for organophilic pervaporation are presented in Figure 2-19.

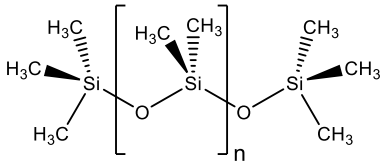

Polydimethylsiloxane (PDMS)

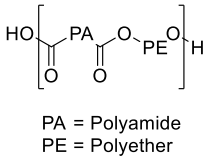

Polyether-block amide (PEBA)

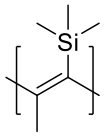

Poly(1-trimethylsilyl-1-propyne) (PTMSP)

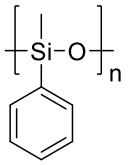

Polymethylphenylsiloxane (PMPS)

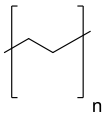

Polyethylene

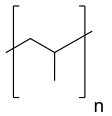

Polypropylene

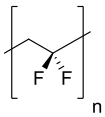

Polyvinylidene fluoride (PVDF)

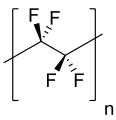

Polytetrafluoroethylene (PTFE)

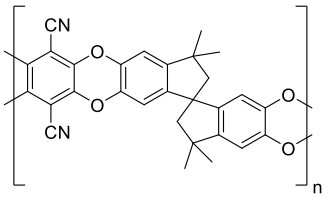

Polymer of Intrinsic Microporosity-1 (PIM-1)

Figure 2-19. Examples of polymers for organophilic pervaporation membranes.

Again the choice of polymer will have a significant effect on the performance of a pervaporation process, with a number of studies for organophilic pervaporation by polymer membranes summarized in Table 2-4. A number of studies have also looked at the effect of modifying the functional groups of a polymer[73, 74] or the creation of new block copolymers[75] on the overall performance of the polymeric membrane.

Table 2-4. Organophilic pervaporation by various polymer membranes.

Organophilic Pervaporation of:	Polymer	Membrane Performance		Temp (°C)	Membrane Thickness (μm)	Ref:
		Total Flux ($kg \cdot m^{-2} \cdot h^{-1}$)	Separation Factor (α)			
1 wt% Ethanol	PTMSP	-	10.7	75	100	[76]
2 wt% Ethanol	PTFE (0.2 μm pore diameter)	12	2	60	175	[77]
5 wt% Ethanol	PTFE (0.2 μm pore diameter)	4	8	30	80	[78]
1 wt% Ethanol	PIM-1	0.47	10.7	30	25–40	[79]
5 wt% Ethanol	Poly(octylmethyl siloxane) POMS	0.12	3.95	50	-	[80]
5 wt% Ethanol	PEBA 2533	0.37	2.4	23	100	[81]
1.5 wt% Butanol	PDMS	0.72	33.7	55	30	[82]
5 wt% Butanol	PEBA 2533	0.65	8.2	23	100	[81]

In Chapters 4 and 5 PDMS was used as the polymer of choice for the fabrication of the MMMs. PDMS has a high performance for organophilic pervaporation of alcohols from water, as can be seen from the comparison with other polymers in Table 2-4. It is also a cheap and readily available polymer that can easily be cast into flat sheets. This has led to its use in many of the MMM examples for organophilic pervaporation described in Section 2.4.4. The membranes fabricated within Chapters 4 and 5 can therefore be directly compared to a number of literature examples.

2.4.2 Inorganic Membrane Materials and Mixed Matrix Membranes for Pervaporation

There are a vast number of different inorganic membrane materials that are either commercially available or have been investigated within the literature. Although many exhibit remarkable selectivities for a number of significant fermentative separations, there are drawbacks to their use. The membranes are generally brittle and difficult to produce, and are usually manufactured with thicknesses in excess of 10 μm, resulting in low permeances.[83] Inorganic membranes are also generally more expensive to produce compared to their polymeric alternatives. There are; however, a variety of novel fabrication techniques being developed to lessen the cost of highly permeable inorganic membranes.[84] To overcome the disadvantages to inorganic membranes, mixed-matrix membranes (MMMs) have been developed. MMMs consist of a dispersed inorganic material within a polymer matrix (Figure 2-20). MMMs are intended to combine the processability

and low cost of polymer membranes with the high separation performance of inorganic membranes. Although these hybrid MMMs generally exhibit enhanced permeabilities and separations compared to purely polymeric membranes, developments must still be made within polymer chemistry to overcome the problems of aging, sensitivity to cleaning agents and fouling. A number of common, significant, inorganic materials for incorporation into MMMs within fermentative separations are discussed below; however, examples of many other fillers for MMMs can be found amongst the literature.

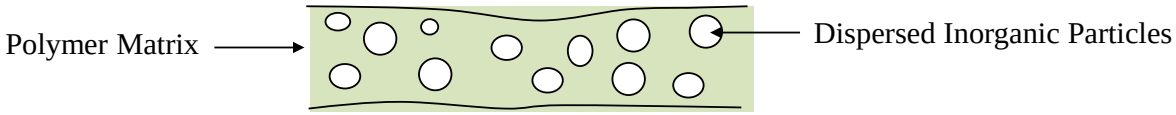

Figure 2-20. Schematic of a mixed-matrix membrane.

2.4.2.1 Zeolites

Zeolites are silicalite or aluminosilicate microporous materials (Figure 2-21) meaning that they exhibit pores that are less than 2 nm (20 Å) in diameter. Formed of SiO_4 and AlO_4 tetrahedra, they can form a vast number of structures. Zeolites are an ideal membrane material due to consisting of uniform, molecularly sized pores as well as possessing high thermal, mechanical, and chemical stability. Although more than 190 zeolite structures have been reported, only 20 have been shown to give a worthwhile separation performance when prepared as membranes[85] with examples of zeolite membranes present for NF/RO[86, 87] and pervaporation processes.[88]

In the recovery of fermentation products, zeolites have been studied extensively for their adsorption properties of certain organic products. Hydrophobic and hydrophilic zeolites have been investigated for the recovery of fermentation products. Studies on the adsorption of various fermentation products from aqueous solutions have been conducted on zeolites with high silica ratios due to their increased hydrophobicity. The adsorption of 1-butanol from aqueous solutions has been demonstrated for zeolites with high silica ratios such as silicalite and ZSM-5 and the adsorption studied within the context of the ABE fermentation.[89-91] Other fermentation products have also been investigated for adsorptive recovery by zeolites such as acetic acid[15] and lactic acid.[92] Therefore, it is clear how zeolites have become popular inorganic fillers within MMMs for fermentative separation processes due to their ability to separate water from organic solutes.

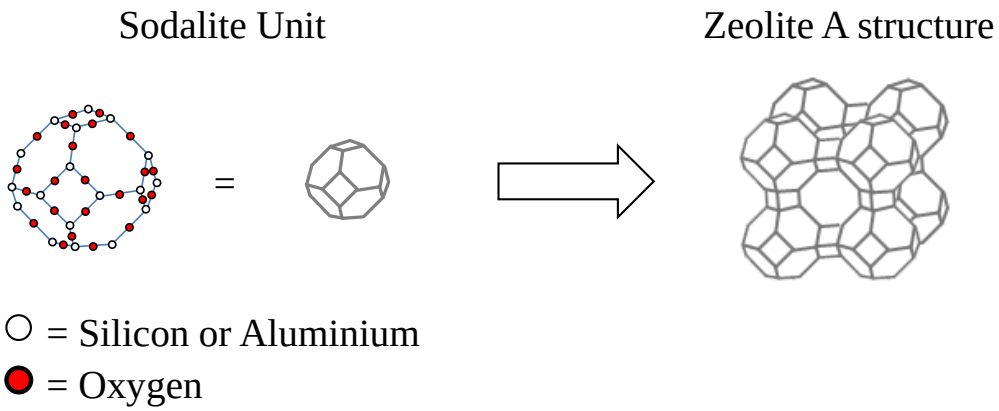

Figure 2-21. Schematic of a typical zeolite structure made up of sodalite units.

2.4.2.2 Metal-Organic Frameworks

Metal-organic frameworks (MOFs) are a novel type of microporous material (Figure 2-22), and like zeolites they exhibit pores that are less than 2 nm in diameter. These crystalline materials are comprised of an organic linker coordinated to a metal or metal oxide cluster (denoted secondary building unit—SBU).[93] The ability to systematically change the SBU or organic linker allows tailoring of the specific size and chemical environment of the pores. Widely studied for their gas storage and separation properties, their use within liquid separations has received much less attention. For applications within liquid separations, especially those of fermentation broths, MOFs that are chemically stable towards water and organic solvents are required.[94] Although historically MOFs have been highly sensitive to moisture and aggressive media, there are ever increasing examples of robust MOFs that can withstand the conditions required for fermentative separation applications.

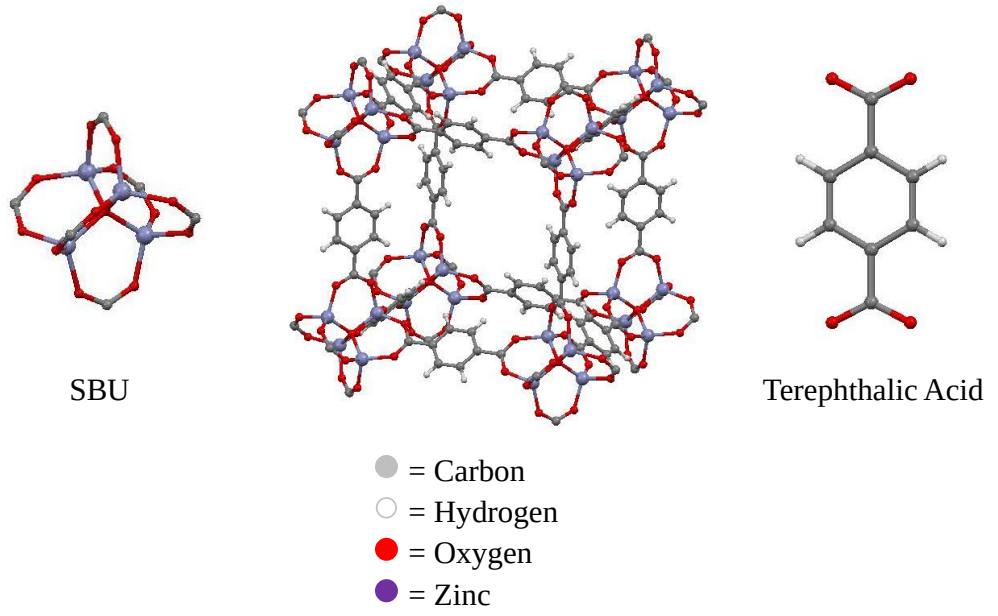

Figure 2-22. Schematic of the Metal-organic Framework (MOF), MOF-5, produced from the crystallographic data from.[95]

With a number of examples of MMMs incorporating MOFs present in the literature for application within gas separations,[96] utilization of MOFs within MMMs for liquid and vapour separations (as are needed for separations from fermentations) has received much less attention. Initial investigations have looked into the alcohol / water separation ability of a number of MOFs to ascertain their properties for application in recovery of fermentation products. Initial computational studies have identified a number of MOFs that exhibit suitable water / alcohol separation properties.[97-99] For example, De Lima *et al*. investigated the mechanism for alcohol-water separation in the MOF $Zn_2(bdc)_2(TED)$ (TED = 1,4-diazabicyclo[2.2.2]octane).[100] From the density functional theory (DFT) calculations conducted, they deduced that the increased adsorption of ethanol over water was due to a combination of hydrogen bonding between the alcohol hydroxyl group and oxy group of $Zn_2(bdc)_2(TED)$ and the van der Waals interactions between the alcohol alkyl chain with the phenyl ring. It is the promise of computational predictions such as this that in part have led to an increasing interest in the use of MOFs for the separation and recovery of fermentation products.

A number of experimental studies have also been conducted on MOFs to identify their water / alcohol adsorption properties. The effect of functional groups on the water adsorption on the MOF MIL-101 was studied.[101] MIL-101 is a MOF that shows high water sorption, and the water sorption profile was successfully manipulated by altering the functionality of the terephthalic acid linker from MIL-101, to MIL-101-NH_2 to MIL-101-SO_3H. This ability to alter

the sorption behaviour of MIL-101 demonstrates the ability to tailor the pore environment of MOFs through synthetic chemistry tools. Water adsorption has also been investigated on a number of other MOFs (HKUST-1, ZIF-8, MIL-101, MIL-100(Fe), DUT-4) with both hydrophilic and hydrophobic materials studied.[102]

The adsorption of alcohols on a number of different classes of MOFs has also been investigated.[103] As a sub category of MOFs, zeolitic-imidazolate frameworks (ZIFs) have received much attention recently for biofuel separations due to their high thermal, water and chemical stability.[104] Being composed of tetrahedral metal ions (Zn, Co, *etc.*) bridged by an imidazolate ligand, the M-Im-M angle of ZIFs is similar to the Si-O-Si angle (145°) present in zeolites and the synthesis of many ZIFs with zeolite-type tetragonal properties has been achieved.[105] Having high stability towards water and generally exhibiting quite hydrophobic pores, the alcohol and water adsorption within a number of these ZIFs demonstrate great potential for alcohol / water separations.[106-111] It has been claimed; however, that ZIF-8 is not a suitable membrane material for removal of ethanol from water due to its extremely low initial ethanol uptake, unfavourable diffusion selectivity, and competitive uptake of water.[108] Despite this, it is clear why there are a huge number of recent studies including these ZIFs within MMMs for both gas separations and pervaporation.

2.4.2.3 Carbon Nanotubes

Carbon nanotubes (CNTs) are a novel form of carbon, which can be described as cylinders of graphene sheets (Figure 2-23). They have many potential applications in electronics and materials chemistry due to having high strength as well as being highly conducting.[112] Single-walled carbon nanotubes (SWCNTs) consist of a single sheet of graphene rolled into a cylinder and multi-walled carbon nanotubes (MWCNTs) consist of concentric CNTs within each other.[112] It is easy to see how CNTs can be applied toward separation applications due to their uniform channels which can be formed at various sizes and are structurally stable. Therefore, they have found a great number of applications within MMMs.[113]

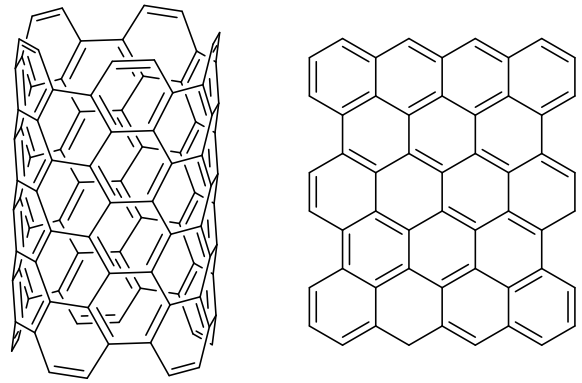

Figure 2-23. Schematic of carbon nanotubes and graphene.

2.4.3 Mixed Matrix Membranes for Hydrophilic Pervaporation

Pervaporation has been successfully applied industrially for dehydration of various organic solvents. The most successful commercial example of this being for high purity ethanol for pharmaceutical applications. This is because the pervaporation process can overcome the azeotrope formed with water at ~ 96 wt% ethanol which becomes problematic in distillation requiring additional carcinogenic entrainers (e.g. benzene) or a semi-batch (potentially more costly) pressure-swing adsorption process.[36] Other solvents including isopropanol, n-butanol, ethyl acetate, acetone, acetonitrile, pyridine, tetrahydrofuran and n-propanol can also be dehydrated in this way and have been applied commercially.[114] Therefore, there has been much research into the pervaporative dehydration of various alcohols and other organic solvents.[115] Fermentation products which form azeotropes with water include ethanol at around 4 wt% water, isopropanol at around 12 wt% water and each isomer of butanol (45 – 12 wt% water). Pervaporation therefore provides an attractive way to dehydrate these fermentation products to > 99 % purity. Again, MMMs provide an intermediate alternative to costly inorganic membranes and the poorer performing polymeric membranes. The examples of MMMs studied for hydrophilic pervaporation presented in the next sections have been collated within Table 2-5.

2.4.3.1 MMMs containing Zeolites for Hydrophilic Pervaporation

Gao *et al.* studied a series of zeolites as potential inorganic fillers dispersed in poly(vinyl alcohol) (PVA) for pervaporative dehydration of alcohols.[72] This systematic study looked at a series of zeolites with increasing pore sizes at 11 wt% in PVA and their separation performance of a

number of different sized alcohols to investigate the molecular sieving effect of the zeolites. It was found that the zeolites increased the flux of the membranes due to the increased porosity of the composite; zeolites with larger pore sizes generally increasing the flux the most. The separation factor of small alcohols such as methanol and ethanol was decreased through the addition of zeolites due to their increased permeation through the zeolite pores. However, for larger alcohols the separation factor was increased as well as the flux, mostly for the smaller pore sized zeolites e.g., KA and NaA as the pore sizes are large enough to allow permeation of water, but too small for isopropanol or t-butanol to permeate. This demonstrates the importance of understanding the porosity of the inorganic filler and how it will affect the alcohol/water separation to be achieved. Therefore, there have been many other investigations into the performance of different zeolites and aluminosilicates within MMMs for dehydration of organic-aqueous mixtures.[116-123]

2.4.3.2 MMMs containing MOFs for Hydrophilic Pervaporation

MOFs have been investigated for their use as inorganic fillers within MMMs for the dehydration of fermentation products. As described earlier, ZIFs exhibit high chemical and thermal stability as well as relatively high water stability and so it is clear why they were identified as some of the most promising candidates for mixed matrix membranes for pervaporation.

ZIF-8 (Figure 2-24) has been studied as the inorganic filler within hydrophilic pervaporation membranes for dehydration of alcohols. Examples include the dispersion of ZIF-8 in PVA,[124] polybenzimidazole (PBI),[125, 126] and polyimide (PI).[127] Although addition of ZIF-8 into the polymer matrix of the hydrophilic polymers increased the flux in each instance, it has generally been observed to be detrimental to the separation factor. For isopropanol dehydration the flux was increased to 992 g m^{-2} h^{-1} and the separation factor decreased to 91 at 7.5 wt% loading of ZIF-8 in PVA (virgin membrane flux = 135 g m^{-2} h^{-1} and separation factor = 163). At 58.7 wt% loading in PBI the flux increased to 246 g m^{-2} h^{-1} whilst the separation factor decreased to 310 (virgin membrane 13 g m^{-2} h^{-1} and > 5000). When the pervaporative dehydration of ethanol was compared for a polyimide membrane with either ZIF-8, mesoporous silica (MCM-41) of two particle sizes (3.1 μm and 0.51 μm) and mesoporous silica coated in ZIF-8, it was expected that because the ZIF-8 aperture size of 0.34 nm is smaller than that of ethanol (0.43 nm) but larger than water (0.27 nm) it would aid the permeation of water.[127] The hydrophobic nature of ZIF-8, however, means it is a poor choice for a hydrophilic membrane as it exhibits no adsorption of water before the onset of capillary condensation,[102] whilst also exhibiting high adsorption of alcohols such as ethanol and isopropanol due to the flexibility of the framework.[107] Essentially, by addition of ZIF-8, the membranes have been given a more hydrophobic character, leading to a decrease in separation factor due to increasing the permeance of the alcohols. The ZIF-8 coated

mesoporous silica also exhibited poor pervaporation performance within PI due to the ZIF-8 preventing water from entering the silica core. The best performing membrane in the paper was that for inclusion of mesoporous silica of particle size ~ 0.53 μm, which increased the flux to 440 g m^{-2} h^{-1} with only a marginal decrease in separation factor to 252 compared to the virgin polyimide membrane (240 g m^{-2} h^{-1} and 260).

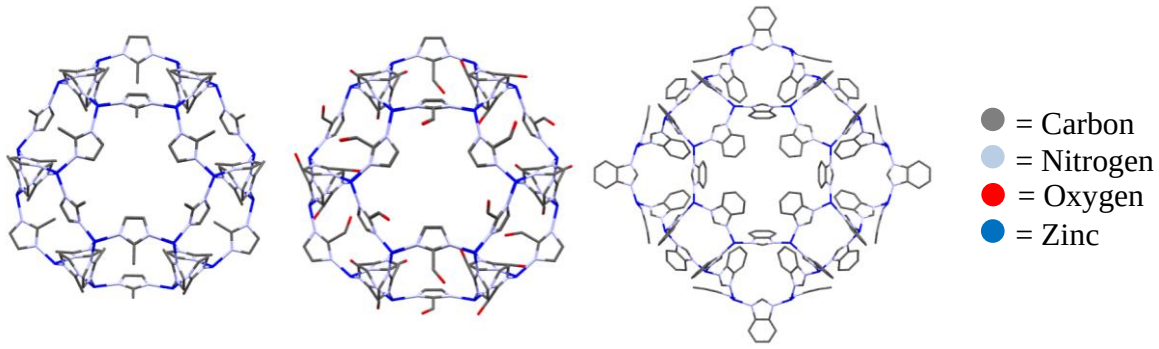

ZIF-8 ZIF-90 ZIF-7

Figure 2-24. Structures of ZIF-8, ZIF-90 and ZIF-7, generated from the crystallographic data in.[104]

ZIF-90 on the other hand exhibits a much higher adsorption of water in comparison with isopropanol,[107] potentially due to the increased pore hydrophilicity due to the addition of an aldehyde to the imidazole structure (Figure 2-24). Therefore, the addition of ZIF-90 into a P84 polyamide membrane was a more obvious choice of filler to enhance both the flux and separation factor of a polymer membrane. Having been included in a P84 polyimide membrane for pervaporative dehydration of isopropanol, the flux of the membrane was increased to 14 g m^{-2} h^{-1} when compared with the virgin membrane whilst retaining a relatively high water concentration in the permeate (98.4 wt%).[128] The separation factor was further enhanced by pre-treating the ZIF-90 nanoparticles with sulfonated poly(ether sulfone) (SPES), designed as a primer for nanoparticles, before dispersion in a polymer matrix.[129] The use of SPES to prime the ZIF-90 nanoparticles provides increased particle dispersion by preventing agglomeration of the nanoparticles, improves the affinity between the polymer matrix and inorganic filler and also increases the hydrophilicity of the membrane. The use of SPES as a primer had little effect on the total flux / permeability, but dramatically increased the separation factor of the MMM from 385 to 5668, potentially due to the reduction of defects between the ZIF and polymer matrix.

ZIF-7 enhanced the performance within a chitosan membrane for the pervaporative dehydration of ethanol.[130] The performance of the pure chitosan membrane was improved through inclusion of

ZIF-7 due to an increased chain rigidification of the polymer which arose from the amino groups of the chitosan interacting with the Zn of the ZIF-7 particles. Although ZIF-7 exhibits the same hydrophobicity and topology as ZIF-8, the framework exhibits a narrower pore aperture (0.30 nm compared to ZIF-8 = 0.34 nm) [104] and a more rigid framework,[131] which has been used to explain the much lower adsorption of isobutanol when compared to ZIF-8.[132] This means that ZIF-7 does not easily allow the permeation of water or ethanol which decreases the flux of the chitosan membrane; however, the rigidification of the polymer means that ethanol does not pass as easily through the membrane whilst smaller water molecules can still freely pass. This resulted in an increase in separation factor for the MMM; at 5 wt% loading of ZIF-7 the chitosan MMM exhibits a flux of 322 $g \cdot m^{-2} \cdot h^{-1}$ and separation factor of 2812 when compared to the chitosan membrane; flux = 602, separation factor = 148.

The ability to systematically modify the organic linker used within MOFs is one of the main attractions to their use for many applications, including separations. This has been studied in the context of a MMM for pervaporative dehydration of ethanol for the MOF MIL-53(Al)-NH_2. The surface of the MOF was modified with formic acid, valeric anhydride and heptanoic anhydride (Figure 2-25). It was found that with the increased surface hydrophobicity of the MOF, the ethanol permeance rose and separation factor decreased when incorporated into PVA MMMs.[133] This demonstrates how MOFs could be tailored through surface modification to create tunable MMMs for specific separations.

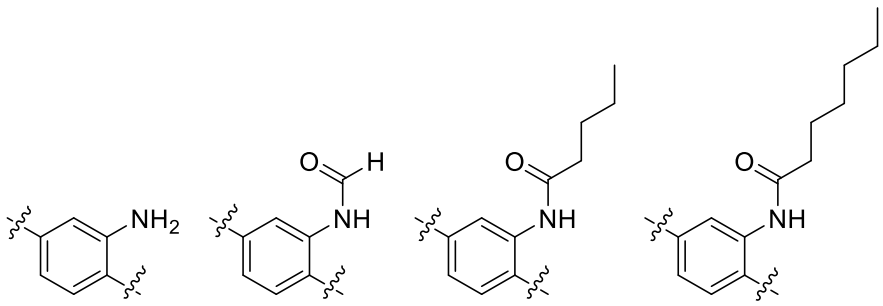

Figure 2-25. Modification of the organic linker within MIL-53(Al)-NH_2 to tune the surface environment of the MOF.[133]

2.4.3.3 Nanotubes, Carbons and Other Inorganic Fillers for Hydrophilic Pervaporation MMMs

The use of CNTs for pervaporative dehydration of alcohols has also been investigated. Shirazi *et al.* incorporated CNTs into a PVA membrane for pervaporative dehydration of isopropanol.[134] CNTs are prone to agglomeration due to strong Van der Waal forces between molecules, which

means that dispersion within a polymer matrix can be difficult. Acid treatment of the CNTs produced via chemical vapour deposition (CVD) was used to purify, and improve the dispersion of the CNTs. Addition of CNTs decreased the permeation flux of the membrane but increased selectivity from 119 for the pure membrane to 1794 for the membrane loaded with 2 wt% of CNT. At a 4 wt% loading of CNT, flux increased but a lowered separation factor was observed due to agglomeration of the CNTs creating nonselective voids within the membrane. Another strategy used to prevent agglomeration of CNTs within a PVA membrane was to wrap the carbon nanotubes in poly(alylamine hydrochloride) (PAH).[135] PVA membranes were prepared with MWCNTs produced via CVD with and without wrapping with PAH. The selectivity of the membranes for dehydration of an isopropanol / water (90 / 10 wt%) feed at 30 °C were increased through addition of the MWCNT-PAH and at 1 wt% loading increased the separation factor (141 to 945) with only a marginal decrease in total flux (229 to 207 g m^{-2} h^{-1}) when compared to the virgin PVA membrane. However, above 1 wt% loading the MWCNT-PAHs agglomerated and decreased the separation factor of the membrane.

Functionalised graphene sheets (FGS) have been utilized as an inorganic filler for hydrophilic membrane preparation. Firstly incorporated into sodium alginate chitosan membranes, the FGS improved the hydrophilicity of the membrane with increased loading and the performance of the membrane improved with an optimum selectivity at 2 wt% of FGS when applied to isopropanol dehydration.[136] Further work by Dharupaneedi *et al.* prepared FGS-chitosan membranes for ethanol and isopropanol dehydration.[137]

Shivanand *et al.* prepared MMMs from a heteropolyacid (HPA) and PVA.[138] Increased loading of the acid dramatically decreased the flux of the membrane, whilst dramatically increasing the separation factor of the membrane.

The addition of sodium montmorillonite (Na^+MMT) clay into PVA membranes for dehydration of organic solvents has also been studied. By incorporating the hydrophilic Na^+MMT particles into the membrane the hydrophilicity was increased, increasing the separation factor as well as demonstrating increased mechanical properties of the MMMs. This increased the membrane separation factor from 77 to 2241 for 10 wt% loading of the clay with a flux of 77 g m^{-2} h^{-1}.[139]

Another filler used within MMMs for ethanol dehydration is polyhedral oligomeric silsesquioxanes (POSSs) (Figure 2-26). POSSs are cages of silicon and oxygen with each silicon atom bonded to three oxygens as well as an alkyl, halide, aryl or alkoxy group. POSSs have been embedded within the polymer matrix of copoly (1,5-naphthalene/3,5-benzoic acid-2,2′-bis(3,4-dicarboxyphenyl) hexafluoropropanedimide (6FDA-NDA/DABA) hollow fibres. The separation factor for these hollow fibres for ethanol/water mixtures was 166 and total flux of 1900 g m^{-2} h^{-1}.[140] POSS was also incorporated into a novel polymer blend of the polyimide and

sulfonated polyimide material to further improve the performance characteristics of these hollow fibre membranes.[141]

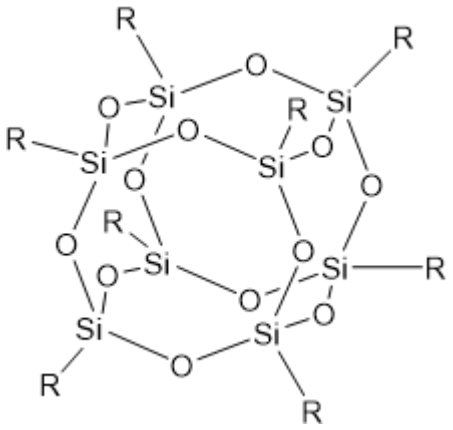

Figure 2-26. Chemical structure of a typical polyhedral oligomeric silsequioxane.

Table 2-5. Collation of Examples of MMMs for Hydrophilic Pervaporation.

Dehydration of: Alcohol/Water (wt% / wt%)	Inorganic Filler	Polymer	Neat Membrane Performance		MMM Performance		Temperature (°C)	Ref:
			Total Flux (g m^{-2} h^{-1})	Separation Factor (α)	Total Flux (g m^{-2} h^{-1})	Separation Factor (α)		
Ethanol/Water (90/10)	H-ZSM-5 (8 wt%)	Chitosan	54.18	158	231	153	80	[122]
Ethanol/Water (90/10)	MPTMS-modified H-ZSM-5 (8 wt%)	Chitosan	120	175	278	274	80	[123]
Ethanol/Water (90/10)	Functionalized-MWCNT (2 wt%)	Chitosan	112	580	337	570	30	[142]
Ethanol/Water (80/20)	Zeolite KA (11 wt%)	PVA	140	40	164	40	50	[72]
Ethanol/Water (80/20)	Zeolite NaA (11 wt%)	PVA	140	40	172	36.6	50	[72]
Ethanol/Water (80/20)	Zeolite CaA (11 wt%)	PVA	140	40	194	22.3	50	[72]
Ethanol/Water (80/20)	Zeolite NaX (11 wt%)	PVA	140	40	214	19.4	50	[72]
Ethanol/Water (85/15)	ZIF-8 (33.7 wt%)	PBI	151	4	106	25.4	60	[125]
Ethanol/Water (85/15)	ZIF-8 (58.7 wt%)	PBI	151	4	992	10	60	[125]
Ethanol/Water (90/10)	ZIF-7 (5 wt%)	Chitosan	602	148	322	2812	25	[130]
Ethanol/Water (90/10)	ZIF-8 (12 wt%)	Matrimid 5218 (polyimide)	240	260	260	300	42	[127]

Ethanol/Water (90/10)	MCM-41 3.1 μm (12 wt%)	Matrimid 5218 (polyimide)	240	260	310	190	42	[127]
Ethanol/Water (90/10)	MCM-41 0.53 μm (12 wt%)	Matrimid 5218 (polyimide)	240	260	440	252	42	[127]
Ethanol/Water (90/10)	MCM-41-ZIF-8 coated (12 wt%)	Matrimid 5218 (polyimide)	240	260	200	137	42	[127]
Ethanol/Water (85/15)	POSS (AMO273) (2 wt%)	6FDA-NDA/DABA	-	-	1900	166	60	[140]
Ethanol/Water (85/15)	POSS (SO1440)	6FDA-NDA/DABA (3 wt% sulfonated polyimide)	-	-	2000	237	60	[141]
IPA/Water (90/10)	Na^+MMT (5 wt%)	PVA	95	77	51	1116	30	[139]
IPA/Water (90/10)	Na^+MMT (10 wt%)	PVA	95	77	75	2241	30	[139]
IPA/Water (90/10)	Silicalite-1 (20 wt%)	PVA	95	77	69	2241	30	[143]
IPA/Water (87.7/13.3)	Aluminosilicate (6 wt%)	PVA-glutaraldehyde crosslinked			109.8	73	40	[120]
IPA/Water (90/10)	ZSM-5 (6 wt%)	PVA	-	-	320	216	30	[144]
IPA/Water (80/20)	Zeolite KA (11 wt%)	PVA	146	223	179	410	50	[72]
IPA/Water (80/20)	Zeolite NaA (11 wt%)	PVA	146	223	183	328	50	[72]
IPA/Water (80/20)	Zeolite CaA (11 wt%)	PVA	146	223	190	233	50	[72]

IPA/Water (80/20)	Zeolite NaX (11 wt%)	PVA	146	223	216	233	50	[72]
IPA/Water (90/10)	Zeolite 5A (20 wt%)	P84	30	3000	40	4200	60	[117]
IPA/Water (90/10)	Zeolite 13X (40 wt%)	P84	30	3000	110	2700	60	[117]
IPA/Water (90/10)	Zeolite 4A (10 wt%)	Matrimid 5218	14	12716	18	8991	30	[119]
IPA/Water (90/10)	ZSM-5 (10 wt%)	Matrimid 5218	14	12716	16	3904	30	[119]
IPA/Water (95/5)	NaY (30 wt%)	Chitosan	32	422	115	2620	30	[145]
IPA/Water (87.4/12.6)	Zeolite-K-LTL (10 wt%)	Sodium Alginate	-	-	140	3847	30	[116]
IPA/Water (90/10)	ZIF-8 (5 wt%)	PVA	135	163	868	132	30	[124]
IPA/Water (90/10)	ZIF-8 (7.5 wt%)	PVA	135	163	952	91	30	[124]
IPA/Water (85/15)	ZIF-8 (33.7 wt%)	PBI	13	>5000	103	1686	60	[125]
IPA/Water (85/15)	ZIF-8 (58.7 wt%)	PBI	13	>5000	246	310	60	[125]
IPA/Water (85/15)	ZIF-90 (30 wt%)	P84	-	-	114	385	60	[128]
IPA/Water (85/15)	ZIF-90-SPES (30 wt%)	P84	-	-	109	5668	60	
IPA/Water (90/10)	CNTs (1 wt%)	PVA	-	-	96	817	30	[134]
IPA/Water (90/10)	CNTs (2 wt%)	PVA	-	-	79	1794	30	[134]

IPA/Water (90/10)	MWNT-PAH (1 wt%)	PVA	229	141	207	945	30	[135]
IPA/Water (90/10)	HPA 40–50 μm (7 wt%)	PVA	132	77	32	89991	30	[138]
n-Butanol/Water (85/15)	ZIF-8 (33.7 wt%)	PBI	11.6	>5000	81	3417	60	[125]
n-Butanol/Water (85/15)	ZIF-8 (58.7 wt%)	PBI	11.6	>5000	226	698	60	[125]

2.4.4 Mixed Matrix Membranes for Organophilic Pervaporation

As discussed in Section 2.3, organophilic pervaporation can recover / remove dilute volatile organics from aqueous solutions. When compared to hydrophilic pervaporation, organophilic pervaporation has found little commercial success despite being intensively researched. The process could in theory provide huge potential energy savings in the recovery of fermentation products. The process has generated a lot of interest in the recovery of 1-butanol from the ABE fermentation to increase the production efficiency,[146] with a number of polymeric membranes being studied.[147] For organophilic pervaporation to become viable the key issues which must be addressed include: improvement of the alcohol–water separation factor, increasing the membrane flux, and a greater understanding with regards to fouling and module stability.[12] It is hoped that the use of novel inorganic fillers within polymeric pervaporation membranes may be able to alleviate or resolve some of these key issues for pervaporation as a biofuel recovery method. This is the motivation for the work presented within Chapters 4; where the effect of different fermentation products have been tested on a MMM of ZIF-8 and PDMS, and Chapter 5; where the effect of the morphology of two Cu-MOFs on their performance within organophilic MMMs for recovery of acetone from water is tested. Consequently, the development of stable and high performing MMMs is key to the future of organophilic pervaporation. The discussed examples of MMMs used for hydrophobic pervaporation are summarised within Table 2-6.

2.4.4.1 Zeolite filled MMMs for Organophilic Pervaporation

As discussed in Section 2.4.2.1, zeolites have been reported to possess the required functionalities for the separation of water / alcohol mixtures. Therefore, there are many examples of zeolite MMMs for pervaporation. Silicalite-1 is a hydrophobic sorbent that exhibits preferential adsorption of alcohols from aqueous solutions, as well as desorption of these alcohols at relatively mild conditions. Therefore, it is obvious why Hennepe *et al.* utilised silicalite-1 as an inorganic filler for a polydimethylsiloxane (PDMS) organophilic pervaporation membrane.[148] The inclusion of silicalite-1 into the PDMS matrix increased the separation factor and flux for pervaporation of methanol, ethanol, 2-propanol and 1-propanol. Hennepe *et al.* also presented how part of the transport through the membrane was through the pores of the silicalite-1 particles. Jia *et al.* prepared a thin film composite membrane of silicalite-1 and PDMS.[149] The membrane exhibited higher fluxes than that of Hennepe as well as a greater separation factor for the pervaporation of ethanol from water. Silicalite-1-PDMS membranes have also been applied to the pervaporation of 1-butanol.[150] To aid application within fermentative separations of 1-butanol, silicalite-1-PDMS

membranes have been studied at low concentrations of 1-butanol relevant for in-situ removal of butanol from a fermentation broth[151] and studied in relation to the ABE fermentation process.[152, 153]

Various efforts have been made to improve the performance of these membranes by increasing the dispersion and homogeneity of silicalite-1 within PDMS. One approach was to use nanosized silicalite-1[154] and recently the effect of different sizes of nano silicalite-1 has been investigated.[155] Both studies also investigated the effect of surface modification through silylation of the nano-scale silicalite-1 and this has become a popular method of increasing the compatibility between silicalite-1 and PDMS. Other reports of silylation of silicalite-1 for MMMs of PDMS include modification with vinyltriethoxysilane (VTES)[156] and vinyltrimethoxysilane (VTMS)[157] (Figure 2-27). For the VTMS modified silicalite-1, the separation factor was improved from 120 to 145 when compared to the unmodified silicalite-1-PDMS membrane. Chlorosilanes have also been used to increase the surface hydrophobicity of silicalite-1 for pervaporation within a PDMS MMM.[158]

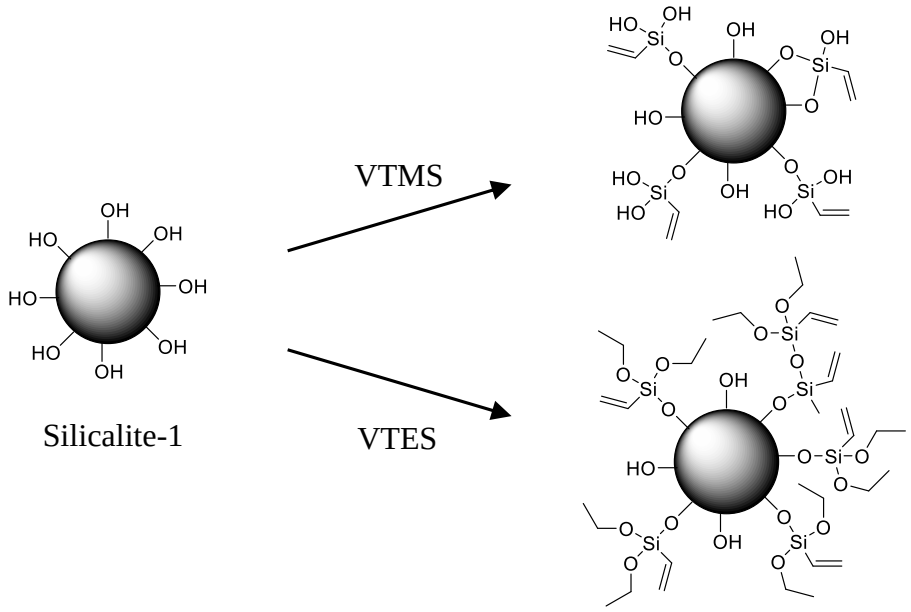

Figure 2-27. Schematic of the modification of silicalite-1 with VTES and VTMS indicating the incorporation of vinyl groups to the silicalite surface.

Investigations have also looked at the inclusion of silicalite-1 within different polymers that have shown high pervaporation performance such as polyether-block amide (PEBA)[159] and polymers of intrinsic microporosity (PIMs). PIMs are novel polymers that utilize inefficient packing of the polymer chains through restricting the rotational freedom of the polymer backbone to induce microporosity.[160] PIMs have been shown to produce organophilic membranes[79, 161, 162] and the

inherent microporosity means that they are an ideal pervaporation membrane material. A Silicalite-1-PIM-1 MMM has been fabricated for the pervaporation of ethanol from dilute aqueous solution.[163] The incorporation of silicalite-1 at high loadings increased the separation factor compared to that of the purely PIM-1 membrane to 5.68 compared to 3.61.

Another zeolite, ZSM-5, has been reported by Vane to enhance the ethanol permeability of a PDMS membrane with increased zeolite loading.[164] After this Vane also reported on the long term operation of these membranes with an S. cerevisiae broth.[165] Exposure to the broth caused a large decline in permeability of the membrane due to the many components of the broth. ZSM-5 has also been incorporated into PEBA for pervaporation of 1-butanol.[166]

2.4.4.2 MOF filled MMMs for Organophilic Pervaporation

MOFs have gained a huge amount of interest for inclusion within organophilic pervaporation membranes in recent years. The first example of a MOF MMM for organophilic pervaporation looked at two analogous single crystal adsorbents.[167] The vapour adsorbency of methanol, ethanol, 1-propanol, 1-butanol and 1-pentanol were studied for the single crystal adsorbents $[M^{II}_2(bza)_4(pyz)]_n$ (M = Rh or Cu, bza = benzoate, pyz = pyrazine). The copper adsorbent was fabricated into a PDMS membrane and the alcohol water separation for methanol and ethanol studied. The inclusion of the copper complex increased both flux and separation factor in both instances; however, the membrane performance is well below that for other MMMs.

- *ZIF-8 containing Mixed Matrix Membranes*

ZIF-8 has been demonstrated to separate alcohols from water due to its hydrophobic pores exhibiting high uptakes of alcohol and low uptakes of water.[107, 109-111] Therefore, it is clear to see why it was originally incorporated into a polymethylphenylsiloxane (PMPS) membrane.[132] MMMs of ZIF-8 and PMPS were produced within alumina capillaries by a solution-blending dip-coating method. The membrane was mainly tested for the pervaporation performance for removal of isobutanol from an aqueous solution due to the high adsorption of isobutanol observed for ZIF-8. The high permeance of isobutanol was attributed to the ZIF-8 particles dispersed in the membrane creating preferential pathways for the permeation of isobutanol, even though the pore aperture of ZIF-8 (as calculated from crystal structure data) is smaller than the size of isobutanol. It was suggested that the high adsorption of isobutanol and increased permeance of the membranes was therefore due to the gate-opening[168] effect of ZIF-8, where the imidazole linkers rotate to create a larger pore aperture. To confirm this, a ZIF-7 / PMPS membrane was also fabricated, as ZIF-7 has

the same sodalite topology as ZIF-8 and hydrophobic pores, but shows little adsorption of isobutanol due to the rigid framework structure and smaller pore aperture (Figure 2-24). This membrane exhibited much poorer separation and permeance properties for isobutanol, which further demonstrated how ZIF-8 was responsible for the increased permeance and separation factor. The as-synthesized ZIF-8/PMPS membrane was also used to concentrate dilute solutions of ethanol, 1-propanol, 1-butanol, isobutanol and 1-pentanol. For isobutanol, it was calculated that the synthesized membrane uses half the amount of energy required per unit of isobutanol when compared to a distillation process.

ZIF-8 and ZIF-7 have also been incorporated within PDMS membranes for pervaporative recovery of 1-butanol and acetone respectively. The ZIF-7-PDMS membrane demonstrates the highest known separation of acetone from water (1237 g m^{-2} h^{-1} and separation factor 39.1, 60 °C, 1 wt% acetone).[169] ZIF-7-PDMS membranes have also recently been studied for the pervaporation of 1-butanol from water. For removal of 1 wt% 1-butanol from water a total flux of 1689 g m^{-2} h^{-1} and separation factor of 66 were observed for the 20 wt% loaded membrane.[170] For ZIF-8, membranes were fabricated with loadings of between 1 and 5 wt%. Incorporation of ZIF-8 into the PDMS matrix increased the 1-butanol selectivity and permeability up to a loading of 2 wt%; however, at higher loadings the selectivity towards 1-butanol was reduced. This was explained by the increased chain rigidity of the PDMS, the aggregation of ZIF-8 particles at higher loadings causing defects in the membrane, and poor compatibility between ZIF-8 and the polymer.[171] This demonstrates the importance of creating a homogenously dispersed filler within the polymer matrix and the difficulty in obtaining this at high particle loading.

Fan *et al.* have since undertaken investigations into alternative methods to fabricate ZIF-8 / PDMS membranes to prevent aggregation at higher loadings of the inorganic filler. The use of a simultaneous spray self-assembly method for fabrication of a ZIF-8-PDMS MMM was conducted.[172] A solution of ZIF-8 and PDMS and a second solution of the crosslinking agent tetraethyl orthosilicate (TEOS) and catalyst dibutylin dilaurate (DBTDL) were sprayed onto a polysulfone substrate. When compared to membranes cast from a doctor blade, the sprayed membranes exhibited superior dispersion of ZIF-8 nanoparticles throughout the polymer matrices at loadings of up to 40 wt%. For a 1 wt% 1-butanol solution, a ZIF-8-PDMS membrane at 40 wt% loading of ZIF-8 demonstrated a flux of 4846.2 g m^{-2} h^{-1} and separation factor of 81.6 at 80 °C exceeding the performance of membranes produced by Bai[171] or Liu.[132] The ZIF-8-PDMS membrane was then compared to a dia(Zn)-PDMS membrane fabricated using the same procedure. The framework dia(Zn) is composed of the same building blocks as ZIF-8 (Zn and 2-methylimidazole) but it exhibits no porosity. The dia(Zn)-PDMS membranes exhibited increased flux but decreased separation factor indicating that the gaps between the polymer matrix and inorganic filler were water permselective. This also indicated that ZIF-8 nanoparticles contribute

greatly to the increased permeation and separation factor exhibited by the membranes due to the selective adsorption of 1-butanol over water.

Another method employed by Fan *et al.* involved the dispersion of as-synthesised ZIF-8 nanoparticles without drying into PDMS. A polysulfone substrate was dipped multiple times into a ZIF-8 / PDMS solution before dipping in a pre-crosslinked PDMS solution to overcome any defects in the membrane caused by particle agglomeration.[173] The nanodispersed ZIF-8 membrane exhibited a high separation factor of 53 and flux of 2801 g m^{-2} h^{-1} for separation of 5 wt% 1-butanol water at 80 °C. These examples demonstrate the importance of the fabrication method of the membrane and how it can affect the membrane performance. An optimal MMM would ideally contain a high loading of homogenously dispersed porous inorganic filler.

Further studies into improving the performance of ZIF-8-PDMS membranes have looked at increasing the hydrophobicity of the membrane. The surface hydrophobicity of an organophilic pervaporation membrane is closely related to the permeance of water and therefore the performance of the membrane. One approach to improving the surface hydrophobicity of a ZIF-8-PDMS MMM was undertaken by Li *et al.* through surface modification with self-assembled monolayers (SAMs) of semifluorinated organosilanes (Figure 2-28).[174] The water contact angle of the ZIF-8-PDMS membrane was increased from 145.3° to 152.3° after modification with SAMs, producing a superhydrophobic surface. The SAM modified ZIF-8-PDMS membrane also exhibited an increase in separation factor compared to the unmodified ZIF-8-PDMS membrane (84.8 compared to 58.4 respectively).

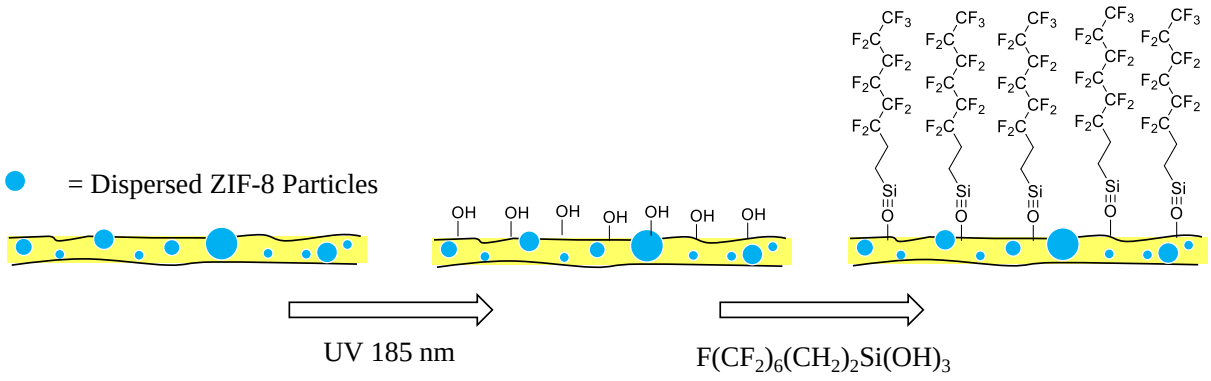

Figure 2-28. Surface modification of a ZIF-8-PDMS membrane with semi-fluorinated organosilanes as conducted in ref. [174]

The improvement of the hydrophobicity of this class of membrane has also been attempted utilising ZIF-8 incorporated into MCM-41 particles. These MCM-41@ZIF-8 particles were then modified with a silane agent and embedded in a PDMS matrix.[175] The membranes exhibited a

much greater flux of 1846 g m^{-2} h^{-1} and separation factor 9.5 than the virgin membrane (total flux = 886 g m^{-2} h^{-1}, separation factor = 6.8) for separation of 5 wt% ethanol at 60 °C.

These examples show that there have been many investigations into ZIF-8 being used as an inorganic phase for preparation of organophilic MMMs for pervaporative separation of alcohols from water. The examples show that inclusion of ZIF-8 shows great promise for improving the water / alcohol separation performance of polymeric membranes, and is one of the most promising inorganic phases utilized within the literature. However, of the examples discussed above, each report has only focused on the separation performance of model aqueous solutions. As discussed in previous sections fermentation broths contain a vast number of different components of the growth media, as well as often a number of different fermentation products. This is what prompted the work conducted within Chapter 4 of this thesis where the effect of 2,3-butanediol and acetate on the pervaporation of ethanol using a ZIF-8-PDMS membrane was undertaken.

- *Mixed Matrix Membranes containing other MOFs*

Another ZIF that has found use as an inorganic filler within MMMs is ZIF-71. The MOF exhibits good separation performance for aqueous mixtures of 1-propanol, 2-propanol and exhibits a greater 1-butanol separation over ZIF-8.[107] Therefore, investigations have included the use of ZIF-71 in an organophilic pervaporation membrane.[176, 177] The first example was of a ZIF-71 filled PEBA MMM.[176] The inclusion of ZIF-71 into the polymer matrix increased both flux and separation factor of the membrane up to a 20 wt% loading of ZIF-71, after this separation factor was improved but flux declined. The membrane with 20 wt% loading of ZIF-71 was tested with model ABE broth solutions as well as real ABE fermentation broth. The membrane exhibited stable performance over a period of 100 hours in the pervaporation of an ABE broth with the average flux 447.9 g m^{-2} h^{-1} and average separation factors of acetone = 8.8, 1-butanol = 18.4 and ethanol = 3.6. However, the obtained values of flux and separation factor are relatively low and have been attributed to the performance of the chosen polymer PEBA. Therefore, ZIF-71 has also been incorporated into PDMS[177] due to PDMS exhibiting superior pervaporation performance for 1-butanol compared to PEBA.[177] More recently studies have combined modelling, through Monte Carlo simulations, and FTIR spectroscopy to give insights into the separation of ethanol from water by ZIF-71 and applied to its performance as an inorganic filler within a PDMS MMM.[178]

The MOF $[Zn(bdc)(ted)]_{0.5}$ (bdc = terephthalic acid; TED = triethylenediamine) has also been incorporated into PEBA for organophilic pervaporation of 1-butanol.[179] The framework exhibits adsorption of many organics and alcohols[180] and has been demonstrated to have good alcohol / water separation ability.[100, 181] The membranes with 20 wt% loading of the MOF

exhibited the greatest separation performance and were tested with a model ABE broth. The membrane had a flux of 630 g m^{-2} h^{-1} and separation factor of 17.4 for 1-butanol at 12 g L^{-1} within a model ABE solution at 40 °C.

The flexible MOF MIL-53 exhibits expansion of the structure upon adsorption of methanol and ethanol[182] and has hydrophobic channels that can provide transport for ethanol molecules and reject water. Therefore, it has also been incorporated into PDMS for ethanol pervaporation.[183] Loading of MIL-53 into PDMS increased the membrane affinity towards ethanol and the flux of the membrane to 5467 g m^{-2} h^{-1} compared to the virgin PDMS membrane of 1667 g m^{-2} h^{-1}. MMMs of PDMS with non-activated MIL-53 or the starting materials for synthesis of MIL-53 (terephthalic acid and $AlCl_3 \cdot 6H_2O$) were also studied. The non-activated MIL-53-PDMS membrane had a higher separation factor but much poorer flux characteristics indicating potential blockage of the pores of the MOF and the MMMs containing the starting materials exhibited performance characteristics similar to PDMS indicating that the pores of MIL-53 created preferential pathways for permeation of ethanol.

These examples show that there have been a number of different MOFs incorporated into MMMs to improve the performance of a hydrophobic polymer towards organophilic pervaporation. Due to the vast number of MOFs possible (section 2.4.2.2) it is clear that there is a huge array of materials that have potential for use within an organophilic pervaporation membrane. This is the motivation for the work conducted within Chapter 5 where two structurally similar Cu-MOFs have been dispersed within PDMS to create two new types of organophilic pervaporation membrane.

2.4.4.3 Other inorganic fillers for MMMs for Organophilic Pervaporation

CNTs have been incorporated into organophilic pervaporation membranes for the recovery of butanol from an ABE fermentation broth.[184] CNTs were dispersed in a PEBA membrane and tested for their use for removal of 1-butanol from a 5 L fermentor. Addition of CNTs increased the removal performance of the PEBA membranes for 1-butanol. When tested with a fed-batch fermentation the mixed matrix membrane controlled the concentration of butanol at between 8 and 12 g L^{-1} and improved the productivity and yield of the fermentation by 20 %.

Another example of nanotubes for organophilic pervaporation membranes is the use of polyphosphazene nanotubes (PZNTs) incorporated into PDMS for ethanol pervaporation.[185] The novel type of nanotube, PZSNTs, increased the swelling of the PDMS membranes for ethanol and successfully increased the separation factor from 5.0 to 10 for a 10 wt% ethanol solution.

The use of POSSs were also studied for creation of organophilic membranes in contrast to the work previously described in Section 2.4.3.3. for creation of hydrophilic membranes. Pebax / POSS (polyether-block-amide / polyhedral oligosilsesquioxane) MMMs were fabricated for ethanol pervaporation.[186] Two types of POSS were used to produce these membranes (Figure 2-29) and the optimum loading being determined at 2 wt% of POSS. At this loading, the MMM prepared with the POSS AL0136 exhibited the greater performance attributed to the POSS exhibiting a higher affinity towards ethanol.

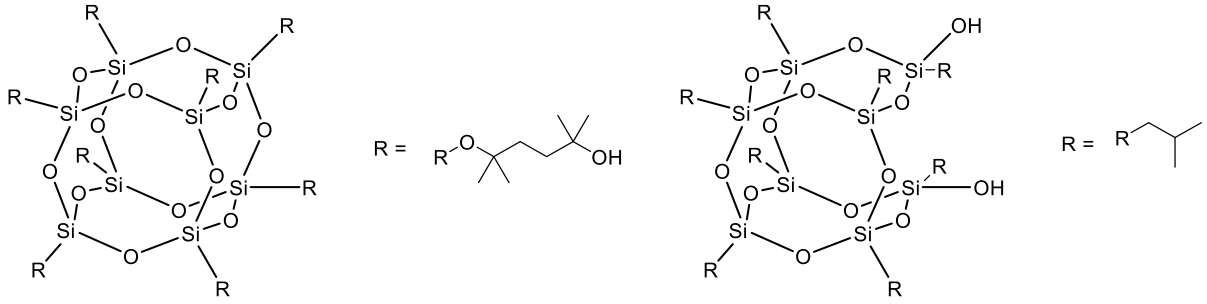

Figure 2-29. Structures of the POSSs incorporated into PEBAX.

Another important example of the incorporation of POSS into organophilic MMMs looked at tuning the free volume of a PDMS membrane to increase the permeability of 1-butanol whilst decreasing the permeability of water.[187] Initially molecular dynamics simulations were undertaken to understand the effect of addition of POSS to the packing of the polymer PDMS and these were related to experimental differential scanning calorimetry (DSC) measurements. The addition of POSS to PDMS was studied for the regulation of packing of the PDMS polymer and the effect this had on free volume of the membrane. The addition of POSS to PDMS was shown to decrease the small free volume of the PDMS membrane, which hinders the transport of smaller molecules, and an increase in the large free volume, which would aid transport of larger molecules. These findings were applied to the pervaporation of a 1 wt% aqueous butanol solution. The membranes with higher loadings of POSS exhibited greater performances in terms of selectivity and butanol permeability due to the increase in the large free volume of the polymer membrane aiding 1-butanol permeation and the decrease in small free volume hindering permeation of water.

Table 2-6. Collation of Examples of MMMs for Organophilic Pervaporation.

Organophilic Pervaporation of:	Inorganic Filler	Polymer	Neat Membrane Performance		MMM Performance		Temperature	Ref:
			Total Flux ($g \cdot m^{-2} \cdot h^{-1}$)	Separation Factor (α)	Total Flux ($g \cdot m^{-2} \cdot h^{-1}$)	Separation Factor (α)		
5 wt% Methanol	$[Cu^{II}_2(bza)_4(pyz)]_n$ (3 wt%)	PDMS	24	2	33	6.5	RT	[167]
5 wt% Ethanol	ZSM-5 (40 wt%)	PDMS	-	-	408	14	40	[188]
5 wt% Ethanol	ZSM-5 HF etched	PDMS	-	-	211	9.2	50	[189]
5 wt% Ethanol	Silicalite-1 (60 wt%)	PDMS	24	7.6	50.7	16.5	22.5	[148]
5.1 wt% Ethanol	Silicalite-1 (77 wt%) TFC	PDMS	530	4.4 (7.0 wt% EtOH Feed)	150	34	22	[149]
1.6 wt% Ethanol	Silicalite-1-VTMS	PDMS	-	-	-	18	50	[157]
5 wt% Ethanol	Silicalite-1 (2 wt%)	PEBA	-	-	833	3.6	40	[159]
1 wt% Ethanol	-	PIM-1	470	10.7	-	-	30	[79]
5 wt% Ethanol	Silicalite-1 (19.3 wt%)	PIM-1	6520	3.61	5460	5.68	60	[163]
5 wt% Ethanol	Silicalite-1 (2 wt%)	PEBA	-	-	833	3.6	40	[159]
5 wt% Ethanol	MIL-53 (40 wt%)	PDMS	1667	7.6	5467	11.1	70	[183]
5 wt% Ethanol	MCM-41@ZIF-8	PDMS	886	6.8	1846	9.5	60	[175]
5 wt% Ethanol	$[Cu^{II}_2(bza)_4(pyz)]_n$ (3 wt%)	PDMS	23	2.3	47	6.2	RT	[167]

10 wt% Ethanol	PZSNTs (10 wt%)	PDMS	-	-	11.9×10^{-3} g·mm^{-2}·h^{-1}	10	40	[185]
5 wt% Ethanol	POSS (AL0136) (2 wt%)	PEBAX 2533	-	-	183.5	4.6	RT	[186]
5 wt% Ethanol	POSS (SO1440) (2 wt%)	PEBAX 2533	-	-	125.8	4.1	RT	[186]
1 wt% 1-butanol	Silicalite-1	PDMS	-	-	607	93	70	[152]
4.3 wt% 1-butanol	ZSM-5 (5 wt%)	PEBA	-	-	719.3	33.3	35	[166]
2.5 wt% 1-butanol	MCM-41 (2 wt%)	PEBA	-	-	> 500	25	35	[190]
1.0 wt% isobutanol	ZIF-8 (10 wt%)	PMPS	-	-	6400	40.1	80	[132]
1 wt% 1-butanol	ZIF-8	PMPS	-	-	5100	36.8	80	[132]
0.96 wt% 1-butanol	ZIF-8	PDMS	2.59 (Permeability of n-butanol × 10^5 barrer)	3.21	1.71 (Permeability of n-butanol × 10^5 barrer)	5.95	40	[171]
5 wt% 1-butanol	ZIF-8 (nanodisperse)	PDMS	-	-	2800.5	52.8	80	[173]
1 wt% 1-butanol	ZIF-8 (40 wt%) Simultaneous spray self-assembly	PDMS	-	-	4846.2	81.6	80	[172]
3 wt% 1-butanol	ZIF-8	PDMS	1065	13.4	1459	58.4	60	[174]
3 wt% 1-butanol	ZIF-8	PDMS^{CF3}	1049	19.4	1339	84.8	60	[174]
3 wt% 1-butanol	MCM-41@ZIF-8	PDMS	-	-	2052	45	60	[175]
Model ABE Broth / 1-Butanol (12 g/L)	ZIF-71	PEBA	-	-	520	18.8	37	[176]

Model ABE Broth 1-Butanol (12 g/L)	$Zn(BDC)(TED)_{0.5}$	PEBA	-	-	630	17.4	40	[179]
1 wt% 1-butanol	CNT (5 wt%)	PEBA	85	17.4	153	19.4	37	[184]
1 wt% 1-butanol	CNT (10 wt%)	PEBA	85	17.4	139	18	37	[184]
1 wt% 1-butanol	POSS	PDMS	-	-	745	40	40	[187]
Acetone	ZIF-7	PDMS	-	-	1236.8	39.1	60	[169]

2.5 Fabrication techniques of MMMs for Pervaporation

As described above, there is a huge library of polymers and inorganic materials that have been utilized within MMMs applicable to the separation of fermentation broths. It is clear that both the inorganic material and chosen polymer can have a large effect on both the permeability and separation ability of the membrane. However, as is evident in several of the examples, the fabrication method of the MMMs can also ultimately have a large influence on the ultimate performance of the membrane.

The majority of MMMs for pervaporation presented above are produced through the creation of a polymer dope solution and solution casting by either pouring on a glass plate or with a doctor blade.[169, 171, 176, 177, 179] Other fabrication methods include dip coating[132, 173] and simultaneous spray self-assembly.[172] The main challenges in fabrication of MMMs for pervaporation are:

- Agglomeration of inorganic particles reducing available surface area and potentially creating non-selective voids.
- Incompatibility between the inorganic phase and polymer matrix creating non-selective voids.
- Leaching of the inorganic phase out of the polymer matrix.

An important procedure in each of these examples is the dispersion of the inorganic particles within the polymer dope solution. Each example uses a combination of stirring and sonication in an attempt to increase the dispersion of the inorganic phase. For their ZIF-8-PMPS membranes, Liu *et al.*[132] noted several ways to improve the dispersion of ZIF-8 within the membrane: the use of newly synthesized ZIF-8 nanoparticles, dispersion of the nanoparticles in isooctane before mixing with the polymer, and utilizing a probe type sonicator rather than an ultrasonic bath.

As described previously (Section 2.4.4.2) Fan *et al.*[172] developed a novel method for improving the dispersion of ZIF-8 within a PDMS membrane called simultaneous-spray self-assembly. The membranes produced have exhibited some of the highest performances for organophilic pervaporation of 1-butanol and this has been attributed to the increased dispersity of the inorganic filler and homogeneity of the membrane. This demonstrates that development of novel fabrication techniques can produce MMMs with superior performance characteristics and will become an important direction for research into MMMs for pervaporation in future.

To overcome the incompatibility between the polymer and inorganic phases of the MMMs, many examples also primed the inorganic particles through surface modification. One of the most common examples presented include silylation of the surface of the inorganic particles.[154, 156-158, 175]

The incorporation of silyl groups onto the surface of the inorganic phases is thought to improve the compatibility with PDMS. Obviously though, the choice of surface modification of the inorganic particle must be compatible with the chosen polymer. Therefore, for the hydrophilic MMM of ZIF-90 and P84 polyimide[128] the ZIF-90 nanoparticles were primed with a sulfonated poly(ether sulfone) surface modification. The effect of the SPES modification is thought to increase particle dispersion through preventing agglomeration, improve affinity between polymer and nanoparticle, and, increase the hydrophilicity of the membrane. Generally an improvement in the membrane performance is observed for these types of modifications, proving that this could be an important step in fabricating MMMs with even greater separation and permeability characteristics.

The particle size of the inorganic phase in a MMM is also important. Smaller nanosized particles - if able to be dispersed well in the casting solutions - would create a more homogenous matrix and create less void space. One example is the use of nanosized silicalite-1 in PDMS.[154] The study found that membranes incorporated with nano-sized silicalite-1 always had a higher total flux and separation factor than those membranes fabricated from micron sized silicalite-1 for pervaporation of a 6 wt% ethanol solution. As the library of available nanosized materials increases and the synthetic procedures for producing these materials simplify[191] many more examples of including these nanosized materials in MMMs for pervaporation should be sought.

Leaching of the inorganic phase out of the polymer membrane would also be problematic for pervaporation membranes. Searching the literature, however, has found little evidence of research into leaching of nanoparticles out of fabricated MMMs for pervaporation. This is incredibly important and should be an area of future research in this field.

The membranes fabricated within Chapters 4 and 5 of this thesis utilised a solution casting process with a doctor blade. This was due to the relatively novel materials being used, the repeatability of this process and the large number of examples that have also utilised solution casting. Although as discussed here the fabrication method can affect the MMM performance; therefore, this will be an important consideration for future studies. Application of techniques such as dip-coating, priming of the inorganic phase, and altering particle size, will all be relevant to the studies described within Chapters 4 and 5.

2.6 Other Examples of MMMs for pervaporation separation of fermentation mixtures

Some fermentation products; however, do not lend themselves towards direct hydrophilic or organophilic pervaporation. For example 2,3-butanediol exhibits relatively high hydrophilicity due

to the two hydroxyl groups present as well as a high boiling point and low vapour pressure, meaning it is difficult to find a material that can preferentially permeate 2,3-butanediol over water. Therefore, a recovery method utilizing solvent extraction then pervaporation was designed (Figure 2-30).[64] 2,3-butanediol was initially recovered from a fermentation broth using 1-butanol as extracting solvent and then 2,3-butanediol was concentrated in the retentate by removing water and 1-butanol with a PDMS pervaporation membrane to purities in excess of 98 wt%. The process was further improved through the use of a ZSM-5 filled PDMS membrane for removal of water and 1-butanol from the extracted phase.[66]

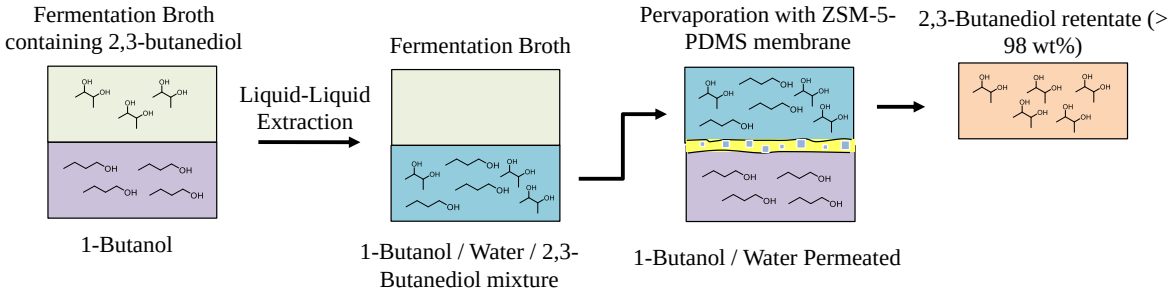

Figure 2-30. Schematic of the recovery process for 2,3-butanediol studied in.[66]

2.7 Conclusions and Implications of the Literature Review

The general concepts of membrane processes have been introduced and a number of examples relevant for the recovery of 2,3-butanediol, acetate, ethanol and a number of other potential fermentation products presented. The membrane separation processes of MF, UF, NF, RO and pervaporation have been identified as the most applicable to the recovery of fermentation products. The requirement to develop novel pervaporation membranes with increased separation performance has been identified as a requirement for the adoption of the process. A number of novel materials for pervaporation membranes have been introduced; however, mixed-matrix membranes have been identified as some of the most promising materials for pervaporative separation as they combine the benefits of both polymeric and inorganic membranes. The following points outline the importance of the discussed literature and concepts to each of the different research chapters presented within this thesis and how they align with the specific objectives of the thesis outlined in Section 1.3:

- **Chapter 3:** Concentration and Purification of a Gas Fermentation Broth with Nanofiltration and Reverse Osmosis.

The literature shows that there have been few investigations into the application of low energy recovery technologies for 2,3-butanediol, acetate, and ethanol from a gas fermentation process. Membrane technologies such as NF and RO have been shown to have promising separation performance of acetate and 2,3-butanediol from water in similar processes. These include separation of acetate from a glucose fermentation[45, 46] and removal of low concentrations of 2,3-butanediol (amongst many other impurities) from distillery condensates.[52] This led to the research conducted in Chapter 3 of this thesis, where a number of commercially available NF and RO membranes have been screened for their separation performance of these products from a gas fermentation broth. The best performing membranes were identified and tested within a membrane series for the purification and concentration of the gas fermentation broth. This has met the aim of "To investigate the feasibility of current commercial membranes for the recovery of gas fermentation products".

- **Chapter 4:** ZIF-8 PDMS MMMs for Ethanol Pervaporation: Effect of 2,3-Butanediol and Acetate; and, **Chapter 5:** Cu-MOF based PDMS Mixed-Matrix Membranes for Acetone Pervaporation: Impact of Glutarate and Bipyridyl ligands on the MOF morphology.

A number of examples of MMMs for pervaporation processes applicable to the removal of fermentation products have been presented. The ability to selectively remove a fermentation product from the broth is an appealing feature of this process and has been introduced and discussed within Chapter 2. However, finding materials with suitable separation performance (such as for pervaporation of 2,3-butanediol)[64] can be difficult. Materials with greater separation performance are required for the process to be applied commercially. For the application of membranes to fermentative separations, novel membranes that can provide greater separation and flux performances are required.

Therefore, the aims of future research within this area, as well as the aims of this thesis have been identified as:

- Further studies into the fouling and long-term stability of high-performing MMMs to help develop measures to overcome fouling from and effects of the many varying components of microbial fermentation broths.
- Further screening of a range of different water stable MOFs as inorganic fillers.

This is what has led to the research conducted within Chapters 4 and 5 which investigate the inclusion of novel inorganic materials, known as metal-organic frameworks (MOFs), within the polymer matrix of a typical pervaporation membrane material. Chapter 4 presents work conducted on the first point above where the effect of 2,3-butanediol and acetate on ethanol pervaporation by a ZIF-8-PDMS membrane has been investigate. Chapter 5 presents work conducted on the second point above where two structurally similar Cu-MOFs that have not been utilised before in a pervaporation membrane are tested to determine the change in performance when incorporated into PDMS. These Chapters have helped meet the aim of "To identify ways to improve the recovery of products from a gas fermentation process".

Further work outside of the scope of this thesis may also include:

- Bespoke polymer development to complement and enhance the different fillers and separations that the resulting MMMs will be applied to.
- Further investigations into the effect of different membrane fabrication techniques on the performance of MMMs for applicable separations to fermentations.

- Improved fabrication and operational methods for preventing the leaching of the inorganic phase out of the polymer membrane.
- Full cost-benefit analysis of the use of novel, expensive, inorganic fillers within these investigated MMMs is needed to determine whether the improved membrane performance characteristics can offset the increased membrane fabrication costs.

- **Chapter 6:** Poly(propylene) glycols as probes for MWCO determination in Organic Solvent Nanofiltration.

The concepts of the performance parameters for separation of NF and RO membranes have been introduced at the beginning of this chapter. These include flux and rejection characteristics and the term MWCO has been defined, as well as a number of other factors which influence rejection. These are important parameters for describing the separation performance of a specific membrane for a specific separation. These concepts are important to the research conducted within Chapter 6 of this thesis where poly(propylene) glycols have been investigated as molecular probes for determining the MWCO of various organic solvent nanofiltration (OSN) membranes. This meets the final aim of this thesis of: "To develop methods to improve the characterisation and understanding of membrane separation processes".

Chapter 3

Concentration and Purification of a Gas Fermentation Broth with Nanofiltration and Reverse Osmosis

The work in this chapter has been published in part as a journal article:

"C. J. Davey, A. Havill, D. Leak, D. A. Patterson, Nanofiltration and reverse osmosis membranes for purification and concentration of a 2,3-butanediol producing gas fermentation broth, *J. Membr. Sci.*, 2016, **518**, 150-158."

3.1 Introduction

As an important commodity chemical, 2,3-butanediol has downstream products with an estimated market of 32 million tons a year, which is valued at around $43 billion in sales.[9] With the majority of 2,3-butanediol sourced from crude oil, alternative sources could provide both a lucrative and sustainable substitute. Gas fermentation can be used to produce 2,3-butanediol alongside acetate and ethanol from carbon rich waste gas streams of varying ratios of CO, CO_2 and H_2. As ethanol and acetate are also important commodity chemicals with markets of 9 and 60 million tons per year respectively[8] this process could provide a route to sustainable commodity chemicals and

fuels. The recovery of these desired organics from the fermentation broth; however, is an energy intensive process which is a limit to its cost effectiveness. This arises from the production of these fermentation products being at low concentrations within the broth and therefore having to be separated from a complex mixture of metabolites, proteins, salts, sugars and other nutrients used as growth media. Distillation is still the dominant separation technology, but for high-boiling organics such as 2,3-butanediol (b.p. = 183 ºC) it is not desirable since it contributes to over half the cost of its microbial production.[10]

A variety of low energy recovery techniques have been investigated for the fermentative production of 2,3-butanediol,[10, 26, 192, 193] acetate[16] and ethanol.[12, 14] For 2,3-butanediol, specific examples include demonstration of liquid-liquid extraction,[21, 22] reactive extraction,[23, 24] salting out,[25] aqueous two phase extraction[194-196] and gas stripping.[26] Membrane technologies; however, present an attractive low energy alternative to these methods.[11, 197]

Nanofiltration (NF) and reverse osmosis (RO) are pressure driven membrane processes that are suitable for the downstream purification and concentration of fermentation products. Examples exist for the purification / concentration of various acidic products from fermentations such as lactate,[48, 49] acetate[45, 46] and succinate.[47] Other examples include the removal of sugars from an ethanol fermentation[198] and purification and concentration of glycerol.[199] Although NF and RO have been studied for the removal of 2,3-butanediol and other fermentation by-products from distillery condensates,[52, 53] no comparison of the purification and concentration of these alcohols as the main target for separation as fermentation products has been undertaken. Consequently, this chapter presents an investigation into the use of NF and RO into the membrane fractionation (Figure 3-1) of 2,3-butanediol and its co-fermentation products, acetate and ethanol, in the context of gas fermentation. The identified membranes could be implemented for purification and concentration of the broth to enable energy savings in further downstream separation processes (such as distillation). The membrane BW30 has also been compared for its potential suitability in the concentration of other alcoholic metabolites.

This meets the specific objectives of this thesis:

- To identify suitable membrane separation processes for the low energy separation of products from a gas fermentation broth.
- To investigate the feasibility of current commercial membranes for the recovery of gas fermentation products, mainly 2,3-butanediol, acetate and ethanol.

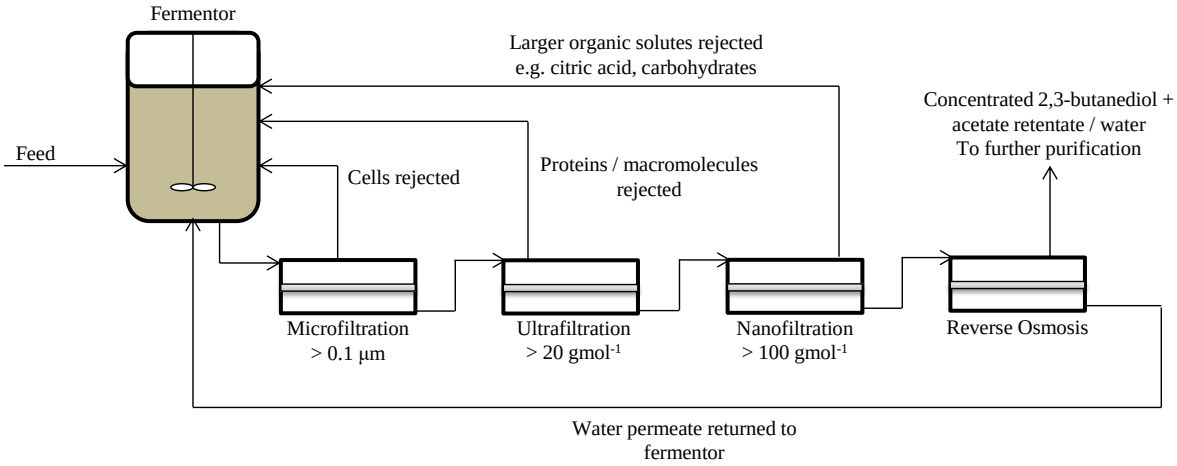

Figure 3-1. Schematic of the ideal membrane series for the purification and concentration of a 2,3-butanediol producing gas fermentation broth.

3.2 Materials and Methods

3.2.1 Materials

The membranes used in all dead-end filtration experiments were purchased from Sterlitech (USA). 2,3-butanediol (98 %), ethanol (≥ 99 %), acetic acid (≥ 99 %), 1,3-propanediol (98 %), 2-propanol (≥ 99.8 %), ethylene glycol (≥ 99.5 %) and methanol (≥ 99.9 %) were purchased from Sigma Aldrich (UK). Ammonium Acetate (97 %), 1-propanol (> 99.5 %), 1,2-propanediol (99.5 %), 1-butanol (99 %), 2-butanol (99 %), Isobutanol (99 %), tert-butanol (99 %), 1,4-butanediol (99 %) and 1,3-butanediol (99 %) were purchased from Alfa Aesar (UK). A series of commercial NF and RO membranes were selected with molecular weight cut-offs (MWCOs) lower than ~ 400 $gmol^{-1}$ as defined by the manufacturer. This is larger than the MW of 2,3-butanediol (90.1 g mol^{-1}), acetic acid (60.1 g mol^{-1}) or ethanol (46.1 g mol^{-1}), however, a range of membranes with varying MWCOs were investigated due to MW not being the only determining factor to effect rejection of organic solutes by NF and RO membranes.[38] Deionised water was taken from a Purelab Option unit (15 MΩ cm at 25 °C).

Table 3-1. Commercial membranes for screening with model solutions.

Manufacturer	Membrane	Membrane type	Active Layer Material	Manufacturers stated MWCO range (g mol^{-1})	Supplier or citation stated Salt Rejection (%)
Dow	NF	NF	Polyamide	200 - 400	99 ($MgSO_4$)
	NF245	NF	Polyamide	200 - 400	99 ($MgSO_4$)
	NF270	NF	Polyamide	200 - 400	80 (NaCl), 50 ($CaCl_2$), 99.3 ($MgSO_4$)[200]
	NF90	NF	Polyamide	200 - 400	90 – 96 (NaCl)[200]
	BW30	RO	Polyamide	100	99.4 (NaCl), 99.4 ($CaCl_2$), 99.7 ($MgSO_4$)[200]
	BW30LE	RO	Polyamide	100	99.0 (NaCl)[52]
	BW30FR	RO	Polyamide	100	
TriSep	TS80	NF	Polyamide	150	99 ($MgSO_4$)[201]
	SB90	NF	Cellulose acetate blend	150	97.0 ($MgSO_4$)
GE Osmonics	SG	RO	Thin film	0	98.2 (NaCl)[52]
	SE	RO	Thin film	0	98.9 (NaCl)[52]
	CE	RO	Cellulose acetate	0	97.0 (NaCl)[52]

The fermentation broth utilised within Section 3.3.4 was provided by LanzaTech (USA), shipped in dry ice, and kept frozen until use. The broth was centrifuged at 5000 rpm for 30 minutes to remove any non-dissolved solids before use. To increase the pH of the gas fermentation broth NaOH was added. The composition of the gas fermentation broth is presented in Table 3-2 and Table 3-3.

Table 3-2. Composition of Organics in LanzaTech gas fermentation broth used in Section 3.3.4.

Component	Concentration in Broth (g L^{-1})	MW (gmol^{-1})
Ethanol	8 - 10	46.1
2,3-Butanediol	3 - 8	90.1
Acetic Acid	3 - 8	60.1
Suspended Biomass	2 - 8	-

Table 3-3. Maximum Inorganic Content of LanzaTech gas fermentation broth.

Characteristic	Fermentation Broth
COD (mg L^{-1})	80000 - 100000
BOD (mg L^{-1})	75000 - 90000
TSS (mg L^{-1})	2500 - 5000
TDS (mg L^{-1})	3000 - 4000
TN (mg L^{-1})	1500 - 2500
TP (mg L^{-1})	250 - 400
Chloride (mg L^{-1})	250 - 500
Potassium (mg L^{-1})	150 - 400
pH	5.1 - 5.3

Chemical Oxygen Demand (COD), Biological Oxygen Demand (BOD), Total Suspended Solids (TSS), Total Dissolved Solids (TDS), Total Nitrogen (TN), Total Phosphorous (TP).

The fermentation broths used within Section 3.3.6 were taken directly from the cell recycle permeates of the continuous fermentors at LanzaTech, USA and had similar inorganic content to that of the previously used broth (Table 3-3). The organic content of the fermentation broths differed slightly, generally having higher ethanol content than the previously used broth (40 – 50 g L^{-1}) (Table 3-2). Permeates of NF270 that were used within subsequent filtrations were stored at ~ 2 – 4 ºC before further use.

3.2.2 Filtrations

Aqueous solutions of 2,3-butanediol, acetic acid, and ammonium acetate at concentrations similar to those observed in a gas fermentation broth bleed stream were used to determine and compare flux and rejection characteristics of the commercial membranes. Then dead end-filtrations were conducted using the gas fermentation broth outlined above with NF270, NF90 and BW30.

Dead end filtrations were carried out in a Sterlitech HP4750 stirred cell made of stainless steel with an active membrane area of 14.6 cm^2 using the standard methodology that has been applied in numerous other studies (Figure 3-2).[202, 203] A magnetic stirrer just above the membrane surface was used for mixing of the feed and minimizing concentration polarization. The dead end cell was placed in a water bath on a heater-stirrer for stirring speed and temperature control (150 – 300 rpm and 30 ^{o}C). Pressure was applied using compressed nitrogen (BOC, 99.998 %) and measured with a pressure gauge. Weight of permeate was recorded using a Sartorius LC3201D-00MS balance with a data logging program developed in LabVIEW. Flat sheet membrane discs of 47 mm diameter were either cut out from larger flat sheets with a scalpel using a membrane size template (to prevent scratching of the surface) or used as received as pre-cut discs. NF and RO membranes were conditioned by permeating reverse osmosis water (15 MΩ.cm at 25 ^{o}C) under pressure before use for ~ 2 hrs, until constant flux was achieved.

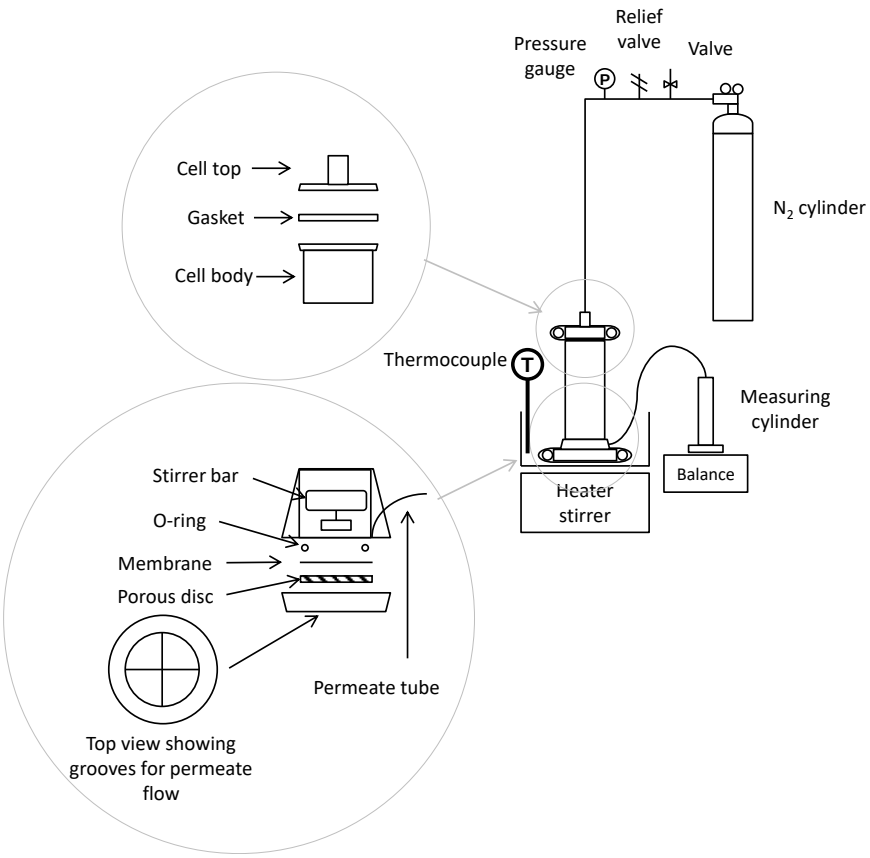

Figure 3-2. Schematic of Dead-End Filtration set-up (Sterlitech HP4750) used for filtrations.

Observed rejections were characterised by permeating half of a 50 mL feed solution (to account for changing concentration) and calculated using Equation 3-1 after measuring the concentration in feed and permeate.

$$R_{j,i} = \left(1 - \frac{C_{i,p}}{C_{i,f}}\right) \times 100\ \% \qquad 3\text{-}1$$

Where: $C_{i,p}$ = Concentration of species *i* in permeate

$C_{i,f}$ = Concentration of species *i* in feed

So when $R_{j,i}$ = 100 % a complete rejection is observed and when $R_{j,i}$ = 0 % no separation has been achieved.

Error bars represent the standard deviation of 3 separate runs with three membrane samples except for in Section 3.3.6 where a single point was repeated thrice with three membrane samples and a

standard deviation of ± 1.22 kg m^{-2} h^{-1} for flux and ± 2.2 % for rejection was calculated and can be inferred across the data.

3.2.3 High-Performance Liquid Chromatography

The concentration of organic solutes in feeds, permeates and retentates were analysed by HPLC using an Agilent Technologies 1200 series instrument. A Phenomenex organic acids column (7.8 x 300 mm) was used at 60 °C with 5 mM H_2SO_4 as mobile phase and a flow rate of 0.7 mL min^{-1}. Solutes were detected with an RI detector and concentrations interpreted through the peak area using external calibration. Fermentation samples were prefiltered with a 0.22 μm syringe filter (Millipore, UK) before analysis to remove any suspended particles.

HPLCs undertaken at LanzaTech, USA were conducted by the analytical team using a method analogous to that described above, except an Alltech IOA-2000 Organic Acids (150mm x 6.5mm, 8μm) was used.

3.2.4 pH Measurements

pH measurements of solutions were conducted on a Denver Instruments 250 pH meter. The pH meter was calibrated to solutions of pH 4, 7 and 10 (Fisher Scientific, UK) before use.

3.2.5 Conductivity Measurements and Apparent Salt Rejection (ASR)

Conductivity measurements were carried out on a Thermo Scientific Orion Versa Star conductivity meter. ASRs were calculated using Equation 3-2:

$$ASR\ (\%) = \left(1 - \frac{C_p}{C_f}\right) \times 100 \qquad 3\text{-}2$$

where C_f is the conductivity of the feed and C_p is the conductivity of the permeate.

3.2.6 Fourier Transform Infrared Spectroscopy (FTIR)

FTIR spectra were recorded over the range 4000 – 600 cm^{-1} using a Perkin Elmer Spectrum 100 FTIR spectrometer fitted with an attenuated total reflectance (ATR) detector. Three ATR-FTIR spectra were recorded in different positions on the membrane sample and the spectrum was averaged over 10 scans with a resolution of 1 cm^{-1}.

3.2.7 Irreversible Fouling Determination

Irreversible fouling was determined by taking the fouled membrane and washing with deionised (DI) water for 5 minutes. Samples of 25 mL of DI water were then permeated through the membrane until the flux stabilised. Then 3 x 25 mL of DI water were permeated through the membrane and an average of the runs was taken.

3.2.8 Scanning Electron Microscopy (SEM)

SEM images were taken on a JEOL SEM6480LV. To achieve cross-sectional images membranes were submersed in liquid N_2 and fractured with a razor blade. Samples were dried in a vacuum desiccator overnight before analysis.

3.3 Results and Discussion

3.3.1 Observed Rejection of 2,3-Butanediol, Acetate and Ethanol

As the gas fermentation studied produces 2,3-butanediol, acetate and ethanol as fermentation products, the individual rejection of these compounds by the selected commercial membranes was investigated at concentrations similar to those found in the broth. Rejection generally correlated well with manufacturers defined MWCOs – however, this is not always the case.[203] Initial studies looked at the rejection of aqueous solutions of 2,3-butanediol (Figure 3-3). High rejections were observed for the denser RO / NF membranes and much lower rejections were observed for the looser NF membranes, as expected. One limit to our approach would be the maximum concentration of the fermentation products achievable before permeance declines beyond a useful level. Experiments conducted at concentrations of 20 g L^{-1} 2,3-butanediol were attempted; however, the permeabilities observed indicate that this would start to be close to the upper limit of concentration with this method.

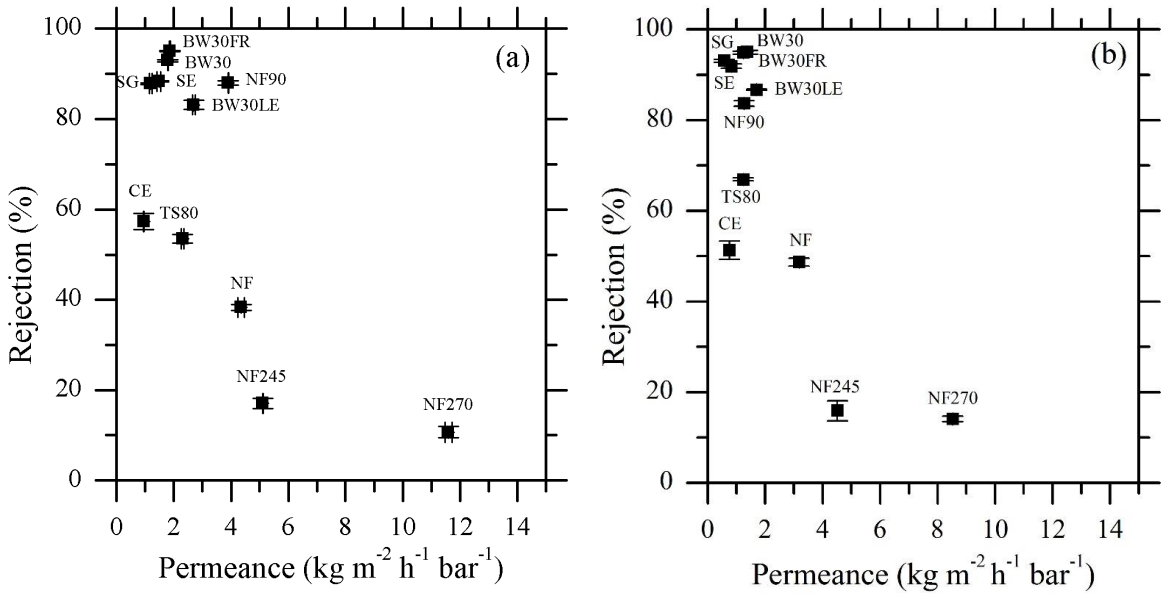

Figure 3-3. Observed Rejection of (a) 4g L^{-1} and (b) 10 g L^{-1} 2,3-Butanediol by various membranes; 15 bar, 30 ºC, 150 rpm.

Acetate rejection was also characterised for each membrane. Every membrane studied exhibited poor rejection (< 40 %) of acetic acid (Figure 3-4.a), whereas ammonium acetate rejection for some membranes was high (> 90 %) (Figure 3-4.b). The difference in the rejection is due to

Donnan Exclusion, based on the charge of the acetate ion and membrane surface.[45] As the pH of the solution is lower than the pK_a of acetic acid (pH = 3.39 vs. AcOH pK_a = 4.75), it will exist mainly as AcOH in solution. When ammonia is present, the pH of the solution increases (pH = 6.81) and therefore acetic acid exists mainly as its conjugate base AcO^-. As the majority of membranes studied exhibit negatively charged surfaces (e.g. BW30, NF90 and NF270),[204] the increase in rejection is thought to be mainly due to an increase in electrostatic repulsion between the membrane surface and the acetate anion. However, MWCO is still an important factor in the rejection of acetate, as the membranes with a smaller MWCO still exhibit a higher rejection than those with a greater MWCO. Therefore, for this particular separation, the membrane selection has been based in the main on both charge and MWCO / pore size – however, other criteria are also important for membrane selection (long term robustness and performance, cost, availability, fouling, ease and robustness to cleaning) many of which are beyond the scope of this work. During the filtration of the fermentation broth, however, it is possible that further interaction effects and membrane fouling may alter the rejection and has been investigated in more detail in Sections 3.2 and 3.3.

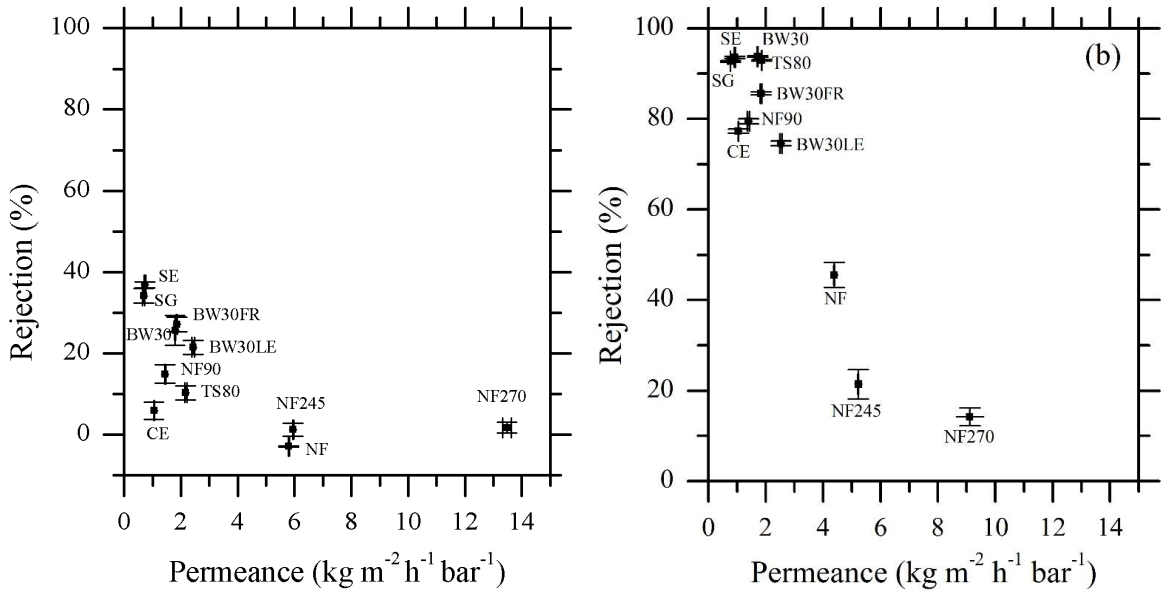

Figure 3-4. Observed rejection of (a) 5 g L^{-1} and (b) 2.5 g L^{-1} ammonium acetate by various membranes; 15 bar, 30 ºC, 150 rpm.

Three membranes were chosen for further investigation; NF270, a poorly rejecting membrane; NF90, a medium to high rejection membrane; and BW30, a high rejection low flux membrane. The performance of NF270, NF90, and BW30 were investigated at different pressures to investigate the variance in rejection performance with flux (Figure 3-5). BW30 exhibited a general

increase in rejection of 2,3-butanediol with flux, whereas NF270 exhibited the opposite behaviour with a decrease in rejection with an increase in flux. NF90 exhibited a relatively stable rejection with increasing flux. Each membrane exhibited a linear relationship between flux and pressure.

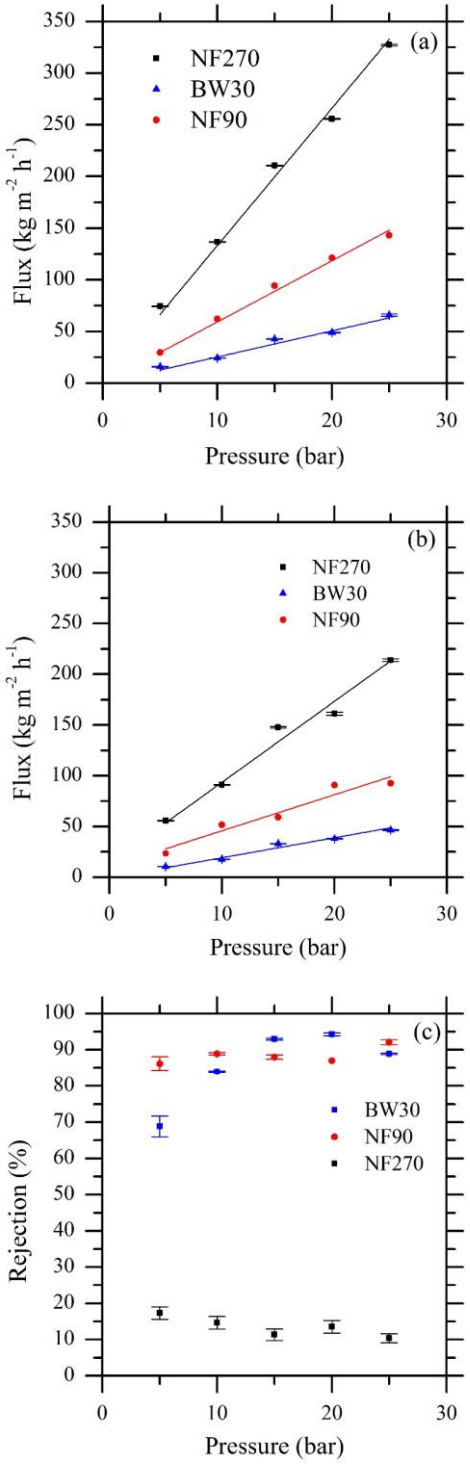

Figure 3-5. (a) Pure water flux, (b) flux and (c) rejection of 4 g L^{-1} 2,3-butanediol with different applied pressures; 30 ºC, 150 rpm.

The rejection of ethanol was investigated for these membranes (Table 3-4) that had different performances in the rejection of 2,3-butanediol and acetate. Each membrane tested showed very low rejection (< 15 %) of ethanol: this is in accordance with previous literature.[205] It is envisaged that ethanol could not be concentrated within the gas fermentation broth, as for 2,3-butanediol and acetate, and therefore would need to be recovered from the purified permeate stream from one of these membranes.

Table 3-4. Ethanol Rejection and Permeance data, 10 g L^{-1} Ethanol, 30 ºC, 150 rpm, 15 bar.

Membrane	Permeance (kg m^{-2} h^{-1} bar^{-1})	Ethanol Rejection (%)
NF270	11.0 (± 0.0814)	2.50 (± 1.69)
NF90	4.29 (± 0.690)	14.8 (± 0.382)
BW30	1.56 (± 0.382)	14.5 (± 1.07)

3.3.2 Characterisation of Membranes

A short study was conducted to characterise the chosen membranes NF270, NF90 and BW30 and determine the reason for the differences in rejection of the solutes 2,3-butanediol, acetic acid and ammonium acetate. The structures of these TFC membranes have been well studied[200, 206] with each one consisting of an ultrathin polyamide active layer on top of a polysulfone support, which itself is supported upon a polyester reinforcing fabric (Figure 3-6).

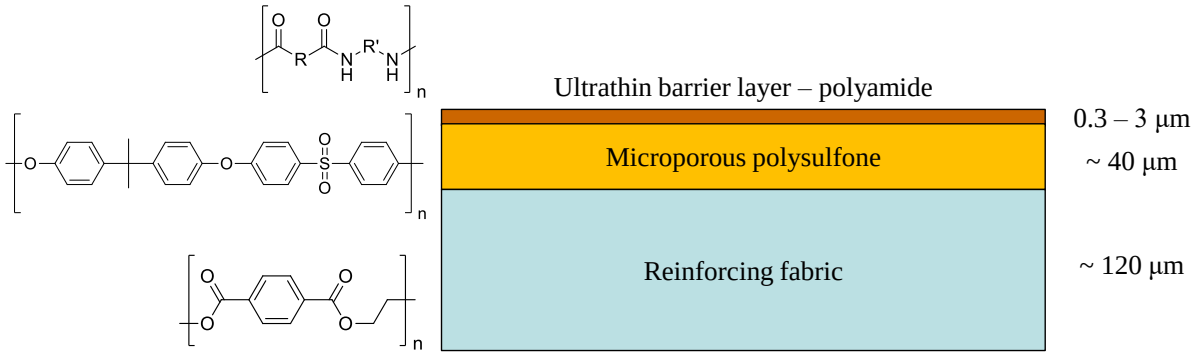

Figure 3-6. Schematic of the structure of a TFC NF / RO membrane.

The polysulfone support and polyester backing layer can be imaged by SEM as presented in Figure 3-7. Energy-dispersive X-ray spectroscopy (EDX) confirmed the presence of sulphur in the microporous polysulfone support layer and only carbon and oxygen were detected within the

polyester backing layer. The ultrathin polyamide layer (0.2 μm thick) could not be visualized by SEM due to the thickness of the layer being beyond the resolution of the SEM.

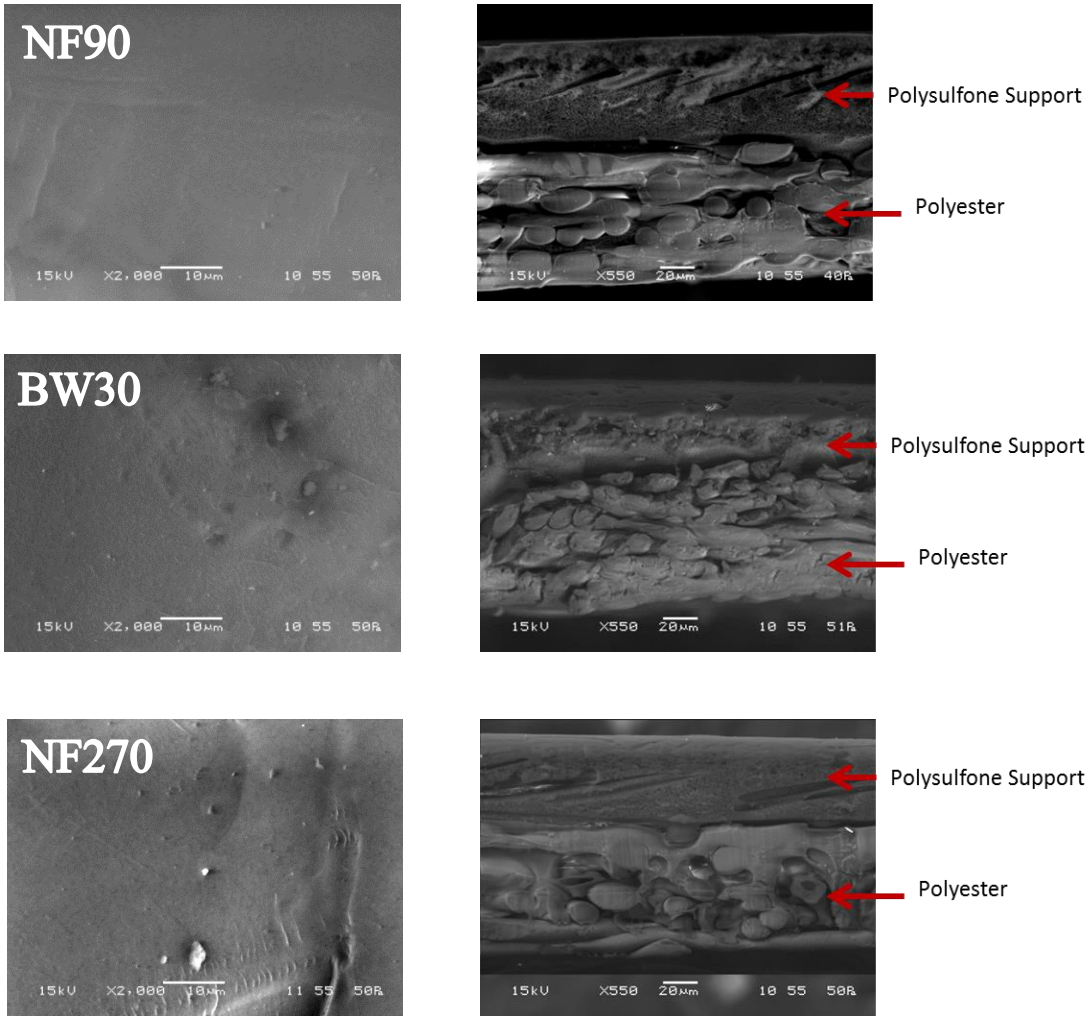

Figure 3-7. Surface and cross-sectional SEM images of NF90, BW30 and NF270.

It is mainly the polyamide layer which achieves the separation exhibited by these TFC membranes (Figure 3-8). The membranes NF90 and BW30 consist of a fully aromatic polyamide (Figure 3-8.a) and NF270 consists of a semi-aromatic poly(piperazineamide) (Figure 3-8.b) each with a high degree of crosslinking of the polyamides.[204, 206]

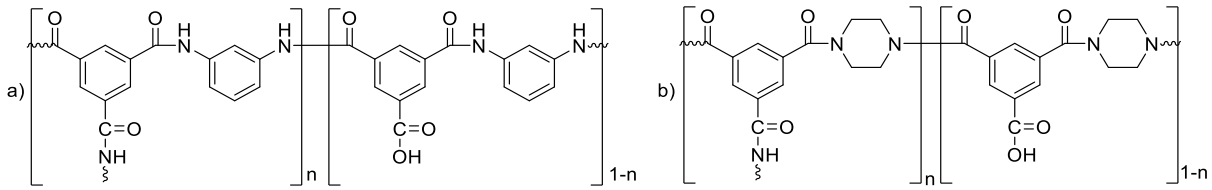

Figure 3-8. Chemical structures of the active polyamide layer of (a) NF90 and BW30 and of (b) NF270. The value of n denotes the amount of cross-linking of the polyamide (n = 1 when fully cross-linked and n = 0 when fully linear.

The active polyamide layer can be probed by FTIR. Figure 3-9 shows the FTIR spectra of NF270, NF90 and BW30. The characteristic absorbances for the polysulfone support (1585, 1503, 1487 cm^{-1}) are present in each spectra due to the penetration of the IR radiation beyond the polyamide on the membrane surface. BW30 exhibits peaks at (1663, 1609, 1543 cm^{-1}) and the absorbances correlate with those reported elsewhere[206] for the fully aromatic polyamide. NF90 exhibited the same absorbances in the FTIR spectra as for BW30 due to the active layer consisting of the same fully aromatic polyamide. The FTIR spectra of NF270 displays the relevant absorbance for the semi-aromatic poly(piperazineamide) (1635 cm^{-1}) as well as not exhibiting an Amide II band, attributed to the absence of N-H bending vibrations in the polyamide structure.[206]

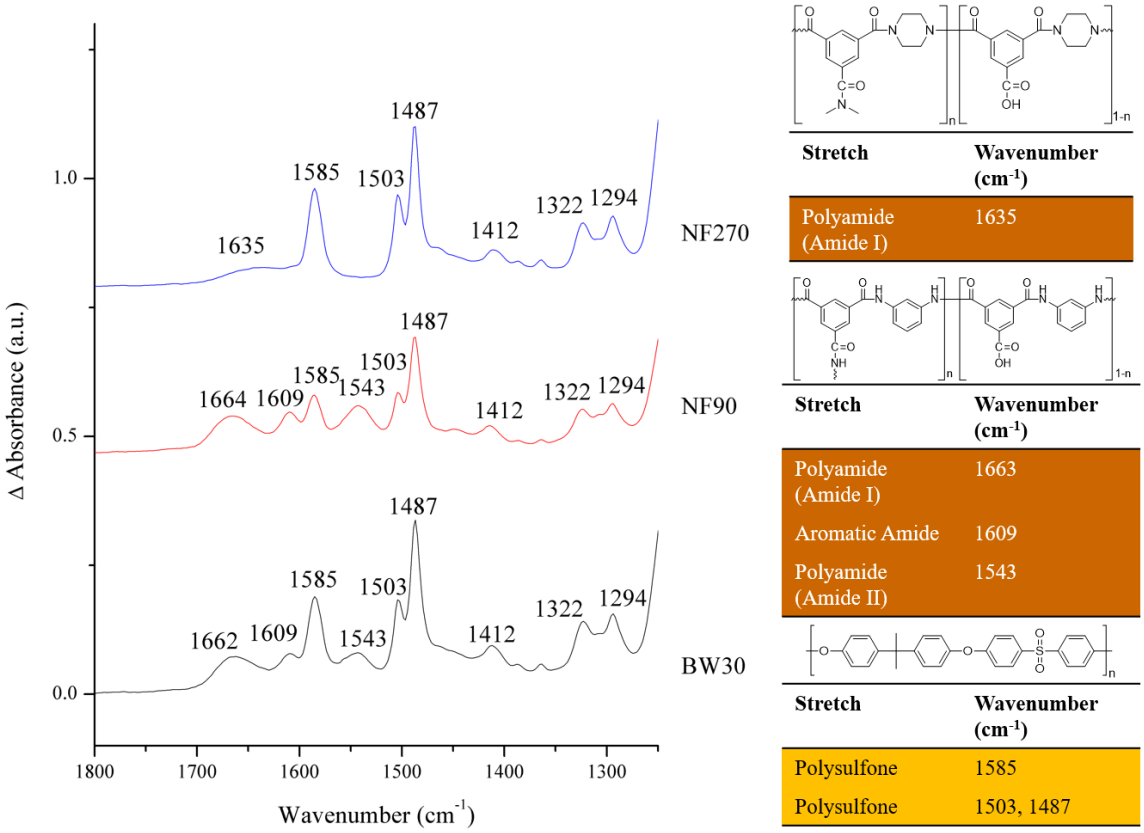

Figure 3-9. FTIR of BW30, NF90 and NF270 showing the characteristic absorbances of the aromatic polyamide / semi-aromatic poly(piperazineamide) barrier layer and polysulfone support, consistent with absorbances presented in.[206]

Even though the membranes NF90 and BW30 contain the same fully aromatic polyamide active layer they exhibited very different rejection characteristics, 78.9 % and 92.9 % respectively, for 4 g L^{-1} of 2,3-butanediol. These membranes differ in the degrees of cross-linking of the polyamide as well as having differences in the surface chemistries of the membranes. In addition to the structure presented in Figure 3-8, BW30 also contains a coating on the surface. The application of surface coatings on membranes can be used to protect the surface of the membrane and / or improve the performance of the membrane.[204, 206, 207] The difference in the surface chemistry of NF90 and BW30 can be determined in part from their respective effective water contact angles (Table 3-5).

Table 3-5. Measured water effective contact angles for NF270, NF90 and BW30.

Effective Contact Angle (º)		
NF270	**NF90**	**BW30**
9.91 (± 1.5)	80.7 (± 3.5)	59.7 (± 2.5)

The apparent hydrophobicity of the surface of NF90 is much greater than BW30, attributed to the hydrophilic PVA coating of BW30.[204] It can also be seen that the poly(piperazineamide) membrane NF270 is much more hydrophilic than the fully-aromatic NF90 or surface coated BW30. The surface properties of NF270, NF90 and BW30 have been probed in more detail by a variety of techniques (FTIR, X-ray photoelectron spectroscopy, atomic-force microscopy, contact angle, zeta potential) elsewhere.[204, 206]

3.3.3 Rejection of Mixtures of 2,3-Butanediol and Acetate

The rejection of mixed component solutions by NF270, NF90 and BW30 was investigated to ascertain any effect the combination of solutes may have on the rejection of the organic species. The rejection of 2,3-butanediol by BW30, NF90 or NF270 (Table 3-6) was unaffected by the addition of either acetic acid or ammonium acetate. Likewise, the rejections of acetic acid or ammonium acetate were unaffected by the presence of 2,3-butanediol (Table 3-6). As the pK_a of 2,3-butanediol (pK_a = 14.9) is much higher than the pH of either the acidic or neutral solution (pH 3.40 and 6.95 respectively), 2,3-butanediol does not form its conjugate base in either solution, so rejection is still mainly based on molecular size / MW. On the other hand, the addition of 2,3-butanediol has negligible effect on the pH of the solution, so the rejection of acetate is unaffected for its respective solutions. This indicates that the membranes and selectivities obtained in the single component runs are applicable still in the mixtures and further justifies the selection of these membranes. Figure 3-10 shows the reduction in flux for each membrane over the concentration of a mixed solution of 2,3-butanediol and ammonium acetate demonstrating only a small reduction in flux over the course of the experiment.

Table 3-6. Permeance and rejection of a mixed solution of 2,3-butanediol and ammonium acetate.

Membrane	Permeance (kg $m^{-2} h^{-1} bar^{-1}$)	2,3-Butanediol Rejection (%)	Acetate Rejection (%)
NF270	7.92	14.3	37.8
NF90	2.53	80.8	76.1
BW30	1.27	96.0	94.2

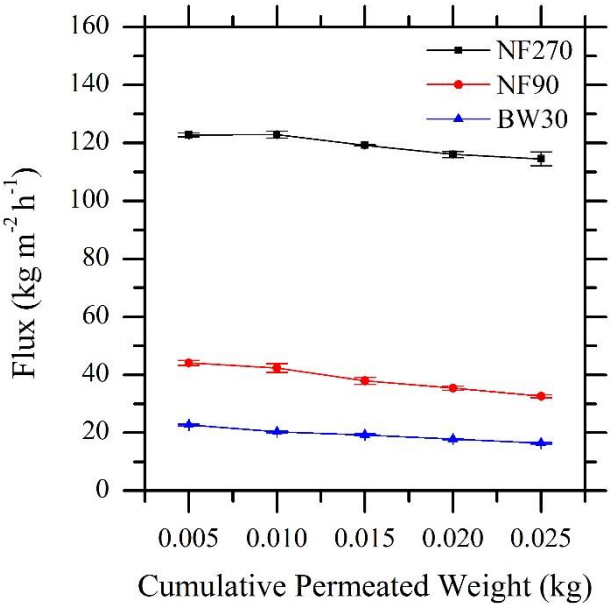

Figure 3-10. Reduction in flux by a mixed solution of 2,3-butanediol (4 g L^{-1}) and ammonium acetate (2.5 g L^{-1}), 30 ºC, 15 bar, 300 rpm.

3.3.4 Initial Performance of Membranes for Concentration of a Gas Fermentation Broth

The rejection and flux characteristics of each organic component by the membranes NF270, NF90 and BW30 within a gas fermentation broth was determined. Figure 3-11 shows the flux profiles for BW30, NF90 and NF270 for the concentration of the gas fermentation broth at natural pH (pH = 5.1). It can be seen that the concentration of the fermentation broth greatly reduces the flux of the membranes compared to that of the model solutions of 2,3-butanediol and acetate (Figure 3-10, Table 3-6). Rejections of each component reflected those of the model solutions (Table 3-7) with BW30 and NF90 exhibiting high rejections (94.6 and 92.6 % respectively). The rejection of

acetate by BW30 and NF90 is between that of the model solutions with values of 74.4 and 70.5 % respectively.

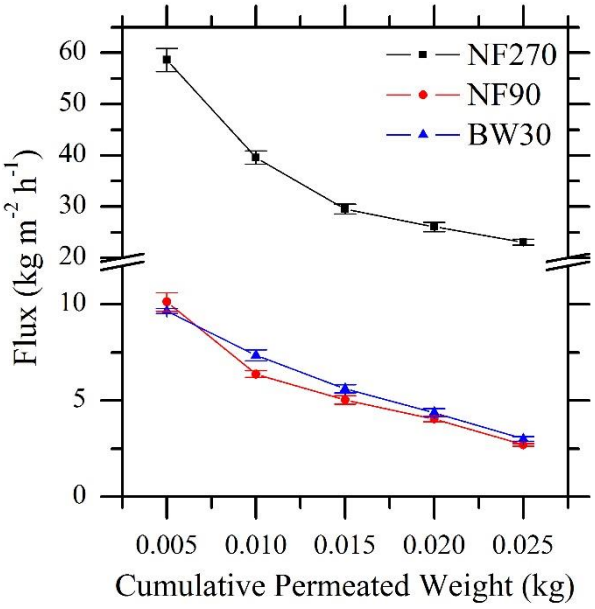

Figure 3-11. Reduction in flux by gas fermentation broth, 30 °C, 15 bar, 300 rpm (±SD).

Table 3-7. Rejection data for filtration of the gas fermentation broth.

Concentration	**Feed**	**NF270**		**NF90**		**BW30**	
		Permeate	**Retentate**	**Permeate**	**Retentate**	**Permeate**	**Retentate**
2,3-Butanediol (g L^{-1})	3.34	2.31	3.67	0.25	5.62	0.18	5.58
Rejection (%)		**30.9**		**92.6**		**94.6**	
Acetate (g L^{-1})	6.51	4.72	7.01	1.92	10.3	1.67	9.93
Rejection (%)		**27.5**		**70.5**		**74.4**	
Ethanol (g L^{-1})	9.2	8.0	8.74	7.11	9.29	7.51	9.47
Rejection (%)		**13.2**		**22.7**		**18.4**	
ASR (%)		**25**		**82**		**88**	
pH	5.1	5.0	5.2	4.3	5.3	4.1	5.2

The reduction in flux from irreversible fouling can be seen in Figure 3-12. After the rejection experiments, membranes were washed with deionised water and the pure water flux measured. NF90 experienced the greatest amount of irreversible fouling with a decline of pure water flux by 55 %, followed by BW30 exhibiting a decline of 43 %. NF270 experienced the least amount of fouling with a decrease in pure water flux of 9.0 %. The greater decline in flux exhibited by NF90 compared to BW30 may be attributed to an increase in fouling from the rougher surface of NF90[204] creating more grooves to trap potential foulants from the fermentation broth.

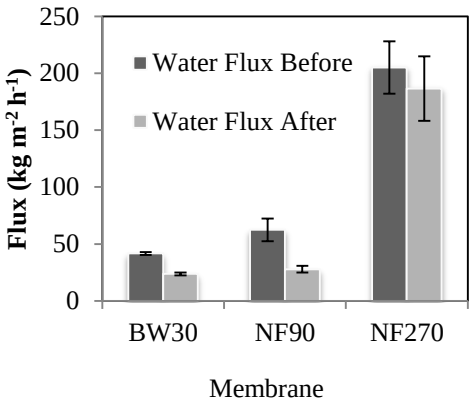

Figure 3-12. Pre-use and post-cleaning water fluxes for membranes after concentration of broth dead-end filtration, 30 ºC, 15 bar, 300 rpm.

The FTIR of NF90 also indicates irreversible fouling due to a general increase in absorbance of the cleaned membrane due to foulants on the membrane surface (Figure 3-13). The contact angles for BW30 and NF90 also indicate some fouling due to an increased hydrophilicity of the fouled and cleaned membranes compared to the virgin membrane (Figure 3-14). An increase in contact angle was observed for NF270 from conditioned to fouled to cleaned (Figure 3-14). As can be seen from the ATR-FTIR of the used NF270 membranes (Figure 3-13) there is an increase in the peaks at 1640 cm^{-1} and 1533 cm^{-1}. This has been attributed to the partial breaking down of the polyamide barrier layer (Figure 3-15). The shoulder at 1635 cm^{-1} in the conditioned NF270 FTIR is due to polyamide C=O stretching,[206] the increase in the absorbance and shift to 1640 cm^{-1} has been attributed to an increase in carboxylic acid C=O stretching shifting, increasing and pronouncing the absorbance. The increase in amide II N-H stretching, not present in the tertiary amide structure, has been attributed to the increase in absorbance at 1533 cm^{-1}.

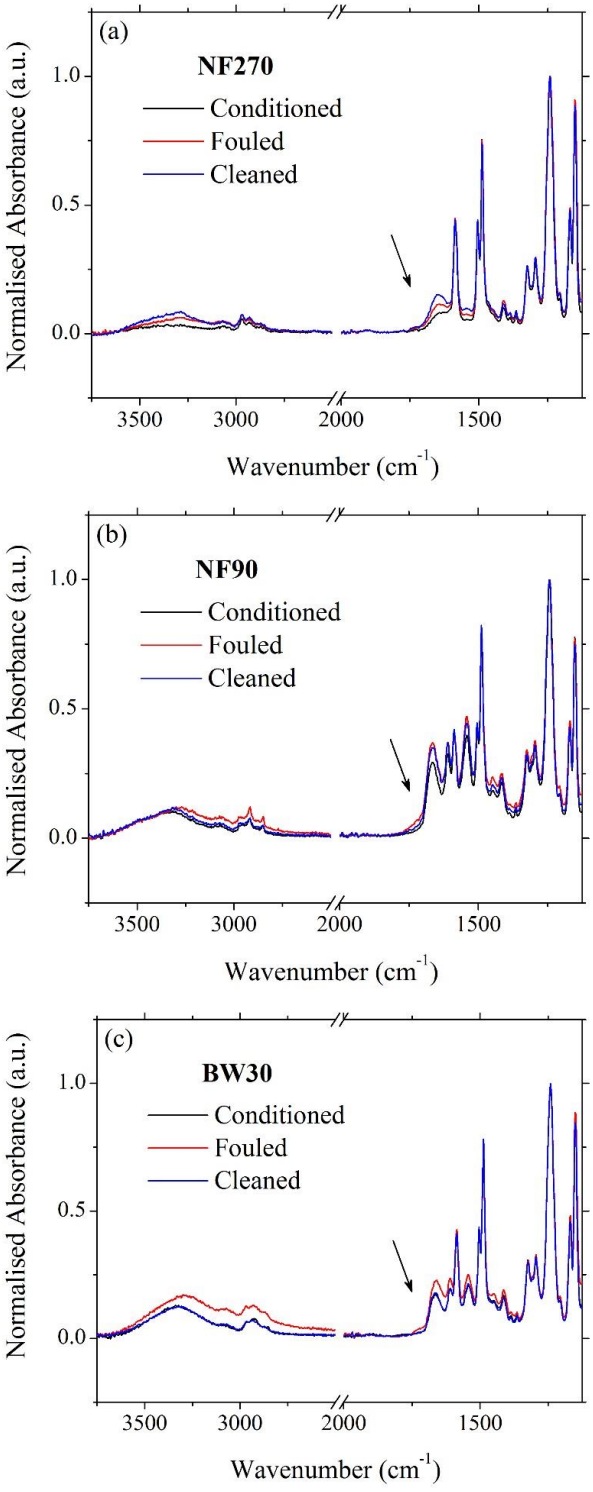

Figure 3-13. FTIR spectra of conditioned, fouled and cleaned membranes of (a) NF270, (b) NF90 and (c) BW30.

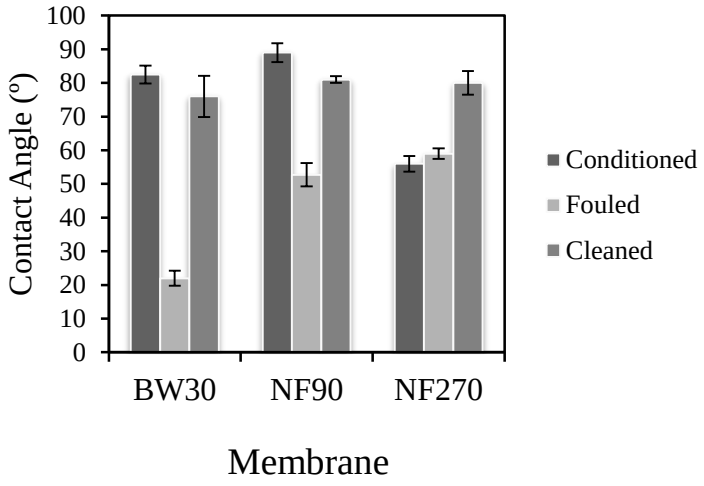

Figure 3-14. Contact Angles for Membranes used in the Concentration of Broth.

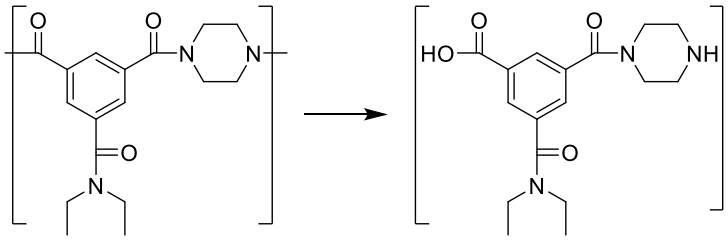

Figure 3-15. Possible partial degradation of NF270 membrane.

Avoiding irreversible fouling is important for a robust membrane separation. Changing solution pH will also change the zeta potential of the membrane surface, altering the interaction of foulants with the membrane. Moreover, changing pH can also affect acid-base species equilibrium, altering rejection of these species in solution. For acetate, as discussed earlier, increasing the pH of the solution will also increase the rejection. Consequently, the pH of the broth was increased to 6.5 to increase acetate rejection and an increase to 94.6 % by BW30 was observed (Figure 3-16.a). An increase in transmembrane pressure was also utilised to increase membrane flux. The filtration observed a lower reduction in flux during the experiment (81 % reduction compared to pure water flux; Figure 3-16.b). The amount of irreversible fouling measured by the post-cleaning pure water flux was also found to be less: a 36 % reduction as opposed to the natural pH broth experiment. The reduction in irreversible fouling of the membrane is thought to be due to the higher pH of the broth creating an increased number of deprotonated foulants, therefore increasing the number of foulants repulsed by the negatively charged membrane surface. This increased repulsion could create less membrane surface fouling and pore blocking.

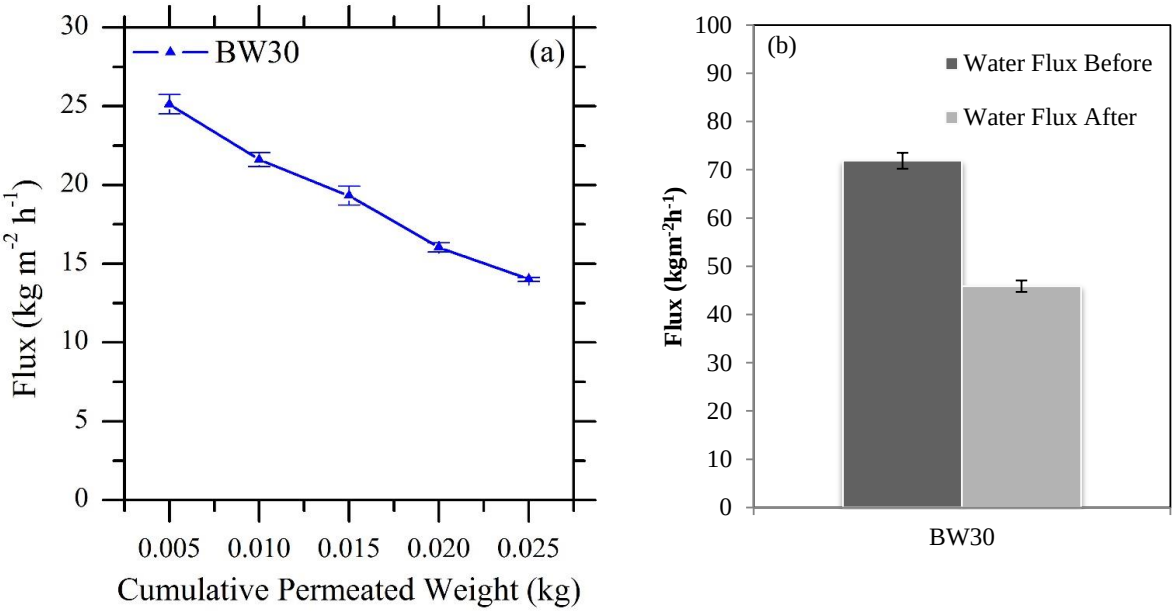

Figure 3-16. (a) Reduction in flux of a gas fermentation broth at pH 6.5, 30 bar; (b) pre-use and post-cleaning water flux for BW30 after concentration of broth.

Table 3-8. Rejection of fermentation products by BW30 at pH 6.5.

Molecule / Property	Concentration in respective stream			
	Feed	Permeate	Retentate	Rejection / ASR (%)
2,3-Butanediol (g L^{-1})	2.77	0.11	4.85	96.1
Acetate (g L^{-1})	5.38	0.29	9.77	94.6
Ethanol (g L^{-1})	7.64	5.47	8.82	28.3
Conductivity (mS / cm)	12.5	0.934	20.2	92.5
pH	6.5	6.3	6.5	-

Overall these results show that a membrane fractionation purification approach is possible in order to concentrate and purify 2,3-butanediol as per Figure 1. NF270 gives good clarification of the media with relatively low rejections of 2,3-butanediol and acetate, so can be used to purify the broth. NF90 and BW30 exhibited high rejection of 2,3-butanediol and good rejection of acetate; however, NF90 exhibited slightly higher irreversible fouling compared to BW30. When the pH of the broth was increased to 6.5, the rejection of acetate was increased by BW30. Therefore, BW30

is the more suitable membrane for the concentration of 2,3-butanediol and acetate within a gas fermentation broth.

3.3.5 Separation of Alcohols by BW30

As the library of potential fermentation products from gas fermentation is extensive and BW30 had been identified as a suitable membrane for rejection of 2,3-butanediol, it was hypothesised that this membrane could be used to reject other alcoholic products in a gas fermentation broth. For this, the relationship between rejection, flux and MW for BW30 of a number of different alcohols was determined. The general trend of solutes follows - with increasing MW in general a greater rejection is exhibited by BW30; however, flux is compromised by this increase in rejection due to fouling, concentration polarisation and an increase in osmotic pressure, hence it decreases with increasing MW (Figure 3-17). This would indicate that pore flow is the major rejection mechanism in controlling the selectivity in this separation.

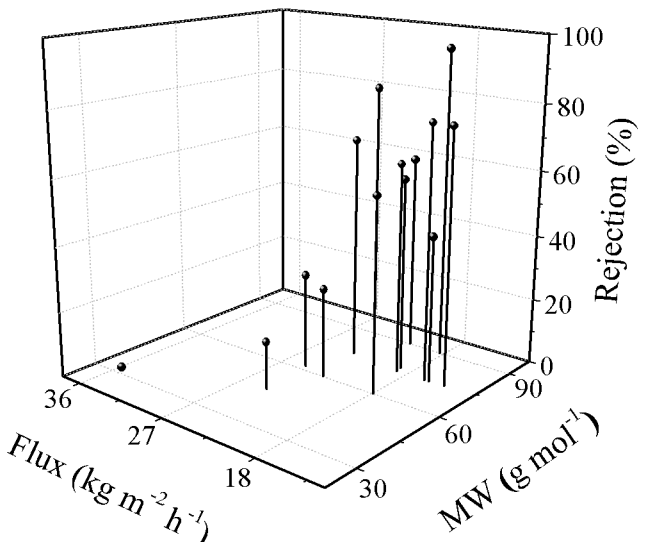

Figure 3-17. Relationship between flux, molecular weight and rejection for BW30.

Figure 3-18 further illustrates the obtained relationship between MW and rejection for the alcohols tested. This clearly shows that although rejection increases with increasing MW, the role of sterics of the alcohols also plays a part in their rejection by BW30. Change in pH with rejection was not investigated because of the relatively high pK_a's of alcohol (~16), the pH would have to be increased beyond an acceptable degree for a fermentation media to achieve dissociation of the alcoholic protons.

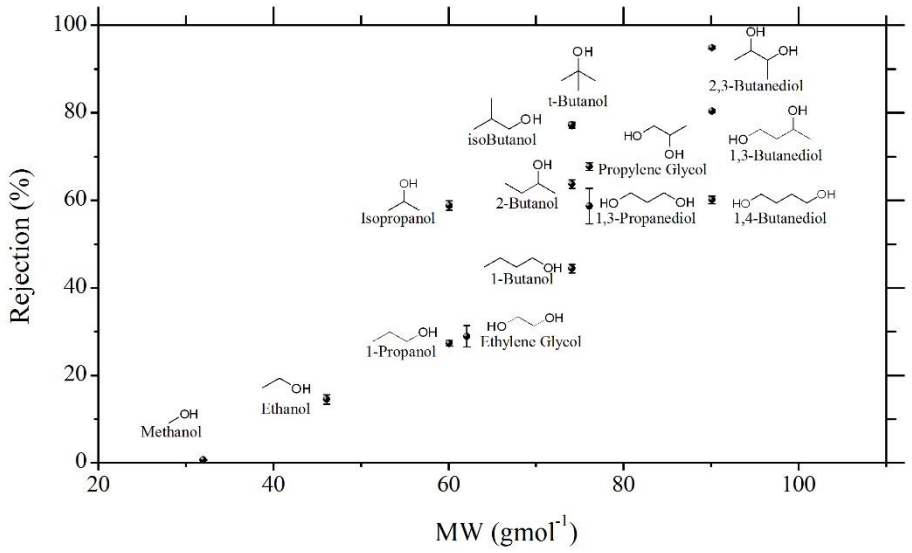

Figure 3-18. Rejection of different alcohols by BW30.

The relatively high rejection of isobutanol ~ 77 % would be sufficient for concentration using BW30 as membrane modules could be numbered up to increase the efficiency of rejection. In addition to this, the property of isobutanol to be only partially soluble in water (8.7 mL / 100 mL) requires the concentration of the solution to < 10 wt% before it will partition out of the aqueous solution. It should be noted; however, that data on the chemical stability of these membranes towards various alcohols is limited and the long term performance will need to be characterised before implementation. It has previously been shown that solutions of high concentration of alcohols can have a detrimental effect on the flux and rejection properties of RO and NF membranes.[208, 209]

These results indicate that the membrane fractionation strategy purification approach investigated in detail for 2,3-butanediol in this work could be applied more widely to the range of alcohol molecules being produced from renewable feedstocks and across industrial biotechnology, hopefully enabling lower energy, more sustainable separations. Future work will require investigating the long term stability of the membranes within these applications. As well as this the effect of concentration of different components of the fermentation broth (e.g. citric acid) on the productivity of the continuous fermentation will need to be studied.

3.3.6 A Membrane Series for Purification and Concentration of the Gas Fermentation Broth

The work in this section was conducted on a visit to LanzaTech, 8045 Lamon Ave Suite 400, Skokie, IL 60077, United States (March - April 2016).

The work in the previous section was expanded upon by a visit to LanzaTech's research and development site in Chicago, IL, USA. The work studied previously of the direct filtration of the broth was furthered through using the NF / RO filtrations in series to purify and then concentrate the broth. Due to the availability of a large volume of broth a systematic study on the effect of operating parameters such as feed pressure, stirrer speed, pH and feed temperature was conducted. An investigation into fermentation broths with different concentrations of metabolites was also undertaken. These will be important process parameters for consideration in the application of these membranes to the purification and concentration of 2,3-butanediol and acetate. Using the fermentation broth directly from the fermenter without having to freeze and thaw the sample to be sent between laboratories also limited the possible precipitation of products from the fermentation broth (i.e. proteins) that could lead to an altered indication of fouling etc. All these studies were not possible in the previous part of the study due to the limited quantity of fermentation broth that could be shipped internationally.

Fermentations conducted at LanzaTech incorporated the use of a cell recycle system. This consisted of a 0.22 μm hollow fibre membrane which would return cells to the fermentor and permeate the broth. This cell recycle system fitted with the membrane series suggested in Figure 3-1. Initially the permeate from the cell recycle system was used directly for the concentration of 2,3-butanediol and acetate with NF90 and BW30 at the natural pH of the broth (pH = 5.1) (mirroring the experiments in Section 3.3.4). For each of these membranes rejections and permeances reflected those within the previous section (Table 3-9). The increased ethanol rejection has been attributed to the much higher concentration within the gas fermentation broth used as the feed (47 g L^{-1}) when compared to the pure solution (10 g L^{-1}) (Table 3-4). The low permeances for NF90 and BW30 at < 0.5 kg m^{-2} h^{-1} bar^{-1} indicate that there would be considerable detrimental

fouling from permeation of the microfiltration permeate with these membranes over a long term use.

Table 3-9. Permeance and rejection data for the filtration of the gas fermentation broth from the cell recycle microfiltration unit. Feed concentrations; ethanol (47 g L^{-1}), acetate (3.5 g L^{-1}), 2,3-butanediol (7.7 g L^{-1}).

Membrane	Permeance	Rejection (%)		
	(kg m^{-2} h^{-1} bar^{-1})	Ethanol	Acetate	2,3-Butanediol
NF270	2.29	13.8	17.3	41.5
NF90	0.426	30.8	76.9	97.5
BW30	0.357	40.1	79.5	98.0

3.3.6.1 Investigation into a series of NF / RO filtrations for purification and concentration of the broth

As initially suggested in Figure 3-1 a membrane series was thus investigated for the concentration of acetate and 2,3-butanediol within the gas fermentation broth, this built on the work within the previous Section of the direct filtration of the broth. This was due to the low permeances exhibited through the direct filtration of the broth observed in Section 3.3.4 and above in Table 3-9. Analogous to the series discussed in the introduction (Figure 3-1), Figure 3-19 shows a schematic of the section of the membrane series to be investigated in the following Section, focusing on the purification using NF and concentration using NF / RO. As NF270 exhibited a relatively low rejection of the fermentation products, it was used to partially purify the broth. Then the NF270 permeate was concentrated with either NF90 or BW30. The ability of the two membranes to concentrate the partially purified fermentation broth could then be compared.

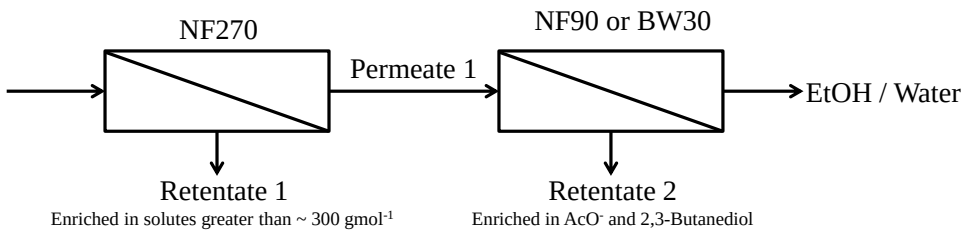

Figure 3-19. Schematic of the membrane series of NF and NF / RO being investigated.

3.3.6.2 Separation Performance of NF270 within the membrane series

Initially the rejection of the metabolites by NF270 was investigated. Figure 3-20 shows a typical feed and permeate stream for this filtration. The loss in colour of the broth has been attributed to the removal of various vitamins and their metabolised products as well as some of the divalent salts which are present within the initial fermentation growth media. The exact composition of these components within the feed and permeate were not fully investigated due to the vast number of components present and complexity in identifying them. The rest of the study has therefore focused on the metabolites ethanol, 2,3-butanediol and acetate.

Figure 3-20. Photograph of solutions of the permeate from the cell recycle (left) and the permeate after filtration with NF270 (right).

An investigation into the process parameters for the filtration using NF270 was undertaken (Figure 3-21). This constituted a more systematic examination than previously done in this Chapter:

- *Filtration Pressure*: An increase in pressure had little effect on the total flux of NF270 when permeating the fermentation broth (Figure 3-21.a). This indicates possible fouling or a large amount of concentration polarisation at the membrane surface. Rejection of ethanol, acetate or 2,3-butanediol remained relatively unchanged with increasing pressure. Rejection of 2,3-butanediol is higher (40.1 % at 15 bar) than for the previously studied fermentation broth (Table 3-7, 30.9 % at 15 bar) possibly due to the higher concentration of 2,3-butanediol within this fermentation broth (7.7 g L^{-1} vs. 3.34 g L^{-1}).
- *Stirring Speed*: A change in the rotational speed of the magnetic stirrer just above the membrane surface had a large effect on the total membrane flux as well as the rejection of 2,3-butanediol. With an increase in stirrer speed from 125 to 1100 rpm the total

permeance increased from 1.95 to 4.47 kg m^{-2} h^{-1} bar^{-1} and the rejection of 2,3-butanediol increased from 31 to 48 % (Figure 3-21.b). This increase in permeance and rejection indicates that the fouling / concentration polarisation at the membrane surface can be limited through an increased turbulence. The increase in 2,3-butanediol rejection indicates that concentration polarisation is present at lower rpm and although the increased permeance would be beneficial to the membrane process an increase in 2,3-butanediol rejection would be undesirable as it would have to be concentrated further in the second stage of the filtration.

- *pH*: Change in the pH of the fermentation broth had the same effect as observed previously within this Chapter for the model solutions of acetate (Figure 3-4). An increase in pH gave a rise in the rejection of acetate due to the level of dissociation of the acetate anion (Figure 3-21.c). From a pH of 4.1 rejection increased from 8.96 % to a rejection of 39.3 % at pH 6.1. Interestingly, the permeance also increased with increasing pH to a maximum of 3.13 kg m^{-2} h^{-1} bar^{-1} at pH 6.1. This has been attributed to a change in the surface charge of the membrane at higher pH. This could in turn effect the level of fouling / concentration polarisation at the membrane surface increasing the permeance at higher pH's. Increased permeance has been observed previously for NF270 at high pH.[210]
- *Feed Temperature*: Change in the feed temperature had the expected effect of an increase in total flux and a decrease in rejection, most obvious for the rejection of 2,3-butanediol (Figure 3-21.d). This is due to the increase in temperature allowing for increased mobility of the polymer chains within the membrane creating a looser structure, which therefore results in an increased permeance and lower rejection.

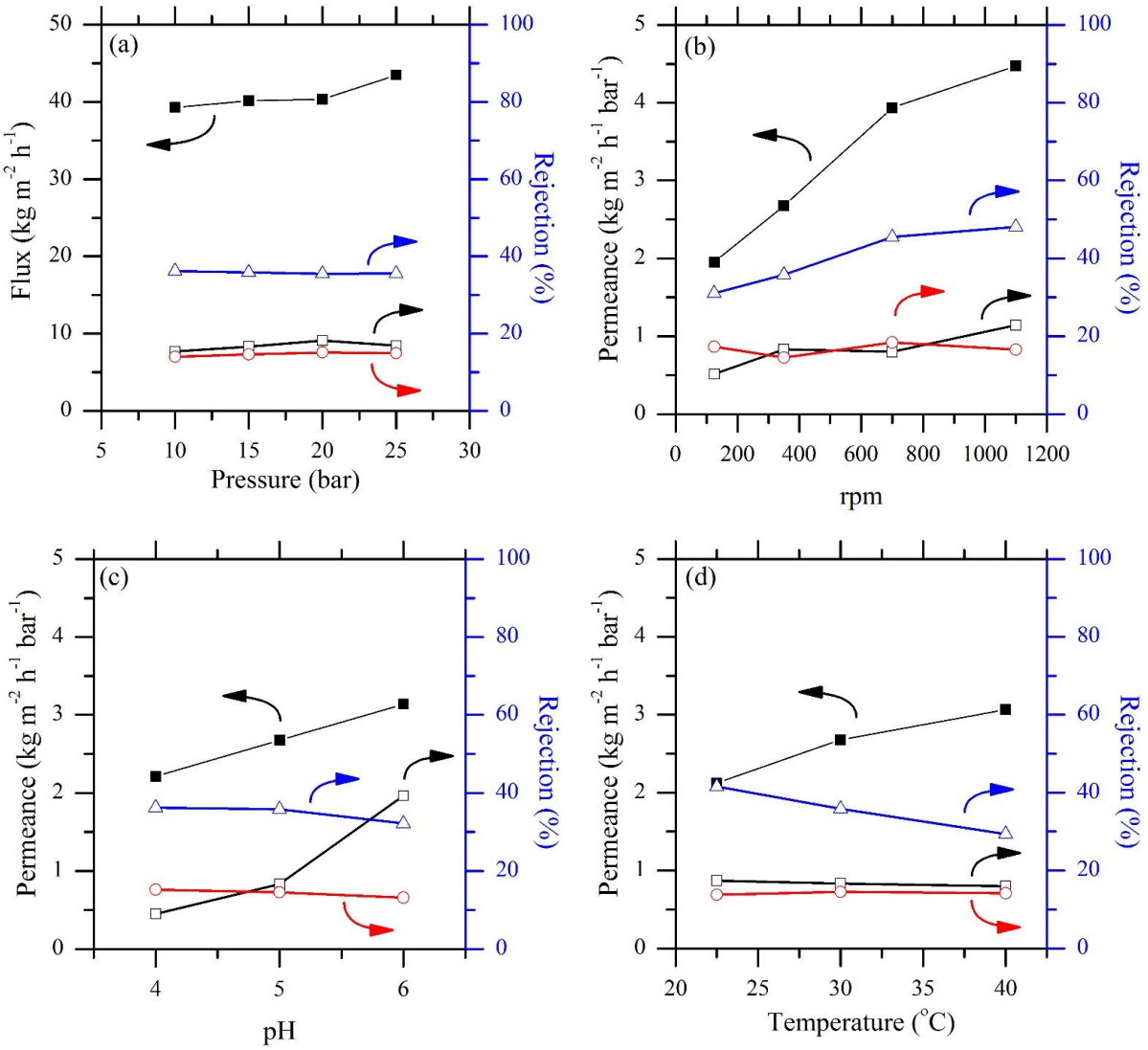

Figure 3-21. **NF270**: *Change in permeance and rejection of metabolites during filtration of the fermentation broth from the microfiltration permeate: (■) total flux or permeance; (Δ) rejection of 2,3-butanediol; (□) rejection of acetate; (○) rejection of ethanol. Graphs show the effect of; (a) change in feed pressure, (b) change in stirrer speed, (c) change in pH and (d) change in temperature. Constant filtration conditions: 30 ºC, 15 bar, 350 rpm, pH 5.1.*

3.3.6.4 Examining the membrane series – NF90 vs. BW30

The permeate from the NF270 filtration of the gas fermentation broth was then used for filtrations with NF90 or BW30 to ascertain the ability of these membranes to concentrate acetate and 2,3-butanediol within the fermentation broth. The average concentrations for each of the metabolites in the feed and the NF270 permeate are presented in Table 3-10.

Table 3-10. Concentrations of ethanol, acetate and 2,3-butanediol within the NF270 feed and permeate.

	Concentration (g L^{-1})		
	Ethanol	**Acetate**	**2,3-Butanediol**
Feed NF270	47	3.5	7.7
Permeate NF270	43	3.0	5.0

3.3.6.5 Separation performance of NF90 within the membrane series

The process parameters for the concentration using NF90 was investigated in the same manner as for the NF270 broth:

- *Filtration Pressure*: An increase in pressure from 15 bar to 30 bar resulted in an increase in the total flux from 27.3 to 50.7 kg m^{-2} h^{-1} (Figure 3-22.a). The rejection of acetate and 2,3-butanediol also slightly increased with increasing transmembrane pressure to a maximum of 87.5 and 90 % respectively. This large increase in total flux indicates that there is limited fouling and concentration polarisation occurring during the filtration and the remaining experiments were run at a pressure of 30 bar due to this. Rejection of 2,3-butanediol was slightly lower than for the gas fermentation broth that hadn't been purified through NF270 (90 % vs 97.5 % respectively at 30 bar). This also reflects the difference in rejection of 2,3-butanediol for the pure (Figure 3-3) and broth (Table 3-7) mixtures reported above (87.9 vs 92.6 % respectively at 15 bar). This could indicate that there is some beneficial fouling aiding 2,3-butanediol rejection when components of the broth are present.
- *Stirring Speed*: The results of altering the rotation speed of the stirrer above the membrane surface (Figure 3-22.b) show that with an increase in revolutions of the stirrer

from 100 to 700 rpm, the permeance increased from 1.47 to 1.92 kg m^{-2} h^{-1} bar^{-1}. The rejection of each metabolite also increased with ethanol, acetate and 2,3-butanediol being rejected at 26.3, 88.9 and 92.6 % respectively at a stirrer speed of 700 rpm. An increased turbulence decreases the small amount of fouling / concentration polarisation present at the membrane surface and a high cross-flow velocity should therefore be utilised when applying this membrane process to limit these factors.

- *pH*: As presented with the previous examples acetate rejection is dependent upon the solution pH (Figure 3-22.c). Acetate rejection increased from 28.2 to 87.5 % with a change in pH from 3 to 6. The rejection of 2,3-butanediol and ethanol; however, remain relatively constant with a change in pH due to the rejection of these components being mainly based on molecular size / shape.[211] The membrane permeance also remains relatively consistent at 1.72 and 1.69 kg m^{-2} h^{-1} bar^{-1} at a pH of 3 and 6 respectively.
- *Feed Temperature*: The change in membrane performance with temperature is also as expected. When increasing the temperature from 22.5 to 40 ºC the total membrane permeance increases from 1.29 to 2.74 kg m^{-2} h^{-1} bar^{-1} and the rejections of ethanol, acetate and 2,3-butanediol all marginally decrease by between 3 to 7 % (Figure 3-22.d).

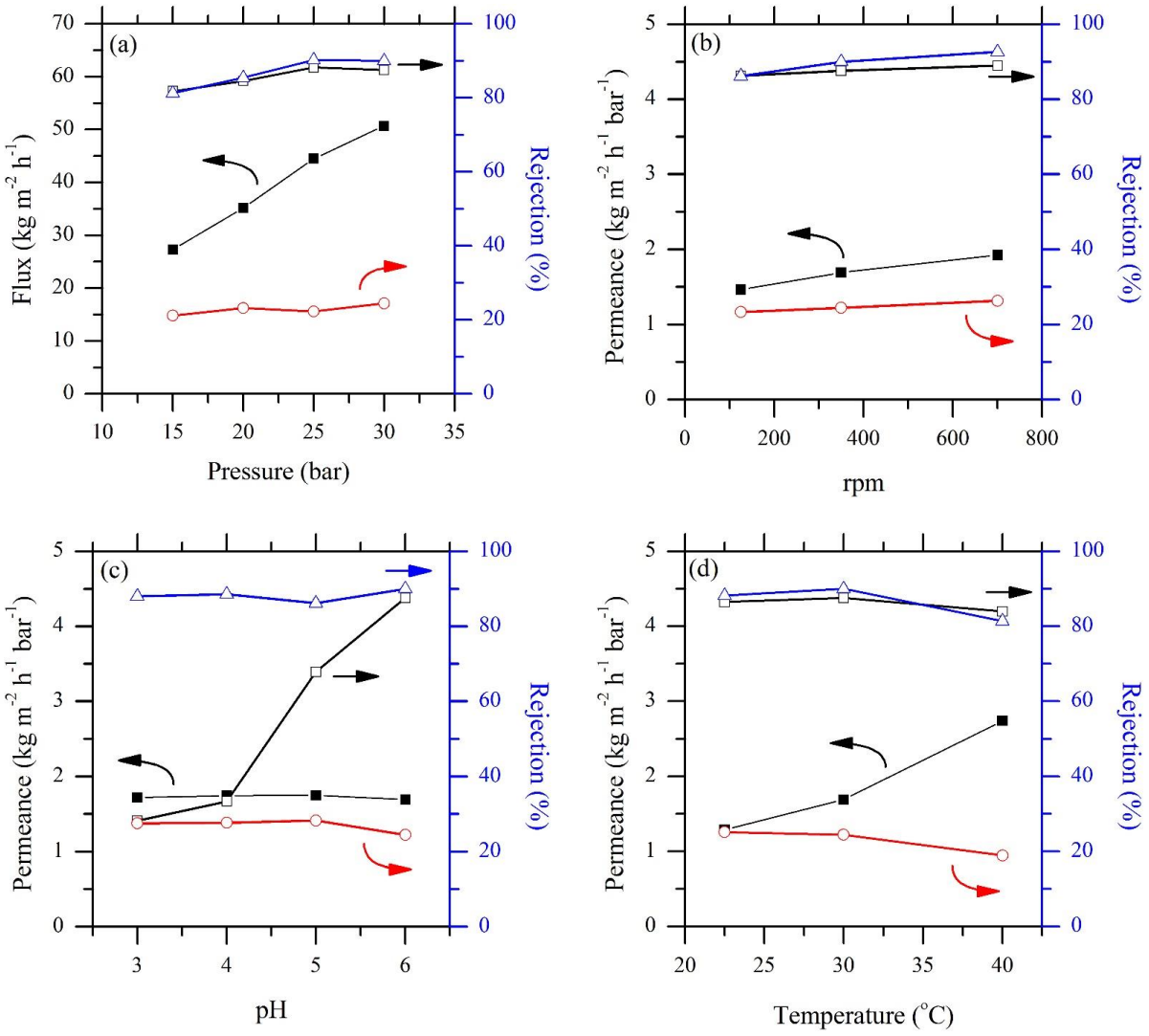

Figure 3-22. **NF90**: *Change in permeance and rejection of metabolites during filtration of the NF270 permeate: (■) total flux or permeance; (Δ) rejection of 2,3-butanediol; (□) rejection of acetate; (○) rejection of ethanol. Graphs show the effect of; (a) change in feed pressure, (b) change in stirrer speed, (c) change in pH and (d) change in temperature.*
Constant filtration conditions: 30 ºC, 30 bar, 350 rpm, pH 6.

3.3.6.6 Separation Performance of BW30 within the membrane series

The ability of BW30 to concentrate acetate and 2,3-butanediol was studied in the same manner as for NF90. BW30 generally exhibited higher rejections of both acetate and 2,3-butanediol, but at a slightly lower total permeance due to the membrane being tighter, classed as a low pressure reverse osmosis membrane as opposed to the nanofiltration membrane NF90 (Table 3-1).

- *Filtration Pressure*: The membrane total flux increased with an increase in applied pressure from 10.2 kg m^{-2} h^{-1} at 15 bar to 24.4 kg m^{-2} h^{-1} at 30 bar (Figure 3-23.a). This flux is over twice that of when the direct broth was filtered (10.7 kg m^{-2} h^{-1} at 30 bar). The rejection of each solute (ethanol, acetate, 2,3-butanediol) also increased with an increase in the applied pressure. This is in accordance to the observations previously with model solutions of 2,3-butanediol (Figure 3-5).
- *Stirring Speed*: With an increase in rpm from 125 to 700 the permeance increased from 0.76 to 0.96 kg m^{-2} h^{-1} bar^{-1} whilst the rejections remained relatively constant (Figure 3-23.b).
- *pH*: An increase in pH gave the respective increase in acetate rejection from 34.9 to 93.9 % when increased from pH 3 to pH 6 (Figure 3-23.c), marginally lower than the 94.6 % rejection reported previously at pH = 6.5 in Section 3.3.4 (Table 3-8). The rejection of 2,3-butanediol and ethanol remained constant throughout the pH range and the permeance exhibited a slight increase from 0.59 to 0.81 kg m^{-2} h^{-2} bar^{-1}. As with the previous membranes this could be due to a change in the surface charge of the membrane changing the amount of fouling or concentration polarisation at the membrane surface.
- *Feed Temperature*: Increasing the feed temperature again increased the membrane permeance from 0.60 to 1.26 kg m^{-2} h^{-1} bar^{-1} from 22.5 to 40 ºC (Figure 3-23.d) with only a slight decrease in rejection of metabolites.

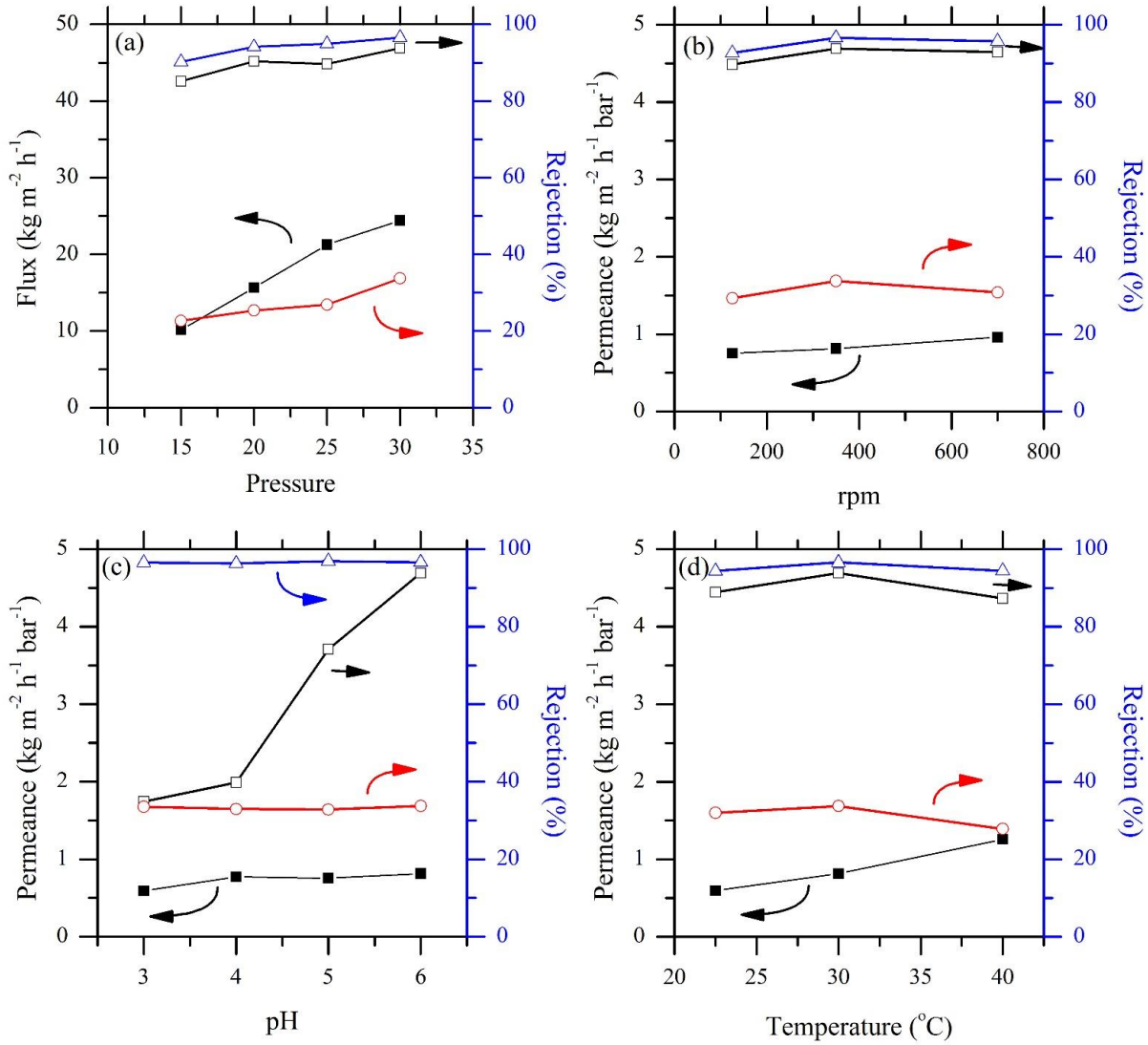

Figure 3-23. **BW30**: *Change in permeance and rejection of metabolites during filtration of the NF270 permeate: (■) total flux or permeance; (Δ) rejection of 2,3-butanediol; (□) rejection of acetate; (○) rejection of ethanol. Graphs show the effect of; (a) change in feed pressure, (b) change in stirrer speed, (c) change in pH and (d) change in temperature.*
Constant filtration conditions: 30 ºC, 30 bar, 350 rpm, pH 6.

The performance of the two membranes NF90 and BW30 under the same process conditions are directly compared in Table 3-11. BW30 exhibits slightly higher rejections of ethanol, acetate and 2,3-butanediol at less than half the permeance of NF90. This is expected due to BW30 being a tighter membrane; however, NF90 still exhibits comparatively high rejections of acetate (87.5 %) and 2,3-butanediol (90.0 %) and a lower ethanol rejection (24.4 %). A number of process parameters will need to be evaluated to determine if the NF90 or BW30 membrane would be most suitable such as pump flow rates and costs etc. Both the NF90 and BW30 membranes were tested

to ascertain the maximum concentrations of acetate and 2,3-butanediol achievable. NF90 was able to achieve concentrations of acetate (22.5 g L^{-1}) and 2,3-butanediol (39.3 g L^{-1}) and BW30 achieved concentrations of acetate (19.8 g L^{-1}) and 2,3-butanediol (37.6 g L^{-1}) after permeation of 90 % of 50 mL of NF270 permeate.

Table 3-11. Comparison of the performance of NF90 and BW30 for the concentration of the NF270 permeate.

Membrane	Permeance	Rejection (%)		
	(kg m^{-2} h^{-1} bar^{-1})	Ethanol	Acetate	2,3-Butanediol
NF90	1.69	24.4	87.5	90.0
BW30	0.81	33.8	93.9	96.6

Process conditions: 30 bar, 30 ºC, pH 6, rpm 350. Feed concentrations: ethanol (43 g L^{-1}), acetate (3.0 g L^{-1}), 2,3-butanediol (5.0 g L^{-1}).

3.3.6.7 Effect of varying fermentation broths

Two additional gas fermentation broths with different metabolite concentrations were then investigated (fermentation broths B and C in Table 3-12). The broths were filtered through NF270 and the permeate concentrated with either NF90 or BW30 as already presented in Figure 3-19. The concentrations of ethanol, acetate and 2,3-butanediol within each broth tested are presented in Table 3-12.

Table 3-12. Metabolite concentrations of the different gas fermentation broths tested.

Fermentation Broth	Concentration (g L^{-1})		
	Ethanol	**Acetate**	**2,3-Butanediol**
A – High 2,3-butanediol	47.0	3.50	7.70
NF270 Permeate A	43.0	3.00	5.00
B – Medium 2,3-butanediol	47.8	3.27	1.69
NF270 Permeate B	43.6	2.89	1.16
C – high acetate, low 2,3-butanediol	45.0	5.53	0.53
NF270 Permeate C	42.0	4.45	0.4

The total permeance of NF270 (Figure 3-24.a) was found to be dependent on the gas fermentation broth used with the lowest permeance exhibited with broth A which had the highest concentration of 2,3-butanediol. The rejection of acetate and 2,3-butanediol were dependent on their concentrations within the broth. At higher concentrations their rejections were higher (Figure 3-24.b). This could be a limitation of this method as if the fermentation was optimised to produce much higher concentrations of these metabolites the increased rejection will mean a comparatively smaller increase in concentration within the NF270 permeate. NF90 and BW30 exhibited similar rejections of each metabolite within each of the gas fermentation broths (Figure 3-24.c, Figure 3-24.d). The permeances for NF90 were reasonably consistent for each broth; however, broth B had the highest permeance and broth C the lowest, this could be related to the acetate concentration being highest in broth C and lowest in broth B; although, there may be a combination of factors that are also affecting the permeance. BW30 exhibited no significant change in permeance for each gas fermentation broth.

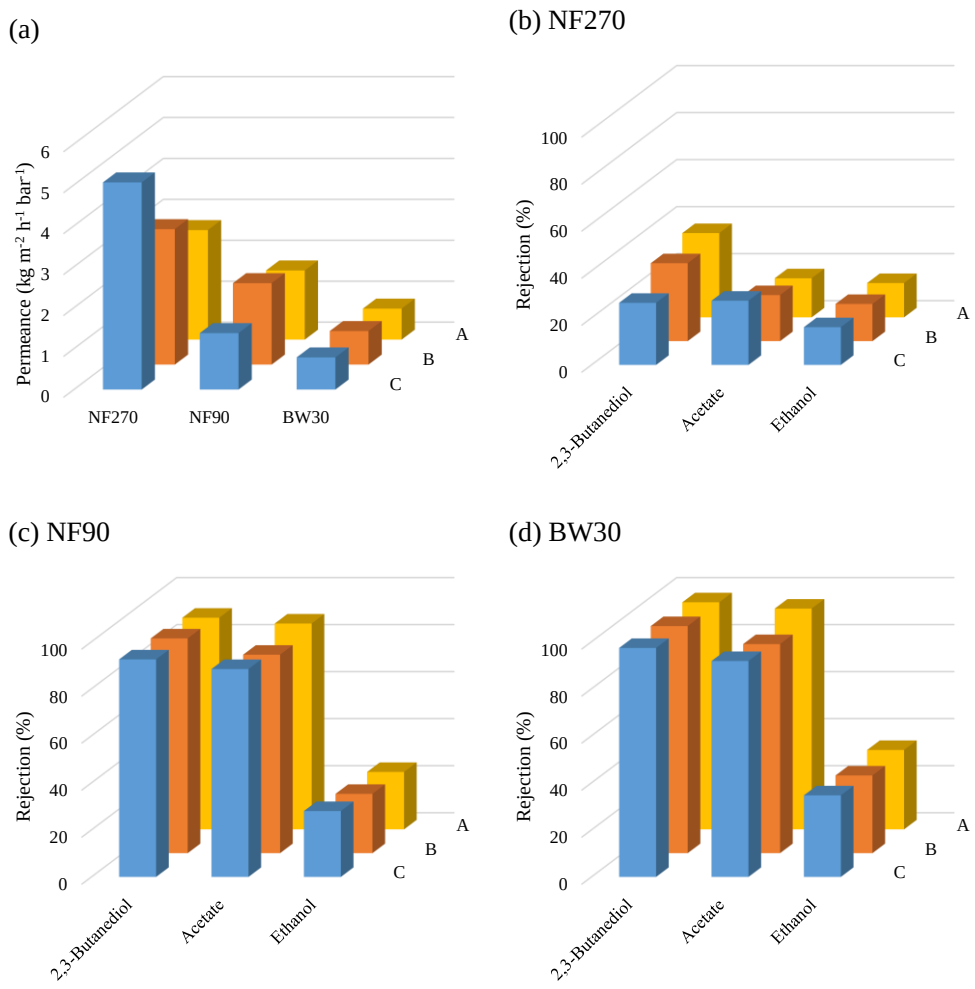

Figure 3-24. Comparison of the flux (a) and rejection characteristics (b) NF270, (c) NF90, (d) BW30 with the three tested gas fermentation broths with varying metabolite concentrations. Conditions: 350 rpm, 30 ºC, NF270 = pH 5.1, 15 bar, NF90 and BW30 = pH 6.1, pressure 30 bar.

These results indicate that the membrane series of NF270 and either NF90 or BW30 could be used to concentrate acetate and 2,3-butanediol before further purification. The process schematic presented in Figure 3-25 shows the process used within these experiments. A number of costs will need to be weighed up before this process could be applied to a fermentation including the equipment costs such as for the membranes and associated pumps etc. as well as the cost of NaOH required to alter the pH of the NF270 permeate to > 6. One major problem identified with this process is that the membranes are non-selective towards ethanol. This requires an ethanol separation from both the NF90 / BW30 permeate and retentate. The concentration in each of these streams was ~ 30 g L^{-1} and ~ 50 g L^{-1} for the permeate and retentate respectively. This separation; however, could be achieved through the use of a pervaporation process[59] and is the focus of the work carried out within the following Chapter 4.

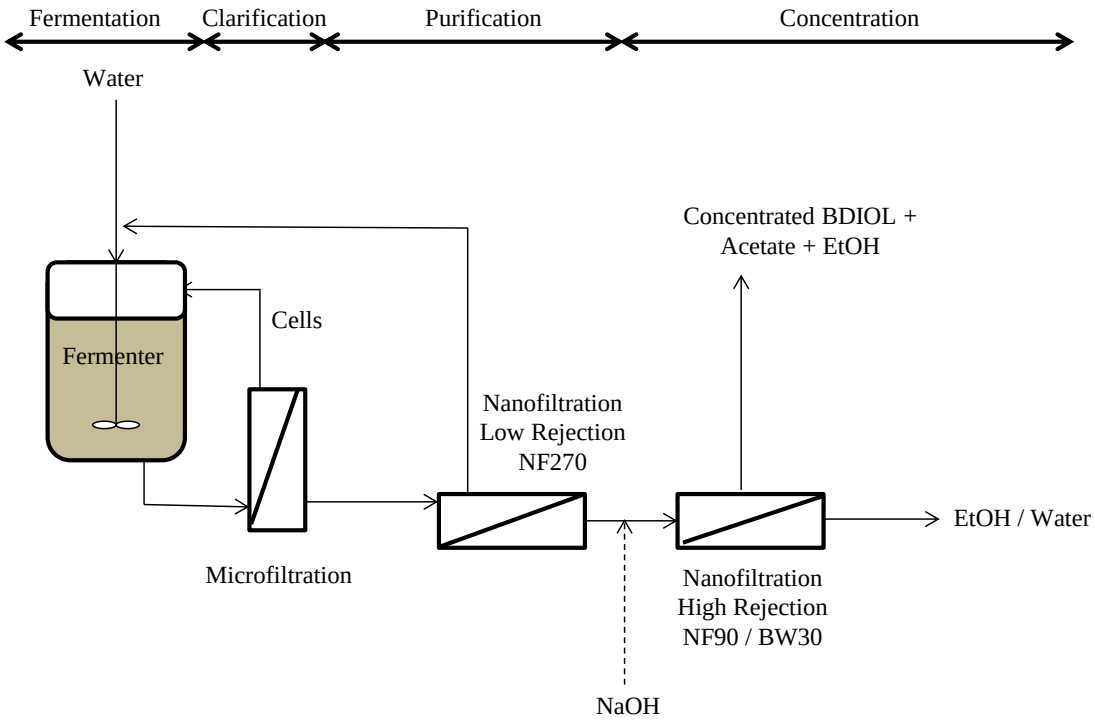

Figure 3-25. Schematic of the process used in the membrane series experiments performed at LanzaTech.

3.4 Conclusions

NF and RO have been studied for the partial purification and concentration of the fermentation products ethanol, acetate and 2,3-butanediol within a gas fermentation broth.Initially a number of different commercial membranes were investigated and the flux and rejection characteristics determined for aqueous solutions of 2,3-butanediol, acetic acid and ammonium acetate. A number of membranes were identified to exhibit high rejection of 2,3-butanediol (BW30FR, BW30, SE, SG) as well as a number with very poor rejection (NF270, NF245, NF). Acetate rejection varied with pH for each membrane with a number exhibiting high rejection of ammonium acetate (BW30, SE, BW30FR, SG), but all membranes exhibited a relatively poor rejection of acetic acid (< 40 %).

NF270, NF90 and BW30 were investigated for the purification / concentration of a gas fermentation bleed stream. Results indicate NF270 can purify the broth due to relatively low rejections of 2,3-butanediol and acetate but good clarification of the media. NF90 and BW30 exhibited high rejection of 2,3-butanediol (92.6 and 94.6 % respectively) and good rejection of acetate (70.5 and 74.4 % respectively); however, NF90 exhibited slightly higher irreversible fouling compared to BW30. When the pH of the broth was increased to 6.5, the rejection of acetate

was increased by BW30. BW30 has been identified as a suitable membrane for the concentration of 2,3-butanediol and acetate within a gas fermentation broth.

By investigating the rejection of other alcohols by BW30 it was identified that its exceptional rejection of 2,3-butanediol can be attributed to the steric properties of the molecule and not solely upon its MW. Isobutanol was also identified as a possible fermentation product that could be concentrated within a fermentation bleed stream by BW30 due to its relatively high rejection (77 %).

The use of NF270, NF90 and BW30 to purify and concentrate the gas fermentation broth was studied further with a number of different fermentation broths. The membrane series of NF270 to partially purify the broth and NF90 or BW30 to concentrate acetate and 2,3-butanediol was investigated. The process parameters of pressure, overhead stirring, pH and temperature were investigated for each separation. The membranes also exhibited similar separation performance with a variety of fermentation broths. Overall, the membrane series of NF270 followed by either NF90 or BW30 has been identified as a suitable process for the concentration of 2,3-butanediol and acetate within a fermentation broth. Concentrations of 2,3-butanediol up to 39.3 g L^{-1} and acetate up to 22.5 g L^{-1} were achieved equating to a > 5 fold increase in concentration within a partially purified fermentation bleed stream.

Overall this work has shown that NF and RO membranes could potentially be used to replace part of the distillation separation of low volatility alcohols from fermentations. This membrane fractionation purification approach to fermentations can be more widely applied across Industrial Biotechnology, hopefully enabling lower energy, more sustainable separations.

Chapter 4

ZIF-8-PDMS MMMs for Ethanol Pervaporation: Effect of 2,3-Butanediol and Acetate

The work within this chapter stems from initial studies conducted during a visit to the University of Stellenbosch under the supervision of Prof. Len Barbour and Dr. Percy van der Gryp. There, preliminary experiments were conducted on the pervaporation of 2,3-butanediol and ethanol by the described MMMs and the interactions these fermentation products may have with ZIF-8. These preliminary investigations led to the work outlined within the following Chapter.

4.1 Introduction

As discussed in Chapter 2, pervaporation could provide a low energy alternative for the recovery of volatile fermentation products when compared to distillation, the dominant separation technology in this field.[12] Despite this, improved alcohol-water separation is required from pervaporation membranes to meet the performance necessary for their implementation.[50] New membrane materials are being developed with the aim of improving the separation performance and of these novel materials Mixed-Matrix Membranes (MMMs) have some of the highest

performances.[11] Comprised of an inorganic phase dispersed within a polymer matrix, they are a trade-off between the high-performance of inorganic materials and the processability and low-cost of polymer membranes.

Of the different inorganic materials used in MMMs, MOFs are novel microporous materials that have exhibited high water-alcohol separation performance, with many improving the pervaporative performance when incorporated into MMMs.[11] One subclass of MOFs, Zeolitic Imidazolate Frameworks (ZIFs), have produced some of the highest performing membranes in terms of flux and separation factor when incorporated into MMMs. One of the first examples of a MOF MMM for organophilic pervaporation was ZIF-8 in a polymethylphenylsiloxane (PMPS) matrix. The study mainly looked at isobutanol pervaporation, but the synthesised membrane also demonstrated improved ethanol, 1-propanol, 1-butanol and 1-pentanol pervaporation properties.[132] Other studies have also fabricated membranes of ZIF-8 in PDMS for butanol pervaporation[171] and the performance further enhanced by improving the fabrication method.[172, 173]

However, of these ZIF-8 MMMs, there has been limited studies on the effect a combination of fermentation products may have on the pervaporation performance. Most have been limited to single solutes and the ABE fermentation process. Fermentation mixtures on the other hand are incredibly complex with numerous organic and inorganic components as either the growth media or different fermentation products and by-products. It can be argued that it is cost effective to produce more than one fermentation product simultaneously to be able to off-set the production costs with products of differing value. It is also sometimes impossible to produce one fermentation product without another due to the metabolic pathway of the microorganism used. Therefore, the majority of fermentations consist of a mixture of valuable products. This study focuses on a gas fermentation process, introduced in Chapters 1 and 3, which produces ethanol as a main fermentation product, but also acetate and 2,3-butanediol (Figure 4-1) as co-products and the effect that these co-products may have on the pervaporation performance of a MMM of ZIF-8-PDMS. Pervaporation could be used as a low energy separation process to remove ethanol from the fermentation mixture before further downstream separation of 2,3-butanediol and acetic acid. It is intended that this study provides an insight into the effect other organic products may have on MMMs. Therefore, any positive or negative synergistic effects of the mixture of fermentation products can be identified and allow for further tailoring of these membranes to achieve greater organic / water separations in pervaporation. Therefore, current distillative separations could be replaced and a reduction in energy costs for recovery of these fermentation products achieved.

This meets the specific objectives of this thesis:

- To identify suitable membrane processes for the low energy recovery of products from a gas fermentation broth.

- To identify ways to improve the recovery of products from a gas fermentation process.
- To improve the understanding of membrane separation processes.

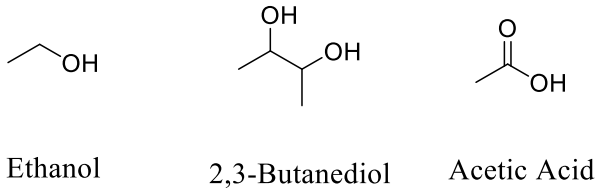

Figure 4-1. Chemical Structures of Ethanol, 2,3-Butanediol and Acetic Acid.

4.2 Materials and Methods

4.2.1 Materials

Materials were purchased from common laboratory suppliers, specifically; Zinc Nitrate Hexahydrate (99 %, Alfa Aesar, UK), 2-Methylimidazole (97%, Alfa Aesar, UK), Polydimethylsiloxane RTV615 (Techsil, UK), Hexane (HPLC grade, VWR), Methanol (Reagent Grade, VWR), Ethanol (Reagent Grade, VWR), Acetic Acid (99.7 %, Sigma Aldrich), 2,3-Butanediol (Mixture of isomers, 98 %, Acros, stored in a desiccator), Sulphuric Acid (96 %, Acros), N-methyl-2-pyrrolidinone (99 %, Alfa Aesar), Poly(vinylidene fluoride-co-hexafluoropropylene) (M_w ~400 000, Sigma Aldrich). Water for pervaporation experiments was taken from an MIDI-RO 10-200-EP unit (< 1 μS cm^{-1} @ 25 ºC). Water for HPLC eluent was taken from a Milli-Q system (0.02 μS cm^{-1} @ 25 ºC). The polypropylene (PP) / polyethylene (PE) nonwoven backing layer for membranes (Novatexx 2431) was supplied by Freudenberg (Germany).

4.2.2 Synthesis of ZIF-8

The synthesis of ZIF-8 was adapted from the procedure presented by Cravillon *et al*.[212] In a typical experiment, a solution of zinc nitrate hexahydrate (2.92 g, 9.82 mmol) in methanol (200 mL) and 2-methylimidazole (6.30 g, 76.8 mmol) in methanol (200 mL) were poured together and stirred at room temperature for 1 hour. The reaction mixture was then centrifuged at 6000 rpm for 10 minutes. The supernatant was decanted off and replaced with an equal amount of fresh methanol. This was repeated 3 times to remove any unreacted starting materials. The as-

synthesised ZIF-8 material was then dried at 40 ºC in a vacuum oven and lightly ground to produce a free flowing powder before use in further experiments.

4.2.3 Synthesis of PDMS and ZIF-8-PDMS membranes

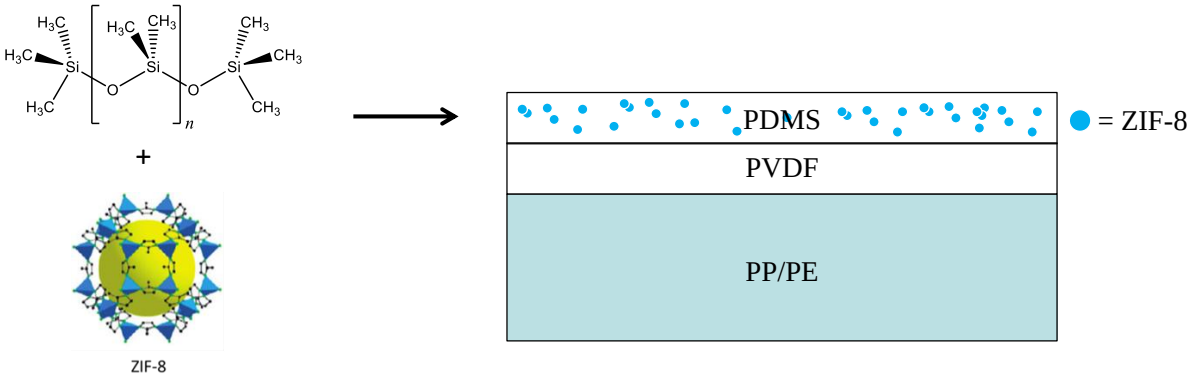

Figure 4-2. Schematic of the as-synthesised composite MMMs.

The mixed matrix membranes were composed of PDMS on a PVDF support on a PP / PE nonwoven backing layer (Figure 4-2). PVDF supports were prepared by dissolving 20wt% PVDF in N-methyl-2-pyrrolidone (NMP) via overhead stirring for 6 hours. The solution was then sonicated for 2 hours and allowed to stand overnight for removal of trapped air bubbles. The polymer doped solution was then cast onto a PP / PE support (Novatexx 2431) taped onto a glass plate, with a doctor blade set to a height of 200 µm. A casting speed of 90.0 mm s^{-1} was used and controlled with a casting machine (Elcometer 4340). The cast membrane was then immersed in water overnight to achieve phase inversion. After phase inversion the membrane was removed from the water bath and allowed to dry in air overnight.

For synthesis of the PDMS and mixed matrix membranes, 8 g of RTV 615A and 0.8 g of RTV615B (Techsil, UK) (Figure 4-3) were mixed together with 10 mL hexane. For the synthesis of ZIF-8 / PDMS membranes ZIF-8 was added to the polymer dope solution (Table 4-1). The solutions were then stirred (15 mins) and sonicated (15 mins) alternately at room temperature and this was repeated 3 times. The solution was then heated with stirring at 60 ºC and once the solution became viscous (< 2 hours), it was cast onto the PVDF supports with a casting knife and doctor blade set to a height of 300 µm. The membranes were then cured in an oven at 60 ºC for 3 hours.

Table 4-1. Mass of ZIF-8 added to the polymer dope solution.

Weight Loading of ZIF-8 in membrane (wt%)	Mass of ZIF-8 added to polymer dope solution (g)
0	0
2.5	0.226
5	0.463
7.5	0.714
10	0.978

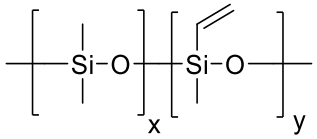

RTV 615A:
poly(dimethylsiloxane-*co*-vinylmethylsiloxane)

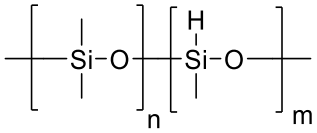

RTV 615B:
poly(dimethylsiloxane-*co*-methylhydrosiloxane)

Figure 4-3. Chemical Structures of RTV615A and RTV615B.

4.2.4 N_2 Adsorption Isotherms

Low pressure nitrogen (BOC, 99.998 %) isotherm data was collected on a Micrometrics 3Flex at 77 K. Before analysis samples were activated on the instrument under vacuum at 150 ºC for 19 hours.

4.2.5 Powder X-Ray Diffraction

Powder diffraction (PXRD) data was collected in flat plate mode on a Bruker D8 Advance equipped with monochromated Cu Kα radiation (λ = 1.54056 Å) in reflection geometry at 298 K. Crystalline samples were lightly ground before analysis. The simulated ZIF-8 PXRD pattern was calculated from single crystal data in[104] using the visualization program Mercury.[213]

4.2.6 Elemental Analysis

Elemental analyses for the dried as-synthesised ZIF-8 powder was carried out by Mr. Stephen Boyer at London Metropolitan University.

Elemental Analysis (%): **Calculated for ZIF-8**; ($C_8H_{10}N_4Zn$ = 227.6 g mol^{-1}); (C, 42.2; H, 4.43; N, 24.6); **Found**; (C, 42.1; H, 4.5; N, 24.5).

4.2.6 Thermal Gravimetric Analysis

Measurements were conducted on a Setaram TGA 92 thermogravimetric analyser from room temperature to 800 ºC with a ramping rate of 5 ºC min^{-1} under an atmosphere of either air or nitrogen. An original sample mass of ~ 15 mg was used.

4.2.7 Fourier Transform Infrared Spectroscopy (FTIR) spectroscopy

FTIR spectra were recorded over the range 4000 – 600 cm^{-1} using a Perkin Elmer Spectrum 100 FTIR spectrometer fitted with an attenuated total reflectance (ATR) detector. Spectra were averaged over 10 scans with a resolution of 1 cm^{-1}.

4.2.8 Contact Angle Measurements

Static contact angles were measured using the sessile drop method with a Dataphysics contact angle system OCA goniometer (Dataphysics, Germany). Measurements were taken 1 s after a drop of ultrapure water (18.2 MΩ cm at 25 °C) of 5 μL was placed on the surface of the membrane at room temperature. Membranes were dried at 80 ºC under vacuum for 16 h before analysis and the reported contact angle is averaged over 10 repeats.

4.2.9 Scanning Electron Microscopy (SEM)

SEM images were taken on a JEOL SEM6480LV. To achieve cross-sectional images membranes were submersed in liquid N_2 and fractured with a razor blade. Samples were then dried in a

vacuum desiccator overnight before coating with a thin layer of gold (Edwards S150B sputter coater, 2 minutes coating time) to prevent sample charging.

4.2.10 Degree of Solvent Uptake

Degree of solvent uptake experiments (sometimes called degree of swelling)[170, 171, 177] were conducted by measuring the change in mass of a piece of membrane after soaking in pure solvent. First a piece of membrane was dried at 80 ºC overnight. The mass of this dried membrane was recorded and the sample placed in a solution of pure solvent. After 24 h the sample was removed from the solution, excess solvent was removed by dabbing the sample on a filter paper and then the wet mass was recorded. The degree of solvent uptake was then measured using Equation 4-1:

$$Degree\ of\ Solvent\ Uptake = \left(\frac{w_{wet} - w_{dry}}{w_{dry}}\right) \times 100 \qquad 4\text{-}1$$

where w_{wet} is the mass of the membrane after solvent uptake and w_{dry} is the mass of the dry membrane.

4.2.11 Liquid-Phase Adsorption Determination

Samples of dried ZIF-8 (0.05 g) were placed in separate glass vials and heated at 150 ºC in a vacuum oven for 18 h. The samples were then mixed with 2.5 g of an aqueous solution of either ethanol or 2,3-butanediol (0.1 - 20 wt%) for 24 h on a shaker (IKA Vibrax) at room temperature (22 ºC). After 24 h, the sample was then centrifuged for 5 min at 13 000 rpm and filtered through a 0.22 μm syringe filter (Millipore) and the equilibrium concentration of the supernatant was obtained using HPLC (see below). The adsorbed amount of alcohol was determined using the Equation 4-2:

$$Q = \frac{M(C_i - C_e)}{m} \qquad 4\text{-}2$$

where Q is the amount adsorbed by ZIF-8 (g g^{-1}), M is the mass of solution added to the adsorption experiment (g), C_i is the initial concentration of the alcohol (g g^{-1}), C_e is the equilibrium concentration of the alcohol (g g^{-1}) and m is the mass of ZIF-8 used in the experiment (g).

4.2.12 Pervaporation Performance

Pervaporation was conducted on a homemade bench-scale set-up (Figure 4-4, Figure 4-5) where the flat sheet membrane supported on a porous sintered disc was sealed in a stainless steel (316) pervaporation cell with an active membrane area of 14.6 cm^2. The feed was circulated over the surface of the membrane using a peristaltic pump (25.7 L h^{-1}). The vacuum on the permeate side was maintained at below 2 mbar with a rotary vane vacuum pump (RV8, Edwards, UK) and monitored with a digital vacuum gauge (VG64, Cole Parmer, UK). The membrane was allowed to condition at the required operating conditions until steady state flux had been reached (1 hour). Permeate vapour was collected in alternating liquid nitrogen cold traps every hour for 4 hours and the membrane flux was recorded gravimetrically by weighing the amount of permeate condensed in the glass trap. Flux (J) was calculated by Equation 4-3:

$$J = \frac{\Delta w}{At} \qquad \textit{4-3}$$

where Δw is the weight of collected permeate (kg), t is the duration of the run (h), and A the effective membrane surface area (m^2). The reported data shows the average of the collected data points at steady state and error bars show the standard deviation of these.

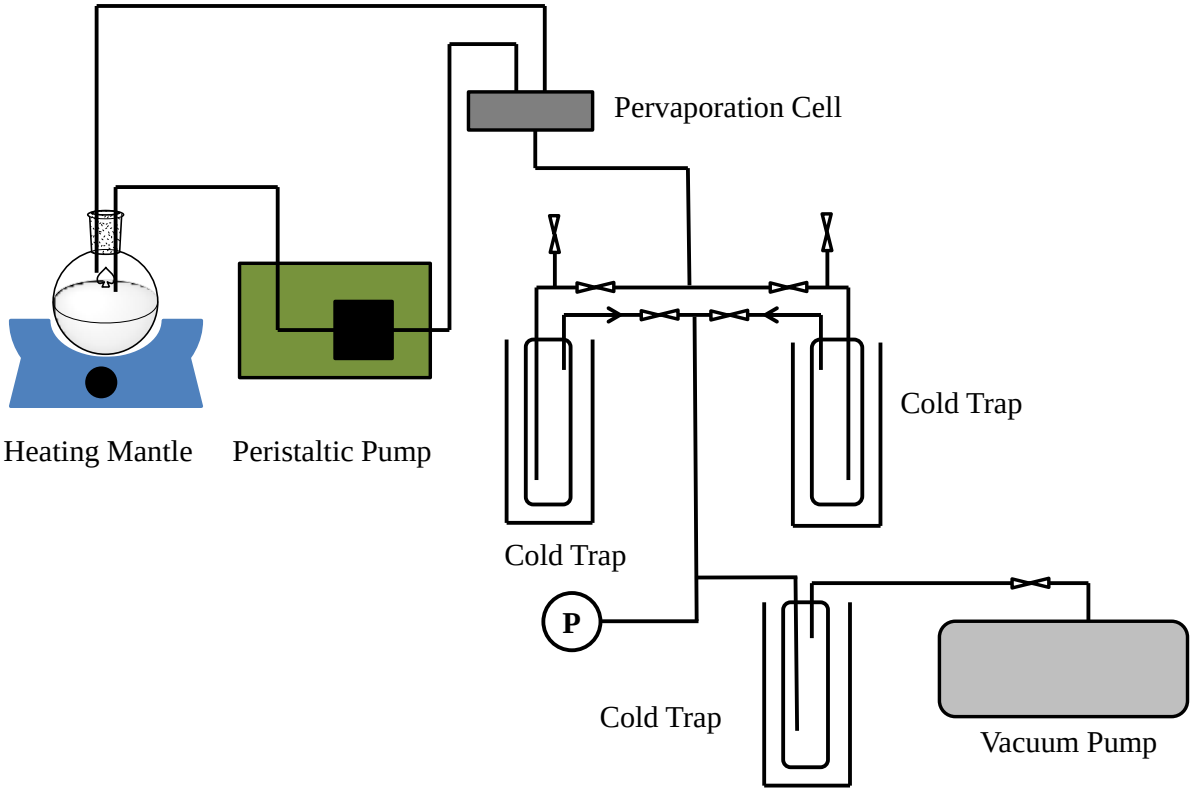

Figure 4-4. Schematic of pervaporation set-up.

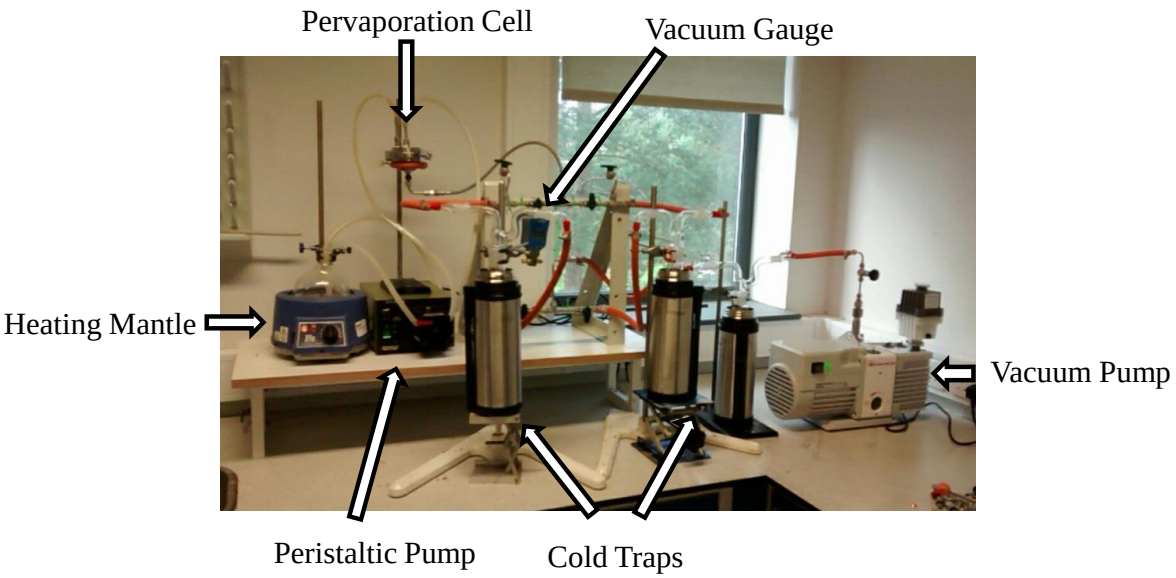

Figure 4-5. Photograph of pervaporation set-up.

4.2.13 High-Performance Liquid Chromatography

HPLC was used to determine the concentration of organic solutes in feeds, permeates and retentates using an Agilent Technologies 1260 series instrument. An ion exchange column (Agilent Hi-Plex H, 300 x 7.7 mm, 8 μm, 8 % crosslinked) fitted with a guard column of the same stationary phase (Agilent Hi-Plex H, 50 x 7.7 mm, 8 μm, 8 % crosslinked) was used at a temperature of 60 ºC. The mobile phase was 5 mM H_2SO_4 at a flow rate of 0.7 mL min^{-1}. The refractive index (RI) detector was set to 35 ºC and concentrations of solutes were interpreted through the peak area using an external calibration. Permeate samples were diluted by addition of 2 mL of water to wash out the sample from the pervaporation condenser. The reported data shows the average of the collected data points at steady state and error bars show the standard deviation of these.

Separation factor was calculated using Equation 4-4:

$$\alpha = \frac{C_P/(1 - C_P)}{C_F/(1 - C_F)} \qquad 4\text{-}4$$

where α is the separation factor of the alcohol / water studied, C_F is the weight fraction of the alcohol in the feed and C_P is the weight fraction of the alcohol in the permeate and 100 wt% = 1.

4.2.14 Fermentation Broth

The spent fermentation broth was received from Dr. Eric Liew from the University of Nottingham (now at LanzaTech, USA) and was kept frozen until use. The components of the growth medium are presented in Table 4-2 which give an indication of the composition of the spent broth.

Table 4-2. Components of growth medium used for fermentation broth.

Component	**Concentration in growth medium (g L^{-1})**
NH_4Cl	1.0
KCl	0.1
$MgSO_4$	0.098
NaCl	0.8
K_2HPO4	0.1
$CaCl_2$	0.015
Yeast Extract	1.0
Trace Elements	10 mL
Wolfe's Vitamin Solution	10 mL
$NaHCO_3$	2.0
Fructose	5.0
Reducing Agent	10 mL

The concentrations of metabolites present within the fermentation broth are given in Table 4-3. The concentrations of acetate, 2,3-butanediol and ethanol were made up to the required concentrations through addition of the appropriate amounts of each metabolite. The broth was adjusted to pH 6 through addition of NaOH.

Table 4-3. Fructose and metabolite concentrations within the spent fermentation broth before spiking with additional acetate, 2,3-butanediol and ethanol.

Component	**Concentration in broth (g L^{-1})**
Fructose	1.49
Acetic Acid	1.16
2,3-Butanediol	0.25
Ethanol	0.38

4.3 Results and Discussion

4.3.1 Synthesis of ZIF-8

Adapting the synthesis of Cravillon *et al*.[212] produced ZIF-8 with characteristic properties. The PXRD pattern of ZIF-8 was consistent with literature values (Figure 4-6.a). This indicated the successful synthesis of the structure of ZIF-8 due to the high-crystallinity observed. The thermal stability of the as-synthesised ZIF-8 was characterised through the use of TGA. As can be seen from the TGA (Figure 4-6.b) the as-synthesised ZIF-8 is stable in air up to ~ 300 ºC and up to ~ 500 ºC in an atmosphere of nitrogen. This demonstrates the high thermal stability characteristic of ZIF-8 and one of the properties why the MOF has received so much attention throughout the literature in various applications. The porosity of the ZIF-8 was probed through nitrogen physisorption experiments (Figure 4-6.c). This gave a typical isotherm characteristic of the microporosity of ZIF-8 with an apparent surface area of 1637.9 $m^2 g^{-1}$ (± 9.58) (BET). No hysteresis between the adsorption / desorption was observed. The fingerprint of the FTIR data (Figure 4-6.d) also matched well with literature values,[104, 214] indicating no presence of impurities within the sample. As the analysis reflected those of other studies the ZIF-8 synthesised was then used in the preparation of the MMMs with PDMS.

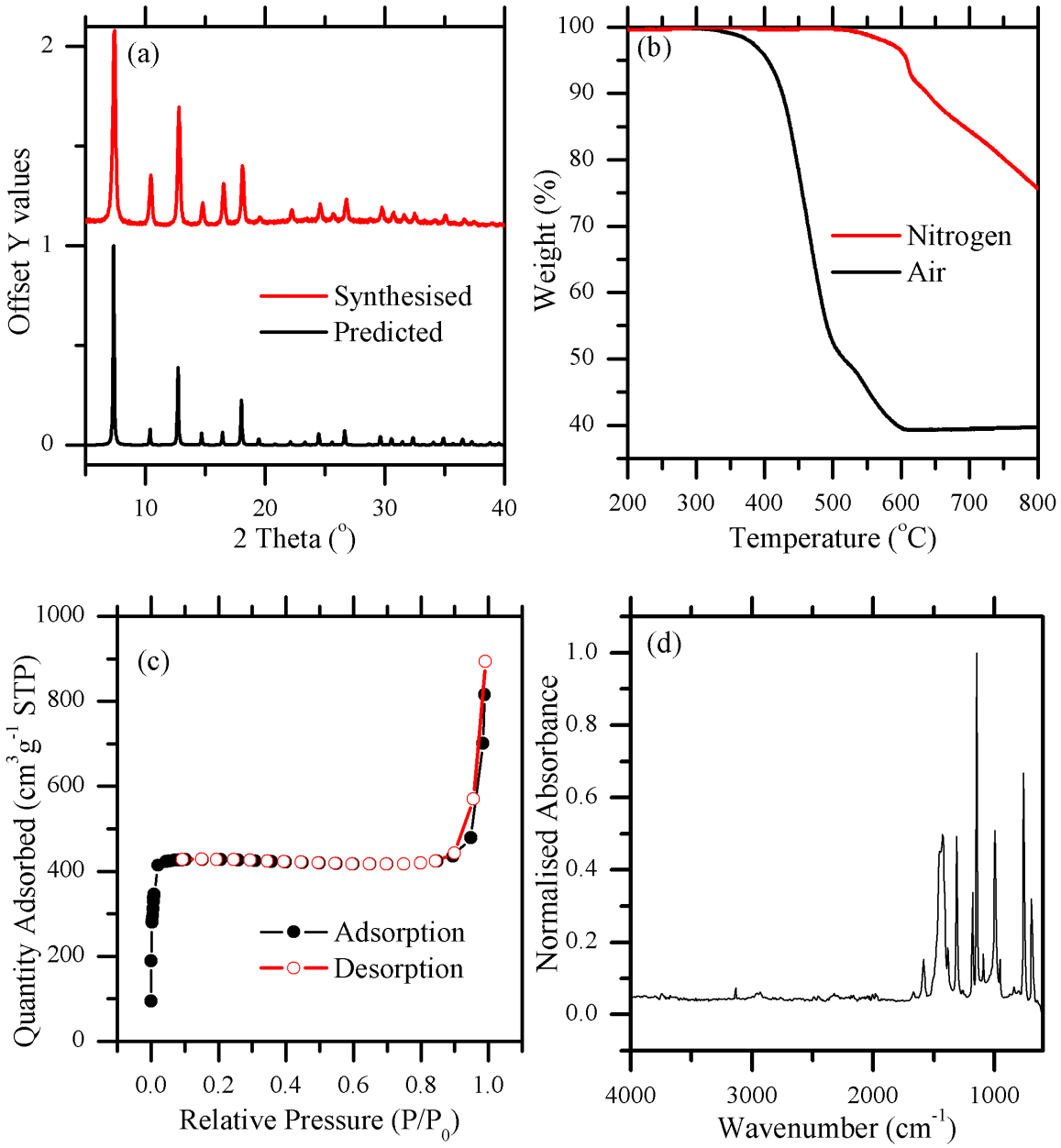

Figure 4-6. Analysis of ZIF-8 (a) PXRD showing characteristic peaks for ZIF-8, (b) TGA indicating the high thermal stability of ZIF-8, (c) N_2 Isotherm demonstrating the microporosity of the as-synthesised framework, (d) FTIR showing the characteristic absorbances of ZIF-8.

4.3.2 Characterisation of ZIF-8 Membranes

ZIF-8-PDMS MMMs were synthesised at different wt% loadings of ZIF-8 within PDMS. This was to investigate whether the co-fermentation products would have an effect on the polymer or MOF or both. The as-synthesised ZIF-8 membranes were characterised using a variety of analytical techniques. PXRD patterns of the differing wt% loading of ZIF-8 within PDMS can be seen in Figure 4-7. It is clear that with an increased loading of ZIF-8 the intensity of the peaks relative to the amorphous bump of PDMS increases. This is due to the increased loading of ZIF-8 within the membrane and the increased crystallinity arising from this.

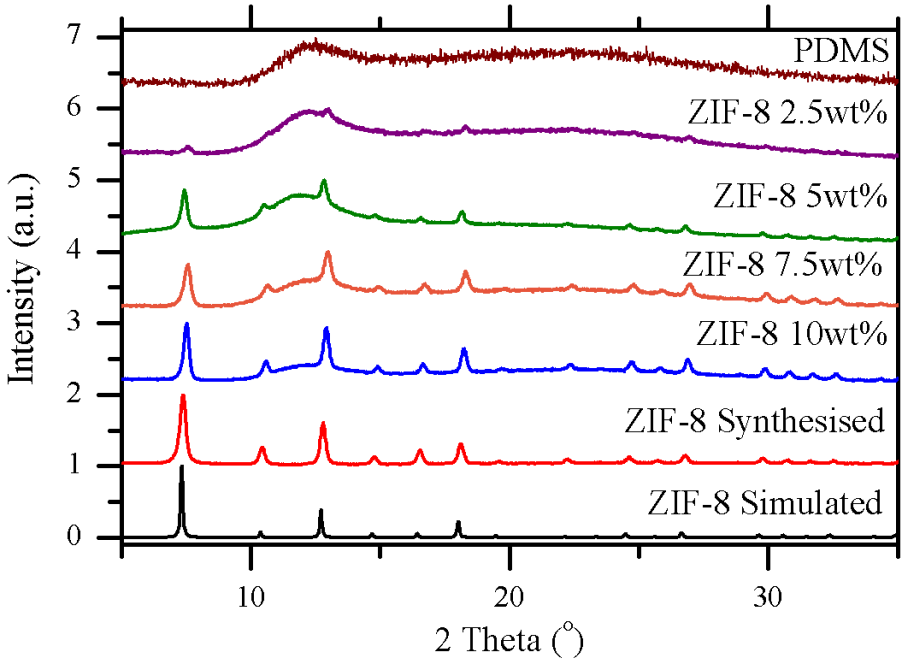

Figure 4-7. PXRD of the as-synthesised ZIF-8 PDMS membranes with different wt% loadings of ZIF-8.

TGA in an atmosphere of air provides another indication to the loading of ZIF-8 into the membrane (Figure 4-8). The analysis shows that with an increased loading of ZIF-8, an increased total mass loss between 300 and 700 ºC is observed. This is due to a higher proportion of the mass being composed of the MOF which as can be seen from Figure 4-8 has a larger % decomposition. This is due to PDMS $[Si(CH_3)_2O]_n$ being composed of mainly silica. In contrast, ZIF-8 $[Zn(C_8H_{10}N_4)]_n$ is composed of Zn and the organic linker which will combust to various CO_2 and NO_x which will be removed as gases, leading to a greater % mass loss due to a greater ratio of organic components to inorganics within the membrane.

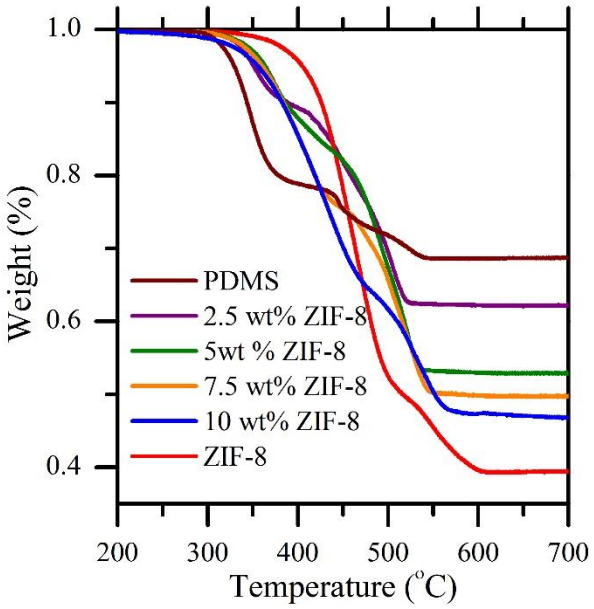

Figure 4-8. TGA of the as-synthesised ZIF-8 membranes in air.

Another property of ZIF-8 is the high level of hydrophobicity exhibited by the material. Despite the highly porous structure and large enough pore aperture of 3.4 Å to accommodate water, ZIF-8 exhibits a hydrophobic structure that exhibits virtually no adsorption of water. The high-hydrophobicity of ZIF-8 is attributed to the methyl-functionalized imidazole ligands and the saturation at the coordination with the metal centres.[109] As can be seen from the effective contact angles in Figure 4-9, an increase in the ZIF-8 loading increased the water contact angle of the membranes. This is thought to be due to an increased loading having an increased amount of ZIF-8 and therefore a higher proportion of ZIF-8 on the surface of the membrane. This would in turn give the increase in contact angle with increased loading and has been observed in other studies.[171] It can therefore be taken from this that ZIF-8 has an increased hydrophobicity compared to PDMS. An increase in surface hydrophobicity is generally thought to help improve the separation performance of a pervaporation membrane due to aiding the alcohol / water selectivity.

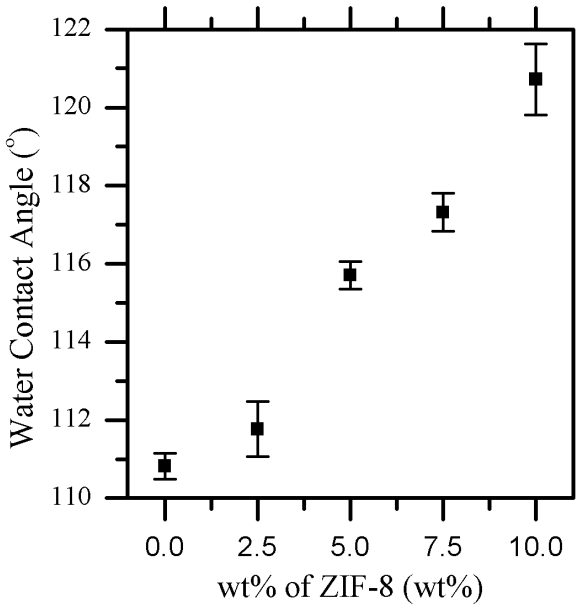

Figure 4-9. Water contact angle of the as-synthesised ZIF-8 PDMS membranes.

The FTIR data of the ZIF-8 membrane with a 10wt% loading clearly shows characteristic peaks for the ZIF-8 incorporated into the membrane (Figure 4-10). It is thought that these peaks can be mainly attributed to the different organic bonds within the imidazole ligand. This confirms the successful incorporation of ZIF-8 within the polymer matrix of PDMS.

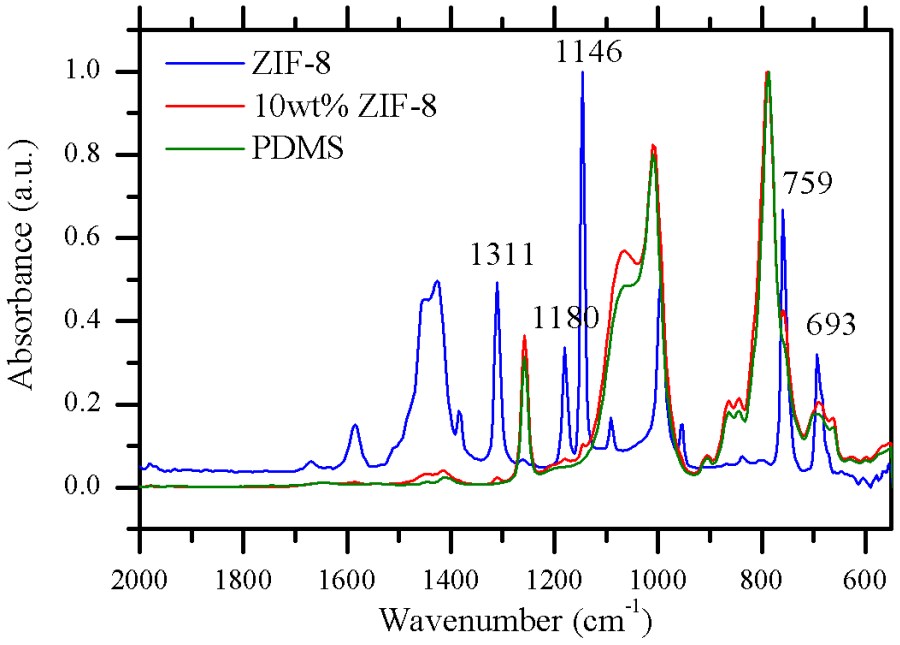

Figure 4-10. FTIR of as-synthesised membrane and pure ZIF-8 and PDMS.

The surface and cross sections of the ZIF-8 MMMs have been imaged (Figure 4-11) with SEM as well as the ZIF-8 material used for fabricating the MMMs (Figure 4-12). The ZIF-8 particles were identified on the surface of the membrane (Figure 4-11). As the wt% of ZIF-8 loaded within the membrane is increased the particle size of the ZIF-8 can be seen to generally increase due to agglomeration of the particles. The 2.5 wt% membrane appears to have many dispersed smaller ZIF-8 particles; however, as the wt% is increased the ZIF-8 particles appear to increase in size due to their agglomeration. An ideal MMM would have a uniform distribution of small particles throughout the polymer matrix to create the most effective pathways for transport of the selected species. The agglomeration of ZIF-8 has been noted before within a PDMS membrane[171] and a number of studies have developed novel techniques for the increased dispersion of the material within a PDMS membrane.[172, 173] The agglomeration of the ZIF-8 particles is also observed from the pervaporation performance of the membranes (section 4.3.5) and reflects that observed by Bai *et al*.[171] In future studies it should be noted that an improvement in dispersion of the ZIF-8 should be undertaken.

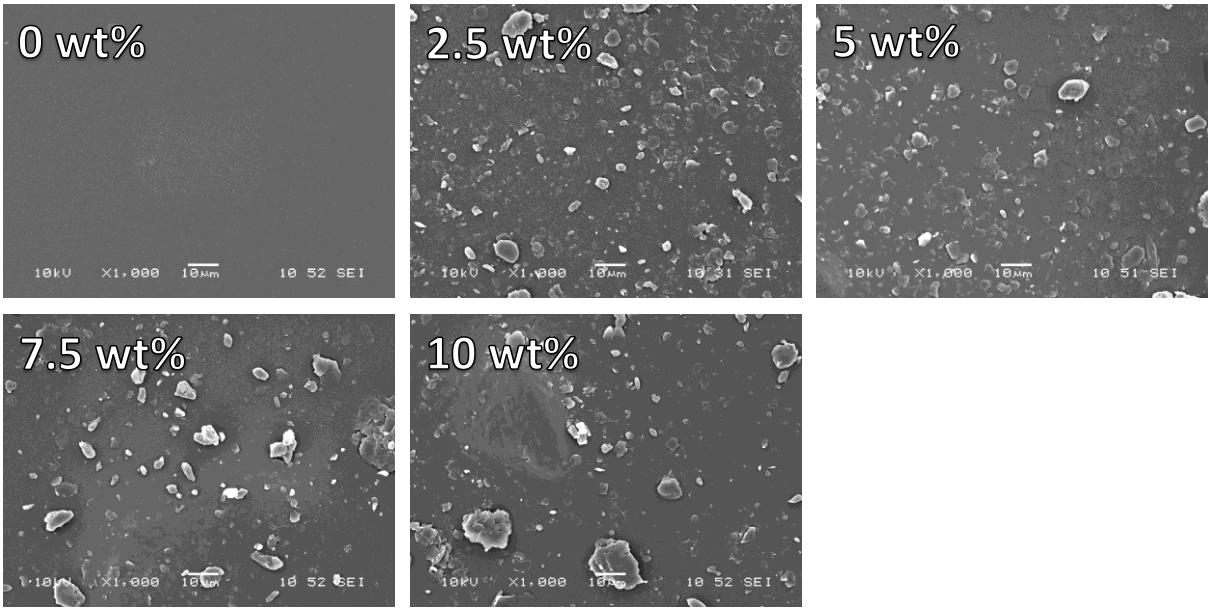

Figure 4-11. Surface SEMs of PDMS and the as synthesised ZIF-8 mixed matrix membranes at different wt% loading of ZIF-8, magnification x1000, scale bar 10 μm.

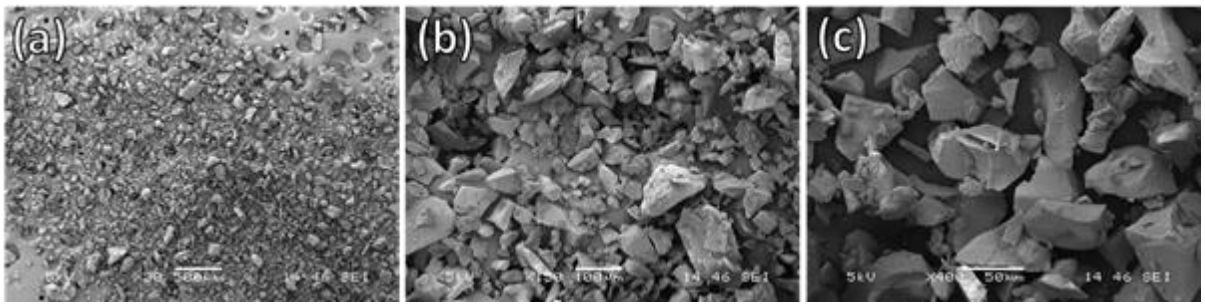

Figure 4-12. SEMs of as-synthesised ground ZIF-8 used for fabrication of the MMMs.

The cross-sectional SEMs of the as-synthesised membranes clearly show the three layers of the composite structure (Figure 4-13). The PP / PE nonwoven support layer and on top of this the porous structure of the PVDF layer are easily identified due to their different morphologies. The top layer of the membrane (far right in Figure 4-13) is the selective ZIF-8-PDMS layer and can be identified due to the dense nature of the rubbery polymer PDMS and the ZIF-8 particles in the membrane.

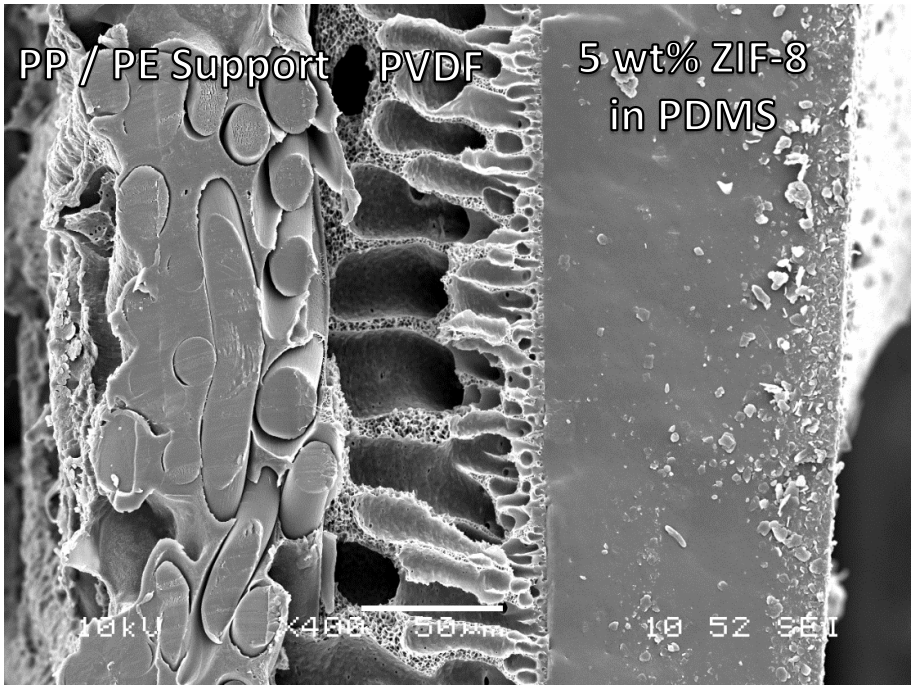

Figure 4-13. Typical cross-section of a ZIF-8 MMM showing the two layers of the support PP / PE and PVDF, and on top of this the selective ZIF-8-PDMS layer, magnification x400, scale bar 50 μm.

The cross sectional SEMS of the different wt% loadings of the MMMs are presented in Figure 4-14. As the wt% of ZIF-8 is increased, again an increase in the number of ZIF-8 particles within the membrane matrices can clearly be identified. Also with an increase in the wt% loading agglomeration of the ZIF-8 can again be observed with a general increase in particle size from 2.5 wt% to 10 wt% loading of ZIF-8.

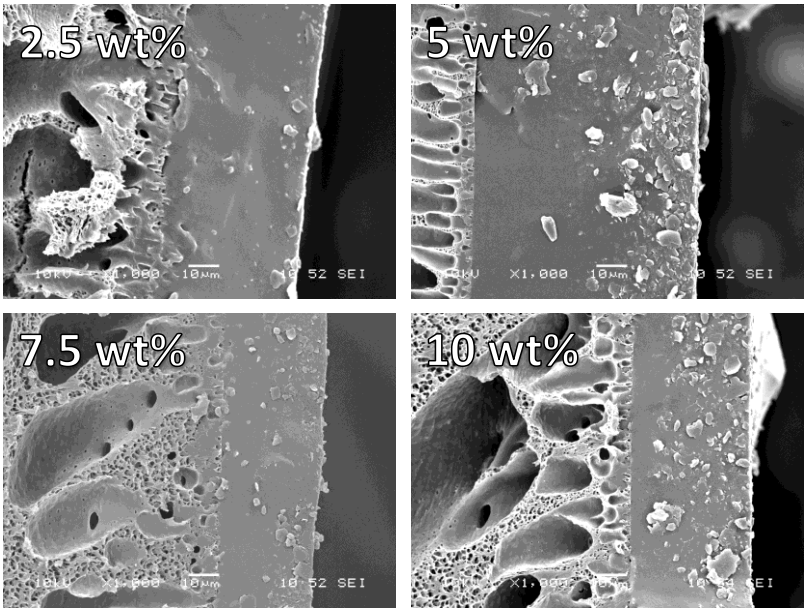

Figure 4-14. Cross sectional SEMs of the as-synthesised ZIF-8-PDMS membranes at different wt% loading of ZIF-8, magnification 1000x, scale bar 10 μm.

4.3.3 Degree of Solvent Uptake of ZIF-8 Membranes and ZIF-8 Adsorption

The solvent uptake of the membranes in water, ethanol and 2,3-butanediol is shown in Figure 4-15. The increase in ZIF-8 content of the membrane increased the uptake of both ethanol and 2,3-butanediol. A slight increase in water uptake was also observed; however, this was much less than that for ethanol indicating the membranes would still exhibit high alcohol / water selectivity.

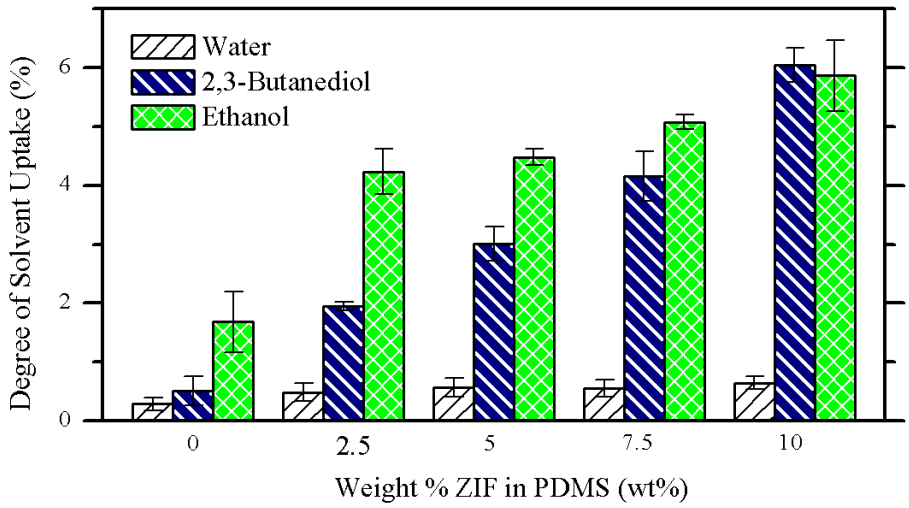

Figure 4-15. Degree of Solvent Uptake of ZIF-8 membranes.

The initial uptake of the PDMS membrane by 2,3-butanediol and ethanol is in contrast with the Hildebrand solubility parameters (Table 4-4). From these it would be expected that 2,3-butanediol would have a greater uptake on the membrane than ethanol due to its closer value to that of PDMS. The exact uptake of PDMS is; however, affected by the higher than predicted polarity of 2,3-butanediol, due to the presence of the two alcohol groups in the structure. These are not accounted for in the simplistic Hildebrand parameter, although it does give a general indication as the two alcoholic compounds are taken up by the polymer greater than water.

Table 4-4. Hildebrand solubility parameters for solvents and PDMS.[215]

Solvent / Polymer	Hildebrand Solubility Parameter at 25 ºC (MPa)
Water	47.9
Ethanol	26.0
2,3-butanediol	22.7
Acetic Acid	20.7
PDMS	15.5

With an increase in loading of the ZIF-8, an increased uptake of both ethanol and 2,3-butanediol was observed. It is clear from previous literature that ZIF-8 has a high adsorption capacity of ethanol.[107, 110, 111] Therefore, the increase in ethanol uptake will be due to the increased loading of ZIF-8 and ethanol adsorbing into the pores of the material. However, a short investigation was undertaken to ascertain whether 2,3-butanediol would be adsorbed by ZIF-8 or whether the increased uptake was due to other factors such as defects between the ZIF-8 particles and polymer, or a change in the polymer chain packing of the membrane introducing a change in the free volume creating more adsorption sites for the diol.

The liquid-phase adsorption isotherms of the alcohols in water were determined (Figure 4-16). At low concentration (< 0.05 g g^{-1} of alcohol) a very weak adsorption was observed, which increased at concentrations greater than this. ZIF-8 exhibited a greater adsorption of ethanol than 2,3-butanediol over the concentration range studied. The uptake of ethanol is comparable to that of previous adsorption studies with an uptake of 0.304 g g^{-1} at an initial ethanol concentration of 0.1 g g^{-1}.[110] The typical s-shaped isotherms; however, are not clear due to the low resolution of the experiment. Although the adsorption of 2,3-butanediol by ZIF-8 is weaker than for ethanol a similar increase in uptake with initial concentration can be observed. The liquid adsorption studies indicated that there is a weak adsorption of 2,3-butanediol from water by ZIF-8 at concentrations < 0.2 g g^{-1}.

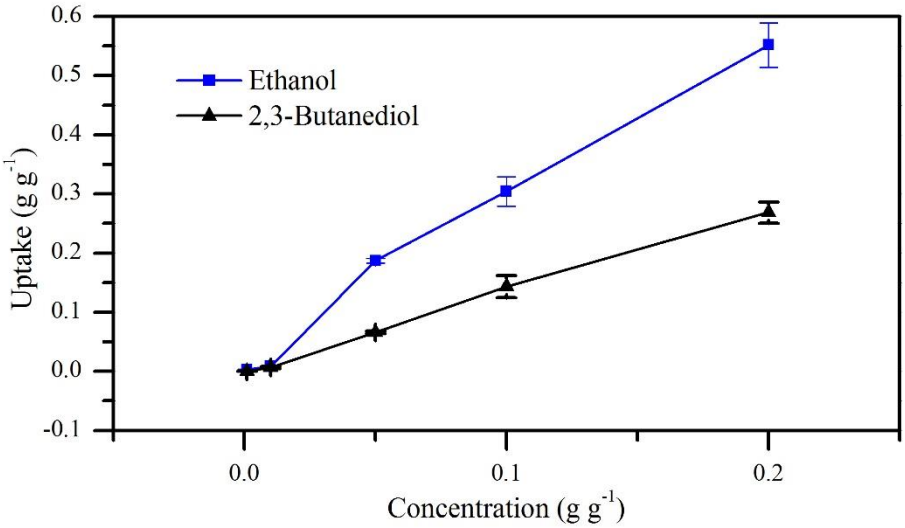

Figure 4-16. Liquid-phase adsorption isotherms of ethanol and 2,3-butanediol in water on ZIF-8.

After soaking a sample of ZIF-8 within 2,3-butanediol for 24 h a significant change in the relative peak intensities of the PXRD pattern was observed. It is known that the imidazolium organic linkers of ZIF-8 can rotate about its axis, and that their orientation determines the aperture of the framework as well as the total cavity size. Originally observed with a dependence on pressure,[216] the orientation also changes with gas adsorption.[168] Recently, the orientation of the imidazolium linkers of ZIF-8 have also been observed to be affected by the adsorption of isobutanol[132] and 1-butanol.[110] In both of these studies, upon adsorption of either butanol isomer, the PXRD pattern was observed to have a large decrease in the intensity of the first reflectance, along with changes in the relative intensity of other reflectances. As is observed in Figure 4-17.a, the reduction in the intensity of the first reflectance of ZIF-8 is also observed for the adsorption of 2,3-butanediol. The change in reflectance intensities is also observed with a 10 wt% ZIF-8-PDMS membrane; however, the change is less clear due to the noise created from the scattering of the x-rays by the amorphous polymer. These results are a clear indication that 2,3-butanediol is adsorbed into the pores of ZIF-8 and there is a gate-opening effect occurring. This also gives an indication of the stability of the framework structure towards 2,3-butanediol.

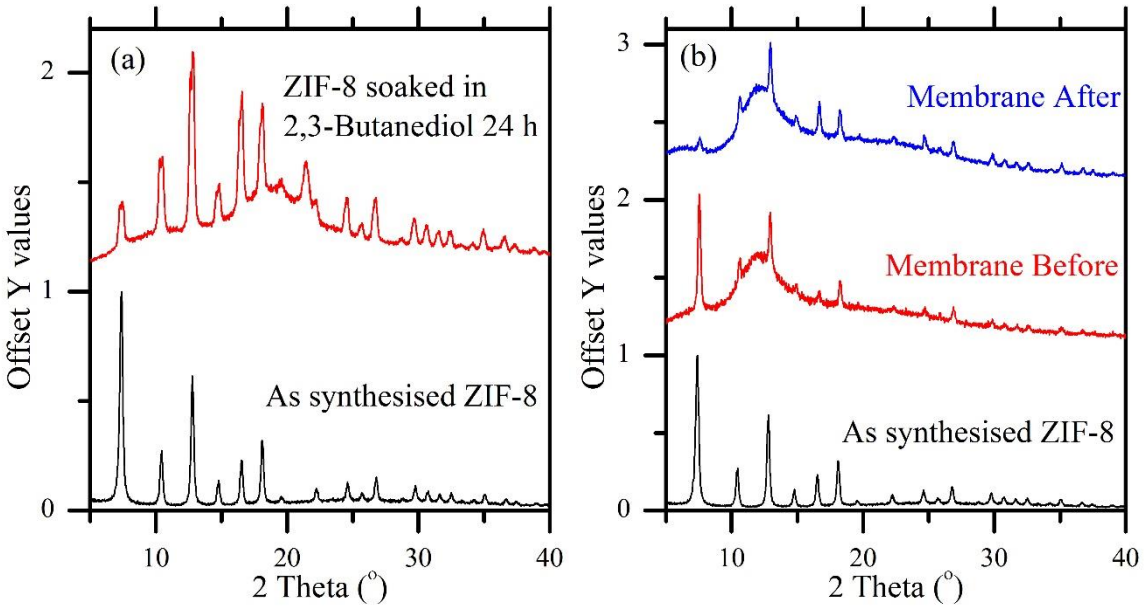

Figure 4-17. PXRDs of (a) ZIF-8 after 24 h soaked in pure 2,3-Butanediol at RT, (b) a 10wt% ZIF-8 PDMS MMM before and after soaking in pure 2,3-butanediol at RT for 24 h.

4.3.4 Membrane Stability towards Acetic Acid

Another important factor for the ZIF-8 MMMs was their stability towards the different gas fermentation products. As acetic acid is a main by-product of the ethanol gas fermentation, a study into the stability of the membrane towards an acetic acid solution was investigated. A small piece of 10 wt% ZIF-8-PDMS was immersed in either a 0.1 M acetic acid or ammonium acetate solution for 24 h at room temperature. PXRDs were run before and after the sample was immersed in the acetate solutions. After 24 h it was determined that the ZIF-8 within the matrix of PDMS for the acetic acid sample had a complete loss in its crystallinity and the porous structure of ZIF-8 (Figure 4-18.a). For the sample soaked in the ammonium acetate solution, the membrane still exhibited characteristic peaks within the PXRD pattern for the ZIF-8 incorporated into the membrane (Figure 4-18.b). However, an increase in noise is observed and so a small loss of crystallinity is expected to have occurred. This difference is due to the varying acidities of the two solutions. With the high pH ammonium acetate solution, the negative charge of the acetate anion will prevent it from solubilising into the hydrophobic polymer PDMS, thereby protecting the ZIF-8. However, the low pH solution will contain the uncharged acetic acid, which will be able to solubilise into the polymer. The acetic acid will then act as an oxidizing agent due to the acidic proton and oxidize ZIF-8, resulting in a loss of the porous structure. Therefore, in the pervaporation experiments, the pH of any acetic acid containing solution was adjusted to pH 6 by the addition of NaOH. The

charged acetate anion would be mainly present and this would limit the oxidation of the ZIF-8 structure.

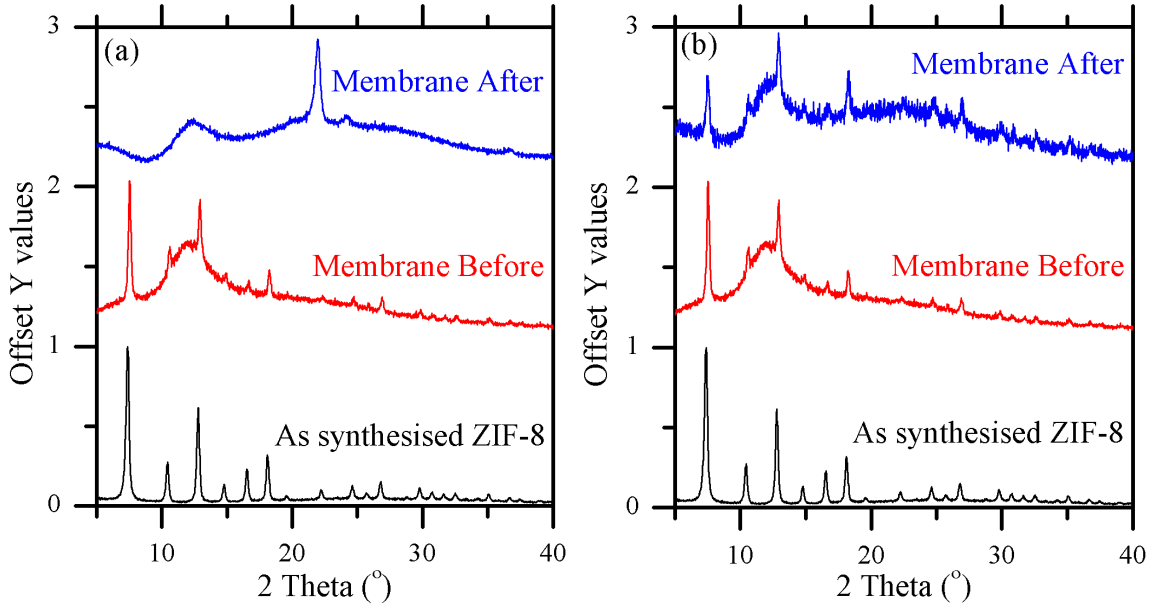

Figure 4-18. PXRDs of a 10wt% ZIF-8 PDMS membrane before and after immersion in (a) 0.1 M acetic acid or (b) 0.1 M ammonium acetate solution for 24 h.

4.3.5 Pervaporation performance of Membranes

The pervaporation performance of the mixed matrix membranes was then investigated.

4.3.5.1 Ethanol Pervaporation

The pervaporation of ethanol was studied at a temperature of 70 ºC and a concentration of 10 g L^{-1} (a typical concentration produced within the gas fermentation broth). It can be seen from Figure 4-19 that with an increasing wt% of ZIF-8 within the membrane, a slight increase in separation factor is observed up to a loading of 7.5 wt%. At a higher loading of 10 wt% the separation factor decreases along with the total flux. The behaviour of the total flux initially shows an increase from 0 – 2.5 wt% ZIF-8. This is due to inclusion of the MOF within the polymer matrix leading to an increased permeance due to the increased permeability of the MOF, as well as a change in the polymer chain packing of the PDMS. As the loading of ZIF is then increased, agglomeration of the ZIF-8 particles within the matrix is occurring and leads to a decrease in the total flux. This is exacerbated further at 10 wt% where a decrease in both flux and separation factor is evidenced, as the high degree of agglomeration inhibits the permeation through the porous particles.

In other studies looking at butanol separation, a much larger increase in the permeability of butanol was observed due to its higher affinity towards ZIF-8.[132, 171-173] The proportionally small increase in separation factor has been attributed to the fact that the ethanol water separation capability of ZIF-8 is lower than that for various butanol / water mixtures[108, 109] and is reflected in previous studies for this class of membrane for ethanol pervaporation.[132] However, the increase in performance is what has driven the use of ZIF-8 as an inorganic filler within MMMs for pervaporation.

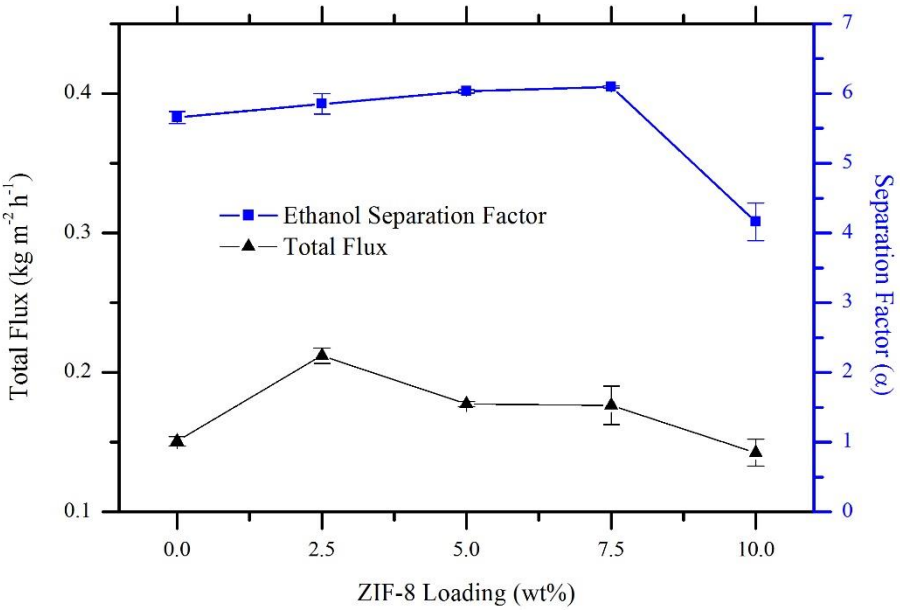

Figure 4-19. Ethanol pervaporation with increasing ZIF-8 wt%, 70 ºC.

4.3.5.2 Ethanol and 2,3-Butanediol Pervaporation

The effect of 2,3-butanediol on the pervaporation of ethanol from their aqueous mixture was then investigated. This was studied for a PDMS membrane by increasing the 2,3-butanediol concentration whilst maintaining ethanol concentration at 10 g L^{-1} and the feed temperature at 70 ºC. Figure 4-20 shows that with an increase in the concentration of 2,3-butanediol from 0 to 8 g L^{-1} that there was a general trend of a slight decrease in both the total flux and separation factor from 0.151 to 0.133 kg m^{-2} h^{-1} and 5.66 to 5.46 respectively. Chovau *et al*. also found that addition of 1 g L^{-1} of 2,3-butanediol to a 50 g L^{-1} ethanol solution decreased the total flux of a PDMS membrane at 30 ºC from 0.555 to 0.517 kg m^{-2} h^{-1} and decreased the enrichment factor from 6.5 to 5.4.[217] This previous study demonstrated that the decrease in ethanol flux can be attributed to 2,3-butanediol swelling into the membrane and competing with ethanol for adsorption sites within the polymer matrix. Due to the low vapour pressure and high boiling point it was not

evaporated from the permeate side of the membrane readily and therefore swelled and stayed within the membrane.

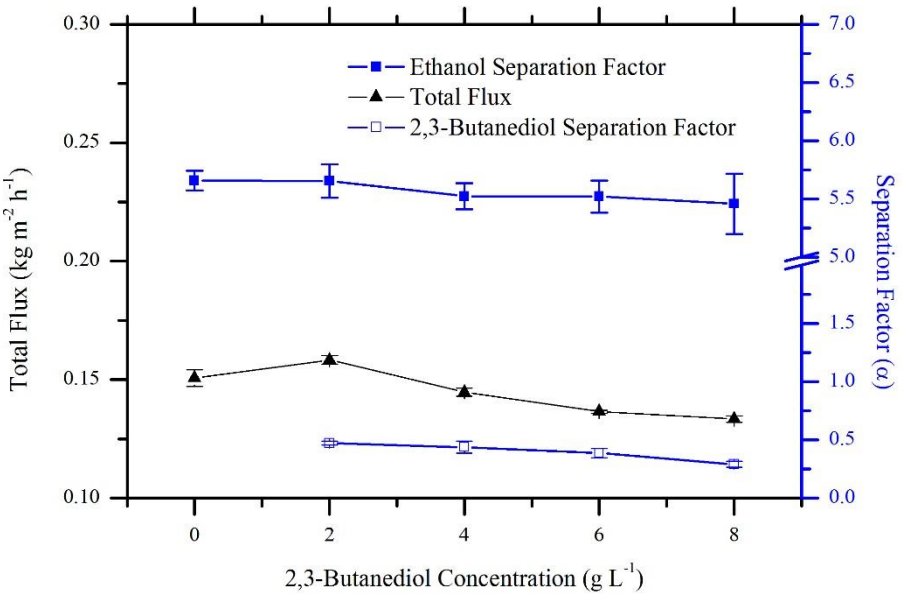

Figure 4-20. Effect of increasing 2,3-Butanediol concentration on ethanol pervaporation for PDMS membrane.

The 7.5 wt% ZIF-8 loaded membrane was then investigated for the effect increasing 2,3-butanediol concentration will have on the ethanol pervaporation performance. The 7.5 wt% ZIF-8 loaded PDMS membrane was chosen as it had the greatest pure ethanol separation factor along with the highest degree of solvent uptake from pure 2,3-butanediol (except for the 10 wt% loaded membrane which exhibited poor ethanol pervaporation performance). Therefore, the membrane would give an indication of any effect 2,3-butanediol may have on the separation performance. Again the ethanol concentration was maintained at 10 g L^{-1} within the mixture and the concentration of 2,3-butanediol increased from 0 – 8 g L^{-1} and the temperature maintained at 70 ºC. As can be seen from Figure 4-21, generally there was an increase in the total flux and the separation factor decreases as the concentration of 2,3-butanediol increases and is in contrast to the pure PDMS membrane.

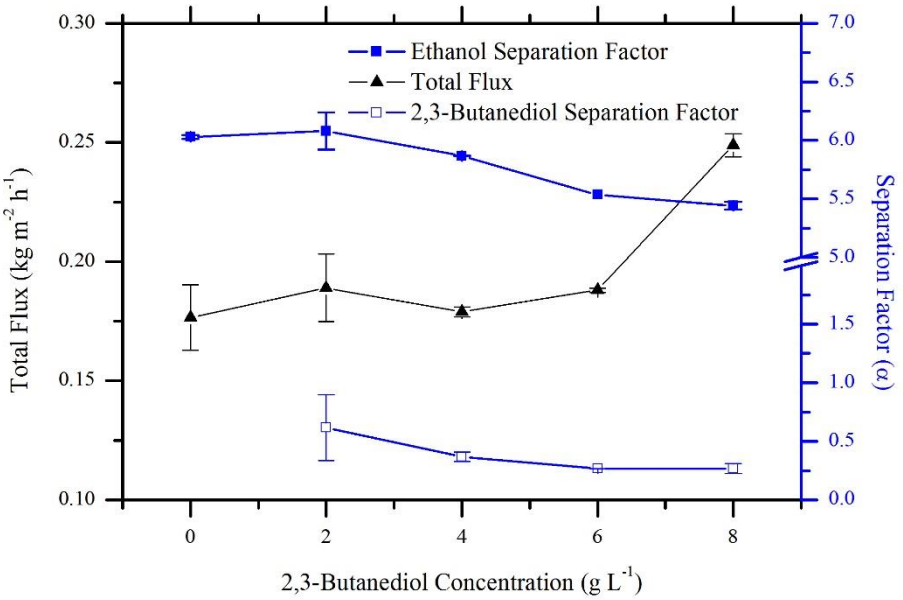

Figure 4-21. Flux and Separation factor of 7.5 wt% ZIF-8 membranes with changing 2,3-butanediol concentration.

This increase in total flux and decrease in separation factor with increasing concentrations of 2,3-butanediol has been attributed to an increase in the water flux through the membrane. An increased 2,3-butanediol concentration would yield a greater uptake of the 7.5wt% ZIF-8 membrane compared to the PDMS membrane. It is clear that the increased permeation of water should be due to the ZIF-8 rather than the polymer (which has been shown to lead to a decreased flux with increased diol concentration). Therefore, the uptake of 2,3-butanediol into the ZIF-8 may change the hydrophobicity of the pores potentially creating preferential pathways for water to permeate through the membrane due to its increased hydrophilicity. This could be either between defects in the ZIF-8 particles or through the pores. As the structure of 2,3-butanediol contains both hydrophobic and hydrophilic moieties (Figure 4-22), the hydrophobic methyl groups could align with the hydrophobic surfaces of ZIF-8 to reveal the hydrophilic alcohol groups of the diol allowing for a pathway of water through the membrane.

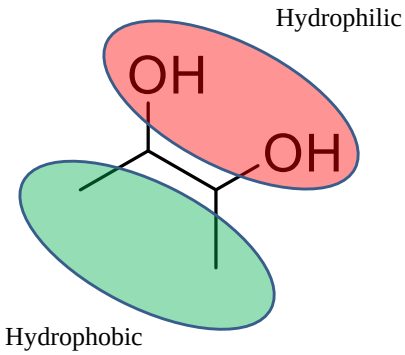

Figure 4-22. Structure of 2,3-butanediol showing the hydrophilic and hydrophobic elements of the structure.

Alternatively, non-selective voids would be evidenced by an increase in total flux and a decrease in separation factor due to the creation of space which would facilitate unselective permeance. These could be created from the degradation of the crystalline ZIF-8 structure leaving non-selective voids in its place. However, degradation of ZIF-8 could also present a decrease in the total flux due to non-porous fillers blocking pathways of ethanol or water diffusing through the membrane matrix. An investigation was undertaken to ascertain if the structure of ZIF-8 within the membrane was degrading due to pervaporation of ethanol in the presence of 2,3-butanediol. PXRDs of the membranes were taken after pervaporation and it was found that the ZIF-8 structure was still evident within the PXRDs so a complete loss in structure was not evident, and there was no discernible difference between the PXRDs of the membrane from a pure ethanol solution and that with the addition of 2,3-butanediol (Figure 4-23). Therefore, the increased water flux at high concentrations of 2,3-butanediol is due to the increased uptake of 2,3-butanediol into the membrane and the increased hydrophilicity of the membrane arising from this creating pathways for water to permeate the membrane.

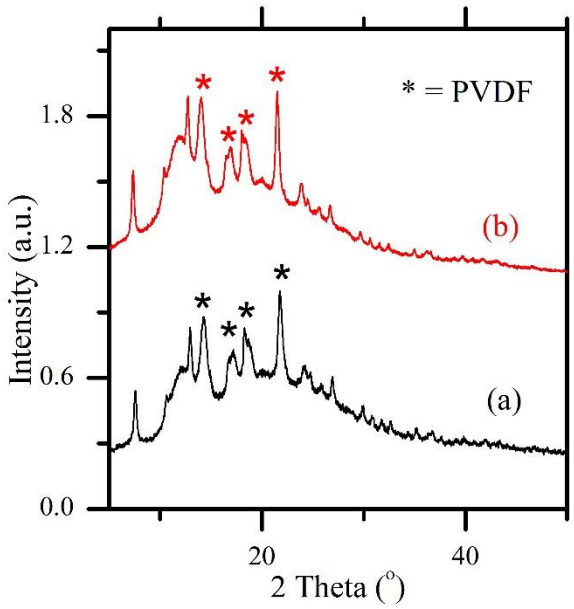

Figure 4-23. PXRDs of the 7.5 wt% ZIF-8 loaded membranes after pervaporation of solutions of (a) 10 g L^{-1} ethanol and (b) 10 g L^{-1} ethanol with 8 g L^{-1}2,3-butanediol. The asterisks indicate reflectances characteristic of the PVDF support layer of the membrane.

Figure 4-24 shows the effect an increase in the wt% of ZIF-8 has on the pervaporation performance of a 10 g L^{-1} ethanol and 4 g L^{-1} 2,3-butanediol mixture at 70 ºC. At low ZIF-8 loading (2.5 wt%) the membrane performs well with an increased flux and separation factor when compared to the PDMS membrane. This is thought to be due to the low level of agglomeration of the ZIF-8 particles in the membrane and lower uptake of 2,3-butanediol due to the greater ratio of polymer to ZIF. Therefore, the membrane would still be relatively unsaturated with 2,3-butanediol. As the ZIF-8 wt% increases the uptake of 2,3-butanediol increases and a decrease in separation factor is observed between 2.5 and 10 wt% loading of ZIF-8. The flux initially decreases between 2.5 and 5wt% due to a decrease in ethanol permeance and then increases again as the uptake of 2,3-butanediol will increase leading to greater water permeance through the membranes. At a 10 wt% loading of ZIF-8 the total flux is over 2.5 times greater than for the PDMS membrane.

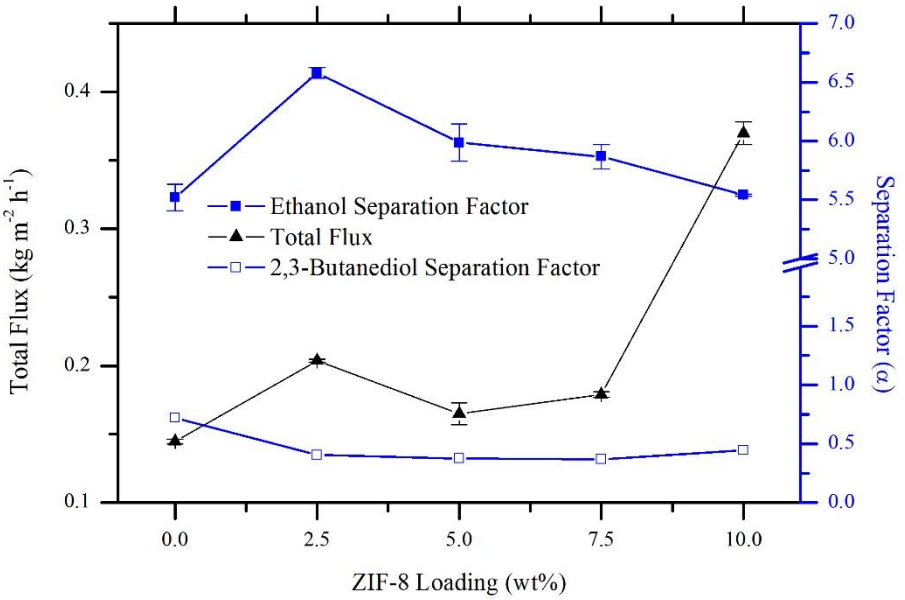

Figure 4-24. Ethanol and 2,3-butanediol pervaporation performance with increasing wt% ZIF-8.

4.3.5.3 Ethanol and Acetate Pervaporation

Figure 4-25 shows the effect of an increasing acetate concentration on the pervaporation performance of ethanol 10 g L^{-1} at 70 ºC and pH 6 for a PDMS membrane. As can be seen from Figure 4-25, initially the membrane performance is quite stable with addition of 5 g L^{-1} of acetic acid with a similar total flux (0.150 vs. 0.146 kg m^{-2} h^{-1}) and a similar separation factor (5.66 vs. 5.7). Further increasing the concentration of acetate to 10 g L^{-1} demonstrates a large increase in total flux to 0.198 kg m^{-2} h^{-1} with only a slight decrease in separation factor to 5.6. Chovau *et al.*[217] showed that addition of 1 g L^{-1} of acetic acid to a 50 g L^{-1} ethanol solution increased the flux of a PDMS membrane when pH was not controlled. At a pH above the pK_a of the carboxylic acids tested, no significant change in performance was observed. It is therefore expected that the increase in total flux is due to the effect of the acetic acid dissolving into the polymer membrane. As the pH was adjusted to 6, less carboxylic acid could dissolve into the polymer and so a large concentration of acetic acid (10 g L^{-1}) was required to effect the membrane performance. As the dissociation of the acetate anions is an equilibrium with an increased concentration there will be an increased amount of undissociated acetic acid at any point in time which would then swell into the membrane which will cause the observed increase in total flux.

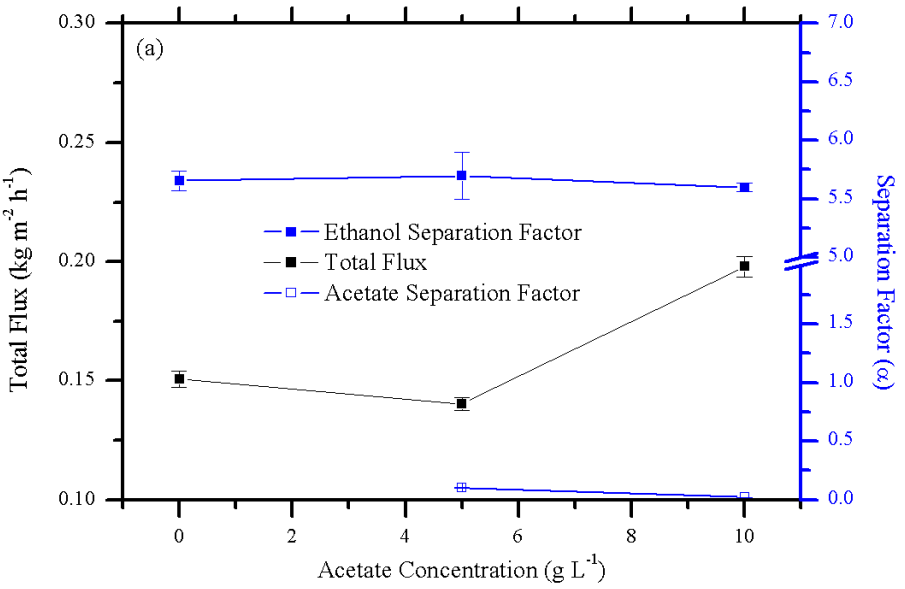

Figure 4-25. Effect of Acetate Concentration on the pervaporation of ethanol with a PDMS membrane.

In contrast to the purely PDMS membrane, the ZIF-8-PDMS membrane with a ZIF-8 loading of 7.5 wt% exhibits a relatively stable pervaporation performance for ethanol over the concentration range of 0 – 10 g L^{-1} acetic acid at pH 6 (Figure 4-26). It is proposed that this increased stability with increasing acetate concentration arises from the increased surface hydrophobicity of the membrane compared to that of the virgin PDMS membrane. An increase in the surface hydrophobicity would increase the rejection of acetate anions from swelling into the membrane. Therefore, there would be less acetate swelled into the membrane and the performance will be more consistent over a changing concentration.

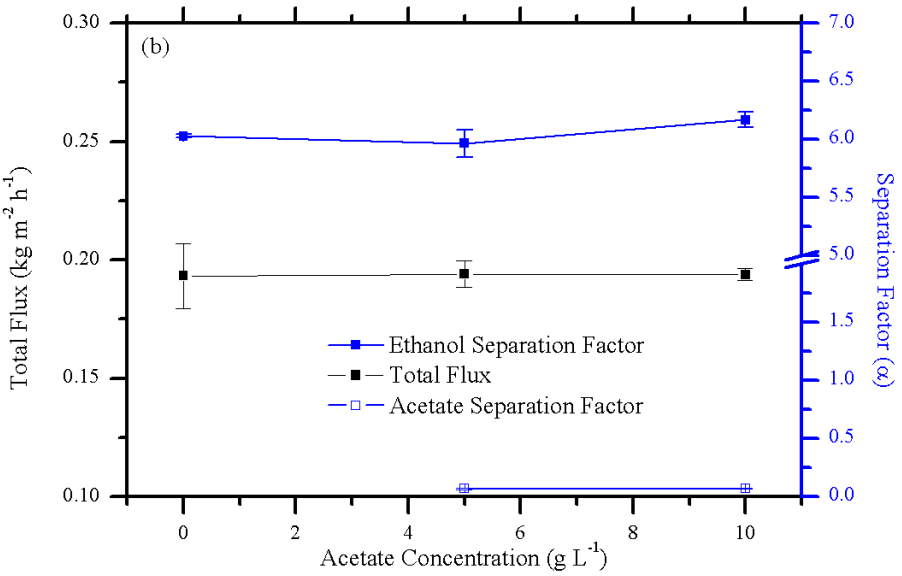

Figure 4-26. Effect of Acetate Concentration on the pervaporation of ethanol with a ZIF-8-PDMS membrane.

4.3.5.4 Model Solution and Fermentation Broth Pervaporation

The pervaporation performance of the 7.5 wt% ZIF-8-PDMS membrane was then evaluated with a mixture of ethanol (10 g L^{-1}), 2,3-butanediol (4 g L^{-1}) and acetic acid (5 g L^{-1}) at the concentrations they would be produced within a gas fermentation broth. The temperature was kept at 70 ºC and the pH adjusted to 6 with the addition of sodium hydroxide. Figure 4-27 shows the trend of the total flux and separation factor for ethanol throughout the experiment. Over the course of 7 hours the separation factor remains stable at around 6 as well as the total flux which increases marginally from 0.164 to 0.176 kg m^{-2} h^{-1}. The total flux and separation factor are therefore similar to the binary solutions of ethanol with either 2,3-butanediol (4 g L^{-1}) or acetate (5 g L^{-1}). This indicates that there is little combinatorial effect of these two additional components in the solution.

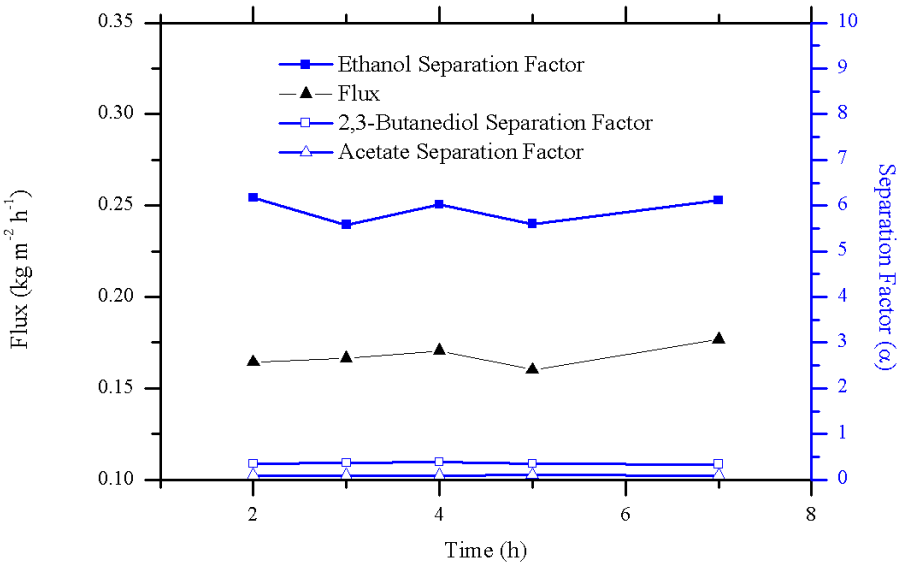

Figure 4-27. Pervaporation performance of a solution of 10 g L^{-1} Ethanol, 4 g L^{-1} 2,3-butanediol and 5 g L^{-1}Acetic Acid, pH 6, 70 ºC by a 7.5 wt% ZIF-8 membrane over 7 hours.

A fermentation broth similar in composition to the gas fermentation broth used by LanzaTech was then tested. The fermentation broth was collected from a fructose-fermenting continuous bioreactor rather than the syngas mixture used by LanzaTech but is similar in composition to the gas fermentation broth (details of the broth are given in section 4.2.14). The broth was spiked with ethanol, acetic acid and 2,3-butanediol to the required concentrations and the pH was adjusted to 6 through addition of NaOH. The pervaporation performance of a 7.5 wt% ZIF-8-PDMS membrane was tested for the removal of ethanol from this fermentation mixture (Figure 4-28). As for the model solution the total flux and ethanol separation factor were relatively stable over the course of 7 hours. The total flux; however, was almost twice that of the model solution with a marginally lower average ethanol separation factor (5.36 vs. 6.0 for the broth and model solution respectively). This was thought to be due to the additional components within the fermentation mixture. A number of publications have investigated the effect of various salts and sugars on the pervaporation performance of purely PDMS membranes. Chovau *et al.* found that addition of either glucose, xylose (5 g L^{-1}) or $(NH_4)_2SO_4$ (1 g L^{-1}) reduced ethanol flux but increased water flux; however, no combinatorial effects of different components were studied.[217] Wood *et al.* found that addition of fructose to an ethanol / water feed increased the water selectivity but decreased the total permeation for a silicone rubber hollow fibre membrane.[218] For a silicalite membrane an increase in permeation was identified from the adsorption of salts (K_2HPO_4, $MgSO_4$, $CaCl_2$, NH_4Cl; all of which are also present in the studied broth) into the membrane during ethanol pervaporation.[219] Due to the number of different combinatorial effects arising from the vast quantity of different components within the fermentation broth it is difficult to identify the exact

cause to the increase in total flux, and likely due to a number of components of the broth. However, as discussed earlier an increase in total-flux can be attributed to an increased hydrophilicity of the membrane so it is likely that a number of components such as acids, salts and 2,3-butanediol may have dissolved into the membrane and changed its hydrophilicity and / or changed the vapour liquid equilibrium governing the separation.[217] The important point is that the increase in flux and marginal decrease in separation factor arising from this leads to a higher average pervaporation separation index (PSI –see Section 2.3 for definition) value of 1281 for the membrane when used for the fermentation broth compared to 804.5 for the model solution. These components of the fermentation broth indicate that the effect enhances the membrane performance. The positive effect of additional components from fermentation broths has been observed in a number of studies previously.[219-221]

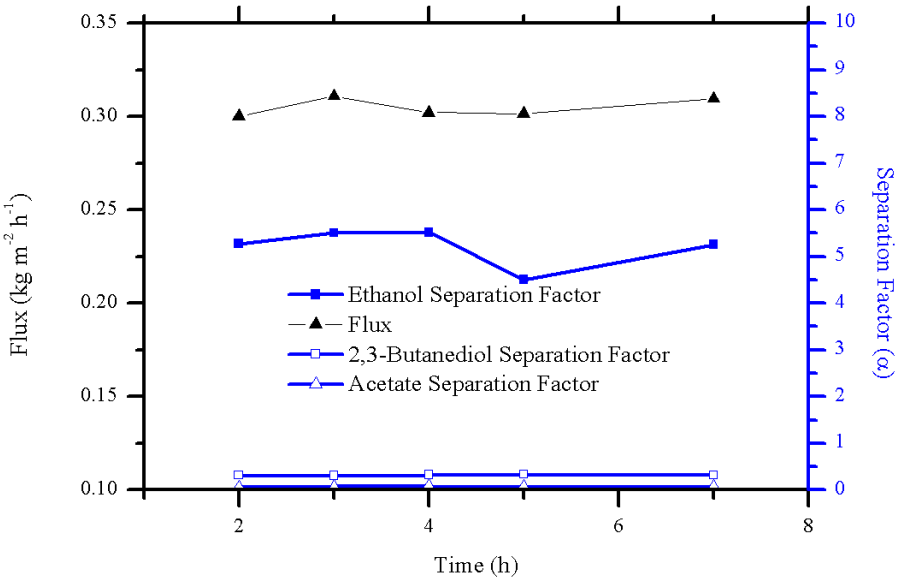

Figure 4-28. Pervaporation performance of a fermentation broth spiked with 10 g L^{-1} Ethanol, 4 g L^{-1} 2,3-butanediol and 5 g L^{-1}Acetic Acid, pH 6, 70 ºC by a 7.5 wt% ZIF-8 membrane over 7 hours.

4.4 Conclusions

The use of a MMM consisting of ZIF-8 and PDMS for the pervaporation of ethanol from a potential gas fermentation mixture has been investigated. Most studies of MMMs containing MOFs have focused on pure alcohol / water solutions with few studies investigating potential combinatorial effects or the effect of a fermentation broth. Here, the specific effect that 2,3-butanediol and acetic acid have on the pervaporation of ethanol from a fermentation mixture using a ZIF-8-PDMS MMM has been studied. The ZIF-8 MMMs were synthesised and found to have characteristic properties in accordance with previous literature examples.[132, 171] It was found that increasing the wt% of ZIF-8 loaded within the membrane increased the uptake of 2,3-butanediol. This has been shown to be due to the adsorption of 2,3-butanediol by ZIF-8. The membranes are also susceptible to acidic solutions of acetic acid but are stable when the pH is increased due to the hydrophobicity of the membrane preventing charged solutes from solubilizing into it. When applied in pervaporation of ethanol, 2,3-butanediol has been shown to increase both the total flux and decrease the ethanol separation factor for a 7.5 wt% loaded ZIF-8-PDMS membrane. This is due to the uptake of 2,3-butanediol increasing the hydrophilicity of the membrane increasing the water permeance and increasing the amount of hydrophilic pathways for water to permeate through the membrane. The 7.5 wt% ZIF-8-PDMS membrane exhibited a stable performance for ethanol pervaporation with changing acetate concentration at pH 6. This was attributed to an increased surface hydrophobicity of the membrane compared to the pure PDMS membrane, preventing uptake of the uncharged ions into the membrane which decrease the membranes hydrophilicity and subsequently increase the water flux. When the pervaporation of ethanol was applied in the presence of both 2,3-butanediol and acetate, the membrane performance was similar as for the individual components indicating little further combinatorial effect between these two fermentation products. Finally, the pervaporation performance of a fermentation broth containing ethanol, 2,3-butaediol and acetate was tested. A large increase in total flux was observed and only a slight decrease in ethanol separation factor. This led to an increased PSI of 1281 compared to the model solution and has been attributed to beneficial effects of the components of the fermentation broth.

This chapter has therefore outlined a number of design considerations for MMMs for pervaporation of ethanol when 2,3-butanediol and acetate are both sought as co-fermentation products. This work demonstrates that before the increased performance of MMMs can be implemented to fermentation processes, the effect of the other components within the fermentation broth on the membranes must be thoroughly understood, indicating where the majority of research currently being done in this area should be extended to. As part of this extension, MMMs of ZIF-8-PDMS have demonstrated suitable performance characteristics for ethanol pervaporation in

the presence of acetate and 2,3-butanediol as co-fermentation products. Further work should be conducted on the effect that the salts and various other components within the fermentation broth have on the membrane. This could then aid design considerations earlier upstream in the fermentation process to enhance the recovery using pervaporation e.g. through addition of specific growth media components that could aid pervaporation as well as the fermentation.

Chapter 5

Cu-MOF based PDMS mixed-matrix membranes for Acetone Pervaporation: Impact of Glutarate and Bipyridyl ligands on the MOF morphology

The work within this chapter started during a visit to the laboratory of Prof. Len Barbour at the University of Stellenbosch. Discussions with Dr. Vincent Smith and Charl X. Bezuidenhout led to initial investigations into the feasibility of using the Cu-MOFs described within this Chapter as the inorganic phase within a MMM. The following Chapter describes the resulting work.

5.1 Introduction

As discussed in the previous Chapters, the removal of volatile organics from water is an important separation process in the production of chemicals using microbial fermentation. Pervaporation is a promising low energy alternative to the traditional approach of using distillation to achieve this separation.[50, 67] However, current commercial organophilic pervaporation membranes do not provide sufficient separation properties to realise its application. A number of novel materials have been introduced in Chapter 2 that have been used to help enhance the performance of traditional

polymeric pervaporation membranes through their inclusion in various mixed-matrix membranes. Therefore, the discovery and application of, new materials to difficult separations will play a large part in the facilitation of low-energy separation technologies such as pervaporation.

MOFs, when used as the inorganic phase within a MMM, have been shown to enhance the separation performance of polymeric membranes for the pervaporation of various organics from water (Section 2.4.4.2). Some of the first examples of MOFs as the inorganic phase within MMMs, as well as the best performing, are those using ZIFs such as ZIF-8,[132, 171-173] ZIF-71[176-178, 222] and ZIF-7.[169, 170] Other examples of MOFs used are $Zn(bdc)(TED)_{0.5}$ in PEBA for butanol pervaporation[179] and MIL-53 in PDMS for ethanol pervaporation,[183]

Within the field of MOFs there have recently been a number of articles introducing copper MOFs with glutarate and bipyridyl ligands.[223-228] Of these examples the Cu-MOFs have been shown to exhibit organic / water separation properties that could be applied to fermentative separations. Chen *et al*. reported a framework that exhibited selective adsorption of water over methanol due to the specific pore size of the Cu-MOF created.[224] Dey *et al*. have shown that a Cu-MOF with larger pores consisting of N,N'-bis-pyridin-4-ylmethylene-hydrazine and glutarate exhibits type 1 adsorption of methanol and ethanol but a gated adsorption of water, and has been attributed to the hydrophobic pores of the framework.[225] As well as this, Hwang[226] and Seco[227] have developed, two structures of Cu-MOFs consisting of the same ligands (glutarate and 4,4'-Trimethylenedipyridine) but with slight structural differences in terms of the orientation of the bipyridyl ligand. The reported Cu-MOFs have been shown to form solvates with acetone and water respectively during their synthesis. Therefore, in this chapter an investigation into the application of these two similar frameworks into PDMS to create MMMs for pervaporative separations was undertaken. The work has aimed to identify the effect that the structures of the Cu-MOFs may play on their performance within a MMM for pervaporation and to try and elucidate any design factors that could be taken forward when designing MOFs for use in MMMs for pervaporative separations.

This meets the specific objectives of this thesis:

- To identify ways to improve recovery of products from a gas fermentation process.
- To improve the understanding of membrane separation processes.

5.2 Materials and Methods

5.2.1 Materials

Materials were purchased from common laboratory suppliers, specifically; Copper (II) nitrate hemi(pentahydrate) (Alfa Aesar, 98 – 102 %), 4,4'-Trimethylenedipyridine (98 %, Alfa Aesar), Glutaric Acid (99 %, Alfa Aesar), 1,2-Bis(4-pyridyl)ethane (97 %, Acros), Acetone (Reagent Grade, VWR), Methanol (Reagent Grade, VWR), Polydimethylsiloxane RTV-615 (Techsil, UK), Hexane (HPLC grade, VWR), and 0.1 μm PVDF membrane filters of 90 mm diameter (EMD Millipore).

5.2.2 Synthesis of CuGluBpp

The Cu-MOFs were synthesised in batches from hydrothermal reactions of:

CuGluBpp-Acetone: Glutaric acid (1.19 g, 9 mmol) and sodium hydroxide (0.360 g, 9 mmol) were dissolved in water (400 mL). This was then mixed with a solution of $Cu(NO_3)_2 \cdot 2.5\ H_2O$ (1.86 g, 8 mmol) and 4,4'-trimethylenedipyridine (0.793 g, 4 mmol) in an acetone / water 1 : 1 mixture (400 mL). A hydrothermal reaction of this solution at 80 ºC for 2 days afforded emerald green crystals of CuGluBpp-Acetone. The crystals were collected by vacuum filtration and washed with water to remove any unreacted starting material (average 1.49 g, 56.5 %). CuGluBpp-MeOH was synthesised using the same procedure except that acetone was replaced with methanol in the copper containing reactant solution (average 1.35 g, 51.3 %).

Vacuum oven dried samples (120 ºC, 16 h) were sent off for elemental analysis;

Elemental Analysis (%): **Calculated for CuGluBpp·4 H_2O;** ($C_{23}H_{32}Cu_2N_2O_{12}$ = 657.6 g mol^{-1}); (C, 42.0; H, 5.21; N, 4.26); **Found** (CuGluBpp-Acetone)**;** (C, 41.4; H, 5.17; N, 4.25), **Found** (CuGluBpp-MeOH)**;** (C, 41.2; H, 5.07; N, 4.26),

5.2.3 Synthesis of PDMS and CuGluBpp / PDMS Membranes

The synthesis of the MMMs followed the same procedure as in section 4.2.3 except the amounts of MOF added to the polymer dope solution were as follows:

Table 5-1. Mass of MOF added to the polymer dope solution.

Weight loading of Cu-MOF in membrane (wt%)	Weight of Cu-MOF added to polymer dope solution (g)
5	0.463
10	0.978
15	1.55
20	2.20
30	3.77

5.2.4 General experimental methods

The methods for characterisation and analysis are largely the same as for Chapter 4, for further details on general experimental methods please refer to Section 4.2; any differences in the experimental procedures are outlined below. For TGA a ramping rate of 10 ºC min^{-1} was utilised. Membranes were dried at 60 ºC under vacuum for 16 h before water contact angle analysis. Aqueous acetone solutions between 0.01 and 0.3 g g^{-1} were used for the liquid-phase adsorption determination and the Cu-MOFs were dried at 120 ºC under vacuum for 16 h before testing. For N_2 and CO_2 isotherm analysis samples were soaked in chloroform for 2 days before drying in a vacuum oven overnight at 100 ºC before further activation under vacuum at 120 ºC. BFDH crystal morphologies[229-231] were calculated from single crystal data using the program Mercury[213], which was also used for structure visualisation. Single crystal data was collected by the author for CuGluBpp-MeOH and by Charl X. Bezuidenhout for CuGluBpp-Acetone at the University of Stellenbosch and reflect the structures presented in[227] and[226] respectively. HPLC was used to determine the concentration of acetone in solution (see section 4.2.13), feed and retentate samples were diluted by a factor of 10 before HPLC analysis.

5.2.5 Microscope Images

Optical microscope images of single crystals of the as-synthesised MOFs were captured on a Leica DM1000 microscope that had been fitted with an Infinity 2 microscopy camera. Images were taken at x 4 magnification. Digital microscope images were taken with a USB digital microscope (2 megapixel and 50 – 500 X digital zoom).

5.2.6 CO_2 Isotherms

Low pressure CO_2 adsorption isotherm data were collected on a Micrometrics ASAP 2020 at 273 K. CO_2 isotherm data were collected over the partial pressure range 0 – 0.035. Samples were soaked in chloroform for 2 days and dried in a vacuum oven for 16 h at 100 ºC before activation at 120 ºC and 0.01 mbar for 16 h. A water / ice bath was used to regulate the temperature at 273 K.

5.2.7 Pervaporation Performance

For details of the pervaporation setup please refer to section 4.2.12. Membranes were dried in a vacuum oven at 60 ºC for 16 h before analysis. The membrane was allowed to condition at the required operating conditions until steady state flux had been reached (1.5 hour). Permeate vapour was then collected in alternating liquid nitrogen cold traps every 2 h for 6 h and the membrane flux was recorded gravimetrically by weighing the amount of permeate condensed in the glass trap. Permeate samples were diluted with 2 mL of water to wash them out of the trap for HPLC analysis.

5.2.8 Contra-Diffusion Membrane Synthesis

In a typical experiment, a solution of $Cu(NO_3)_2 \cdot 2.5\ H_2O$ (1.86 g, 8 mmol) and 4,4'-trimethylenedipyridine (0.793 g, 4 mmol) in acetone / water (1 : 1) (400 mL) and a solution of glutaric acid (1.19 g, 9 mmol) and sodium hydroxide (0.360 g, 9 mmol) in water (400 mL) were placed either side of a 0.1 μm PVDF membrane (90 mm diameter) in a custom-made glass setup (Figure 5-1) and stirred at room temperature. The concentration of NaOH was altered to investigate the effect this had on film growth; the concentrations used were 9 mmol, 13.5 mmol and 18 mmol. After 20 h (or 60 h for the double concentration sample) the membrane was washed with water and allowed to dry at room temperature.

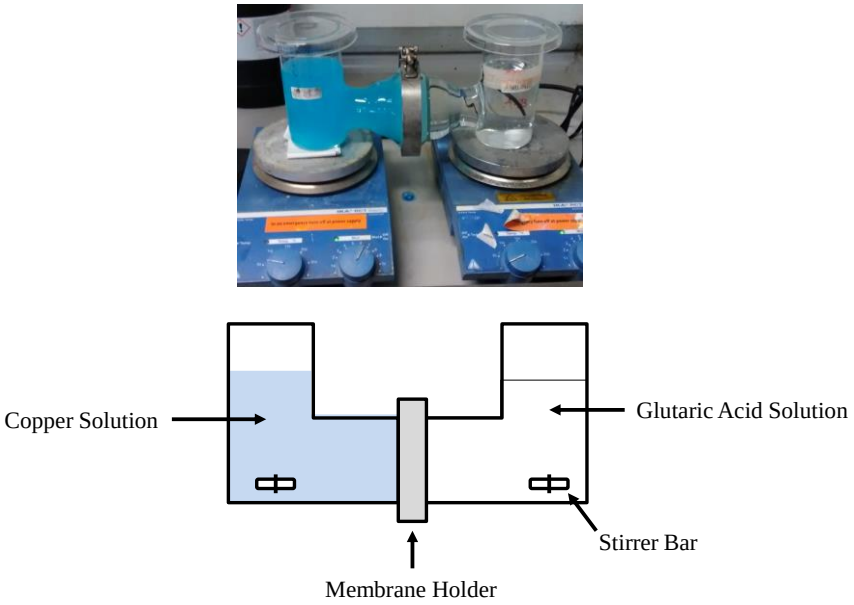

Figure 5-1. Photograph and schematic of the contra-diffusion cell used for preparation of films of the Cu-MOFs.

5.3 Results and Discussion

5.3.1 Synthesis of the CuGlu Frameworks

The Cu-MOFs were synthesised from hydrothermal reactions of copper(II) nitrate hemi(pentahydrate), glutaric acid and 4,4'-trimethylenedipyridine in either an acetone / water or methanol / water solution. This produced emerald green micrometre size single crystals of both Cu-MOFs and have been denoted from herein as CuGluBpp-Acetone and CuGluBpp-MeOH respective to the solvent used in the reaction mixture. The reaction in the presence of acetone produced smaller thicker crystals whereas in the presence of methanol, larger plate like crystals were formed (Figure 5-2). The differences in the crystal shape is due to a combination of the structural differences within the framework, due to the differences in the orientation of the bipyridyl ligand, as well as the different growth conditions due to the presence of either acetone or methanol within the hydrothermal reaction.

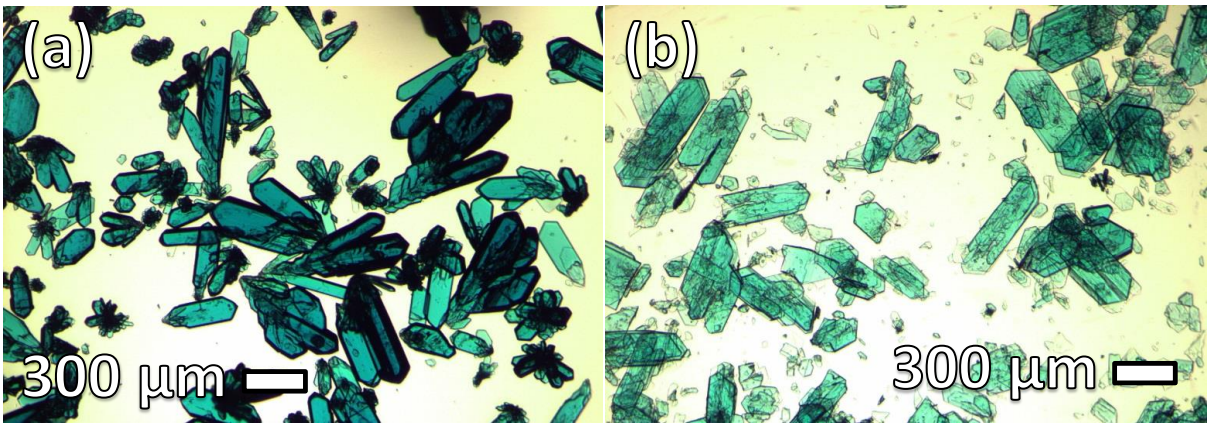

Figure 5-2. Optical microscope images of the as-synthesised single crystals of (a) CuGluBpp-Acetone and (b) CuGluBpp-MeOH showing the difference in the crystal morphologies of the two Cu-MOFs.

SEMs of the as-synthesised frameworks (Figure 5-3) give a clearer indication of the differences in the crystal morphologies. Figure 5-3.b shows crystals of the as-synthesised CuGluBpp-MeOH which compared to the structure of the CuGluBpp-Acetone (Figure 5-3.a) are thinner and have a plate-like structure. From the calculated BFDH morphology, from single crystal data, it can be inferred that the largest face for the CuGluBpp-Acetone crystals is the (0, 2, 0) face (Figure 5-4.a) and for the CuGluBpp-MeOH crystals it is the (2, 0, 0) face (Figure 5-4.b).

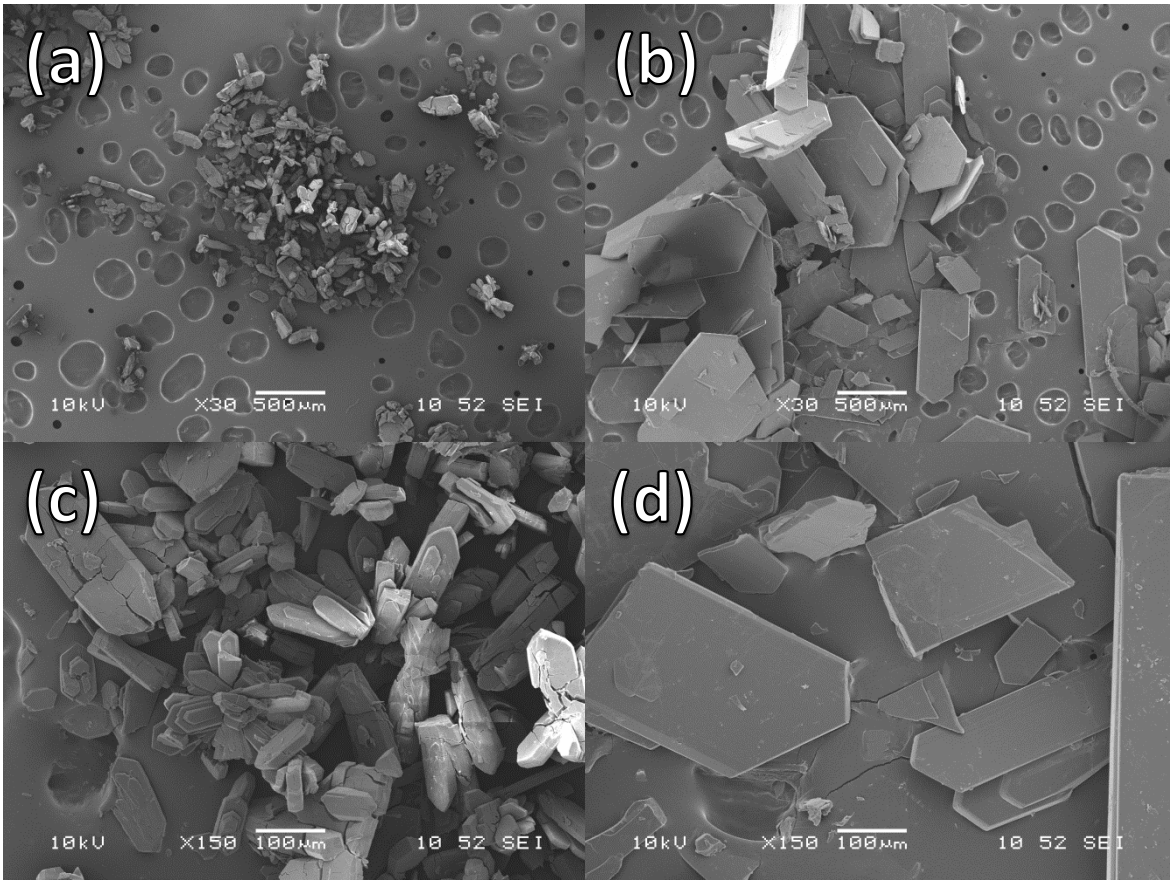

Figure 5-3. SEM images of single crystals of (a),(c) CuGluBpp-Acetone and (b),(d) CuGluBpp-MeOH.

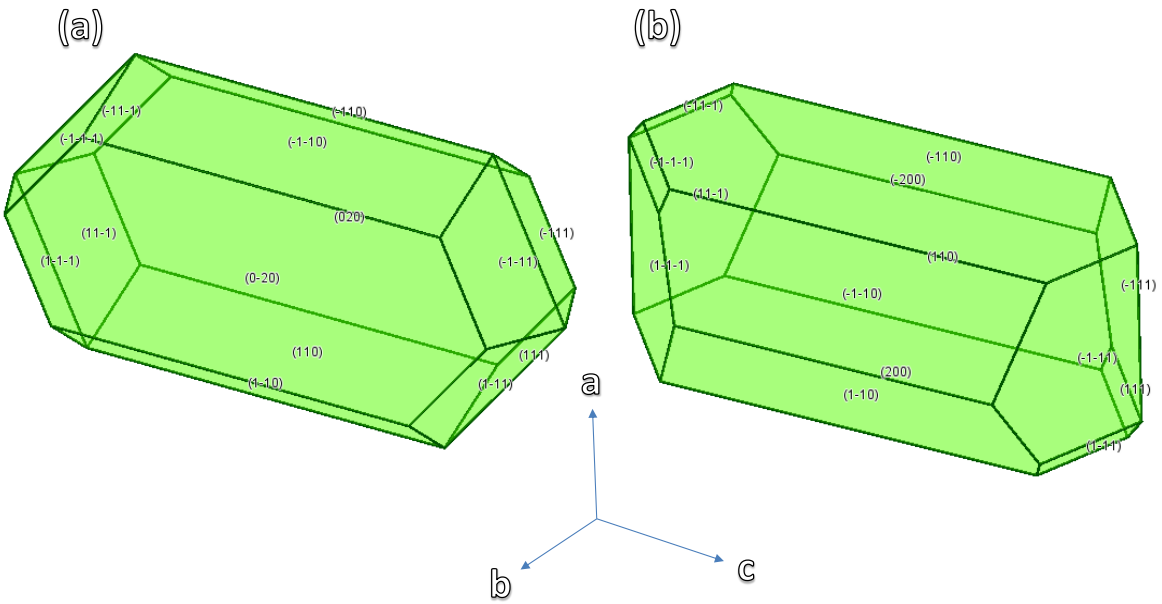

Figure 5-4. BFDH calculated crystal morphologies from single crystal data of (a) CuGluBpp-Acetone and (b) CuGlubpp-MeOH.

The two MOFs, CuGluBpp-Acetone and CuGluBpp-MeOH, exhibit similar pore structures but can be differentiated by the angle of the bipyridyl ligand within the structure (Figure 5-5).[226, 227] It is intended to use these two similar MOFs to understand what role the differences in this structure of the MOF as well as the overall crystal morphology may have on their performance within a MMM with PDMS for application within a pervaporation process.

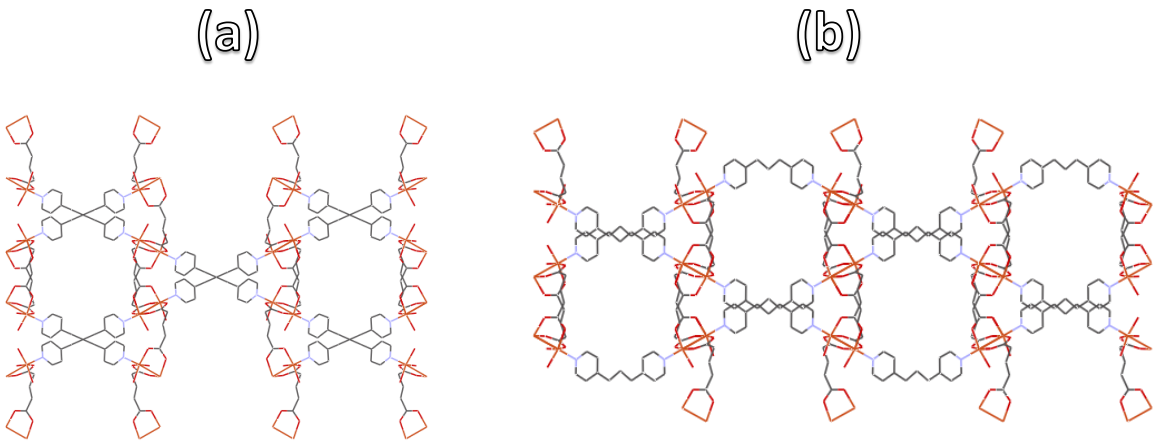

Figure 5-5. Showing the pores of (a) CuGluBpp-Acetone and (b) CuGluBpp-MeOH looking down the c-axis of the crystal structures. The contrast in the tilting of the propane chain compared to the pyridyl groups can be seen.

The microcrystalline nature of the as-synthesised Cu-MOFs means that they are too large (some in excess of 300 μm in length, (Figure 5-2) to successfully cast into a PDMS pervaporation membrane. This is due to the typical thickness of the PDMS layer of a pervaporation membrane being < 100 μm in total thickness, as the thickness of the membrane will limit the total membrane flux and ideally would be as thin as possible. It is also generally considered that smaller particles create a more homogenous dispersion within a polymer matrix and therefore exhibit greater separation properties when compared to the same membranes consisting of larger inorganic particles.[154] Therefore, the crystals were lightly ground with a pestle and mortar and sieved to reduce the particle size. SEM images of the ground Cu-MOFs are shown in Figure 5-6. As can be seen the Cu-MOFs retain similar morphologies to those presented at the microcrystalline size after being ground.

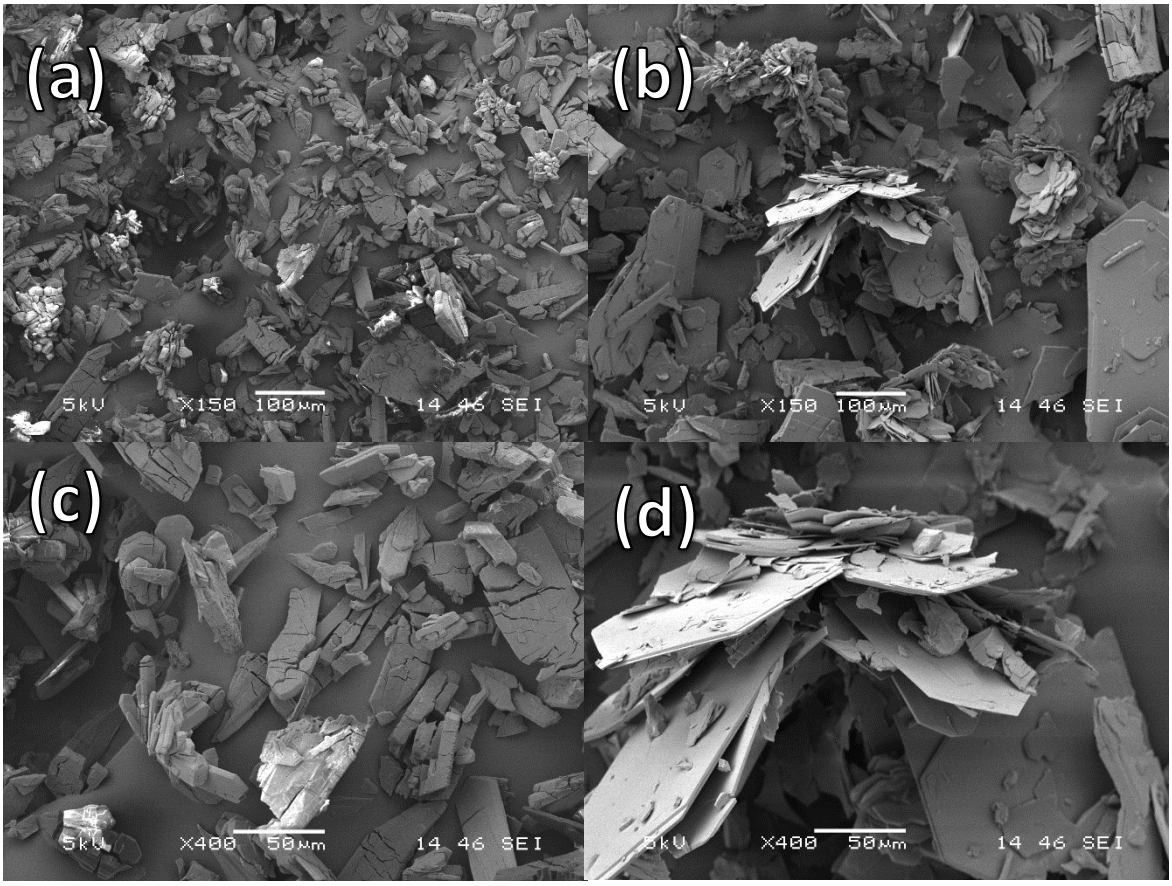

Figure 5-6. SEM images of the ground CuGluBpp-Acetone (a, c) and CuGluBpp-MeOH (b, d) at different magnifications. The plate like structure of CuGluBpp-MeOH can be seen to still be present after grinding (d) and the thicker more random crystal morphologies of CuGluBpp-Acetone (c) can be seen.

The structures of the ground as-synthesised MOFs were confirmed through comparison of the PXRD patterns with those simulated from crystal structure data. PXRD patterns of the as-synthesised bulk Cu-MOF samples matched those of the simulated patterns determined from crystal structure data (Figure 5-7). This demonstrated that the Cu-MOFs with the crystal structures had been obtained.

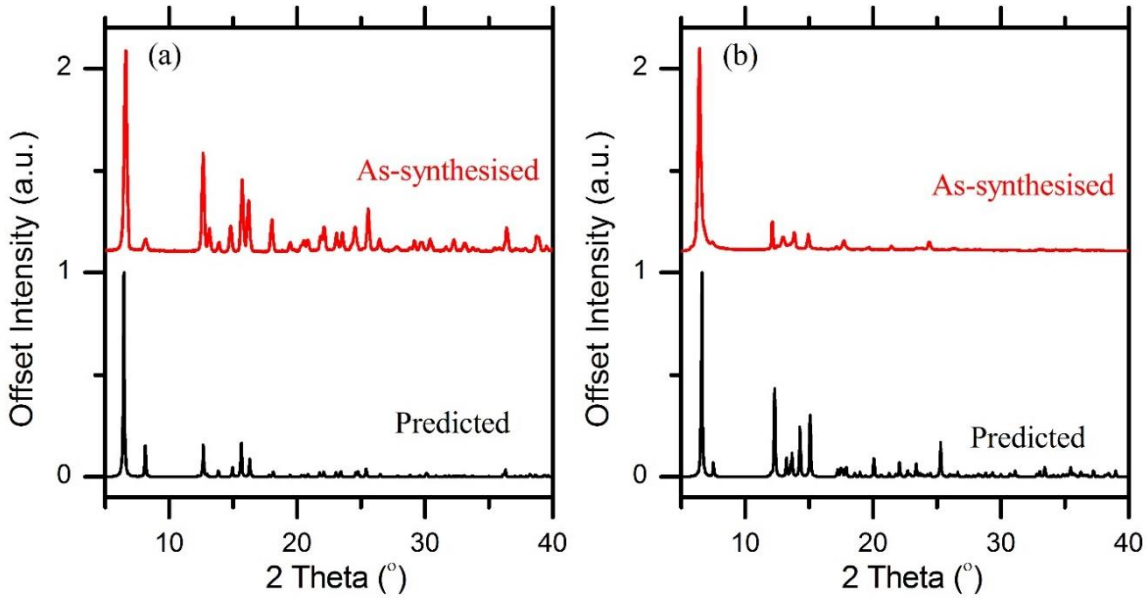

Figure 5-7. PXRDs for (a) CuGluBpp-Acetone and (b) CuGluBpp-MeOH matching predicted patterns from single crystal data.

To determine the porosity of the as-synthesised Cu-MOFs, low pressure gas adsorption isotherms were collected (Figure 5-8). Nitrogen isotherms at 77 K indicate no adsorption at low pressures whereas CO_2 isotherms of both the Cu-MOFs at 273 K indicate type I isotherms characteristic of a microporous material. This behaviour is typical for this class of MOF, with many examples of copper containing MOFs with N-donor ligands exhibiting high CO_2 adsorption but low nitrogen sorption behaviour at low pressures.[225, 226, 228] This behaviour has been previously explained by the different quadrupole moments and polarizability of the different molecules, as well as the differing sizes of N_2 and CO_2. The differences of the adsorption behaviour between the two Cu-MOFs can be attributed to a combination of the different orientation of the bipyridyl ligands[227] as well as the difference in crystal morphology.[232] Seco *et al.* observed differences in adsorption behaviour of the two MOFs and attributed it to the orientation of the bipyridyl ligand;[227] however, no effect of crystal morphology was accounted for which can also be a large contributor to adsorption behaviour.[232, 233] The N_2 adsorption by CuGluBpp-Acetone also shows a much greater adsorption of N_2 at higher relative pressures when compared to CuGluBpp-MeOH. This is indicative of the presence of mesopores which could contribute to the separation behaviour of this MOF within a MMM.

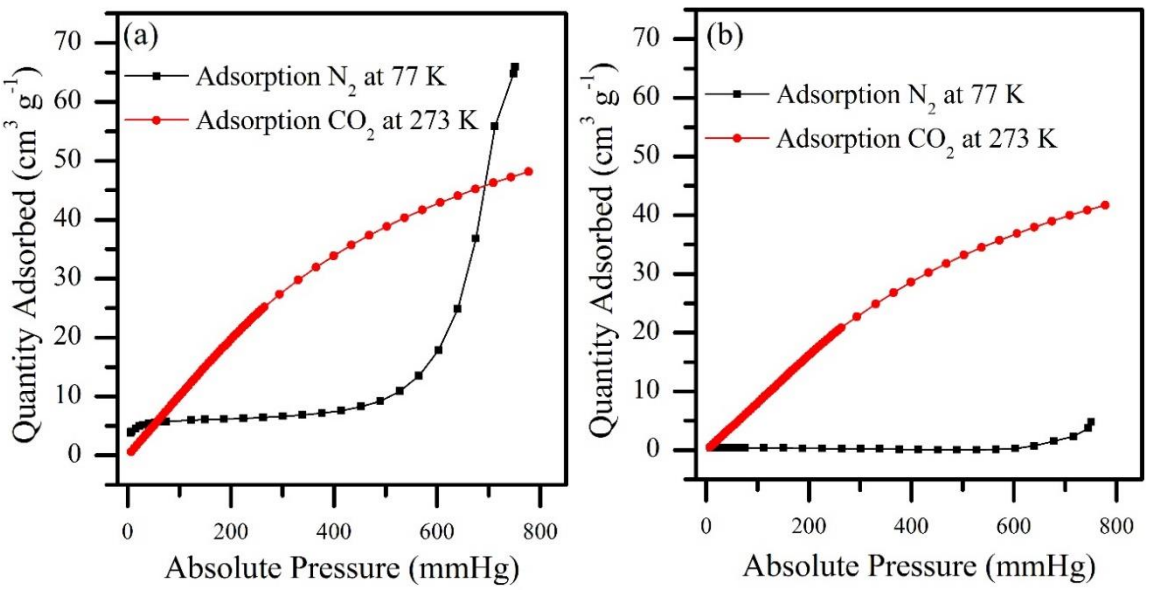

Figure 5-8. Low pressure adsorption isotherms of N_2 at 77 K and CO_2 at 273 K for (a) CuGluBpp-Acetone and (b) CuGluBpp-MeOH. The isotherms show a typical type I isotherm for the adsorption of CO_2 at 273 K and type III isotherms for N_2 adsorption at 77 K typical of these Cu-MOFs.

The TGA of the two synthesised Cu-MOFs are shown in Figure 5-9. The MOFs form solvates with either the acetone or water. The TGA for the Cu-MOF synthesised in the presence of acetone exhibits a loss of 9.1 % between 20 and 100 ºC. This is due to the loss of acetone from the as-synthesised solvated structure and equates to 1 acetone molecule per unit cell (9 % mass loss) which matches crystal structure and previous literature data.[226] The TGA of the Cu-MOF synthesised in the presence of methanol exhibits a loss of 10.6 % between RT and 200 ºC. The mass loss of 10.6 % would equate to four water molecules per unit cell (11 %) and matches the elemental analysis results.

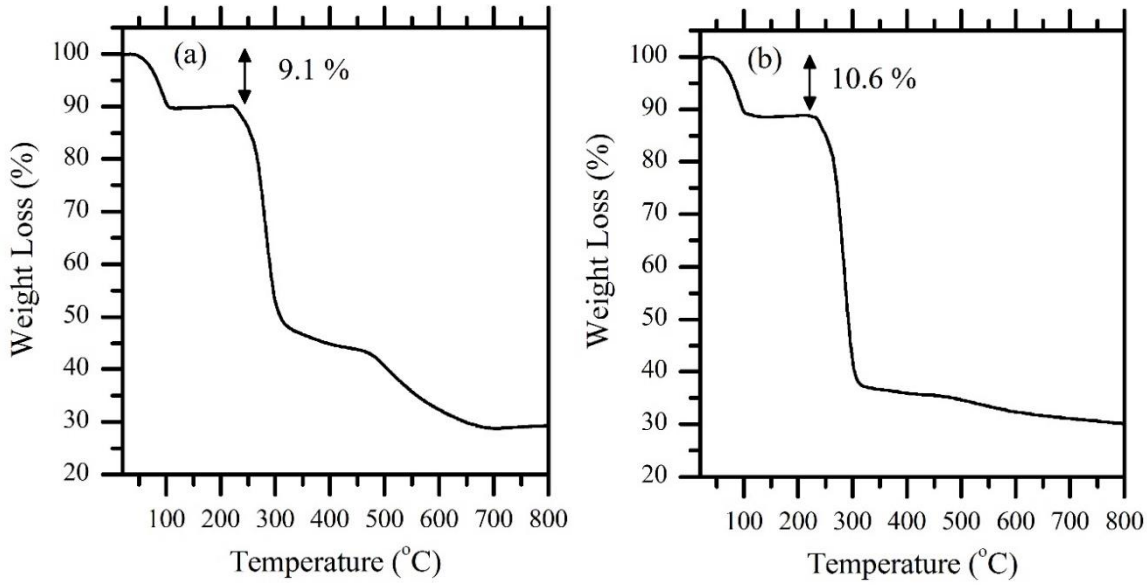

Figure 5-9.TGAs for (a) CuGluBpp-Acetone and (b) CuGluBpp-MeOH, 10 ºC min^{-1} Nitrogen atmosphere.

Liquid phase adsorption isotherms of the MOFs were used to ascertain the adsorption of acetone from water (Figure 5-10). Both MOFs, CuGluBpp-Acetone and CuGluBpp-MeOH, exhibited similar adsorption of acetone from water with adsorptions of 0.60 and 0.53 g g^{-1} respectively from an initial concentration of 0.3 g g^{-1}. The liquid phase adsorption experiments show that the Cu-MOF formed in the presence of acetone exhibits a slightly higher adsorption of acetone than the one formed in the presence of methanol. It is thought that this is due to the formation of an acetone solvate by the CuGluBpp-Acetone which indicates complementary interactions between the solvate and the pore structure of the MOF. CuGluBpp-MeOH on the other hand has a slightly different pore structure to the acetone solvated MOF and therefore is expected to exhibit a different adsorption compared to the CuGluBpp-Acetone. Again the crystal morphology will also play a role in the adsorption behaviour and the slightly lower adsorption of acetone by CuGluBpp-MeOH compared to CuGluBpp-Acetone reflects the difference in the CO_2 and N_2 adsorption isotherms (Figure 5-8).

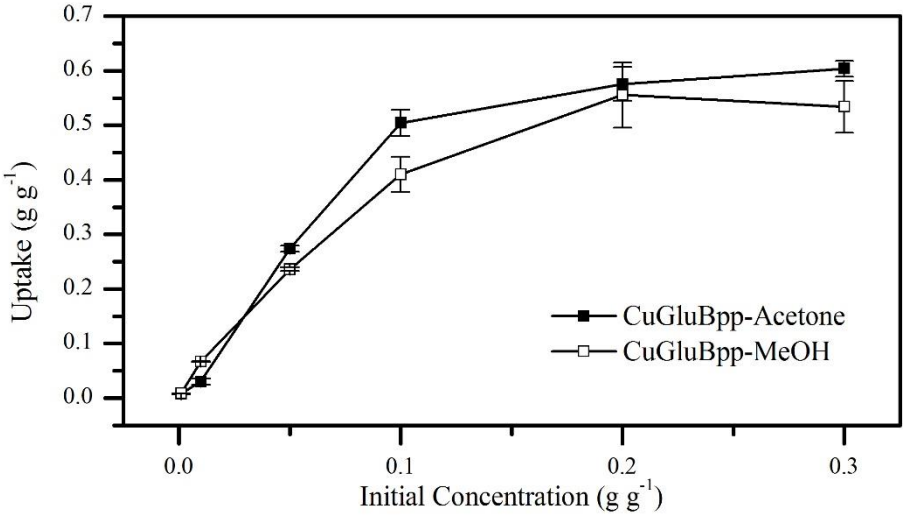

Figure 5-10. Liquid-phase adsorption isotherms of acetone by the MOFs CuGluBpp-Acetone and CuGluBpp-MeOH.

5.3.2 Characterisation of Cu-MOF MMMs

Membranes were fabricated of the two different Cu-MOFs within PDMS with varying wt% at 5, 10, 15, 20 and 30 wt% respectively. A number of analytical techniques were used to ascertain the structural properties of the as-prepared membranes so this could be related to their pervaporation performance:

5.3.2.1 FTIR

FTIRs show the presence of the Cu-MOFs within the membranes. These are clearest within the membranes loaded at 30 wt% of MOF and absorbances at 1604, 1415 and 1303 cm^{-1} can clearly be seen in the MMM due to the presence of the Cu-MOFs embedded within PDMS (Figure 5-11, Figure 5-12).

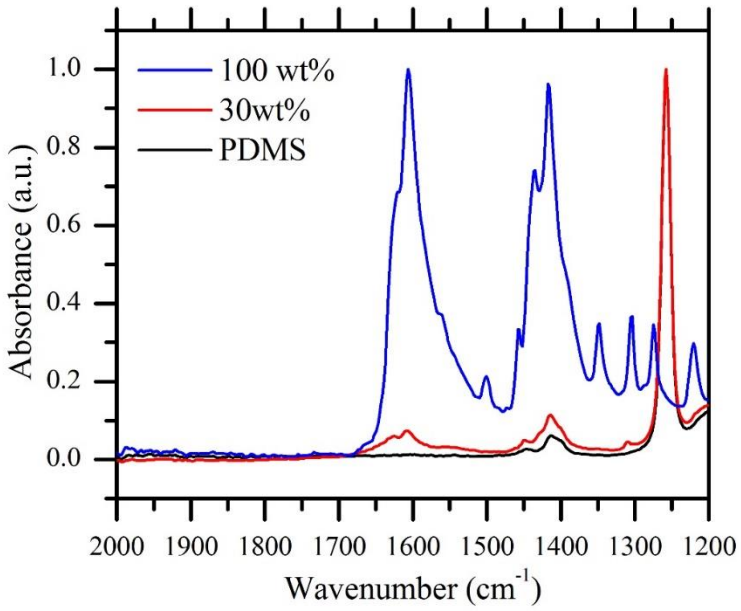

Figure 5-11. Comparison of the FTIRs of PDMS, CuGluBpp-Acetone and the MMM containing 30 wt% of MOF.

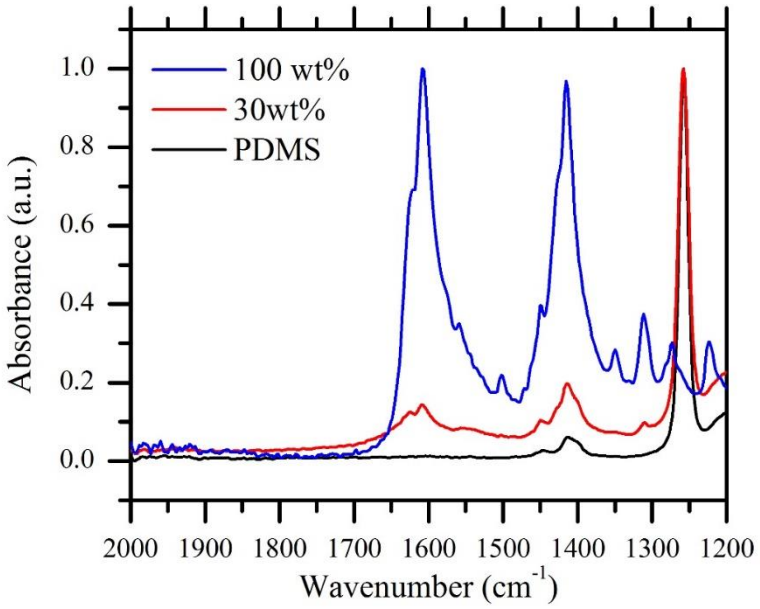

Figure 5-12. Comparison of the FTIRs of PDMS, CuGluBpp-MeOH and the MMM containing 30 wt% of MOF.

5.3.2.2 Imaging of Membranes

Digital microscope images of the as-synthesised MMMs of CuGluBpp-Acetone (Figure 5-13) and CuGluBpp-MeOH (Figure 5-14) give a visual indication of the loading of the Cu-MOFs into the MMMs (photographs of the as-prepared membranes can also be seen in Appendix A.5.1). As can be seen from the images it is clear that an increased loading of the Cu-MOFs was achieved within the MMMs through addition of increased MOF into the polymer dope solution. Another point that can be inferred from the images is the appearance of points within the CuGluBpp-MeOH membranes where there is an increased agglomeration of particles, clearest in the 5 wt% and 30 wt% loaded membranes (Figure 5-14). It is thought that these are due to layers of the plate like crystals of CuGluBpp-MeOH having stacked on top of each other within the PDMS matrix.

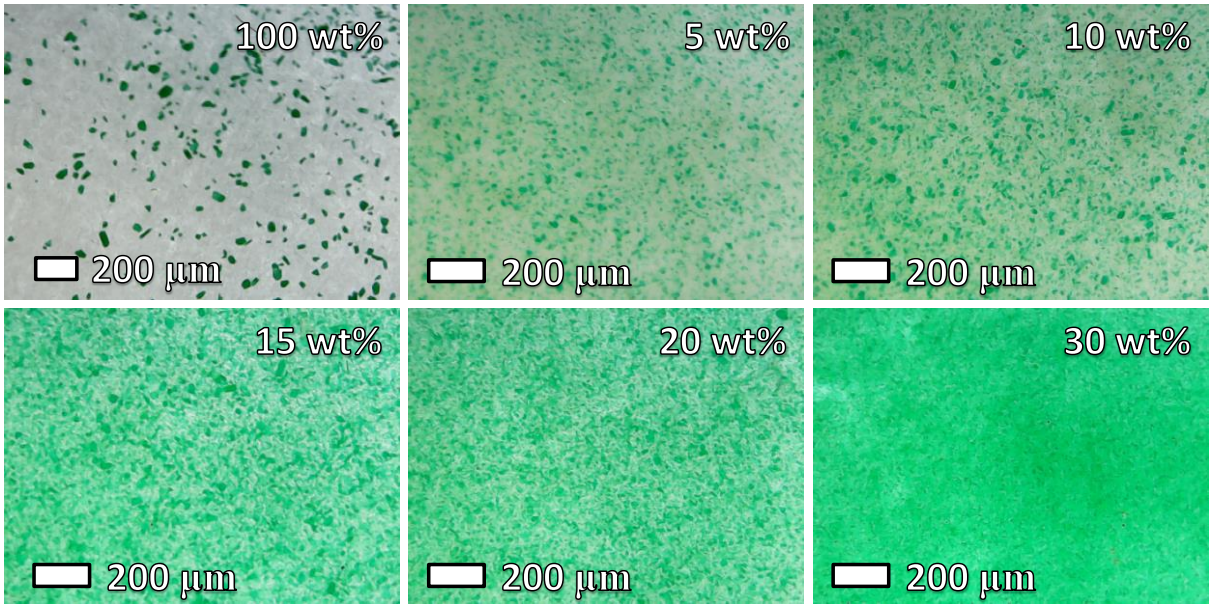

Figure 5-13. Digital microscope pictures of the as prepared CuGluBpp-Acetone membranes.

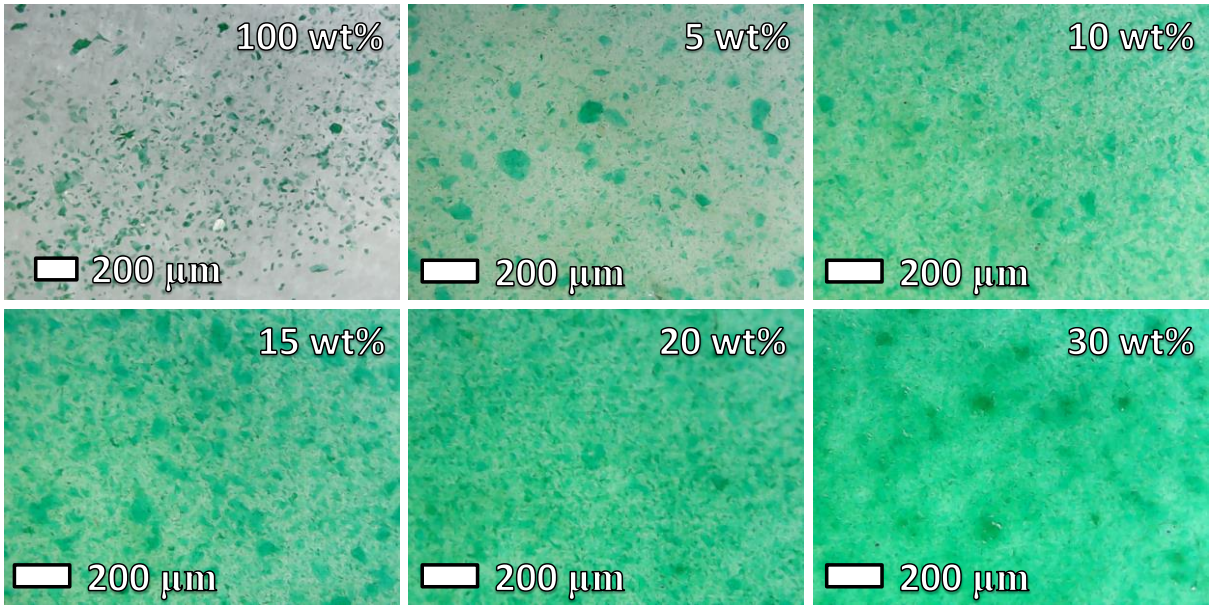

Figure 5-14. Digital microscope pictures of the as prepared CuGluBpp-MeOH membranes.

SEM imaging reflects the digital microscope imaging giving a visual indication of the loading of the MOFs within the MMMs. The surface and cross-sectional images of the membranes produced from CuGluBpp-Acetone (Figure 5-15, Figure 5-16) and CuGluBpp-MeOH (Figure 5-17, Figure 5-18) can easily identify an increase in MOF within the cast membrane with increased addition to the polymer dope. The agglomeration of the MOFs within the polymer matrix can also be seen qualitatively in the surface and cross-sectional SEMs.

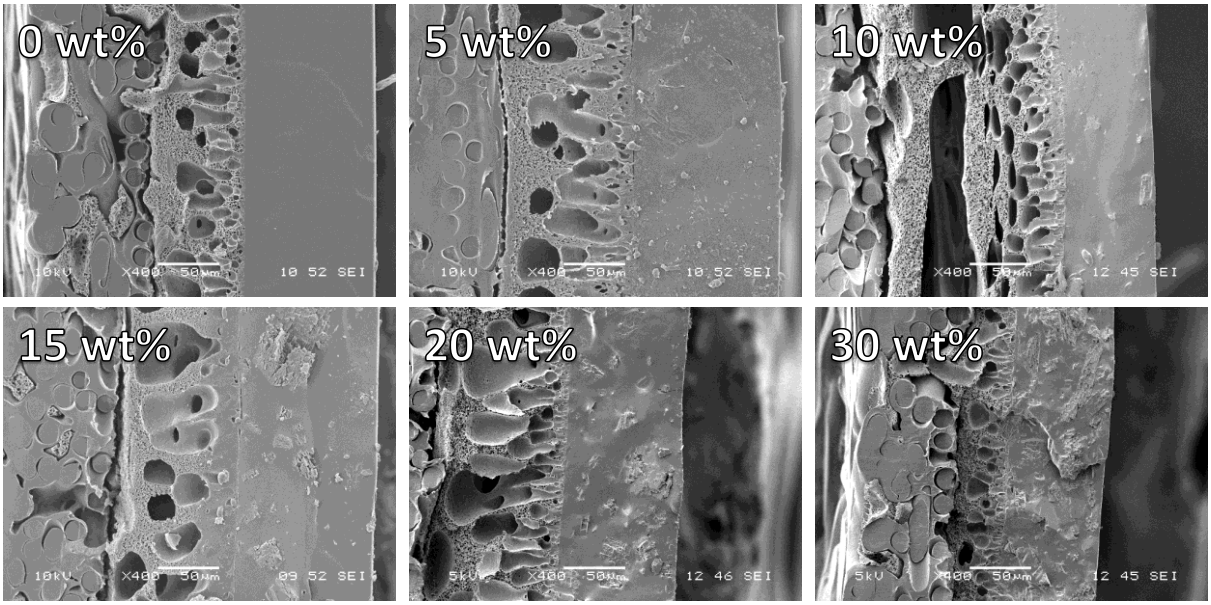

Figure 5-15. Cross-sectional SEM images of the as-prepared MMMs of PDMS and CuGluBpp-Acetone at varying wt% of the Cu-MOF.

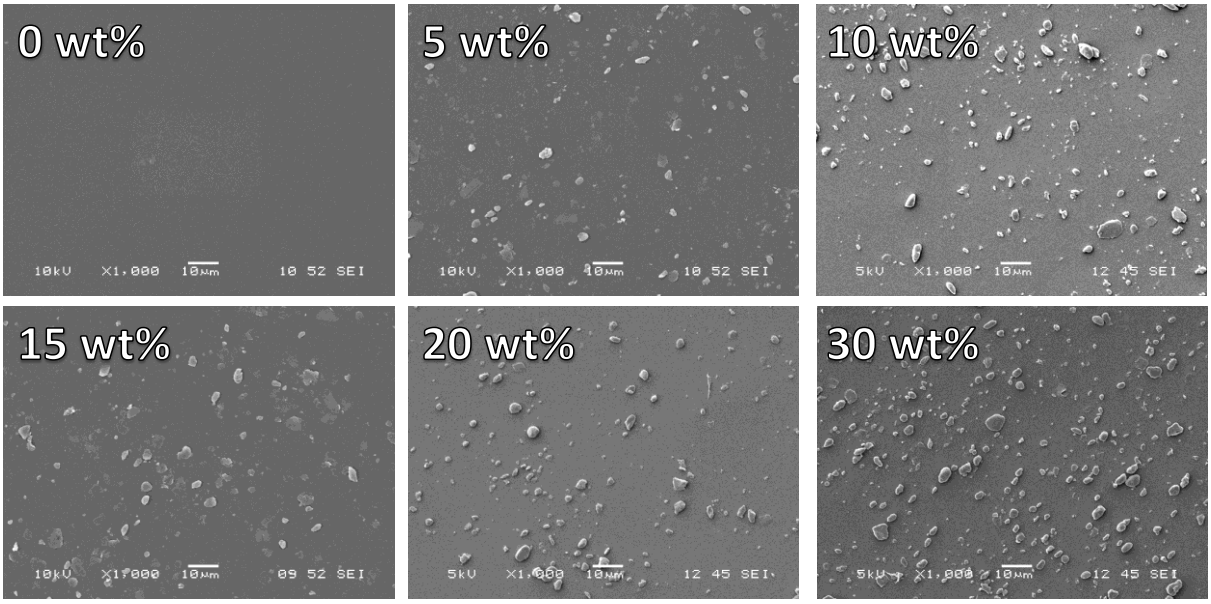

Figure 5-16. Surface SEM images of the as-prepared MMMs of PDMS and CuGluBpp-Acetone at varying wt% of the Cu-MOF.

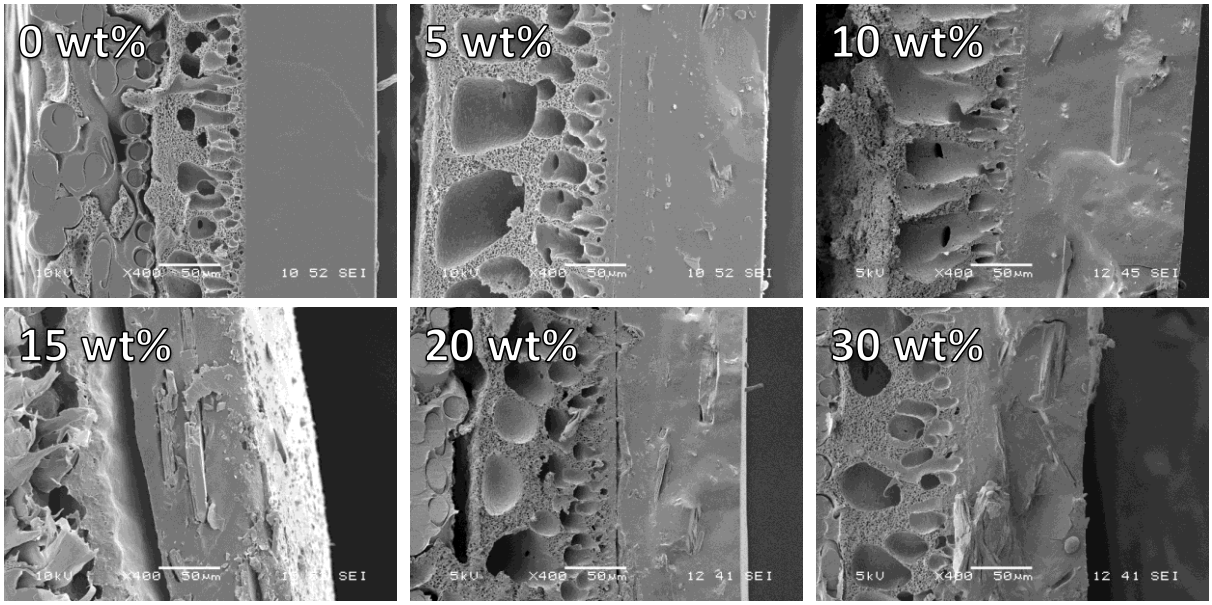

Figure 5-17. Cross-sectional SEM images of the as-prepared MMMs of PDMS and CuGluBpp-MeOH at varying wt% of the Cu-MOF.

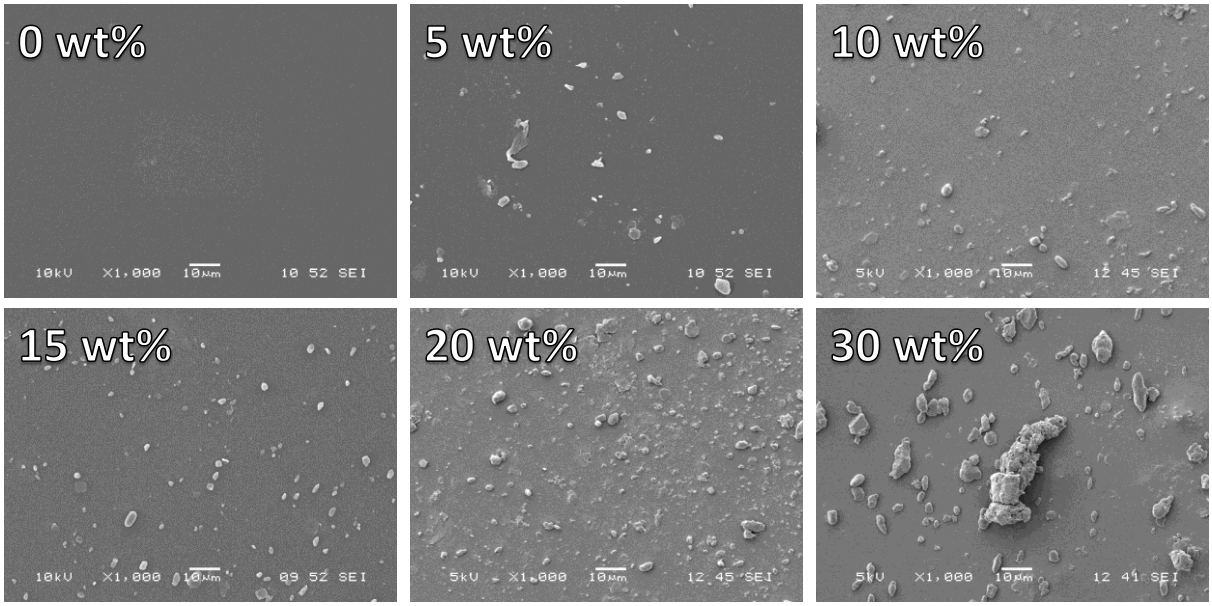

Figure 5-18. Surface SEM images of the as-prepared MMMs of PDMS and CuGluBpp-MeOH at varying wt% of the Cu-MOF.

5.3.2.3 Thermal Gravimetric Analysis

The loading of MOF within the MMMs was investigated using TGA. The TGA curves can be seen in Figure 5-19 and Figure 5-20. With an increased loading of MOF an increased % mass loss was

observed for the membrane material from 5 to 30 wt% for both classes of MMM. This is clearly the case for an increased loading of MOF as the Cu-MOFs exhibit a much larger % mass loss (~ 70 %) compared to PDMS (~ 32 %).

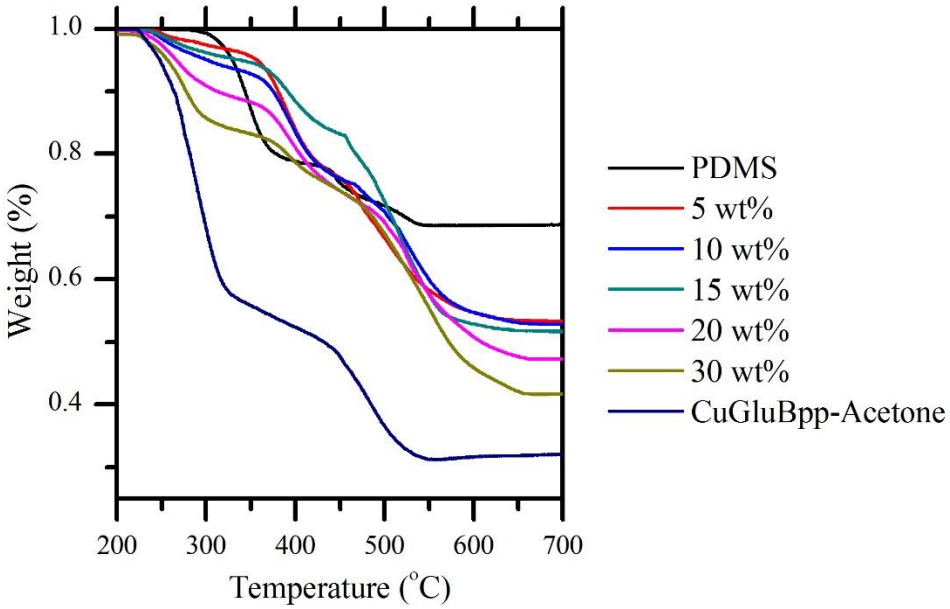

Figure 5-19. TGAs of as-synthesised MMMs of PDMS and CuGluBpp-Acetone at differing wt% loading of the MOF.

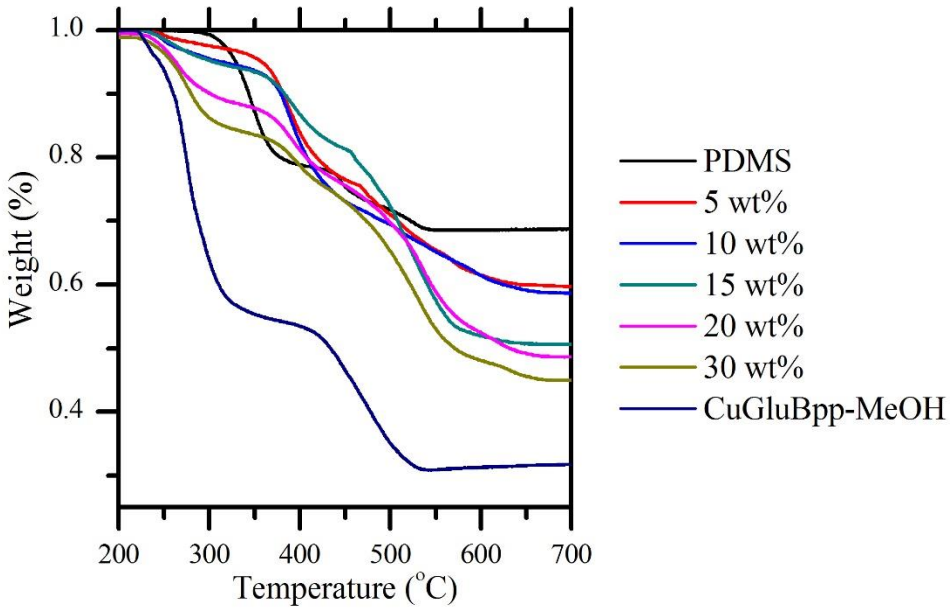

Figure 5-20. TGAs of as-synthesised MMMs of PDMS and CuGluBpp-MeOH at differing wt% loading of the MOF.

5.3.2.4 Powder X-ray diffraction

The PXRD of the as-synthesised membranes of CuGluBpp-Acetone (Figure 5-21) exhibited characteristic reflectances of the simulated pattern of CuGluBpp-Acetone calculated from crystal structure data. This indicates that the structure of the MOF is intact after fabrication of the membrane.

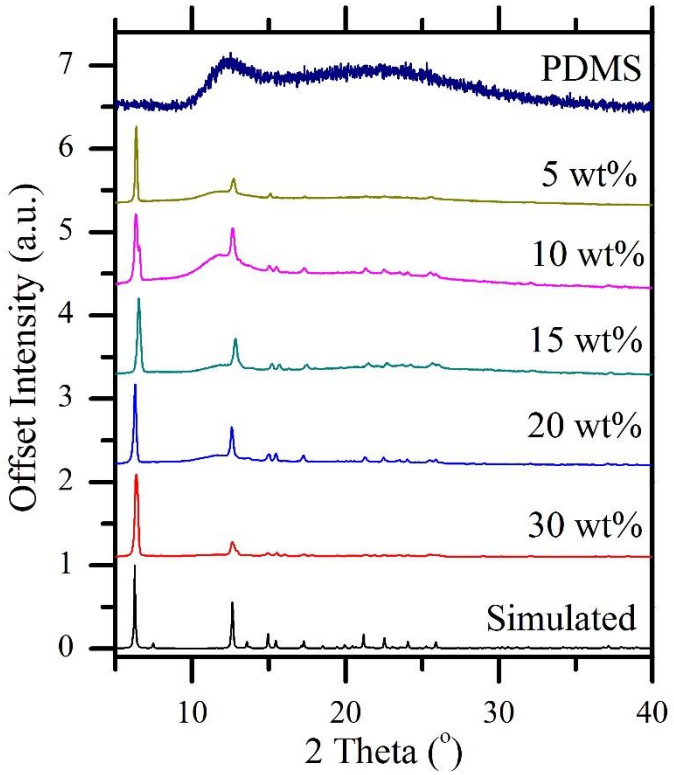

Figure 5-21. PXRDs of the as-synthesised CuGluBpp-Acetone membranes with differing wt% of MOF.

The PXRD of the as-synthesised membranes with CuGluBpp-MeOH are shown within Figure 5-22. The PXRDs of the as-synthesised membranes show a high degree of preferential orientation along the (2, 0, 0), (4, 0, 0) and (8, 0, 0) planes, and reflect the pattern simulated with this preferred orientation in these planes (see Figure 5-23 for a comparison of the simulated PXRD pattern with and without preferred orientation). This would indicate that the majority of the CuGluBpp-MeOH MOFs are aligned parallel to the membrane. This would be a non-ideal orientation of the MOF as it would mean that the 1D channels for permeation would be perpendicular to the permeate flow within the membrane.

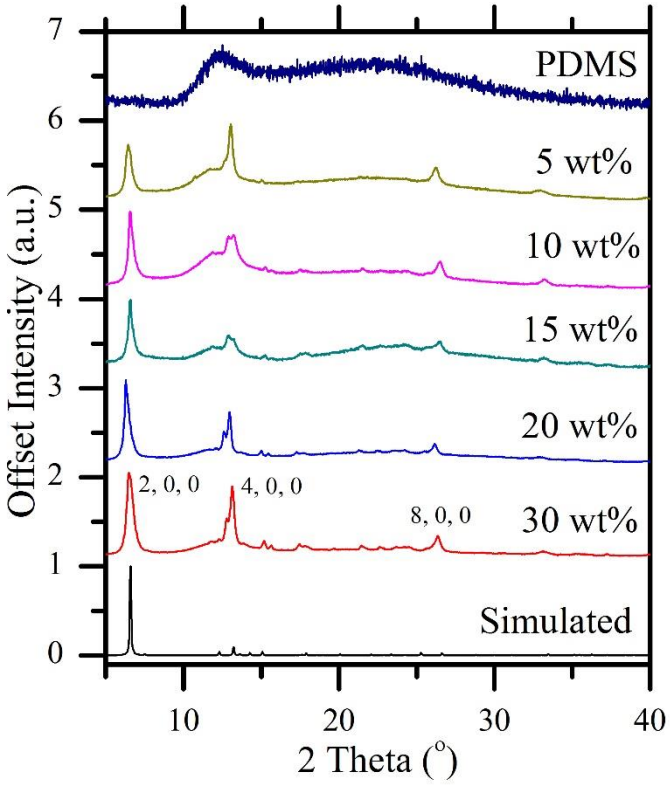

Figure 5-22. PXRDs of the as-synthesised CuGluBpp-MeOH membranes with differing wt% of MOF.

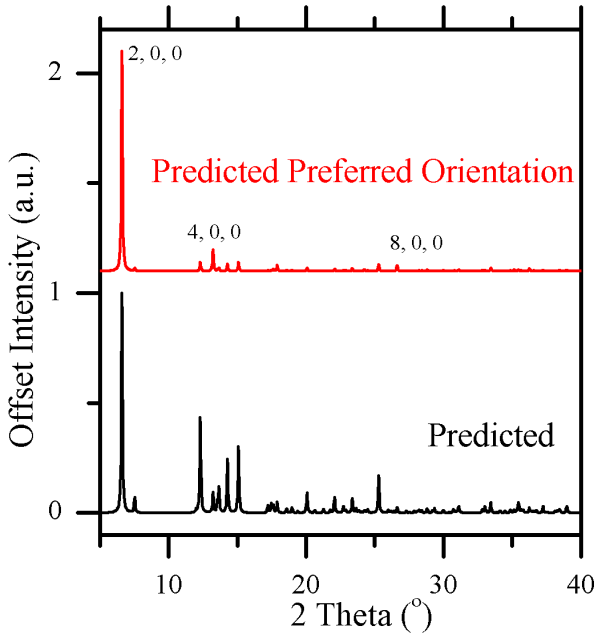

Figure 5-23. Comparison of the PXRD patterns predicted from crystal structure data without (lower) and with (upper) simulated preferred orientation (h = 1, k = 0, l = 0) with March-Dollase parameter of 0.5.

Figure 5-24 highlights the (2, 0, 0), (4, 0, 0) and (10, 0, 0) planes within the crystal structure of CuGluBpp-MeOH. It can be seen that the planes are parallel to the orientation of the 1-dimensional pore of the MOF. As these planes exhibit preferred orientation within the PXRD it can be reasoned that the majority of the crystals are aligned along these planes within the MMM parallel to the membrane surface. Therefore, the majority of the pores of the MOFs are parallel to the membrane. The orientation of pores in this manner would be non-ideal, as they are perpendicular to the permeate flow through the membrane and would likely inhibit the total flux of the material.

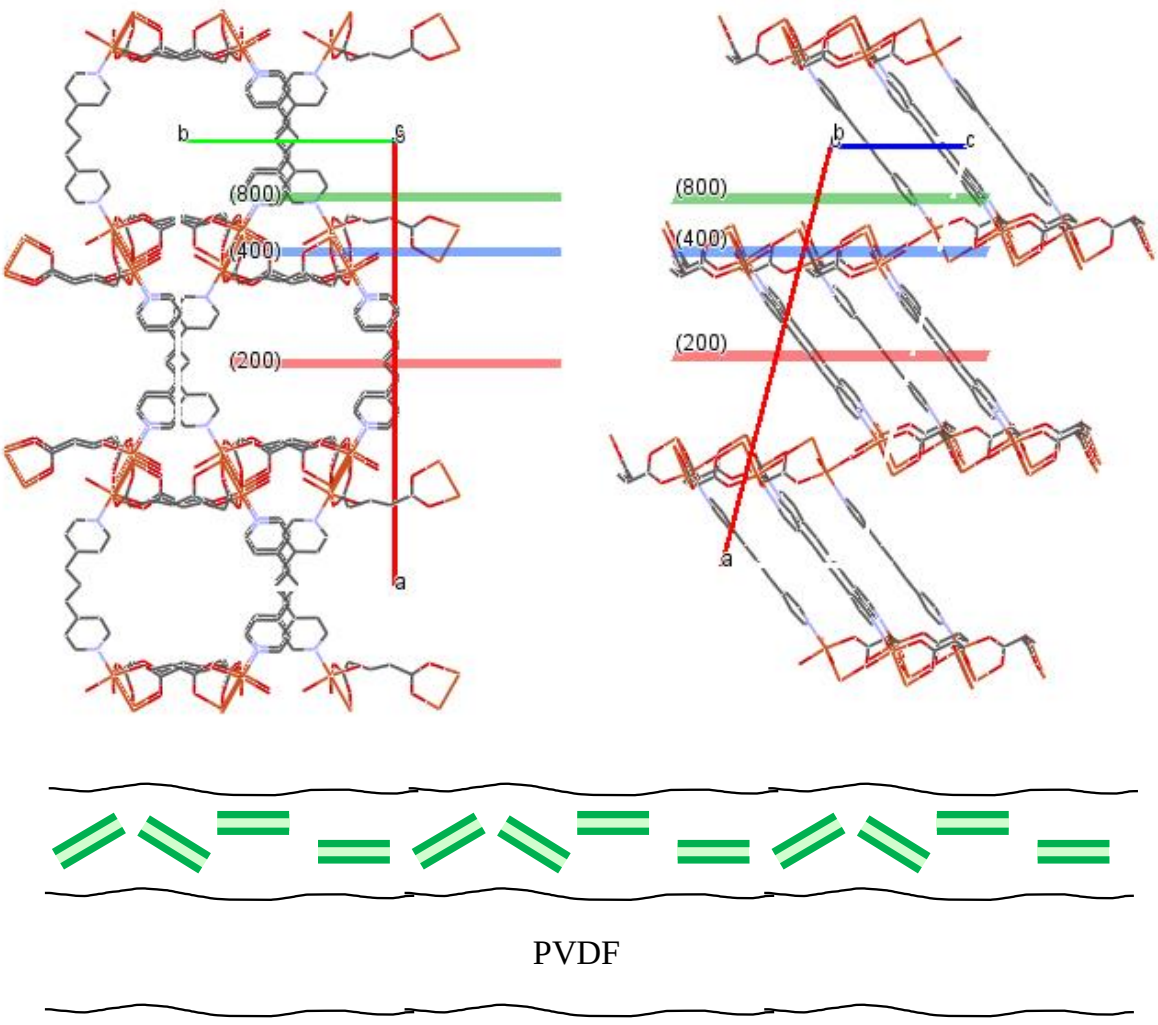

Figure 5-24. Schematic showing the (2, 0, 0), (4, 0, 0) and (8, 0, 0) planes of CuGluBpp-MeOH which show preferred orientation within the PXRD pattern of the membranes and the expected orientation of the 1D channels within the membrane.

An ideal structure (Figure 5-25) for the MMM would be where the pores of the MOF would be oriented perpendicular to the feed flow of the membrane and parallel to the permeate flow through the membrane, as well as the MOF being homogenously dispersed throughout the membrane. The non-alignment of pores in the filler materials is a common problem when fabricating MMMs from inorganic materials exhibiting 1-dimensional pores, with one main example being carbon nanotubes, where the alignment of the 1-dimensional channels has been found to be crucial to a membranes flux and selectivity as well as its overall mechanical strength.[113]

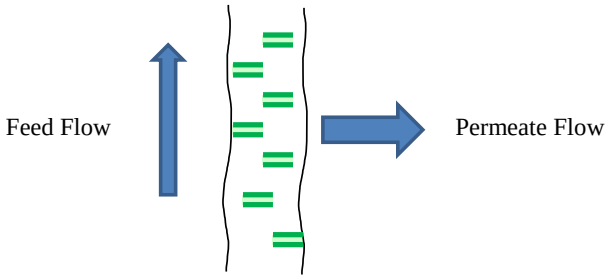

Figure 5-25. Ideal orientation of the MOFs within the MMM to achieve enhanced flux and selectivity.

More detailed cross-sectional SEM images further indicate the orientation of the Cu-MOFs within the membranes (Figure 5-26). As can be seen from Figure 5-26.b, the flat plate-like crystals of CuGluBpp-MeOH can be clearly identified within the PDMS of the membrane with the largest faces parallel to the surface of the membrane. In contrast, no major orientation of the CuGluBpp-Acetone crystals within the MMM could be identified from the SEM analysis, matching PXRD data, indicating that the different morphology allowed for a higher number of orientations of the 1D pores. These matched more closely the ideal orientation of the pores compared to CuGluBpp-MeOH.

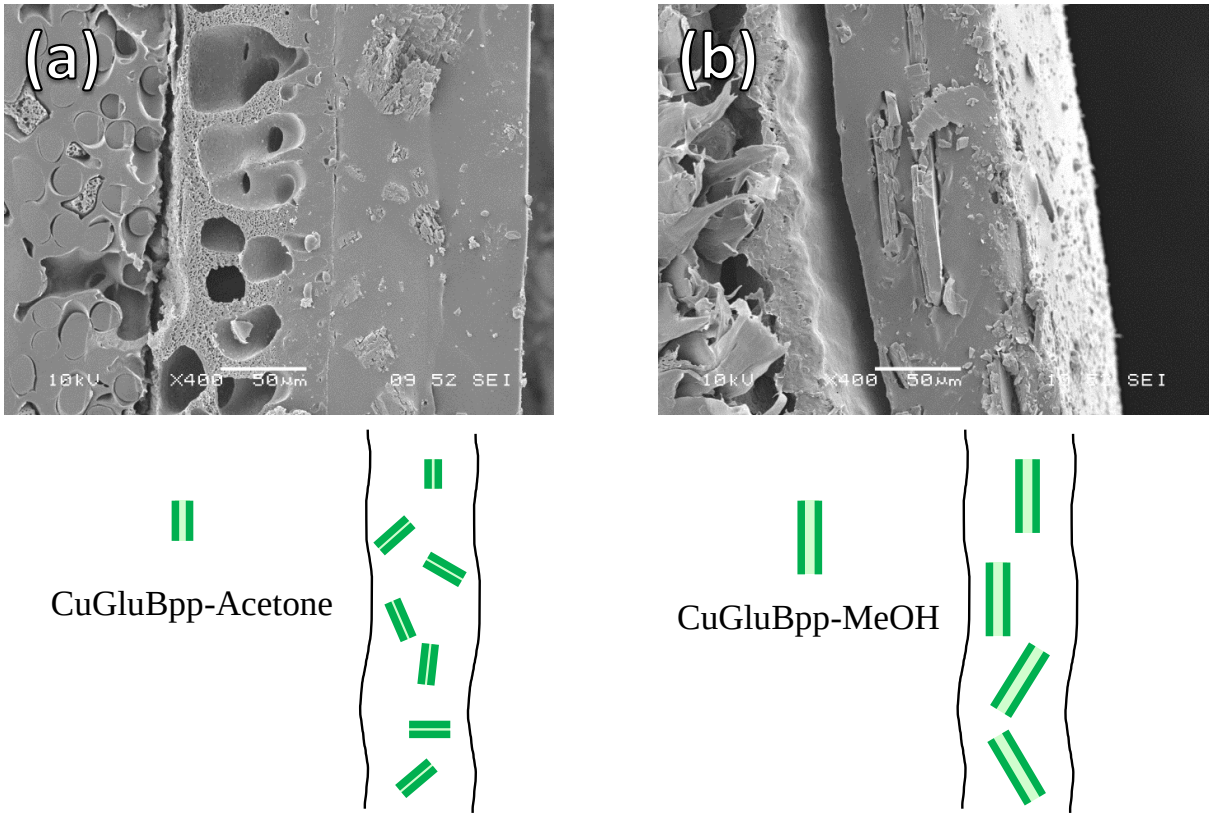

Figure 5-26. The orientation of the two Cu-MOFs differs substantially due to their differing crystal shapes and is demonstrated within their 15 wt% MMMs, SEM images (above) and schematic diagrams (below).

Calculation of the BFDH crystal morphology from the single crystal data of CuGluBpp-MeOH (an approximation of the crystal morphology based on the geometrical considerations of the crystallographic data) confirms SEM analysis of the cross-sections of the as-synthesised MMMs. As can be seen in Figure 5-27, the 1-dimensional pores of CuGluBpp-MeOH run down the c-axis of the structure. From the SEM imaging it can be identified that the (2, 0, 0) face (Figure 5-4) perpendicular to the a-axis will be lying parallel to the membrane surface. This indicates the non-ideal orientation of the crystal within the MMM, as identified through the preferential orientation within the PXRD analysis.

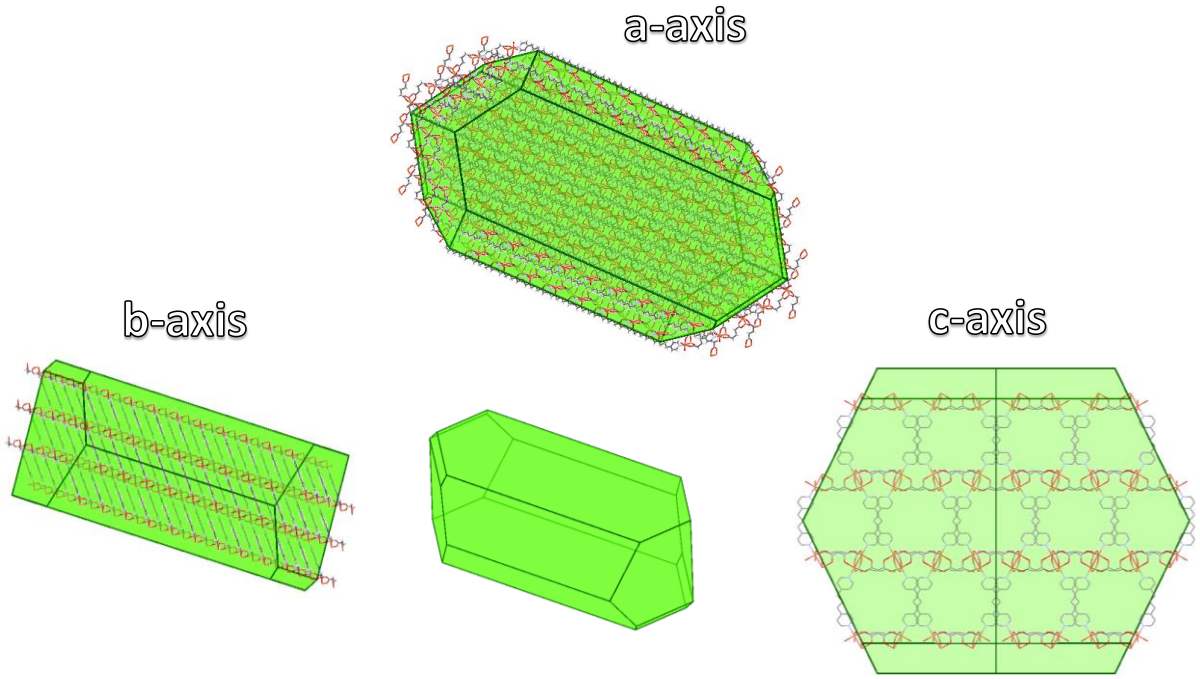

Figure 5-27. BFDH calculated crystal morphology of CuGluBpp-MeOH viewing down the different axes.

This alignment of the CuGluBpp-MeOH particles within the PDMS membrane is thought to arise from a combination of the casting process used and the general morphologies of the crystals. A doctor blade was used to cast the polymer dope solution onto the PVDF support (Figure 5-28). When the larger flat crystals of CuGlubpp-MeOH were cast, these would either be pushed into a parallel direction with the membrane surface or would come to rest at this orientation due to gravity and lying on the largest face. As discussed earlier, the pore orientation is a common problem when fabricating membranes from carbon nanotube materials and a number of different techniques have been studied to achieve an improved alignment of the pores perpendicular to the membranes surface.[113]

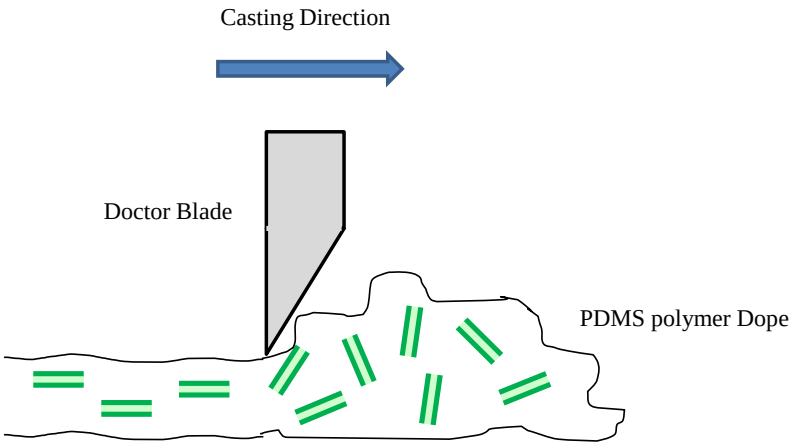

Figure 5-28. Schematic of the casting process for the MMMs using a doctor blade and the potential effect on the orientation of the CuGluBpp-MeOH particles within the MMM.

5.3.2.5 Water contact angles

The water contact angles of the surfaces of the different MMMs were also measured (Figure 5-29). The surfaces of the membranes were all hydrophobic, exhibiting contact angles of > 90 ºC. With an increase in the loading of Cu-MOF, the contact angle for both classes of membrane increased. From comparing the two classes of MMMs, it can be seen that the average water contact angle of the membrane surfaces is higher for the membrane consisting of CuGluBpp-MeOH than for CuGluBpp-Acetone. As both the Cu-MOFs are composed of the same components the change in contact angle has been attributed to the orientation of the MOFs within the membranes and the effect on surface roughness.[234] The alignment of the CuGluBpp-MeOH crystals within the membranes would have the (2, 0, 0) or (-2, 0, 0) faces (Figure 5-4) aligning parallel with the membrane surface creating a smoother surface with less defects or roughness at the surface. CuGluBpp-Acetone which is oriented randomly creates a higher surface roughness with more chances for defects at the surface reducing the contact angle, and would correlate to the increased difference in contact angle at higher MOF loading.

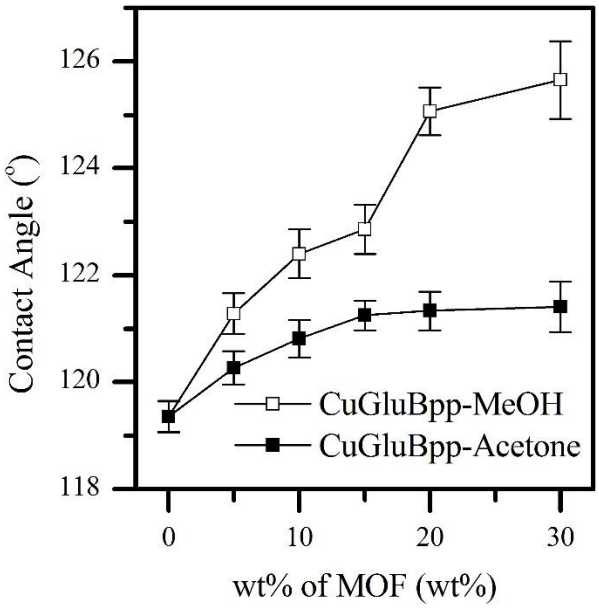

Figure 5-29. Water contact angles of the as-synthesised CuGluBpp-PDMS membranes with different wt% loading of MOF.

5.3.2.6 Degree of Solvent Uptake

The solvent uptake of the membranes was measured with water, methanol and acetone separately for the membranes consisting of CuGluBpp-Acetone (Figure 5-30.a) and CuGlubpp-MeOH (Figure 5-30.b). For the membranes synthesised from CuGluBpp-Acetone, the uptake of acetone initially increases with increased MOF loading to 25.8 % with a 10 wt% loading. However, with further increased MOF loading, the total degree of solvent uptake of the membranes by acetone decreases down to 19.3 %. For the membranes composed of CuGluBpp-MeOH, the uptake of acetone by the membranes correlates well with increasing wt% of MOF within the membrane up to a maximum of 24.7 % at a 20 wt% loading of MOF. At the higher loading of 30 wt% of MOF the uptake decreases to 17.9 %. The uptake of water and methanol by both classes of membranes increased with increasing wt% of loaded MOF. These results are due to a change in the free volume of the PDMS polymer due to the disruption of the polymer chains by the MOF particles. At low loading the looser polymer chains than for pure PDMS will increase the uptake; however, the more entangled the polymer chains become with the MOF crystals at higher loadings they will then start to resist the swelling process.[235, 236] For water and methanol, the membrane will not be saturated with solvent which is a result of the limited uptake of these solvents by PDMS arising from their vastly different Hildebrand solubility parameters (Table 5-2). Decreased uptake at higher wt% loading of MMMs for pervaporation has been previously noted for a number of

examples including: ZSM-5-PEBA,[166] silicalite-filled PEBA,[159] ZSM-5 in polyurethaneurea[237] and ZIF-8 filled PDMS.[171]

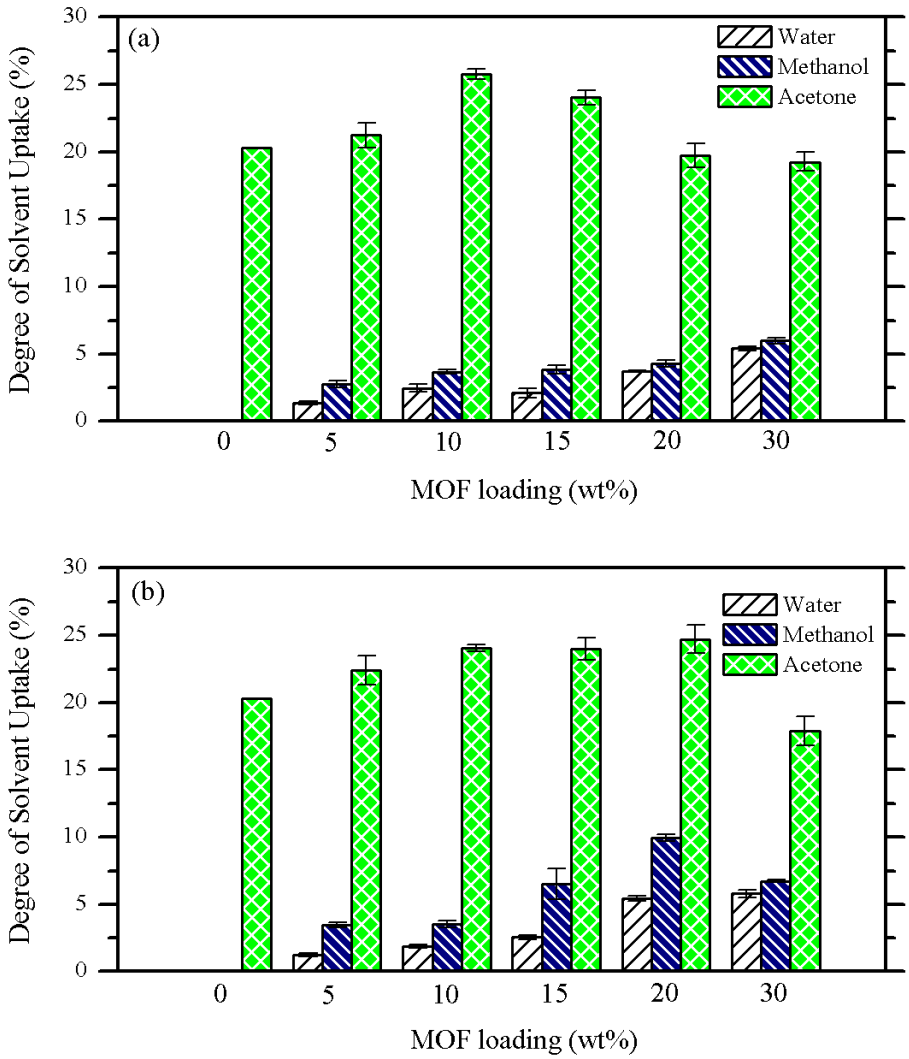

Figure 5-30. Degree of solvent uptake of water, methanol and acetone for the as-synthesised membranes: (a) CuGluBpp-Acetone and (b) CuGluBpp-MeOH.

Table 5-2. Hildebrand solubility parameters for solvents and PDMS[215]

Solvent / Polymer	Hildebrand Solubility Parameter at 25 °C
Water	47.9
Methanol	29.6
Acetone	20.2
PDMS	15.5

The difference between the solvent uptake behaviour of the two membrane classes can be explained by the difference in morphologies of the MOF. The membranes consisting of CuGluBpp-Acetone exhibit a decrease in the acetone uptake at a lower loading (15 wt%) than for those composed of CuGluBpp-MeOH (30 wt%). This is likely due to the smaller crystals of CuGluBpp-Acetone causing greater entanglement of the polymer chains at a lower loading than the larger flatter CuGluBpp-MeOH particles. Similar differences in behaviours has been shown previously for gas separation membranes utilising different morphologies of MOFs.[232, 233]

These results show that the membranes have a solvent uptake selectivity towards acetone over water or methanol. Therefore, in pervaporation testing the selective removal of acetone over water would be expected. The non-ideal alignment of CuGluBpp-MeOH is; however, likely to inhibit the flux and separation performance of the membranes. In the following section the pervaporation performance for the removal of acetone from water is presented and related to the structural properties of the as-prepared membranes.

5.3.3 Pervaporation Performance of the Cu-MOF MMMs

The pervaporation performance of the as-synthesised membranes was then investigated to ascertain what effect the structural differences outlined above may have on the organic / water separation performance of the membranes. Initially a 5 wt% solution of acetone in water was investigated at a temperature of 30 ºC for the membranes of differing wt% loading of the Cu-MOF. For the membranes loaded with CuGluBpp-Acetone there was a strong relationship between increasing separation factor and increasing wt% of the MOF (Figure 5-31). The separation factor increased from 5.5 for the pure PDMS membrane up to 11.9 for the 30 wt% membrane. The total flux initially increased from 0 - 5 wt% of MOF from 0.052 to 0.070 kg m^{-2} h^{-1}, but then decreases with increased loading of MOF down to 0.042 kg m^{-2} h^{-1} at a loading of 30 wt%. It is clear that increasing the loading of MOF aids the separation performance of the PDMS membrane but decreases permeability. At low loadings of MOF (5 wt%) the polymer chain packing is looser than for the pure PDMS membrane and the pores of CuGluBpp-Acetone aid diffusion across the membrane, leading to an increase in permeability. The total flux then decreases at higher loadings due to the partial chain rigidification (as also observed in the solvent uptake results; Figure 5-30.a) and the increasingly tortuous pathway through the membrane due to the increasing number of randomly oriented 1D pores of the MOF. Both of these factors would contribute to a higher transport resistance across the membrane. This reflects the degree of solvent uptake experiments which show that after a maximum uptake of acetone at 10 wt% loading, the uptake decreases. As the pores of CuGluBpp-Acetone are more selective to acetone over water, they will provide an additional pathway for acetone to permeate whereas water would permeate mainly through the polymer that is rigidifying. Therefore, although the permeabilities of both are decreasing, water would decrease faster than acetone with increased loading of CuGluBpp-Acetone. Although a decrease in the total flux is observed, due to the increase in separation factor, the PSI value of the membranes for acetone separation increases to a maximum of 567 (Table 5-3) for the 15 wt% loaded membrane. This is similar to the effect increased concentration of CNTs in PVA had on pervaporation performance[134] and the decreased permeability but increased separation performance of ZIF-71 in PEBA at 20 wt% loading.[176]

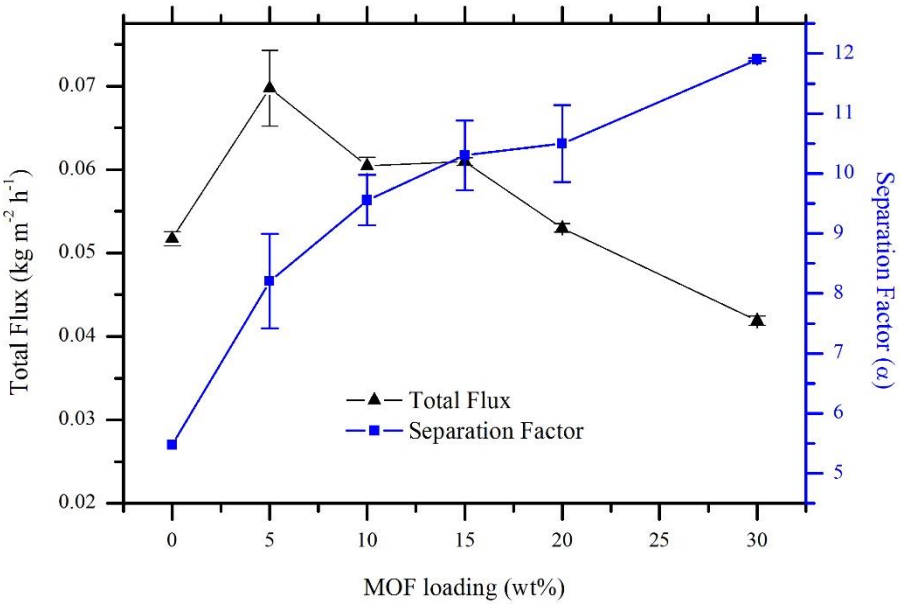

Figure 5-31. Pervaporation performance of membranes with CuGluBpp-Acetone as the inorganic filler. 5 wt% Acetone, 30 ºC.

The pervaporation performance of the membranes loaded with CuGluBpp-MeOH were assessed using the same conditions, with a feed solution of 5 wt% acetone at 30 ºC (Figure 5-32). The as-synthesised membranes exhibited an increase in the separation factor from 0 to 15 wt% MOF loading, to a maximum of 9.18. The separation factor then decreased with further increasing wt% of MOF to 6.33 for the 30 wt% loaded membrane. The total flux exhibited was slightly higher at a 5 wt% loading of MOF (0.079 kg m^{-2} h^{-1}) than for the pure PDMS membrane, but then had a lower total flux at each increasing wt% loading of MOF to a minimum of 0.030 kg m^{-2} h^{-1} at a 30 wt% loading of MOF. The worsened performance of the CuGluBpp-MeOH in terms of a lower total flux and adecrease in separation factor from a 15 wt% loading has been attributed to the orientation of the MOF particles within the membrane compared to the CuGluBpp-Acetone membranes and the difference in chain rigidification of the PDMS at similar MOF loading. At low loading of the MOF (5 wt%) the total flux is thought to have increased through the looser polymer chains from disruption caused by the incorporated MOF and the additional pathways created by the MOF pores. The sharp drop off of the total flux from 5 to 30 wt% indicates that there is likely to be a blockage of the permeating species through the membrane, and could be attributed to the pores of the MOFs being mainly perpendicular to the permeate flow. This would be opposed to the rigidification of the polymer chains through entanglement with the MOF particles as the solvent uptake results indicate this would likely only be an effect at high loadings (30 wt%) (Figure 5-30.b). The decrease in separation factor from 15 to 30 wt%, and sharp decline in total flux, is indicative of pores that are oriented perpendicular to the permeate flow (as shown in the SEM

imaging Figure 5-26 and PXRD results Figure 5-22). Similar trends in total flux and separation factor are found in the literature for ZIF-8-PDMS[171] and ZSM-5-PEBA[238] due to pore blocking which would be similar to the effect of the pores being oriented parallel to the membrane surface.

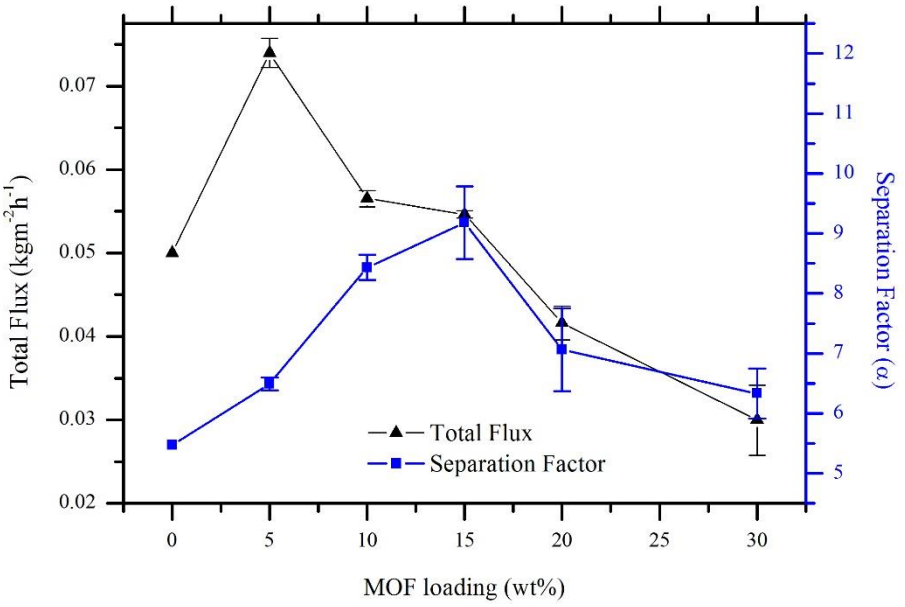

Figure 5-32. Pervaporation performance of membranes with CuGluBpp-MeOH as the inorganic filler. 5 wt% Acetone, 30 ºC.

Table 5-3. PSI values for the as synthesised membranes with varying wt% of Cu-MOF for a feed solution of 5 wt% acetone at 30 ºC.

wt% of MOF CuGluBpp-Acetone	**PSI Value**	**wt% of MOF CuGluBpp-MeOH**	**PSI Value**
0	231	-	-
5	502	5	433
10	516	10	420
15	567	15	447
20	503	20	252
30	457	30	160

For a practical application in a pervaporation process, the operating conditions of feed temperature and composition will have a large effect on the separation performance of an applied membrane. To ascertain the performance of these novel membranes the conditions of feed temperature and acetone concentration were varied. As the membrane composed of 15 wt% CuGluBpp-Acetone possessed the highest PSI value of 567, the performance at varying temperatures and acetone concentrations were analysed for this membrane. The membrane performance over increasing temperature (Figure 5-33) yields an increase in total flux and separation factor. This is due to both an increased evaporation energy of the permeants as well as higher diffusion coefficients at higher temperatures. At a temperature of 40 ºC, a separation factor of 13.7, total flux of 0.074 kg m^{-2} h^{-1} and PSI of 932 is reached.

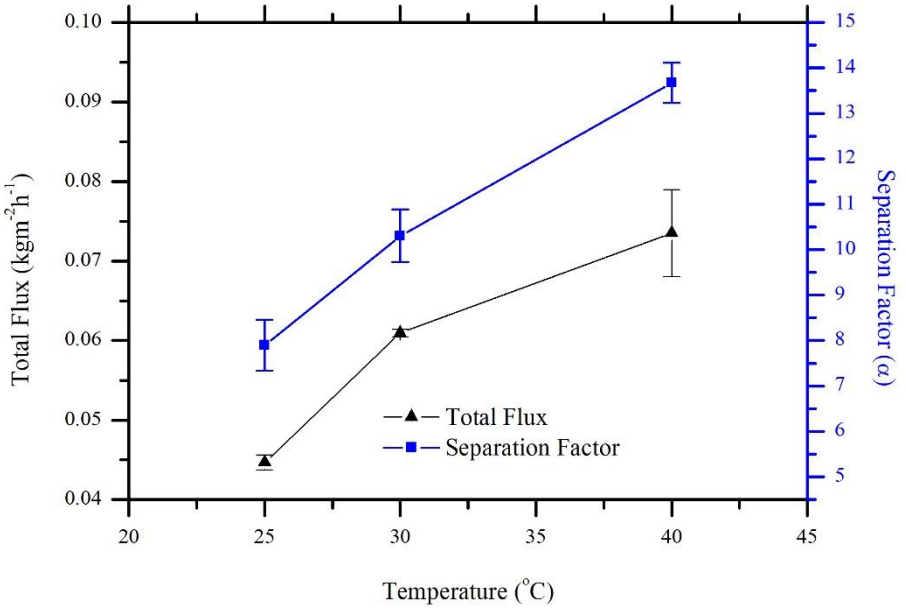

Figure 5-33. Pervaporation performance of a 15 wt% loaded CuGluBpp-Acetone membrane at varying temperatures, 5 wt% Acetone feed.

The effect of varying the feed acetone concentration was then investigated. The pervaporation performance of the 15wt% CuGluBpp-Acetone membrane was studied with acetone concentrations of 2, 5 and 10 wt% (Figure 5-33). With an increase in concentration of acetone both an increase in the total flux and the separation factor were observed. As permeation through these dense MMMs occurs predominantly through a solution diffusion mechanism, a higher feed acetone concentration would increase the transmembrane concentration gradient, and consequently, the rate of permeation of acetone would be greater. The pervaporation performance of the 15wt% CuGluBpp-Acetone with a 10 wt% acetone concentration in the feed had the

maximum performance within the range studied, with a total flux of 0.088 kg m^{-2} h^{-1}, separation factor of 15.2 and PSI of 1243.

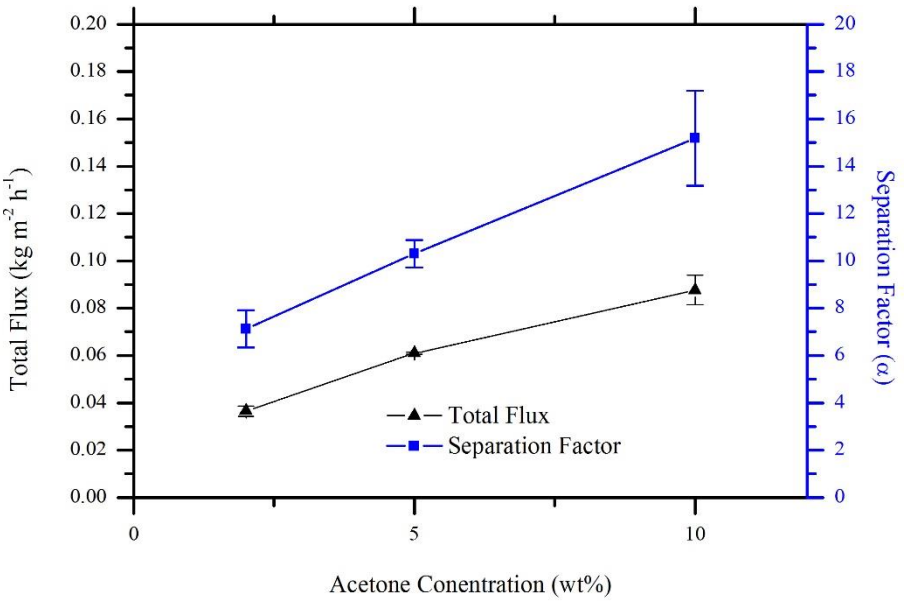

Figure 5-34. Pervaporation performance of a 15 wt% CuGluBpp-Acetone PDMS membrane with varying Acetone feed concentrations of 2, 5 and 10 wt% at 30 ºC.

Overall the total fluxes of these membranes are slightly lower than for some other examples of acetone pervaporation membranes recently reported in the literature. However, this is due to the thicker PDMS layer cast of the composite membranes. This was required due to the microcrystalline nature of the as-synthesised Cu-MOFs. This could be easily rectified within future work through the optimisation of smaller, potentially nano-sized particles of the different CuGluBpp MOFs. This would also aid in dispersion of the MOF within the PDMS matrix, particle agglomeration, and alignment of the 1D pores of the MOF, as a smaller particle size would mean that a non-ideal orientation would have less effect as the pore is shorter.

Another approach is to directly utilise the Cu-MOF in separation without having to compromise with mass transfer limitations and defects in the polymer due to particle orientation e.t.c. Consequently, some preliminary work was undertaken to investigate this possibility.

5.3.4 CuGluBpp Films – Preliminary Investigations

Preliminary investigations have been undertaken towards the synthesis of a continuous film of one of the Cu-MOFs studied within the previous section. Utilising a contra-diffusion synthesis,[239] where a solution of copper and the bipyridine and a solution of glutaric acid and sodium hydroxide were placed either side of a 0.1 μm PVDF membrane, films of the framework CuGluBpp-Acetone was selectively grown on one side of the microporous support (Figure 5-35).

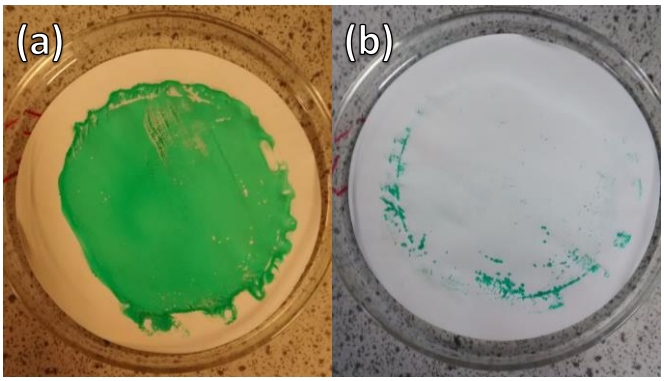

Figure 5-35. Photograph of the as-prepared CuGluBpp-Acetone film showing (a) selective growth on the side of the membrane facing the copper solution (b) and no / limited growth on the side facing the glutaric acid solution.

The formation of the structure of the desired Cu-MOF was verified through comparing the PXRD pattern of the as-synthesised film with that calculated from single-crystal data. As can be seen from Figure 5-36, the PXRD pattern of the as-synthesised film exhibits characteristic reflectances of that simulated from single-crystal data, as well as having reflectances characteristic of the PVDF support.

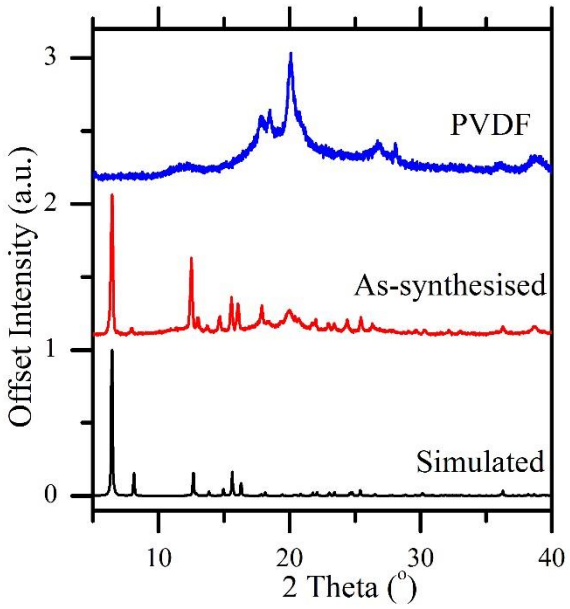

Figure 5-36. PXRDs of the as-synthesised contra-diffusion film, within the PXRD pattern reflectances for that of the Cu-MOF as well as the PVDF support can be identified.

Although growth was selective on one side of the PVDF support, a defect free film was not formed; as can be seen from Figure 5-35. Initial investigations were undertaken in an attempt to optimise the growth to produce a defect free film. The concentration of NaOH within the glutaric acid solution was varied to ascertain the effect this may have on film formation. An increase in NaOH concentration would increase the dissociation of the glutaric acid meaning a faster film growth which would potentially create smaller particles and a more homogenous film. From visual inspection, increasing the concentration of NaOH from 9 to 18 mmol within the solution generally decreased the particle size of the components of the film; however, the films still exhibited defects. With a doubling in concentration of all reactants and an increase in reaction time to 60 h, a thick film was grown on the support which eventually became too thick and detached from the support (Figure 5-37).

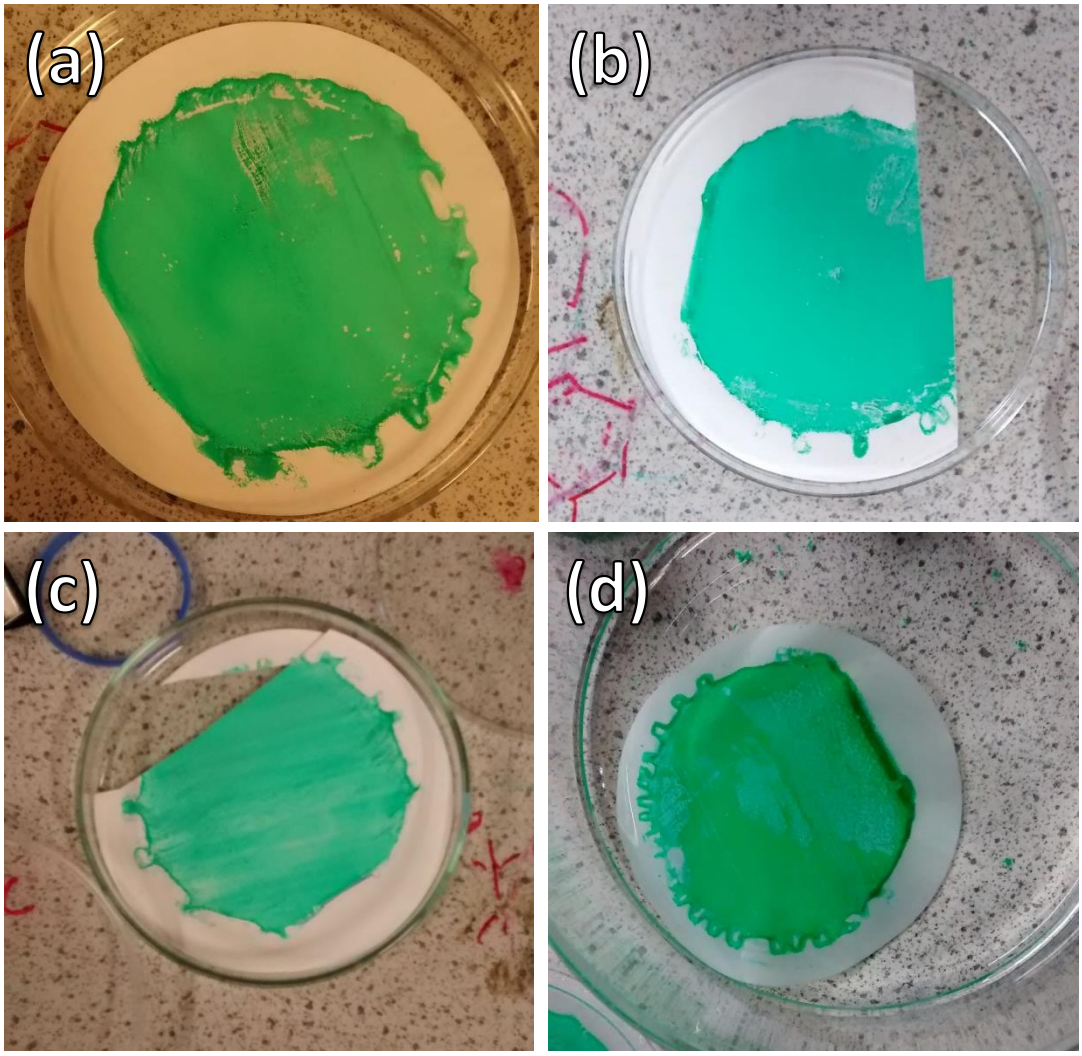

Figure 5-37. Variation in the film of the MOF CuGluBpp-Acetone from different reaction conditions (a) 9 mmol NaOH, (b) 13.5 mmol NaOH, (c) 18 mmol NaOH, (d) double concentration of all reactants and reaction time increased to 60 h.

Although this method has shown promise for the creation of a continuous film of the Cu-MOF, a number of approaches will need to be studied to improve the Cu-MOF films to a point that could be used as barriers for membrane separations. Approaches to improving the film may include:

- A smaller membrane area could be used, as this would make it easier to create a defect free film for testing to ascertain if the selected Cu-MOF film would have suitable separation properties.
- The concentrations of reactants and reaction times could be optimised further.
- Other approaches could investigate different substrates with different pore sizes and materials for improved compatibility with the Cu-MOF, and the substrate could also be

impregnated with copper nitrate to aid growth as shown in previous studies for the growth of MOF films.[240-242]

5.4 Conclusions

Two MOFs which are composed of copper and the same ligands (glutarate and 4,4'trimethylenedipyridine) but differing in the orientation of the bipyridyl ligand within the framework and crystal morphology, have been incorporated into MMMs with PDMS. The two MMMs have been tested for the pervaporation of acetone from its dilute aqueous mixture. The crystal morphologies of the two Cu-MOFs had a large effect on the pervaporation performance of their MMMs. The Cu-MOF produced from a solution in methanol exhibited large plate like crystals which lay parallel to the surface of the membrane. This meant that the 1-dimensional pores of the Cu-MOF lay parallel to the membrane surface and perpendicular to the permeate flow, identified through a combination of PXRD, SEM imaging, and water contact angle. The pervaporation performance of these membranes increased slightly at lower wt% but then decreased drastically at higher wt% due to the non-ideal orientation of the Cu-MOF. The Cu-MOF synthesised from a solution with acetone created smaller thicker crystals which had a more random orientation within their MMMs. These MMMs exhibited superior separation performance when compared to solely PDMS membranes of similar thickness with an optimum loading at 15 wt% of CuGluBpp-Acetone having a PSI of 567 total flux of 0.061 kg m^{-2} h^{-1} and separation factor of 10.3 for pervaporation of a 5 wt% acetone feed at 30 ºC. The 15 wt% loaded membrane exhibited an increase in total flux and separation factor with both increasing temperature and increasing acetone concentration. This study therefore provided an insight into the effect the morphology and structure of MOFs have when included within a MMM for pervaporation.

Preliminary investigations into a continuous membrane of CuGluBpp-Acetone utilising a contra-diffusion synthesis has provided promising results for film formation. Optimisation of the growth conditions must be realised so that defect free films that could be used as barriers for membrane separation processes can be realised.

Chapter 6

Polypropylene glycols as probes for MWCO determination in Organic Solvent Nanofiltration

The work in this chapter has been accepted in part as a journal article within the Journal of Membrane Science as:

"C. J. Davey, Z. Low, R. H. Wirawan, D. A. Patterson, Molecular Weight Cut-Off Determination of Organic Solvent Nanofiltration Membranes Using Poly(propylene) Glycols"

6.1 Introduction

Organic solvent nanofiltration (OSN; also known as solvent resistant nanofiltration, SRNF) is an emerging technology for more efficient separations within the chemical and pharmaceutical industries.[243-246] The principles of OSN are the same as for aqueous NF but is used to denote circumstances of separations where organic solvents are used instead of water. Within the purification of fermentation products there are multiple circumstances where OSN could be applied in the recovery and / or downstream processing of these products. OSN could be used for the treatment of the extractant solvent in a liquid-liquid extraction process, e.g. purifying the solvent for consecutive extraction processes. It may also be useful in the final purification stage of

these fermentation products, where small quantities of impurities may need to be removed. This would be especially useful for solvents such as 2,3-butanediol and acetic acid where thermal separations are energy intensive due to their high boiling points.

When applying a particular membrane to a separation it is important to understand its general separation ability before conducting feasibility testing; or if a new membrane material has been developed it is important to be able to generally quantify its separation potential. As discussed in Section 1.3.3, for NF membranes the MWCO is an important characteristic for determining their usefulness in a particular separation. It is used as a general guide for the separation ability of a membrane and defined as the MW for which 90 % of a solute is rejected.[197, 203] In practice, solutes with a range of different MWs are filtered in the target solvent and the MWCO value is the real or interpolated MW of the solute molecule that gives a 90 % rejection (Figure 2-7). Although in many circumstances a key factor, it is important to note that MW is not the only property to affect separation[38] (for example the rejection of acetate described in Chapter 3). Despite this, the MWCO of a membrane provides an important general description of a membrane's separation ability.

In aqueous solutions, a number of methods have been developed to determine the MWCO of a NF membrane.[203, 210, 247, 248] However, these methods cannot be directly applied for use in organic solvent systems due to various issues such as solute solubility and compatibility in organic solvents, as well as the numerous and complex solute-solvent-membrane interactions present. Suitable techniques for determining the concentration of the probe molecule in the permeate is also problematic when applied across a range of solvents. Thus, several new methods using different solute molecule types have been developed specifically for OSN systems as summarized in Table 6-1. Researchers also use a range of different MW dye molecules (including methylene blue and rose bengal) – these have not been included in Table 6-1, since the rejection is generally due to both charge (Donnan Exclusion) and MW related factors that make them less comparable (and ultimately less accurate and therefore applicable to MWCO determination) than those listed.

Table 6-1. Comparison of important attributes of common methods of MWCO determination in OSN, (✓= advantage, ✗ = disadvantage, ~ = neutral).

Important attributes of the MWCO method	**Solute used in MWCO method**			
	Alkanes Ref:[249]	*Polystyrene* Ref: [202]	*Poly(ethylene) glycols* Ref:[250]	*Poly(propylene) glycols* Ref: this work
Detection method	~ Gas chromatography	✓ Simple detection *via* UV	~ Use of ELSD	~ Use of ELSD
MWCO attributes	✓ Can investigate influence of MW and structure on rejection	MW of solute only	MW of solute only	MW of solute only
MW of solute repeating unit	Not constant	104 g mol^{-1}	44 g mol^{-1}	58 g mol^{-1}
Solvent applicability	✗ Limited solubility in more polar organic solvents	✗ Solvent swap required for solvents that obscure chromatogram (e.g. toluene, hexane, ethyl acetate)	✗ Insoluble in most non-polar solvents ✗ Poor rejection by commercial membranes in organic solvents	✓/✗ Soluble in non-polar solvents however a solvent swap required for non-polar solvents that obscure the chromatogram
Quantitative solute concentration determination	✓ Can determine exact concentrations of each MW	✗ Difficult to determine absolute concentrations of each oligomer	✗ Difficult to determine absolute concentrations of each oligomer	✗ Difficult to determine absolute concentrations of each oligomer
Solutes cost and availability	✗ Lack of pure commercially available alkanes > 400 g mol^{-1}	✗ Expensive Oligomers	✓ Cheap range of available oligomers	✓ Cheap range of available oligomers

One of the more commonly used solutes and methods for MWCO determination of OSN membranes is through the use of polystyrene oligomers.[202, 251-253] Polystyrene oligomers having MWs between 200 and 1000 g mol^{-1} allow a sufficient MW range to be covered to produce suitable MWCO curves for OSN membranes in various polar and non-polar solvents. Polystyrene oligomers have been used since they have four of the five essential properties of MWCO probe molecules:

- *Availability:* polystyrenes are available in a wide range of MWs, unlike proposed alternative probe molecules such as alkanes[249] (which lack commercially available pure species of MW > 400 g mol^{-1}).

- *Molecular similarity:* polystyrenes are available in a homologous series, enabling a range of similar molecules to be used for MWCO determination. Systems which use a selection of different compounds as probes which could vary in structure and functionalities (e.g.

dyes[254] or alkanes[249]) could have differing and varied interactions with a membrane leading to a skewed increase in rejection with MW.[255]

- *Robust analysis method for mixtures in different solvents:* The various MW polystyrenes when dissolved in the different solvents used in OSN can be separated by HPLC analysis and therefore a MWCO can be determined in a single filtration, instead of a series of filtrations, each with a single solute (which is often the case for MWCO methods that use different compounds).

- *Good resolution:* The MWCO curve must be obtained in a reasonable resolution – i.e. a small gap between the MW of molecules in the series to enable the MWCO to be determined with good accuracy. The polystyrene method is not ideal with a 104 g mol^{-1} resolution, which may not as accurately discriminate the differences between some membranes as methods with closer gaps in the molecular series (such as for the DuraMem™ series from Evonik which comes in close MWCOs of 150, 200 and 300 less than the resolution of the polystyrene method).

- *Affordability/low cost:* The polystyrene method; however, fails in the last key requirement – low cost. Pure polystyrene oligomers of low MW and polydispersity are very expensive (Polystyrene 500 £153/g; Polystyrene 1000 £85.9/g; Sigma Aldrich 2016) which can mean that the use of the polystyrene MWCO method is prohibitively expensive if it is to be applied as a routine measurement and/or at large scale. The material costs can in part be ameliorated by synthesising the oligomers prior to testing if the test is to be applied at laboratory scale. However, the synthesis can be time-consuming (accruing potentially prohibitively expensive person-time costs) and may produce oligomers with varying quality and purity (e.g. mixtures of oligomers / oligomers with high polydispersity that may not be able to be properly resolved using the HPLC-UV method commonly applied).[202]

A more cost effective and higher resolution alternative to the polystyrene MWCO method is therefore needed.

Polyether-based molecular probes such as poly(ethylene glycols) (PEGs) have been proposed for determining the MWCO in both aqueous systems[203] and in polar solvents.[250, 256, 257] The analysis of polyethers (such as PEGs) is commonly done by means of reverse phase high-performance liquid chromatography (HPLC) with evaporative light scattering detection (ELSD). This gives suitable separation and detection of the individual polyether oligomers (such as PEGs, poly(propylene glycols) (PPGs) and poly(butylene glycols) (PBGs).[258, 259] However, the insolubility of PEGs in

some non-polar solvents as well as the wide range of conformations that PEG adopts in different organic solvents[260] can sometimes limit the reliability and cross-comparability of this method in OSN. This means PEGs can sometimes give quite different results for MWCO determination when compared to other methods[256] (also see the comparison within Section 6.3.3). If a closely related and inexpensive compound could be found and an analysis method developed to allow the oligomers to be resolved accurately in a range of solvents commonly used in OSN, an additional and further enabling OSN MWCO method to all those currently used could be developed. This can help expand the MWCO determination potential where the current methods cannot be readily used. Poly(propylene glycol) (PPG; Figure 6-1) has therefore been investigated for its potential as a molecular probe for MWCO determination.

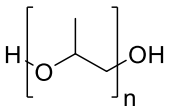

Figure 6-1. Chemical Structure of Poly(propylene glycol) (PPG).

A method for the single filtration determination of MWCO for OSN membranes utilising PPG with oligomer separation by means of reverse phase HPLC coupled with an ELSD has been developed. PPG comes as a homologous series and has the same polyether backbone as PEG, but the extra methyl groups improves the hydrophobicity of the polymer, which increase its solubility in non-polar organic solvents when compared to PEG. The method has a high resolution, with a size increment of 58 g mol^{-1} corresponding to the $OCH(CH_3)CH_2$ structural unit. Also, PPGs with a wide range of MWs are commercially available at a fraction of the cost of polystyrene oligomers. All five essential properties of MWCO probe molecules are therefore potentially satisfied.

MWCO curves have been constructed for a number of commercial OSN membranes in a range of organic solvents (polar aprotic, polar protic and non-polar) and the results have been compared to those of previously reported methods for determining MWCO in OSN. The membranes chosen are commonly used within the literature and industry, and have been chosen due to their differing nominal MWCOs, as defined by the manufacturer, to probe the effectiveness of the designed method. The results indicate a reproducible, single filtration method using inert molecules of regularly incrementing size that is compatible in a range of organic solvents.

This meets the specific objectives of this thesis:

- To develop methods to improve the characterisation and understanding of membrane separation processes.

6.2 Materials and Methods

6.2.1 Materials

Tripropylene glycol (Alfa Aesar), PPG 400 (Alfa Aesar), PPG 725 (Sigma Aldrich), PPG 1000 (Alfa Aesar), PEG 200 (Alfa Aesar), PEG 400 (Alfa Aesar), PEG 600 (Alfa Aesar), PEG 1000 (Alfa Aesar), of reagent grade were used as the oligomer samples. Organic solvents (HPLC grade) methanol, acetone, acetonitrile and toluene were purchased from VWR and used as received. The membranes were purchased from Evonik (UK) (DuraMem™ 150, DuraMem™ 200, DuraMem™ 500 and PuraMem™ 280) and Membrane Extraction Technologies (StarMem™ 240). Ultrapure water (18.2 MΩ·cm at 25 °C) and HPLC grade acetonitrile (Alfa Aesar) were used in the gradient elution of the HPLC method. Nitrogen (BOC, 99.998 %) was used as carrier gas for the ELSD.

6.2.2 Experimental Procedure

The experimental setup consisted of the dead end cell configuration described within Section 3.2.2. Filtration experiments and calculation of rejection of each oligomer was therefore conducted in the same manner as described in Section 3.2.2, but differing in the volume of feed and the applied pressure used. For a typical filtration, solutions of PPG were made up by dissolving 4 g of each of the purchased PPG oligomer samples (tripropylene glycol, 400, 725, and 1000) within 1 L of solvent. A fresh membrane sample was used for each experiment to avoid the effects of cross contamination of samples. After conditioning with the pure solvent at the applied pressure and temperature, (~ 2 hours for consistent flux), 40 mL of feed was added to the cell. Half of the feed was permeated using an applied pressure of 30 bar, except for DuraMem™ 500 where an applied pressure of 10 bar was used. The temperature of the filtrations were maintained at 30 ºC using a water bath.

The maximum standard deviation of the rejection of a single point was calculated to be ±2.47 % from three repeats with three different membrane samples.

6.2.3 Analytical Method for PPG detection

The concentration of each oligomer of PPG in the feed, permeate and retentate samples was conducted using reversed phase HPLC equipped with an evaporative light scattering detector (ELSD). The HPLC consisted of an Agilent Technologies (1260 Infinity) system with a quaternary pump (G1311B), autosampler (G1329B), column oven (G1316A) equipped with a Poroshell 120 EC-C18 (4.6 x 50 mm 2.7 μm) column, and ELSD (GB1530001). An injection volume of 100 μL,

flow rate of 1 mL min^{-1}, column temperature of 25 ºC and a gradient elution of water and acetonitrile which is shown in Table 6-2. The settings of the ELSD detector were a nebulizer temperature of 25 ºC, nitrogen gas flow rate of 1.8 SLM, and an evaporator temperature of 25 ºC.

Table 6-2. Solvent gradient used for separation of PPG oligomers.

Time (min : sec)	Concentration of Water (%)	Concentration of Acetonitrile (%)
0	95	5
2:30	80	20
42:30	0	100
47:30	0	100
50	95	5
57	95	5

All samples within water miscible solvents were diluted with water by 1/3 (400 µL sample and 800 µL water) before analysis. This gave an improved chromatogram by reducing peak fronting and an improved baseline. For the analysis of PPGs within non-polar solvents the solvent was removed *in vacuo* and replaced with an equal amount of methanol. This mixture was then diluted with water as above before HPLC analysis.

The relationship between oligomer concentration and peak area was exponential and characteristic of ELSD[258] (Equation 6-1):

$$y = ax^b \qquad 6\text{-}1$$

where y is the peak area of the response, a and b are coefficients that are dependent upon the separation and experimental conditions and x is the mass of the analyte. Calibration curves (Appendix A.6.2) were constructed by diluting a stock solution of a mixture of PG oligomers at a higher concentration than used (200 % = 8 g L^{-1} of each sample). This gave a relative concentration of each oligomer of PPG that was used for calculation of the rejection and mass balances.

6.2.4 Analytical method for PEG detection

MWCOs using poly(ethylene glycols) as the molecular probe were conducted with a method adapted from[250] and[203] and analogous to the PPG method developed in this paper. PEG 200, 400, 600 and 1000 were used as the oligomer samples. Solutions of PEG were made up by dissolving

4 g of each PEG sample (200, 400, 600, 1000) in 1 L of solvent. Filtrations were performed in the same manner as for the PPG method. For detection of PEG oligomers via HPLC, all solvents tested were evaporated *in vacuo* and replaced with an equal amount of water due to their disruption of the separation method. The permeates and feeds were then diluted by 1/3 with water analogous to the PPG method and the retentates by 1/6 to keep within the higher detection limit of the ELSD.

The concentrations of oligomers of PEG were determined using the same HPLC setup as described above. The experimental parameters used were injection volume 100 µL, a flow rate of 1 mL min^{-1}, a column temperature of 25 ºC and the gradient elution of water and acetonitrile given in Table 6-3. The ELSD settings were kept at a nebulizer temperature of 25 ºC, an evaporator temperature of 25 ºC and a nitrogen gas flow rate of 1.8 SLM.

Table 6-3. Solvent gradient used for PEG analysis.

Time (min : sec)	Concentration of Water (%)	Concentration of Acetonitrile (%)
0	5	95
42:30	30	70
47:30	100	0
50	5	95

This gave suitable separation of the PEG oligomers (Figure 6-2). Calibration curves (see Appendix 6 Section A.6.2.3) were constructed by diluting a stock solution of a mixture of PEG oligomers (100 % = 4 gL^{-1} of each sample). The calibration curves exhibited an exponential relationship between peak area and oligomer concentration as for the PPG samples.

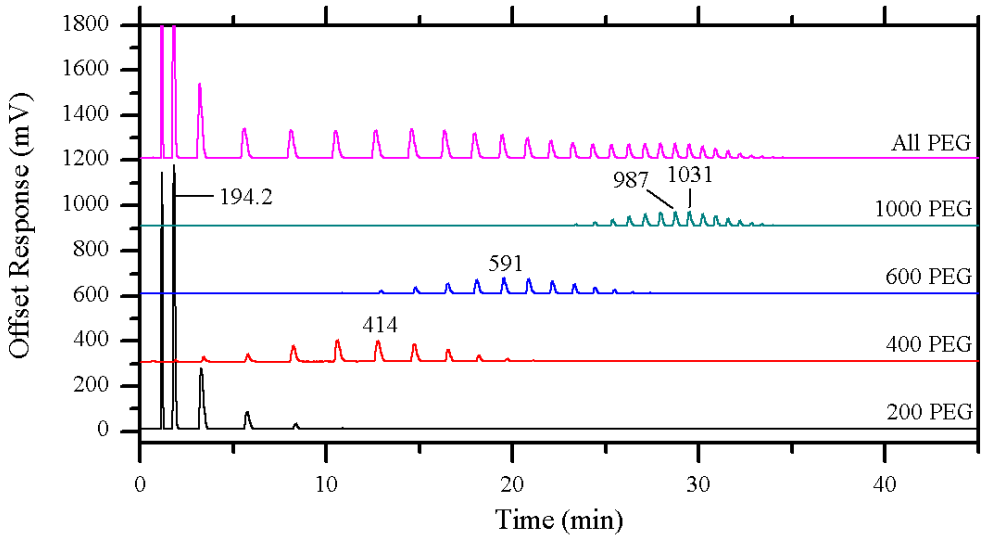

Figure 6-2. Separation of PEG oligomers in water by the described HPLC method.

6.3 Results and Discussion

6.3.1 Development of the analytical method

Previous studies have investigated the influence of the mobile and stationary phases on the separation of PPGs using reverse phase HPLC and ELSD.[259] These methods achieved good separation of the oligomers at relatively high concentrations of PPG in methanol and therefore only required small injection volumes (10 μL). For MWCO determination, the concentration of PPGs is required to be much lower such as to minimise the effects of concentration polarisation and fouling. To allow for this, a higher injection volume was used in the HPLC method (100 μL); however, this led to a much larger amount of organic solvent being introduced to the column at an early stage of the separation, altering the concentration gradient. In these chromatograms peak fronting and poor baseline resolution was observed. It was found that diluting the samples with water (when water miscible solvents were used) greatly improved the separation and resolution of PPG, as this reduced the ratio of organic solvent to PPG being injected (Figure 6-3). Looking at the different amounts of water added (as per Figure 3) it was determined that dilution with water by 1/3 (400 μL sample and 800 μL water) gave an improved chromatogram with reduced peak fronting and a flat baseline, both facilitating repeatable measurements and accurate and repeatable integration of all peaks.

For determination of oligomer concentrations in non-polar and water immiscible solvents, these were solvent exchanged by removing the original solvent *in vacuo* and replacing with an equal volume of methanol. This sample was then diluted with water achieving a suitable chromatogram for MWCO determination. Mass balances showed that there was no significant loss of PPG in the solvent exchange process (< 10 %).

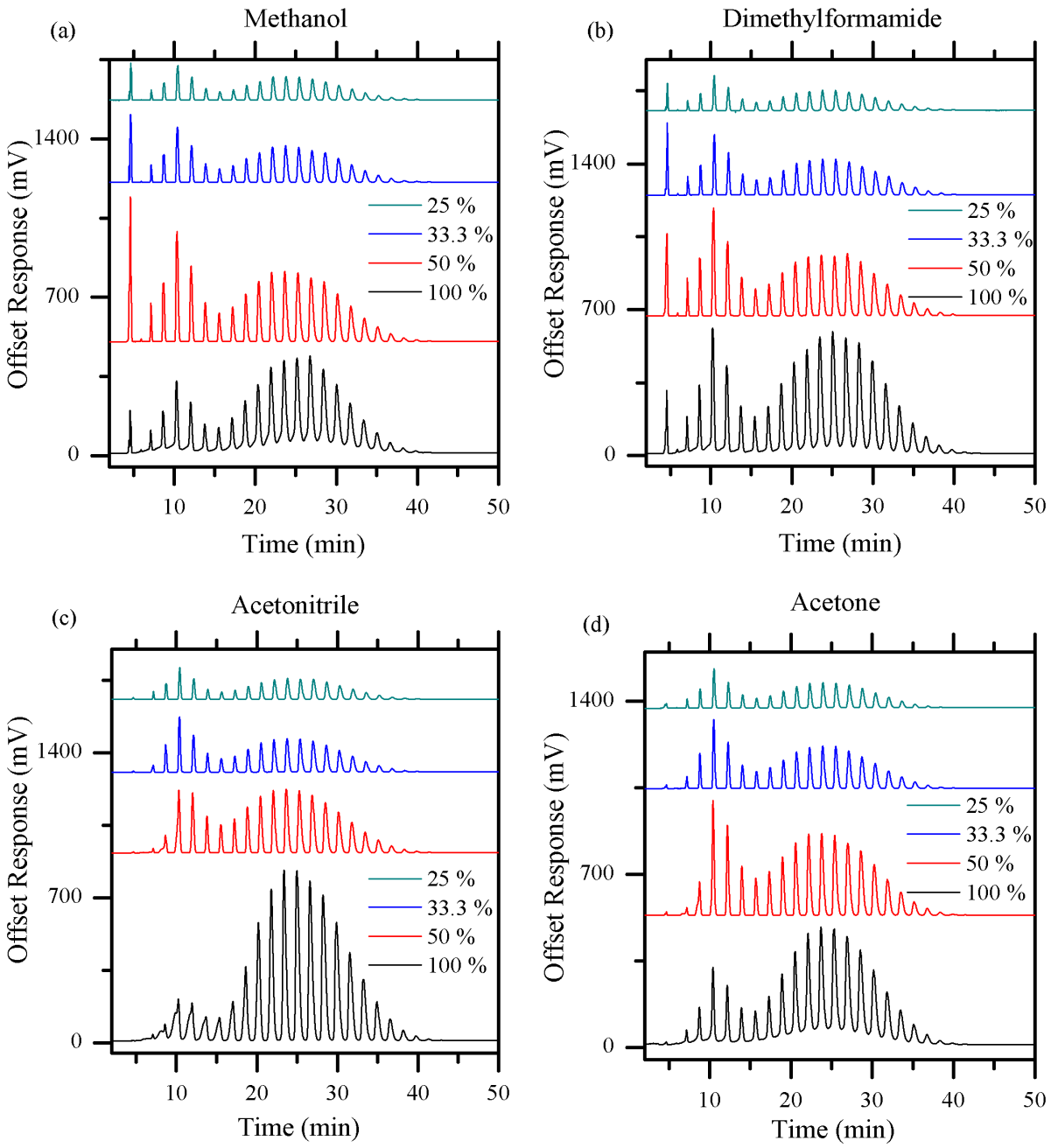

Figure 6-3. Effect of dilution of samples with water on the HPLC chromatogram of PPG dissolved in different solvents (a) methanol, (b) dimethylformamide, (c) acetonitrile, and (d) acetone. In each, percentage (%) refers to the vol% of original sample.

The different molecular weights of each PPG oligomer present within the chromatographic method can be easily identified due to the regularity of elution as shown in Figure 6-4.a. The peak corresponding to tripropylene glycol (MW = 192.1 g mol^{-1}) is first to elute. The oligomer is easily identified due to the presence of isomers in the purchased sample which eluted as shoulders in the chromatogram. These isomers were unable to be separated within the chromatographic method and

were therefore treated as one MW due to their limited difference in sterics. The next PPG to elute is that with a MW of 250.3 g mol^{-1}; however, this oligomer was present at very low concentrations within the PPG 400 sample used and so was not used in this investigation. Each oligomer of PPG can then be identified up to PPG with a MW of > 1179.9 g mol^{-1}. This would be the upper range of a NF membrane which is generally described as rejection of solutes between 150 – 1000 g mol^{-1}. The identification of each PPG oligomer also correlated well with the manufacturer's defined average MW distribution of each sample (Figure 6-4.b).

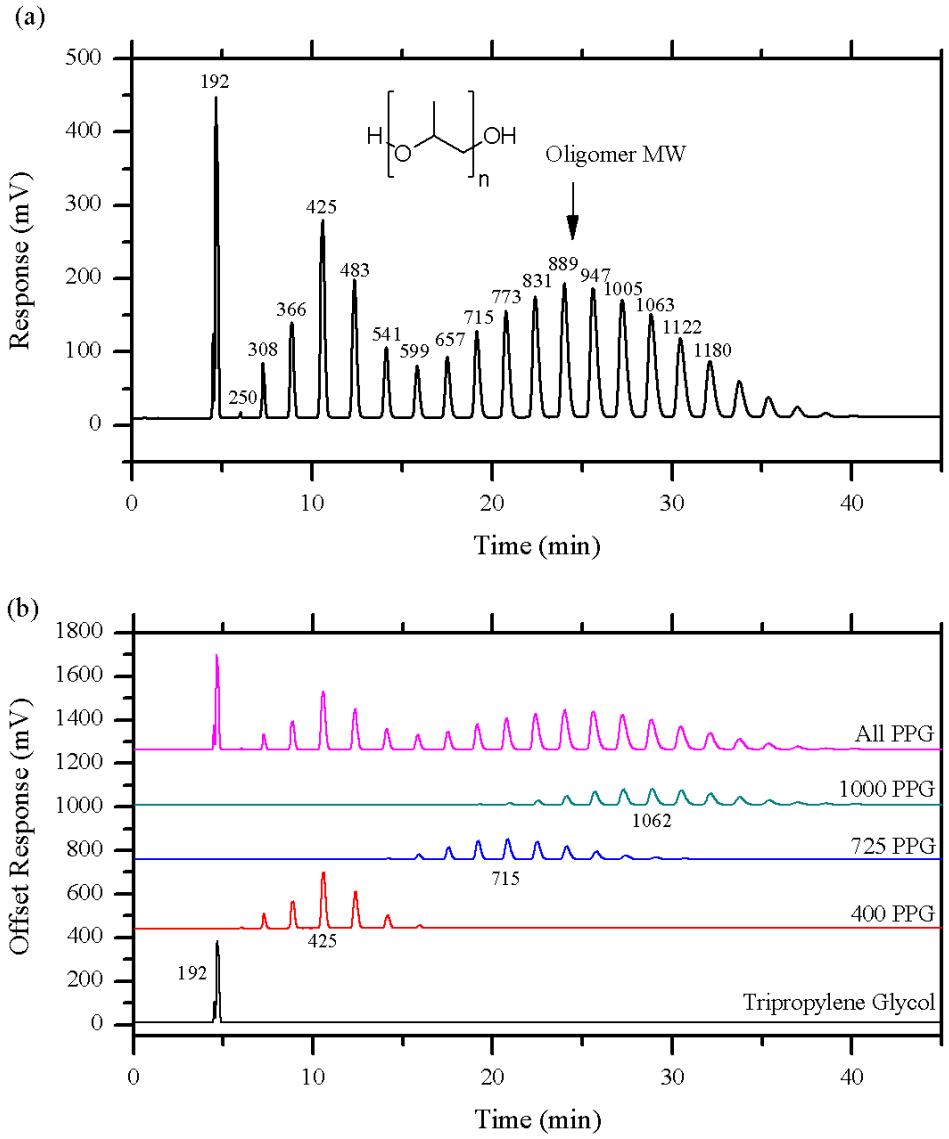

Figure 6-4. Separation of PPG oligomers in methanol by the described HPLC method (a) analysis of feed, (b) analysis of individual commercial samples.

As outlined in Section 6.1, an essential feature of a successful MWCO determination method is the ability for the analysis to work with the MWCO probe molecules used in a number of different solvents. The PPGs were found to be soluble in all solvents investigated in this study at the intended concentration. Therefore, a study of the effect of different organic solvents on the chromatographic separation was undertaken. As can be seen from Figure 6-5, the method can be applied across different organic solvents which are miscible with water. Each solvent exhibits the typical separation of PPG oligomers as presented for methanol. However, due to the disruption of the gradient of the mobile phase in the separation, some of the resolution of the lower MW oligomers is lost in certain solvents. For non-polar solvents (which elute in the middle of the chromatogram) and solvents that did not have high enough resolution for the membrane to be tested, a solvent exchange can be performed where the solvent is removed *in vacuo* and replaced with the same volume of methanol before dilution with water for HPLC analysis, as outlined in Section 6.2.3. This allows for determination of oligomers down to a MW of 192 g mol^{-1} if required.

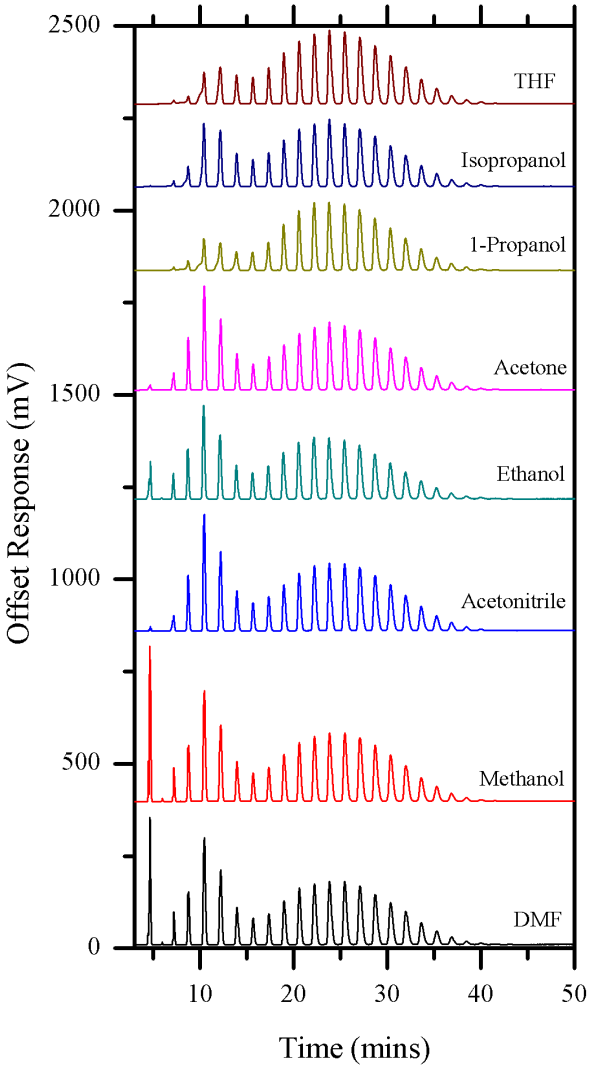

Figure 6-5. HPLC chromatograms of PPGs in different solvents diluted with water.

6.3.2 Determination of MWCO in commercial OSN membranes

The MWCO of a number of commercially available OSN membranes was therefore investigated using the developed method (Figure 6-6). MWCO's were determined in methanol, acetone and toluene as examples of polar, polar aprotic and non-polar solvents, respectively. The MWCOs determined using PPG are within the range of those reported by the manufacturer (and closer than those determined by a PEG MWCO method – see Section 6.3.3) constructed using oligomers of polystyrene in acetone for the DuraMem™ membranes and in toluene for PuraMem™ 280 and StarMem™ 240. Importantly, the shapes of the MWCO curves are comparable to those obtained by other methods in the literature also (e.g. for StarMem™ 240 in [202]), which is essential for understanding how sharp a separation a membrane can give.[197] This is not the case for other methods, such as those using PEG (see Section 6.3.3 for comparison).

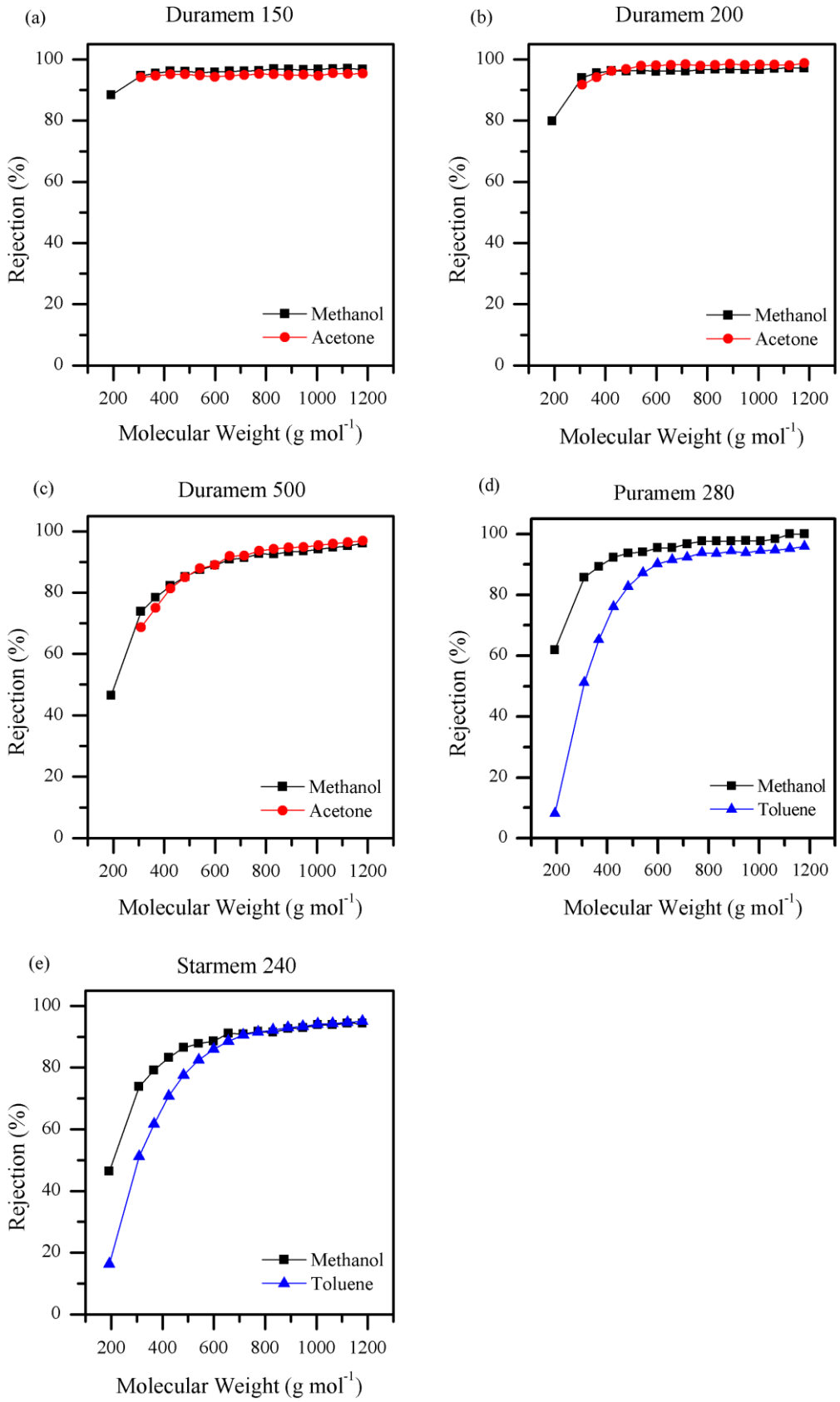

Figure 6-6. MWCO curves of (a) DuraMem™ 150; (b) DuraMem™ 200; (c) DuraMem™ 500; (d) PuraMem™ 280; and (e) StarMem™ 240 using PPGs.

It is also noticeable that the rejection characteristics of StarMem™ 240 and PuraMem™ 280 differ considerably between methanol and toluene. This is most likely due to a combination of the different swelling of the membrane in these two solvents (as indicated also in Toh *et al.*[202]) as well as the high degree of rotational freedom around the polymer backbone for PPG. Previous work has shown that PPGs exist as a tight coil in polar / aqueous systems and open up in non-polar solvents,[261, 262] this reflects the increased rejection observed in methanol compared to toluene. It would be expected that a tightly coiled PPG would be rejected better than an uncoiled PPG chain that could rotate to a preferred orientation to permeate through the membrane.

Figure 6-7 compares the MWCO of the tested membranes using the PPG method with methanol as solvent. The MWCO curves of the membranes correlate well with the increasing MWCO trends as defined by the manufacturer using the polystyrene method; however, MWCO for PPGs are generally slightly higher than those reported for polystyrene (Table 6-4). This has been attributed to the differences in steric bulk and rotational freedom around the backbone of the polymers, as well as the differences between the polystyrene and PPG molecules and their interactions with the membranes in the solvents used. Differences in MWCOs determined using different solute systems have been noted before (e.g. Toh *et al.*[202] and Bhanushali *et al.*[254]). Different molecules may also produce different MWCOs due to differing macromolecular chain deformation, shape, membrane interactions and orientations during filtration, since rejection is not based on MW, but rather a range of shape, charge, chemical interaction and molecular orientation based phenomena. PPGs will be representative of a different set of molecules as compared to the polystyrenes used by the manufacturers of these membranes. Therefore, the MWCOs and MWCO curves generated by the PPG method help to explain why these membranes can give rejections that are far from the MWCO that is specified when used for separations of molecules other than polystyrenes.

Table 6-4. Comparison of the MWCO from the manufacturer using the polystyrene method and from the PPG method in this work.

Membrane	Manufacturers Stated MWCO: (g mol^{-1})		PPG MWCO: (g mol^{-1})		
	Acetone	Toluene	Methanol	Acetone	Toluene
DuraMem™ 150	150	-	308	308	-
DuraMem™ 200	200	-	308	308	-
DuraMem™ 500	500	-	657	657	-
PuraMem™ 280	-	280	366	-	657
StarMem™ 240	-	400	657	-	715

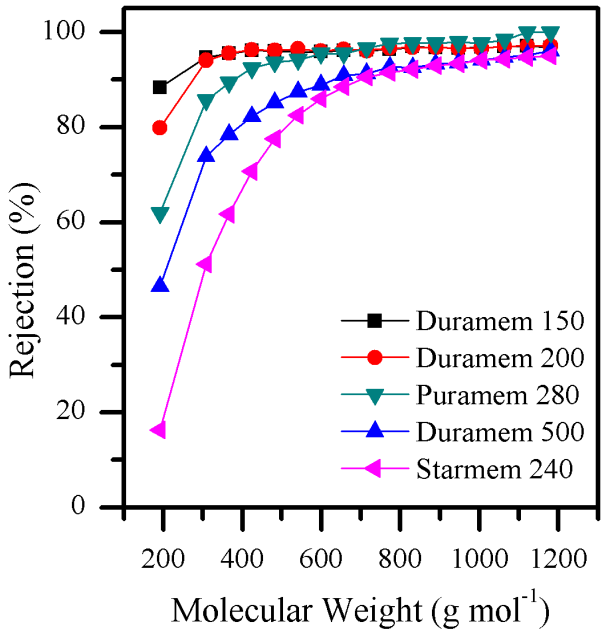

Figure 6-7. Comparison of the MWCO of different OSN membranes with methanol as solvent using the PPG method.

Consequently, since the MWCO curves provide a further way of determining the selectively of OSN membranes for molecules that are dissimilar to the widely used polystyrenes, this new PPG method should be used to complement the PEG and polystyrene techniques where a more robust understanding of OSN performance and selectivity is required (such as for understanding the potential range of performance of a new OSN membrane or for OSN membrane manufacturers to state a more representative range of MWCO values for client potential applications). Moreover, in cases where only a comparative assessment of MWCO is required and so only one MWCO method need be used, the authors propose that this method be adopted as a new standard MWCO test for OSN membranes that could be used, since compared to the current standard of polystyrene, oligomers of PPG can probe a wider range of MWCO, provide higher resolution and cost considerably less.

6.3.3 Comparison of PEG and PPG MWCO Methods

Figure 6-8 compares the rejection of oligomers of PEG and PPG by Starmem 240 in methanol and toluene. It can be seen that PEG is poorly rejected in methanol whereas in toluene has a greater rejection (Figure 6-8.a) although in both solvents rejection is far below 90 %. In contrast, PPG

(Figure 6-8.b) rejection is much greater and suitable MWCO curves can be constructed for both methanol and toluene which give MWCOs of 657 g mol^{-1} and 715 g mol^{-1} in methanol and toluene respectively. These MWCOs are closer to that stated by the manufacturer of 400 g mol^{-1} determined in toluene using polystyrenes as molecular probes. PPG has been shown to form a tight coil in water and polar solvents, and a loose coil in non-polar solvents.[261, 262] This could be the cause for the trend of a slightly higher MWCO for PPG in toluene compared to methanol (Figure 6-8.b). In methanol the tight coil of PPG would have greater steric bulk exhibiting greater rejection at lower molecular weight, compared to the looser coil in toluene which would have less steric bulk leading to lower rejection at equivalent molecular weight. PEG is a more hydrophilic molecule than PPG and could therefore have a more uncoiled nature in polar solvents such as methanol and coiled in non-polar solvents such as toluene.[260] These assumptions would reflect the rejections observed in Figure 6-8.a.

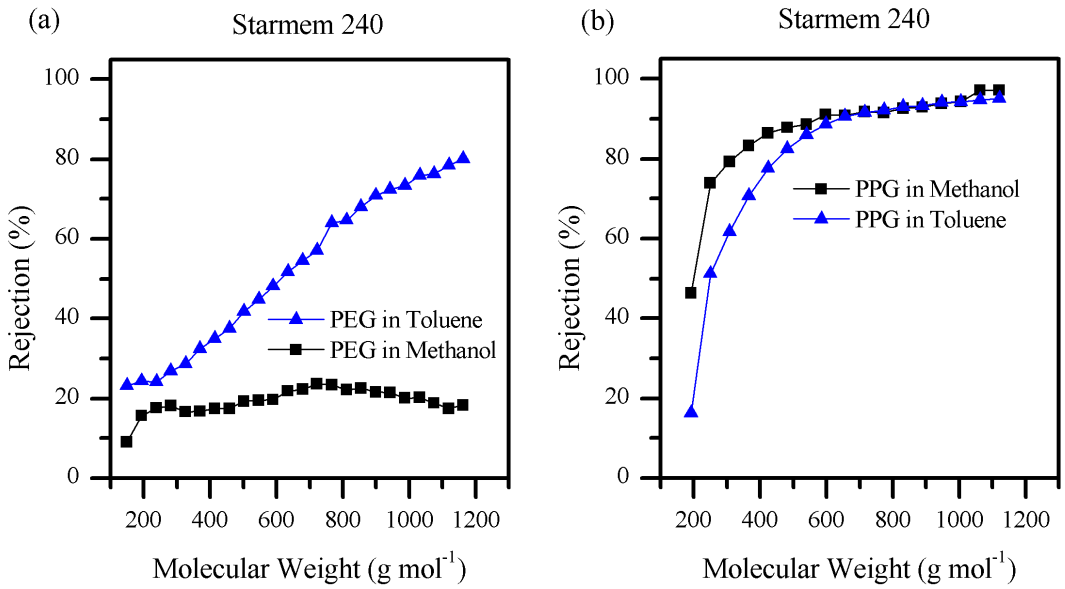

Figure 6-8. Rejection of oligomers of (a) PEG and (b) PPG by Starmem 240 in methanol and toluene.

Figure 6-9 compares the rejection of PEG and PPG in methanol by the tighter OSN membrane Duramem 200. It can be seen that PEG is much more poorly rejected than PPG giving a much higher MWCO of 766 g mol^{-1} compared to that obtained from using PPG (308 g mol^{-1}) or given by the manufacturer using polystyrenes (200 g mol^{-1}). Therefore, the use of PPG to probe the MWCO of a OSN membrane can be seen to reflect the results obtained from the use of polystyrene more closely than when PEG is employed. These different methods could be further developed into a series of complementary analysis to better understand the rejection characteristics of a specific OSN membrane to specific solutes.

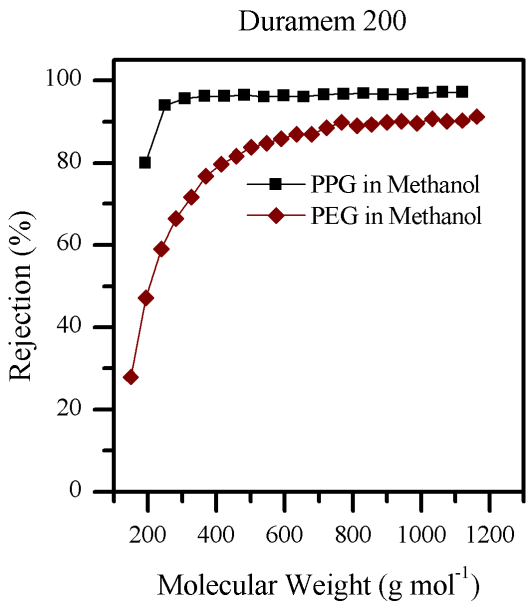

Figure 6-9. Comparison of the rejection of oligomers of PEG and PPG in methanol by Duramem 200.

6.4 Conclusions

A new, single filtration, reproducible method for determining the MWCO of OSN membranes using PPGs has been presented. The method has been used to construct MWCO curves of commercial OSN membranes within the range of 192 - 1180 g mol^{-1} for methanol, acetone, and toluene, indicating a method that can be applied across a number of different solvents (i.e. polar, polar aprotic and non-polar). Utilising ELSD the method can be easily adopted by many researchers already studying PEGs for characterisation of aqueous NF membranes. This method provides an alternative analysis for OSN membranes and overcomes some of the limitations of the previously reported polystyrene and PEG methods, as well as providing a complementary analysis to these methods. Consequently, the authors propose that this method be adopted as a new standard MWCO test for OSN membranes since compared to the current standard of polystyrene, oligomers of PPG can probe a wider range of MWCO, provide higher resolution and cost considerably less.

Chapter 7

Conclusions and Future Work

7.1 Conclusions

This thesis investigated various aspects of membrane separations that could be applicable to the recovery of fermentation products. A majority of the work has focused on the recovery of 2,3-butanediol, acetate and ethanol from a gas fermentation broth produced by LanzaTech. The thesis has also attempted to improve knowledge of membrane separations applicable to the recovery / purification of fermentation products through development of novel pervaporation membranes and development of a new analytical method for MWCO determination of OSN membranes. Summaries of the main conclusions from each Chapter are outlined below:

- **Chapter 3**: Concentration and Purification of a Gas Fermentation Broth with Nanofiltration and Reverse Osmosis.

An investigation into the application of NF and RO for the purification and concentration of 2,3-butanediol and acetate within a gas fermentation broth was undertaken. Screening a number of commercially available NF and RO membranes was conducted to ascertain their rejection characteristics for 2,3-butanediol and acetate. A range of rejections were observed for 2,3-butanediol (10.7 – 95 %) and correlated to the general rejection abilities of the membranes, with the looser NF membranes exhibiting lower rejections and the tighter NF / RO membranes

exhibiting higher rejections. Rejection of acetate was found to be dependent on the pH of the solution due to Donnan exclusion. At higher pH observed rejections of acetate were 14 - 94 % compared to -2.9 - 37 % at lower pH due to the degree of dissociation of acetic acid. The membranes NF270, NF90 and BW30 were tested further for the purification and concentration of a gas fermentation broth. NF270 was shown to have low rejection of 2,3-butanediol and acetate but good rejection of salts and other organics and could be used to purify the broth, NF90 and BW30 were shown to be able to concentrate 2,3-butanediol and acetate within the broth but suffered from low permeabilities due to fouling. The rejection of a number of different potential alcoholic fermentation products by BW30 was then studied and the high rejection of 2,3-butanediol attributed to the steric properties of the molecule and not solely its MW. The rejection of isobutanol by BW30 (77 %) was also shown to be suitable for concentration in the same manner as for 2,3-butanediol.

Studies of a membrane series of NF270 followed by either NF90 or BW30 to purify and then concentrate 2,3-butanediol and acetate within the fermentation broth where then undertaken. Initial purification using NF270 decreased the fouling and flux decline within NF90 and BW30 and a total increase of > 5 fold concentration of 2,3-butanediol and acetate was observed. This work demonstrates that NF and RO can be used to purify and concentrate a gas fermentation broth producing 2,3-butanediol and acetate.

- **Chapter 4**: ZIF-8-PDMS MMMs for Ethanol Pervaporation: Effect of 2,3-Butanediol and Acetate.

The effect of 2,3-butanediol and acetate on a ZIF-8-PDMS MMM was studied for the pervaporation of ethanol from a fermentation broth. The ZIF-8-MMMs were fabricated having similar properties as characterised in previous literature.[132, 171] Studies on the solvent uptake of the membranes by 2,3-butanediol, water and ethanol found that increasing ZIF-8 loading within a membrane increased the uptake of both ethanol and 2,3-butanediol. The increased uptake of 2,3-butanediol has been shown to be due, in part, to adsorption by 2,3-butanediol through a combination of adsorption and PXRD data. The membranes were also shown to be sensitive to acidic solutions of acetic acid, causing oxidation of the ZIF-8 structure, but are stable at higher pH. In ethanol pervaporation 2,3-butanediol was shown to increase the total flux and decrease the separation factor. The increased uptake of 2,3-butanediol by the membrane is thought to increase the amount of hydrophilic pathways for water to permeate through the membrane. The 7.5 wt% ZIF-8-PDMS membrane exhibited a stable pervaporation performance with increasing addition of acetate at pH 6. In contrast the purely PDMS membrane was shown to exhibit an increase in total flux with increasing acetate concentration. The difference has been attributed to the increased

hydrophobicity of the ZIF-8-PDMS membrane compared to the pure PDMS membrane reducing the uptake of acetate. The 7.5 wt% ZIF-8-PDMS membrane exhibited no significant change in total flux and separation factor for ethanol pervaporation in the presence of 2,3-butanediol and acetate. In the presence of a fermentation broth the total flux was much higher with only a small decrease in separation factor. An increased PSI of 1281 compared to the model solution (PSI = 805) was observed, attributed to beneficial effects of the components of the fermentation broth.

- **Chapter 5:** Cu-MOF based PDMS Mixed-Matrix Membranes for Acetone Pervaporation: Impact of Glutarate and Bipyridyl ligands on the MOF morphology.

The performance of two structurally similar Cu-MOFs as the inorganic phase within a MMM for pervaporation of acetone from water have been compared. The frameworks consist of the same ligands (glutarate and 4,4'trimethylenedipyridine) and copper centres but differ in the orientation of the bipyridyl ligand and crystal morphologies depending on if acetone or methanol were used in the synthesis (denoted CuGluBpp-Acetone and CuGluBpp-MeOH respectively). Synthesis from a solution containing methanol resulted in large, flat, plate-like crystals, whereas, when acetone was used smaller thicker crystals were produced. Casting membranes of the two Cu-MOFs within PDMS produced MMMs at differing wt% loading of the MOF and were analysed with a variety of techniques (FTIR, SEM, TGA, PXRD, Contact Angle, Degree of Solvent Uptake). Due to the flat plate-like nature of the crystals produced from the methanol solution, they lay parallel to the surface of the membrane. Through the use of PXRD and SEM analysis this was shown to be a non-ideal direction of the 1D pores of the MOF as they would be perpendicular to the permeation through the membrane. At high wt% loading of the CuGluBpp-MeOH the pervaporation performance was shown to reduce dramatically due to this non-ideal orientation. For the MOF produced from acetone, the smaller crystals had a more random orientation within the polymer and exhibited greater pervaporation performance for the removal of acetone from water. The 15 wt% loaded CuGluBpp-Acetone membrane was shown to have the greatest performance for a 5wt% acetone solution at 30 ºC with a PSI of 567, a total flux of 0.061 kg m^{-2} h^{-1} and separation factor of 10.3. The study has provided insight into design considerations for the effect of morphology and structure of MOFs for inclusion within MMMs for pervaporation applications.

- **Chapter 6**: Polypropylene glycols as probes for MWCO determination in Organic Solvent Nanofiltration

This Chapter has presented investigations into a new method for determining the MWCO of OSN membranes using PPGs. The single filtration method has been used to construct reproducible MWCO curves of a number of commercial OSN membranes using oligomers in the range of 192 - 1180 g mol^{-1} with methanol, acetone and toluene as solvents. The method developed has provided an alternative and complementary analysis for OSN membrane characterisation as it overcomes some of the limitations of the previously reported polystyrene[202] and PEG[250] methods.

The way these studies have met the specific objectives of the thesis as stated in Section 1.3 are outlined below:

- To identify suitable membrane separation processes for the low energy separation of products from a gas fermentation broth.

A review of the literature (Chapter 2) identified a number of different membrane separation processes that could be suitable for the recovery of fermentation products. The processes of NF, RO and pervaporation were identified as being suitable for recovery of 2,3-butanediol, acetate and ethanol from a gas fermentation broth and have been the focus of study within Chapters 3 and 4.

- To investigate the feasibility of current commercial membranes for the recovery of gas fermentation products, mainly 2,3-butanediol, acetate and ethanol.

The commercial membranes NF270, NF90 and BW30 have been used for the purification and concentration of 2,3-butanediol and acetate within a gas fermentation broth. The ZIF-8-PDMS membranes studied within Chapter 4 also give insight into the potential of this relatively new class of membrane which although not commercially available has recently been the subject of many important examples within the literature.[132, 171-173, 222]

- To identify ways to improve recovery of products from a gas fermentation process, this took the form of development of new membrane materials.

MMMs have been identified as promising novel materials for pervaporative removal of fermentation products (Chapter 2). Therefore, the effect of 2,3-butanediol and acetate on the pervaporation performance of a ZIF-8-PDMS membrane has been studied. The development of novel MMMs from the Cu-MOFs presented within Chapter 5 has shown the improvement of the

performance of a traditional PDMS membrane and identified design considerations for future studies.

- To develop methods to improve the characterisation and understanding of membrane separation processes.

Chapter 5 demonstrated the importance of the structure and crystal morphology of MOFs within pervaporation MMMs. The development of a new method for determining the MWCO of OSN membranes aids the understanding of separation within these processes (Chapter 6).

- Overall:

This thesis has presented a number of different investigations into the recovery of dilute organics from fermentation broths using membrane separations. There is; however, a number of studies that will need to be conducted for the successful application of these technologies industrially. A number of short term and long term considerations relevant to the work reported within this thesis are discussed within the next Chapter to help realise this.

7.2 Future Work

This thesis has presented a range of investigations into membrane separations for the lower energy recovery of dilute organics from fermentation broths. This Section presents a number of suggestions for future work stemming from the investigations conducted. These have been split up into suggestions for each Chapter and are outlined below:

- **Chapter 3**: Concentration and Purification of a Gas Fermentation Broth with Nanofiltration and Reverse Osmosis.

The main step to be taken next will be the continuous application of the membrane series coupled to a gas fermentation. A laboratory scale separation as set out in Figure 3-25 should be used to study the long term operational parameters such as fouling, membrane ageing, as well as the effect the separation has on the fermentation. Continuous removal of the fermentation products should have a beneficial effect on the fermentation due to their inherent toxicity towards the fermenting organism. If promising results for the long term operation are shown that can be reproduced at a

pilot scale then the separation presented could potentially provide the energy savings required for the commercial production of 2,3-butanediol and acetate from a gas fermentation process.

Additionally, studies into the further purification of 2,3-butanediol and acetate from their concentrated solution within the NF90 / BW30 permeate should be undertaken. NF at low pH could be used to separate the 2,3-butanediol from acetic acid. Then evaporation, vacuum membrane distillation, or hydrophilic pervaporation could be used to remove water and concentrate the 2,3-butanediol and acetate solutions up to > 95 % purity. The final removal of impurities from the concentrated product could then be conducted using OSN. An overall cost / benefit analysis into the use of the membranes to pre-concentrate the broth before further downstream separation will also need to be conducted. The energy savings due to the concentration will need to outweigh the increased operational costs of the membrane separation process.

- **Chapter 4**: ZIF-8-PDMS MMMs for Ethanol Pervaporation: Effect of 2,3-Butanediol and Acetate.

Future studies should focus on the effects of the components of the fermentation media such as the salts and vitamins etc. A systematic study of different salts such as conducted by Lipnizki *et al*. for 1-propanol pervaporation[221] would give further insight into their effect on the separation process within ZIF-8-PDMS membranes. Further long term studies using fermentation media / broth should also be undertaken to better understand the long-term stability / performance of these pervaporation membranes. Only a relatively short time was used in the experiments presented within the Chapter and so experiments of > 72 h in length should be conducted as well as investigating potential cleaning procedures for regeneration of the membranes performance after fouling by the broth components.

ZIF-71 has also been used within the literature as the inorganic filler within MMMs for both butanol and ethanol pervaporation. Although ZIF-71 in PEBA has been tested with an ABE fermentation mixture,[176] literature examples of ZIF-71 within PDMS have used model alcohol / water mixtures only and focused on the fabrication and characterisation of the membrane material rather than on the performance within a real fermentation mixture.[177, 178, 222] As a number of the studies have shown promise of the material for ethanol pervaporation, a study reflecting the one presented within this Chapter except utilising ZIF-71 as opposed to ZIF-8 could be undertaken. Due to the similarities of the two ZIFs, comparisons could easily be drawn as to the specific features of the MOFs that may aid or hinder the separation process in the presence of 2,3-butanediol and acetate.

- **Chapter 5**: Cu-MOF based PDMS Mixed-Matrix Membranes for Acetone Pervaporation: Impact of Glutarate and Bipyridyl ligands on the MOF morphology.

Due to the relatively low total fluxes exhibited by the prepared MMMs it would be important to reduce the thickness of the PDMS layer of the MMMs in future studies. The inherent thickness of the membranes produced here was a result of the microcrystalline nature of the as synthesised Cu-MOFs. Smaller particles would allow for casting of thinner membranes as well as a more homogenous dispersion within the polymer matrix.[154, 155] There are a number of different approaches used to produce nanosized MOF particles and that could be applied to the synthesis of the Cu-MOFs reported in this study including: microwave heating, changing the molar ratio of the ligands to copper nitrate, or use of additives.[191, 263]

Another investigation could include changing the crystal morphology so that the 1D pores run perpendicular as opposed to parallel to the largest face of the crystals (Figure 7-1). A number of approaches can be used to change crystal morphology such as change in solution pH, synthetic method, heating rate / method and the use of additives.[191, 233, 263-265]

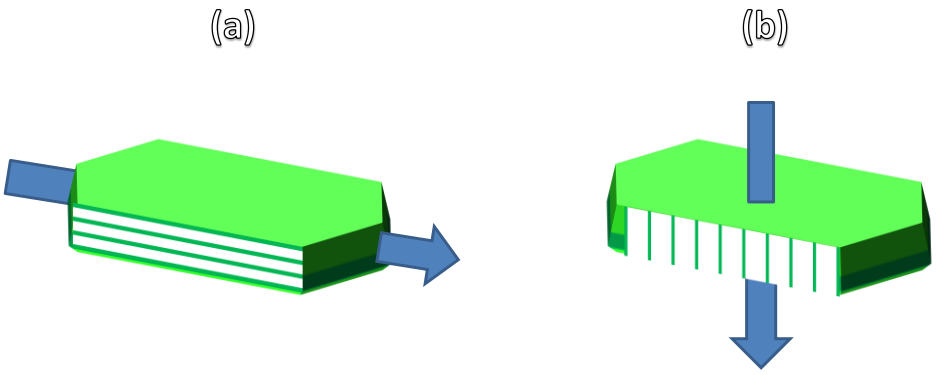

Figure 7-1. Potential change in the crystal morphology of CuGluBpp-MeOH used in this study to improve its performance within a MMM: (a) pores run parallel to the largest face, (b) the pores are perpendicular to the largest crystal face.

For a much more detailed study the effect of a change in the pore size of the Cu-MOFs could be undertaken. This could be conducted by increasing the length of the alkyl chain connecting the pyridines in the bipyridyl ligand (Figure 7-2). Cu-MOFs of glutarate and either 4,4'-bipyridine,[223] 1,2-bis(4-pyridyl)ethane,[226] 4,4'-Trimethylenedipyridine[226, 227] (used in this study), and an analogue of 1,4-di(4-pyridyl)butane[225] have been recorded in the literature. This shows that

Cu-MOFs with steadily increasing pore sizes could be produced and the MMMs of these fabricated. This could yield a systematic study of the effect of the pore size of the MOF used on their performance as the inorganic filler within a MMM. However, as shown in this study and several others[232, 233] it would also be important to consider crystal morphology in any assumptions made.

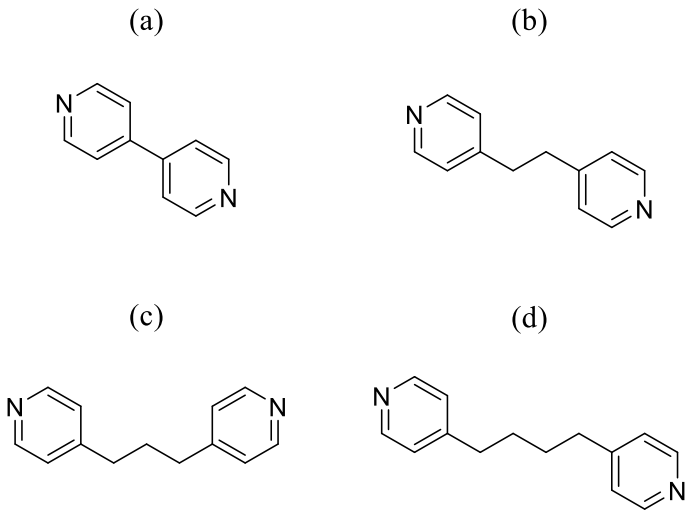

Figure 7-2. Structures of the bipyridines: (a) 4,4'-bipyridine, (b) 1,2-bis(4-pyridyl)ethane, (c) 4,4'-Trimethylenedipyridine and (d) 1,4-di(4-pyridyl)butane that could be used as the bipyridyl ligands in Cu-MOFs to produce MOFs with increasing pore sizes.

Future work in the development of the films of the Cu-MOFs, as described at the end of Chapter 5, should include film formation on a smaller membrane area, variation of the molar ratios of reactants and use of different substrates. Hydrothermal synthesis of films of the Cu-MOFs could also provide a route to defect free thin films.[191, 263, 266] The formation of thin-films of ZIFs on polymer substrates has also recently been reported using an interfacial synthesis method[267, 268] that could be applied to the Cu-MOFs studied within this Chapter.

- **Chapter 6**: Polypropylene glycols as probes for MWCO determination in Organic Solvent Nanofiltration

The main use of the protocol outlined within Chapter 6 within future studies will be in the characterisation of novel membrane materials for OSN. The method will provide a way to both characterise and further improve the understanding of rejection within these new materials as well as for established commercial OSN membranes. It is also suggested that an analogous MWCO method could be developed utilising oligomers of poly(1,2-butylene glycol) (Figure 7-3.c). Rissler

et al. showed that oligomers of poly(1,2-butylene glycol) of ~ 1000 g mol^{-1} can be separated using a similar chromatographic method as PEG and PPG and detected using ELSD.[259] A series of three filtrations of oligomers of PEG, PPG, and PBG may be able to be used to ascertain the importance of sterics and hydrophilicity / hydrophobicity within the rejection mechanism of an OSN membrane.

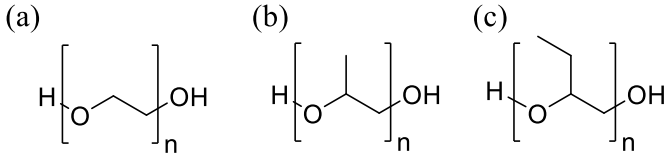

Figure 7-3. Chemical structures of: (a) poly(ethylene glycol), (b) poly(propylene glycol) and (c) poly(1,2-butylene glycol).

7.3 Final Remarks

The production of fuels and chemicals from microbial fermentation is evidently becoming increasingly important in a society that must transition from a linear to a circular economy. However, the recovery of these products from their dilute mixture within a fermentation broth is currently a major barrier to the industrial production of these sustainable chemicals. Of the many low energy separation processes available it is clear that membrane separation processes can provide an array of different low energy separations within this area. Therefore, future research within the area of low energy recovery of dilute organics from fermentation broths should have a specific focus on membrane separations. As described within this thesis and literature,[59, 269, 270] the specific processes of NF, RO and pervaporation have potential to reduce the production costs of fermentatively produced fuels and chemicals.

Dissemination

Journal Publications and Book Chapters

C. J. Davey, Z. Low, R. H. Wirawan, D. A. Patterson, "*Molecular Weight Cut-Off Determination of Organic Solvent Nanofiltration Membranes Using Poly(propylene) Glycols*", 2016, Accepted by the Journal of Membrane Science.

C. J. Davey, A. Havill, D. Leak, D. A. Patterson, "*Nanofiltration and reverse osmosis membranes for purification and concentration of a 2,3-butanediol producing gas fermentation broth*", *J. Membr. Sci.*, 2016, **518**, 150-158.

C. J. Davey, D. Leak, D. A. Patterson, "*Hybrid and Mixed Matrix Membranes for Separations from Fermentations*", *Membranes,* 2016, **6**, 17.

D. A. Patterson, C. J. Davey, R. Rohani, "*Membrane Separations: from Purifications, Minimisation, Reuse and Recycling to Process Intensification*", in: T. Letcher, J. Scott, D. Patterson (Eds.) Chemical Processes for a Sustainable Future, RSC, 2014, pp. 469 - 504.

Manuscripts in preparation

C. J. Davey, A. Havill, D. Leak, P. van der Gryp, L. Barbour, D. A. Patterson, "*ZIF-8-PDMS MMMs for Ethanol Pervaporation: Effect of 2,3-Butanediol and Acetate*" based on the work presented within Chapter 4.

C. J. Davey, V. J. Smith, C. X. Bezuidenhout, D. Leak, P. van der Gryp, L. Barbour, D. A. Patterson, "*Cu-MOF based PDMS mixed-matrix membranes for Acetone Pervaporation: Impact of Glutarate and Bipyridyl ligands on the MOF morphology*" based on the work presented within Chapter 5.

Conference Presentations

C. J. Davey, D. Leak, A. Havill, D. A. Patterson, "*Lower Energy Recovery of dilute organics from fermentation broths*", CSCT Sumer Showcase 2016, Bath, UK, (Flash and Poster Presentations).

C. J. Davey, D. Leak, A. Havill, D. A. Patterson, "*More sustainable separations for renewable feedstocks: membrane fractionation cascades for 2,3-butanediol and other fermented alcohols"*, Emerging and Hybrid Membrane Technologies, Swansea, UK, June 2016, (Poster Presentation).

C. J. Davey, D. Leak, A. Havill, D. A. Patterson, "*Enabling more sustainable separations for Industrial Biotechnology: membrane fractionation cascades for 2,3-butanediol*", Euromembrane 2015, Aachen, Germany, September 2015, (Speaker).

C. J. Davey, D. Leak, A. Havill, D. A. Patterson, "*Lower Energy Recovery of dilute organics from fermentation broths*", CSCT Sumer Showcase 2014, Bath, UK, (Poster Presentation).

Awards

European Membrane Society (EMS) Travel Award – Amount €500. Awarded to give a presentation at the conference Euromembrane 2015 in Aachen, Germany.

Global Research Scholarship (GRS) –University of Bath - Amount: £3000. Awarded to study for 3 months at the University of Stellenbosch, South Africa.

References:

[1] BP, *BP Statistical Review of World Energy 2013*, 2013.

[2] P. Vasudevan, M. Gagnon, M. Briggs, in *Sustainable Biotechnology*, eds. O. V. Singh and S. P. Harvey, Springer Netherlands, 2010, ch. 3, pp. 43-62.

[3] L. R. Radovic, *Energy and Fuels in Society: Analysis of Bills and Media Reports*, McGraw-Hill Custom Publishing, 1997

[4] T. W. Bank, *Turn Down the heat Why a 4 degree centrigrade warmer world must be avoided*, Potsdam Institute for Climate Impact Research and Climate Analytics, Washington DC, 2012

[5] J. Daniell, M. Köpke, S. Simpson, *Energies*, 2012, **5**, 5372.

[6] D. W. Griffin, M. A. Schultz, *Environ. Prog. Sustainable Energy*, 2012, **31**, 219-224.

[7] http://www.lanzatech.com/content/fueling-future-through-carbon-cycling, 25/10/13

[8] P. N. R. Vennestrøm, C. M. Osmundsen, C. H. Christensen, E. Taarning, *Angew. Chem. Int. Ed.*, 2011, **50**, 10502-10509.

[9] M. Kopke, C. Mihalcea, F. Liew, J. H. Tizard, M. S. Ali, J. J. Conolly, B. Al-Sinawi, S. D. Simpson, *Appl Environ Microbiol*, 2011, **77**, 5467-5475.

[10] Z. L. Xiu, A. P. Zeng, *Appl. Microbiol. Biotechnol.*, 2008, **78**, 917-926.

[11] C. Davey, D. Leak, D. Patterson, *Membranes*, 2016, **6**, 17.

[12] L. M. Vane, *Biofuels, Bioprod. Biorefin.*, 2008, **2**, 553-588.

[13] K. Schügerl, *Biotechnol. Adv.*, 2000, **18**, 581-599.

[14] H.-J. Huang, S. Ramaswamy, U. W. Tschirner, B. V. Ramarao, *Sep. Purif. Technol.*, 2008, **62**, 1-21.

[15] T. C. Bowen, L. M. Vane, *Langmuir*, 2006, **22**, 3721-3727.

[16] P. Pal, J. Nayak, *Sep. Purif. Rev.*, 2016, 1-18.

[17] Q. Z. Li, X. L. Jiang, X. J. Feng, J. M. Wang, C. Sun, H. B. Zhang, M. Xian, H. Z. Liu, *J Microbiol Biotechnol*, 2016, **26**, 1-8.

[18] S. Venkatesan, in *Separation and Purification Technologies in Biorefineries*, John Wiley & Sons, Ltd, 2013, ch. 5, pp. 101-148.

[19] *China Pat.*, CN101274876 B, 2011.

[20] J. Zhang, B. Hu, in *Separation and Purification Technologies in Biorefineries*, John Wiley & Sons, Ltd, 2013, ch. 3, pp. 61-78.

[21] D. F. Othmer, W. S. Bergen, N. Shlechter, P. F. Bruins, *Ind. Eng. Chem.*, 1945, **37**, 890-894.

[22] M. Anvari, H. Pahlavanzadeh, E. Vasheghani-Farahani, G. Khayati, *J. Ind. Microbiol. Biotechnol.*, 2009, **36**, 313-317.

[23] M. Senkus, *Ind. Eng. Chem.*, 1946, **38**, 913-916.

[24] Y. Li, Y. Wu, J. Zhu, J. Liu, *Biotechnol. Bioproc. E.*, 2012, **17**, 337-345.

[25] A. S. Afschar, C. E. Vaz Rossell, R. Jonas, A. Quesada Chanto, K. Schaller, *J. Biotechnol.*, 1993, **27**, 317-329.

[26] S. K. Garg, A. Jain, *Bioresour. Technol.*, 1995, **51**, 103-109.

[27] J. A. Wheat, J. D. Leslie, R. V. Tomkins, H. E. Mitton, D. S. Scott, G. A. Ledingham, *Can. J. Res.*, 1948, **26f**, 469-496.

[28] D. Datta, S. Kumar, H. Uslu, *J. Chem.*, 2015, **2015**, 1-16.

[29] J.-Y. Dai, Y.-Q. Sun, Z.-L. Xiu, *Eng. Life Sci.*, 2014, **14**, 108-117.

[30] W. J. Koros, *AIChE J.*, 2004, **50**, 2326-2334.

[31] S. Judd, in *Membranes for Industrial Wastewater Recovery and Re-use*, eds. S. Judd and B. Jefferson, Elsevier Science, Amsterdam, 2003, ch., pp. 13-74.

[32] R. W. Baker, in *Membrane Technology and Applications*, John Wiley & Sons, Ltd, 2012, ch. 2, pp. 15-96.

[33] R. W. Baker, in *Membrane Technology and Applications*, John Wiley & Sons, Ltd, 2012, ch. 7, pp. 303-324.

[34] T. C. Ezeji, Y. Li, in *Biomass to Biofuels*, eds. A. A. Vertès, N. Qureshi, H. P. Blaschek and H. Yukawa, Blackwell Publishing Ltd., 2010, ch. 16, pp. 331-345.

[35] R. W. Baker, in *Membrane Technology and Applications*, John Wiley & Sons, Ltd, 2012, ch. 6, pp. 253-302.

[36] R. W. Baker, in *Membrane Technology and Applications*, John Wiley & Sons, Ltd, 2012, ch. 9, pp. 379-416.

[37] T. Y. Cath, A. E. Childress, M. Elimelech, *J. Membr. Sci.*, 2006, **281**, 70-87.

[38] C. Bellona, J. E. Drewes, P. Xu, G. Amy, *Water Res.*, 2004, **38**, 2795-2809.

[39] D. Green, R. Perry, *Perry's Chemical Engineers' Handbook, Eighth Edition*, McGraw-Hill Education, 2007.

[40] M. Mulder, in *Basic Principles of Membrane Technology*, Springer Netherlands, Dordrecht, 1996, ch. 8, pp. 465-520.

[41] B. Sen Gupta, M. A. Hashim, K. B. Ramachandran, I. Sen Gupta, Z. F. Cui, *Eng. Life Sci.*, 2005, **5**, 54-57.

[42] P. Whittington, *Appl. Biochem. Biotechnol.*, 1990, **23**, 91-121.

[43] A. Persson, A.-S. Jönsson, G. Zacchi, *Biotechnol. Bioeng.*, 2001, **72**, 269-277.

[44] C. Wang, Q. Li, H. Tang, W. Zhou, D. Yan, J. Xing, Y. Wan, *J. Chem. Technol. Biotechnol.*, 2013, **88**, 444-448.

[45] I. S. Han, M. Cheryan, *J. Membr. Sci.*, 1995, **107**, 107-113.

[46] I. Han, M. Cheryan, *Appl. Biochem. Biotechnol.*, 1996, **57-58**, 19-28.

[47] S. H. Kang, Y. K. Chang, *J. Membr. Sci.*, 2005, **246**, 49-57.

[48] J. M. K. Timmer, H. C. van der Horst, T. Robbertsen, *J. Membr. Sci.*, 1993, **85**, 205-216.

[49] J. M. K. Timmer, J. Kromkamp, T. Robbertsen, *J. Membr. Sci.*, 1994, **92**, 185-197.

[50] L. M. Vane, *J. Chem. Technol. Biotechnol.*, 2005, **80**, 603-629.

[51] N. Qureshi, M. M. Meagher, R. W. Hutkins, *Sep. Sci. Technol.*, 1994, **29**, 1733-1748.

[52] C. Sagne, C. Fargues, R. Lewandowski, M.-L. Lameloise, M. Decloux, *Desalination*, 2008, **219**, 335-347.

[53] C. Sagne, C. Fargues, R. Lewandowski, M.-L. Lameloise, M. Gavach, M. Decloux, *Chem. Eng. Process. Process Intensif.*, 2010, **49**, 331-339.

[54] R. A. Diltz, T. V. Marolla, M. V. Henley, L. Li, *Bioresour. Technol.*, 2007, **98**, 686-695.

[55] N. Aydogan, T. Gurkan, L. Yilmaz, *Sep. Sci. Technol.*, 2005, **39**, 1059-1072.

[56] J. P. Choudhury, P. Ghosh, B. K. Guha, *Biotechnol. Lett.*, 1986, **8**, 731-734.

[57] J. P. Choudhury, P. Ghosh, B. K. Guha, *Biotechnol. Bioeng.*, 1985, **27**, 1081-1084.

[58] A. Garcia, E. L. Iannotti, J. L. Fischer, *Biotechnol. Bioeng.*, 1986, **28**, 785-791.

[59] C. Abels, F. Carstensen, M. Wessling, *J. Membr. Sci.*, 2013, **444**, 285-317.

[60] X. Feng, R. Y. M. Huang, *Ind. Eng. Chem. Res.*, 1997, **36**, 1048-1066.

[61] S.-Y. Lu, C.-P. Chiu, H.-Y. Huang, *J. Membr. Sci.*, 2000, **176**, 159-167.

[62] T. Sano, S. Ejiri, K. Yamada, Y. Kawakami, H. Yanagishita, *J. Membr. Sci.*, 1997, **123**, 225-233.

[63] B. Dettwiler, I. J. Dunn, E. Heinzle, J. E. Prenosil, *Biotechnol. Bioeng.*, 1993, **41**, 791-800.

[64] P. Shao, A. Kumar, *J. Membr. Sci.*, 2009, **329**, 160-168.

[65] P. Shao, A. Kumar, *Can. J. Chem. Eng.*, 2011, **89**, 1255-1265.

[66] P. Shao, A. Kumar, *J. Membr. Sci.*, 2009, **339**, 143-150.

[67] W. Kujawski, *Pol. J. Environ. Stud.*, 2000, **9**, 13-26.

[68] T. Uragami, in *Comprehensive Membrane Science and Engineering*, eds. E. Drioli and L. Giorno, Elsevier, Oxford, 2010, ch. 2.11, pp. 273-324.

[69] R. Y. M. Huang, C. K. Yeom, *J. Membr. Sci.*, 1990, **51**, 273-292.

[70] R. Y. M. Huang, C. K. Yeom, *J. Membr. Sci.*, 1991, **58**, 33-47.

[71] R. Y. M. Huang, X. Feng, *Sep. Sci. Technol.*, 1993, **28**, 2035-2048.

[72] Z. Gao, Y. Yue, W. Li, *Zeolites*, 1996, **16**, 70-74.

[73] T. Masuda, B.-Z. Tang, T. Higashimura, *Polym J*, 1986, **18**, 565-567.

[74] T. Masuda, M. Takatsuka, B.-Z. Tang, T. Higashimura, *J. Membr. Sci.*, 1990, **49**, 69-83.

[75] K.-i. Okamoto, A. Butsuen, S. Tsuru, S. Nishioka, K. Tanaka, H. Kita, S. Asakawa, *Polym J*, 1987, **19**, 747-756.

[76] J. R. González-Velasco, J. A. González-Marcos, C. López-Dehesa, *Desalination*, 2002, **149**, 61-65.

[77] A. Aroujalian, A. Raisi, *Desalination*, 2009, **247**, 509-517.

[78] S.-i. Nakao, F. Saitoh, T. Asakura, K. Toda, S. Kimura, *J. Membr. Sci.*, 1987, **30**, 273-287.

[79] S. V. Adymkanov, Y. P. Yampol'skii, A. M. Polyakov, P. M. Budd, K. J. Reynolds, N. B. McKeown, K. J. Msayib, *Polym. Sci. Ser. A*, 2008, **50**, 444-450.

[80] M. Lazarova, P. Bösch, A. Friedl, *Sep. Sci. Technol.*, 2012, **47**, 1709-1714.

[81] F. Liu, L. Liu, X. Feng, *Sep. Purif. Technol.*, 2005, **42**, 273-282.

[82] S. Li, F. Qin, P. Qin, M. N. Karim, T. Tan, *Green Chem.*, 2013, **15**, 2180-2190.

[83] R. W. Baker, in *Membrane Technology and Applications*, John Wiley & Sons, Ltd, 2004, ch. 3, pp. 89-160.

[84] A. Buekenhoudt, A. Kovalevsky, J. Luyten, F. Snijkers, in *Comprehensive Membrane Science and Engineering*, eds. E. Drioli and L. Giorno, Elsevier, Oxford, 2010, ch. 1.11, pp. 217-252.

[85] M. Yu, R. D. Noble, J. L. Falconer, *Acc. Chem. Res.*, 2011, **44**, 1196-1206.

[86] L. Li, J. Dong, T. M. Nenoff, R. Lee, *J. Membr. Sci.*, 2004, **243**, 401-404.

[87] N. Liu, L. Li, B. McPherson, R. Lee, *J. Membr. Sci.*, 2008, **325**, 357-361.

[88] T. C. Bowen, R. D. Noble, J. L. Falconer, *J. Membr. Sci.*, 2004, **245**, 1-33.

[89] I. S. Maddox, *Biotechnol. Lett.*, 1982, **4**, 759-760.

[90] A. Faisal, A. Zarebska, P. Saremi, D. Korelskiy, L. Ohlin, U. Rova, J. Hedlund, M. Grahn, *Adsorption*, 2014, **20**, 465-470.

[91] A. Oudshoorn, L. A. M. van der Wielen, A. J. J. Straathof, *Biochem. Eng. J.*, 2009, **48**, 99-103.

[92] I. H. Aljundi, J. M. Belovich, O. Talu, *Chem. Eng. Sci.*, 2005, **60**, 5004-5009.

[93] S. T. Meek, J. A. Greathouse, M. D. Allendorf, *Adv. Mater.*, 2011, **23**, 249-267.

[94] N. C. Burtch, H. Jasuja, K. S. Walton, *Chem. Rev.*, 2014, **114**, 10575-10612.

[95] H. Li, M. Eddaoudi, M. O'Keeffe, O. M. Yaghi, *Nature*, 1999, **402**, 276-279.

[96] B. Zornoza, C. Tellez, J. Coronas, J. Gascon, F. Kapteijn, *Microporous Mesoporous Mater.*, 2013, **166**, 67-78.

[97] A. Nalaparaju, X. S. Zhao, J. W. Jiang, *J. Phys. Chem. C*, 2010, **114**, 11542-11550.

[98] A. Nalaparaju, X. S. Zhao, J. W. Jiang, *Energy Environ. Sci.*, 2011, **4**, 2107-2116.

[99] A. U. Ortiz, A. P. Freitas, A. Boutin, A. H. Fuchs, F.-X. Coudert, *Phys. Chem. Chem.Phys.*, 2014, **16**, 9940-9949.

[100] G. F. de Lima, A. Mavrandonakis, H. A. de Abreu, H. A. Duarte, T. Heine, *J. Phys. Chem. C*, 2013, **117**, 4124-4130.

[101] G. Akiyama, R. Matsuda, H. Sato, A. Hori, M. Takata, S. Kitagawa, *Microporous Mesoporous Mater.*, 2012, **157**, 89-93.

[102] P. Küsgens, M. Rose, I. Senkovska, H. Fröde, A. Henschel, S. Siegle, S. Kaskel, *Microporous Mesoporous Mater.*, 2009, **120**, 325-330.

[103] D. Banerjee, B. J. Deibert, H. Wang, J. Li, in *Metal–Organic Frameworks: Adsorption of Hydrocarbons and Alcohols - Encyclopedia of Inorganic and Bioinorganic Chemistry*, John Wiley & Sons, Ltd, 2011, ch.

[104] K. S. Park, Z. Ni, A. P. Côté, J. Y. Choi, R. Huang, F. J. Uribe-Romo, H. K. Chae, M. O'Keeffe, O. M. Yaghi, *Proc. Natl. Acad. Sci.*, 2006, **103**, 10186-10191.

[105] A. Phan, C. J. Doonan, F. J. Uribe-Romo, C. B. Knobler, M. O'Keeffe, O. M. Yaghi, *Acc. Chem. Res.*, 2009, **43**, 58-67.

[106] R. P. Lively, M. E. Dose, J. A. Thompson, B. A. McCool, R. R. Chance, W. J. Koros, *Chem. Commun.*, 2011, **47**, 8667-8669.

[107] K. Zhang, R. P. Lively, M. E. Dose, A. J. Brown, C. Zhang, J. Chung, S. Nair, W. J. Koros, R. R. Chance, *Chem. Commun.*, 2013, **49**, 3245-3247.

[108] K. Zhang, R. P. Lively, C. Zhang, W. J. Koros, R. R. Chance, *J. Phys. Chem. C*, 2013, **117**, 7214-7225.

[109] K. Zhang, R. P. Lively, C. Zhang, R. R. Chance, W. J. Koros, D. S. Sholl, S. Nair, *J. Phys. Chem. Lett.*, 2013, 3618-3622.

[110] J. Cousin Saint Remi, T. Rémy, V. Van Hunskerken, S. van de Perre, T. Duerinck, M. Maes, D. De Vos, E. Gobechiya, C. E. A. Kirschhock, G. V. Baron, J. F. M. Denayer, *ChemSusChem*, 2011, **4**, 1074-1077.

[111] J. A. Gee, J. Chung, S. Nair, D. S. Sholl, *J. Phys. Chem. C*, 2013, **117**, 3169-3176.

[112] M. Paradise, T. Goswami, *Mater. Design*, 2007, **28**, 1477-1489.

[113] A. F. Ismail, P. S. Goh, S. M. Sanip, M. Aziz, *Sep. Purif. Technol.*, 2009, **70**, 12-26.

[114] I. F. J. Vankelecom, L. E. M. Gevers, T. Schäfer, J. G. Crespo, in *Green Separation Processes*, Wiley-VCH Verlag GmbH & Co. KGaA, 2006, ch. 3.6, pp. 251-289.

[115] P. D. Chapman, T. Oliveira, A. G. Livingston, K. Li, *J. Membr. Sci.*, 2008, **318**, 5-37.

[116] S. D. Bhat, T. M. Aminabhavi, *J. Membr. Sci.*, 2007, **306**, 173-185.

[117] X. Qiao, T.-S. Chung, R. Rajagopalan, *Chem. Eng. Sci.*, 2006, **61**, 6816-6825.

[118] Z. Huang, H.-m. Guan, W. l. Tan, X.-Y. Qiao, S. Kulprathipanja, *J. Membr. Sci.*, 2006, **276**, 260-271.

[119] S. Mosleh, T. Khosravi, O. Bakhtiari, T. Mohammadi, *Chem. Eng. Res. Des.*, 2012, **90**, 433-441.

[120] P. Das, S. K. Ray, S. B. Kuila, H. S. Samanta, N. R. Singha, *Sep. Purif. Technol.*, 2011, **81**, 159-173.

[121] D. Oh, S. Lee, Y. Lee, *Desalin. Water Treat.*, 2013, **51**, 5362-5370.

[122] H. Sun, L. Lu, X. Chen, Z. Jiang, *Sep. Purif. Technol.*, 2008, **58**, 429-436.

[123] H. Sun, L. Lu, X. Chen, Z. Jiang, *Appl. Surf. Sci.*, 2008, **254**, 5367-5374.

[124] M. Amirilargani, B. Sadatnia, *J. Membr. Sci.*, 2014, **469**, 1-10.

[125] G. M. Shi, T. Yang, T. S. Chung, *J. Membr. Sci.*, 2012, **415–416**, 577-586.

[126] G. M. Shi, H. Chen, Y. C. Jean, T. S. Chung, *Polymer*, 2013, **54**, 774-783.

[127] A. Kudasheva, S. Sorribas, B. Zornoza, C. Téllez, J. Coronas, *J. Chem. Technol. Biotechnol.*, 2015, **90**, 669-677.

[128] D. Hua, Y. K. Ong, Y. Wang, T. Yang, T.-S. Chung, *J. Membr. Sci.*, 2014, **453**, 155-167.

[129] Y. Li, W. B. Krantz, T.-S. Chung, *AIChE J.*, 2007, **53**, 2470-2475.

[130] C.-H. Kang, Y.-F. Lin, Y.-S. Huang, K.-L. Tung, K.-S. Chang, J.-T. Chen, W.-S. Hung, K.-R. Lee, J.-Y. Lai, *J. Membr. Sci.*, 2013, **438**, 105-111.

[131] J. C. Tan, T. D. Bennett, A. K. Cheetham, *Proc. Natl. Acad. Sci.*, 2010, **107**, 9938-9943.

[132] X.-L. Liu, Y.-S. Li, G.-Q. Zhu, Y.-J. Ban, L.-Y. Xu, W.-S. Yang, *Angew. Chem. Int. Ed.*, 2011, **50**, 10636-10639.

[133] G. Wu, M. Jiang, T. Zhang, Z. Jia, *J. Membr. Sci.*, 2016, **507**, 72-80.

[134] Y. Shirazi, M. A. Tofighy, T. Mohammadi, *J. Membr. Sci.*, 2011, **378**, 551-561.

[135] M. Amirilargani, A. Ghadimi, M. A. Tofighy, T. Mohammadi, *J. Membr. Sci.*, 2013, **447**, 315-324.

[136] D. P. Suhas, A. V. Raghu, H. M. Jeong, T. M. Aminabhavi, *RSC Adv.*, 2013, **3**, 17120-17130.

[137] S. P. Dharupaneedi, R. V. Anjanapura, J. M. Han, T. M. Aminabhavi, *Ind. Eng. Chem. Res.*, 2014, **53**, 14474-14484.

[138] S. B. Teli, G. S. Gokavi, M. Sairam, T. M. Aminabhavi, *Colloid Surface A*, 2007, **301**, 55-62.

[139] S. G. Adoor, M. Sairam, L. S. Manjeshwar, K. V. S. N. Raju, T. M. Aminabhavi, *J. Membr. Sci.*, 2006, **285**, 182-195.

[140] N. L. Le, Y. P. Tang, T.-S. Chung, *J. Membr. Sci.*, 2013, **447**, 163-176.

[141] N. L. Le, T.-S. Chung, *J. Membr. Sci.*, 2014, **454**, 62-73.

[142] S. Qiu, L. Wu, G. Shi, L. Zhang, H. Chen, C. Gao, *Ind. Eng. Chem. Res.*, 2010, **49**, 11667-11675.

[143] S. G. Adoor, B. Prathab, L. S. Manjeshwar, T. M. Aminabhavi, *Polymer*, 2007, **48**, 5417-5430.

[144] A. A. Kittur, M. Y. Kariduraganavar, U. S. Toti, K. Ramesh, T. M. Aminabhavi, *J. Appl. Polym. Sci.*, 2003, **90**, 2441-2448.

[145] A. A. Kittur, S. S. Kulkarni, M. I. Aralaguppi, M. Y. Kariduraganavar, *J. Membr. Sci.*, 2005, **247**, 75-86.

[146] V. García, J. Päkkilä, H. Ojamo, E. Muurinen, R. L. Keiski, *Renew. Sust. Energ. Rev.*, 2011, **15**, 964-980.

[147] G. Liu, W. Wei, W. Jin, *ACS Sustainable Chem. Eng.*, 2013.

[148] H. J. C. te Hennepe, D. Bargeman, M. H. V. Mulder, C. A. Smolders, *J. Membr. Sci.*, 1987, **35**, 39-55.

[149] M.-D. Jia, K.-V. Pleinemann, R.-D. Behling, *J. Membr. Sci.*, 1992, **73**, 119-128.

[150] A. Jonquières, A. Fane, *J. Membr. Sci.*, 1997, **125**, 245-255.

[151] E. A. Fouad, X. Feng, *J. Membr. Sci.*, 2009, **339**, 120-125.

[152] J. Huang, M. M. Meagher, *J. Membr. Sci.*, 2001, **192**, 231-242.

[153] H. Zhou, Y. Su, X. Chen, Y. Wan, *Sep. Purif. Technol.*, 2011, **79**, 375-384.

[154] B. Moermans, W. D. Beuckelaer, I. F. J. Vankelecom, R. Ravishankar, J. A. Martens, P. A. Jacobs, *Chem. Commun.*, 2000, 2467-2468.

[155] N. Wang, J. Liu, J. Li, J. Gao, S. Ji, J.-R. Li, *Microporous Mesoporous Mater.*, 2015, **201**, 35-42.

[156] S. Yi, Y. Su, Y. Wan, *J. Membr. Sci.*, 2010, **360**, 341-351.

[157] H. Zhou, Y. Su, X. Chen, S. Yi, Y. Wan, *Sep. Purif. Technol.*, 2010, **75**, 286-294.

[158] X. Zhan, J.-d. Li, C. Fan, X.-l. Han, *Chin J Polym Sci*, 2010, **28**, 625-635.

[159] J. Gu, X. Shi, Y. Bai, H. Zhang, L. Zhang, H. Huang, *Chem. Eng. Technol.*, 2009, **32**, 155-160.

[160] N. B. McKeown, P. M. Budd, *Chem. Soc. Rev.*, 2006, **35**, 675-683.

[161] P. M. Budd, E. S. Elabas, B. S. Ghanem, S. Makhseed, N. B. McKeown, K. J. Msayib, C. E. Tattershall, D. Wang, *Adv. Mater.*, 2004, **16**, 456-459.

[162] M. Žák, M. Klepic, L. Č. Štastná, Z. Sedláková, H. Vychodilová, Š. Hovorka, K. Friess, A. Randová, L. Brožová, J. C. Jansen, M. R. Khdhayyer, P. M. Budd, P. Izák, *Sep. Purif. Technol.*, 2015, **151**, 108-114.

[163] C. R. Mason, M. G. Buonomenna, G. Golemme, P. M. Budd, F. Galiano, A. Figoli, K. Friess, V. Hynek, *Polymer*, 2013, **54**, 2222-2230.

[164] L. M. Vane, V. V. Namboodiri, T. C. Bowen, *J. Membr. Sci.*, 2008, **308**, 230-241.

[165] L. M. Vane, V. V. Namboodiri, R. G. Meier, *J. Membr. Sci.*, 2010, **364**, 102-110.

[166] H. Tan, Y. Wu, T. Li, *J. Appl. Polym. Sci.*, 2013, **129**, 105-112.

[167] S. Takamizawa, C. Kachi-Terajima, M.-a. Kohbara, T. Akatsuka, T. Jin, *Chem. Asian J.*, 2007, **2**, 837-848.

[168] D. Fairen-Jimenez, S. A. Moggach, M. T. Wharmby, P. A. Wright, S. Parsons, T. Düren, *J. Am. Chem. Soc.*, 2011, **133**, 8900-8902.

[169] Y. Ying, Y. Xiao, J. Ma, X. Guo, H. Huang, Q. Yang, D. Liu, C. Zhong, *RSC Adv.*, 2015, **5**, 28394-28400.

[170] X. Wang, J. Chen, M. Fang, T. Wang, L. Yu, J. Li, *Sep. Purif. Technol.*, 2016, **163**, 39-47.

[171] Y. Bai, L. Dong, C. Zhang, J. Gu, Y. Sun, L. Zhang, H. Chen, *Sep. Sci. Technol.*, 2013, **48**, 2531-2539.

[172] H. Fan, Q. Shi, H. Yan, S. Ji, J. Dong, G. Zhang, *Angew. Chem. Int. Ed.*, 2014, **53**, 5578-5582.

[173] H. Fan, N. Wang, S. Ji, H. Yan, G. Zhang, *J. Mater. Chem. A*, 2014, **2**, 20947-20957.

[174] J. Li, N. Wang, H. Yan, S. Ji, G. Zhang, *RSC Adv.*, 2014, **4**, 59750-59753.

[175] N. Wang, G. Shi, J. Gao, J. Li, L. Wang, H. Guo, G. Zhang, S. Ji, *Sep. Purif. Technol.*, 2015, **153**, 146-155.

[176] S. Liu, G. Liu, X. Zhao, W. Jin, *J. Membr. Sci.*, 2013, **446**, 181-188.

[177] Y. Li, L. H. Wee, J. A. Martens, I. F. J. Vankelecom, *J. Mater. Chem. A*, 2014, **2**, 10034-10040.

[178] L. H. Wee, Y. Li, K. Zhang, P. Davit, S. Bordiga, J. Jiang, I. F. J. Vankelecom, J. A. Martens, *Adv. Funct. Mater.*, 2015, **25**, 516-525.

[179] S. Liu, G. Liu, J. Shen, W. Jin, *Sep. Purif. Technol.*, 2014, **133**, 40-47.

[180] J. Y. Lee, D. H. Olson, L. Pan, T. J. Emge, J. Li, *Adv. Funct. Mater.*, 2007, **17**, 1255-1262.

[181] Y. F. Chen, J. Y. Lee, R. Babarao, J. Li, J. W. Jiang, *J. Phys. Chem. C*, 2010, **114**, 6602-6609.

[182] S. Bourrelly, B. Moulin, A. Rivera, G. Maurin, S. Devautour-Vinot, C. Serre, T. Devic, P. Horcajada, A. Vimont, G. Clet, M. Daturi, J.-C. Lavalley, S. Loera-Serna, R. Denoyel, P. L. Llewellyn, G. Férey, *J. Am. Chem. Soc.*, 2010, **132**, 9488-9498.

[183] G. Zhang, J. Li, N. Wang, H. Fan, R. Zhang, S. Ji, *J. Membr. Sci.*, 2015, **492**, 322-330.

[184] H.-W. Yen, Z.-H. Chen, I. K. Yang, *Bioresour. Technol.*, 2012, **109**, 105-109.

[185] Y. Huang, P. Zhang, J. Fu, Y. Zhou, X. Huang, X. Tang, *J. Membr. Sci.*, 2009, **339**, 85-92.

[186] N. L. Le, Y. Wang, T.-S. Chung, *J. Membr. Sci.*, 2011, **379**, 174-183.

[187] G. Liu, W.-S. Hung, J. Shen, Q. Li, Y.-H. Huang, W. Jin, K.-R. Lee, J.-Y. Lai, *J. Mater. Chem. A*, 2015, **3**, 4510-4521.

[188] G. Liu, F. Xiangli, W. Wei, S. Liu, W. Jin, *Chem. Eng. J.*, 2011, **174**, 495-503.

[189] X. Zhan, J. Lu, T. Tan, J. Li, *Appl. Surf. Sci.*, 2012, **259**, 547-556.

[190] H. Tan, Y. Wu, Y. Zhou, Z. Liu, T. Li, *J. Membr. Sci.*, 2014, **453**, 302-311.

[191] V. Valtchev, L. Tosheva, *Chem. Rev.*, 2013, **113**, 6734-6760.

[192] X.-J. Ji, H. Huang, P.-K. Ouyang, *Biotechnol. Adv.*, 2011, **29**, 351-364.

[193] M. J. Syu, *Appl. Microbiol. Biotechnol.*, 2001, **55**, 10-18.

[194] L.-H. Sun, B. Jiang, Z.-L. Xiu, *Biotechnol. Lett.*, 2009, **31**, 371-376.

[195] B. Jiang, Z.-G. Li, J.-Y. Dai, D.-J. Zhang, Z.-L. Xiu, *Process Biochem.*, 2009, **44**, 112-117.

[196] Z. Li, H. Teng, Z. Xiu, *Process Biochem.*, 2010, **45**, 731-737.

[197] D. A. Patterson, C. J. Davey, R. Rohani, in *Chemical Processes for a Sustainable Future*, eds. T. Letcher, J. Scott and D. Patterson, RSC, 2014, ch. 19, pp. 469 - 504.

[198] T. Brás, M. C. Fernandes, J. L. C. Santos, L. A. Neves, *Desalin. Water Treat.*, 2013, **51**, 4333-4342.

[199] J. Bastrzyk, M. Gryta, K. Karakulski, *Chem. Pap.*, 2014, **68**, 757-765.

[200] S. Mondal, S. R. Wickramasinghe, *J. Membr. Sci.*, 2008, **322**, 162-170.

[201] A. R. D. Verliefde, E. R. Cornelissen, S. G. J. Heijman, I. Petrinic, T. Luxbacher, G. L. Amy, B. Van der Bruggen, J. C. van Dijk, *J. Membr. Sci.*, 2009, **330**, 90-103.

[202] Y. H. See Toh, X. X. Loh, K. Li, A. Bismarck, A. G. Livingston, *J. Membr. Sci.*, 2007, **291**, 120-125.

[203] R. Rohani, M. Hyland, D. Patterson, *J. Membr. Sci.*, 2011, **382**, 278-290.

[204] C. Y. Tang, Y.-N. Kwon, J. O. Leckie, *Desalination*, 2009, **242**, 168-182.

[205] K. Košutić, D. Dolar, B. Kunst, *J. Membr. Sci.*, 2006, **282**, 109-114.

[206] C. Y. Tang, Y.-N. Kwon, J. O. Leckie, *Desalination*, 2009, **242**, 149-167.

[207] J. S. Louie, I. Pinnau, I. Ciobanu, K. P. Ishida, A. Ng, M. Reinhard, *J. Membr. Sci.*, 2006, **280**, 762-770.

[208] J. Geens, K. Peeters, B. Van der Bruggen, C. Vandecasteele, *J. Membr. Sci.*, 2005, **255**, 255-264.

[209] J. Geens, B. Van der Bruggen, C. Vandecasteele, *Chem. Eng. Sci.*, 2004, **59**, 1161-1164.

[210] M. Dalwani, N. E. Benes, G. Bargeman, D. Stamatialis, M. Wessling, *J. Membr. Sci.*, 2010, **363**, 188-194.

[211] C. J. Davey, A. Havill, D. Leak, D. A. Patterson, *J. Membr. Sci.*, 2016, **518**, 150-158.

[212] J. Cravillon, S. Münzer, S.-J. Lohmeier, A. Feldhoff, K. Huber, M. Wiebcke, *Chem. Mater.*, 2009, **21**, 1410-1412.

[213] C. F. Macrae, P. R. Edgington, P. McCabe, E. Pidcock, G. P. Shields, R. Taylor, M. Towler, J. van de Streek, *J. Appl. Cryst.*, 2006, **39**, 453-457.

[214] X. Liu, H. Jin, Y. Li, H. Bux, Z. Hu, Y. Ban, W. Yang, *J. Membr. Sci.*, 2013, **428**, 498-506.

[215] A. F. M. Barton, *CRC Handbook of Solubility Parameters and Other Cohesion Parameters, Second Edition*, Taylor & Francis, 1991.

[216] S. A. Moggach, T. D. Bennett, A. K. Cheetham, *Angew. Chem. Int. Ed.*, 2009, **48**, 7087-7089.

[217] S. Chovau, S. Gaykawad, A. J. Straathof, B. Van der Bruggen, *Bioresour. Technol.*, 2011, **102**, 1669-1674.

[218] M. Wood, T. Matsuura, Z. Duvnjak, *Sep. Sci. Technol.*, 1994, **29**, 1609-1619.

[219] M. Nomura, T. Bin, S.-i. Nakao, *Sep. Purif. Technol.*, 2002, **27**, 59-66.

[220] R. H. Bello, O. Souza, N. Sellin, S. H. W. Medeiros, C. Marangoni, *Procedia Engineering*, 2012, **42**, 512-520.

[221] F. Lipnizki, S. Hausmanns, R. W. Field, *J. Membr. Sci.*, 2004, **228**, 129-138.

[222] P. V. Naik, L. H. Wee, M. Meledina, S. Turner, Y. Li, G. Van Tendeloo, J. A. Martens, I. F. J. Vankelecom, *J. Mater. Chem. A*, 2016, **4**, 12790-12798.

[223] B. Rather, M. J. Zaworotko, *Chem. Commun.*, 2003, 830-831.

[224] B. Chen, Y. Ji, M. Xue, F. R. Fronczek, E. J. Hurtado, J. U. Mondal, C. Liang, S. Dai, *Inorg. Chem.*, 2008, **47**, 5543-5545.

[225] R. Dey, R. Haldar, T. K. Maji, D. Ghoshal, *Cryst. Growth Des.*, 2011, **11**, 3905-3911.

[226] I. H. Hwang, J. M. Bae, W.-S. Kim, Y. D. Jo, C. Kim, Y. Kim, S.-J. Kim, S. Huh, *Dalton Trans.*, 2012, **41**, 12759-12765.

[227] J. M. Seco, D. Fairen-Jimenez, A. J. Calahorro, L. Mendez-Linan, M. Perez-Mendoza, N. Casati, E. Colacio, A. Rodriguez-Dieguez, *Chem. Commun.*, 2013, **49**, 11329-11331.

[228] C. X. Bezuidenhout, V. J. Smith, P. M. Bhatt, C. Esterhuysen, L. J. Barbour, *Angew. Chem.*, 2015, **127**, 2107-2111.

[229] A. Bravais, *Études cristallographiques*, Gauthier-Villars, Paris, 1866.

[230] G. Friedel, *Bull. Soc. Franc. Mineral.*, 1907, **30**, 326.

[231] J. D. H. Donnay, D. Harker, *Am. Mineralogist*, 1937, **22**, 446.

[232] A. Sabetghadam, B. Seoane, D. Keskin, N. Duim, T. Rodenas, S. Shahid, S. Sorribas, C. L. Guillouzer, G. Clet, C. Tellez, M. Daturi, J. Coronas, F. Kapteijn, J. Gascon, *Adv. Funct. Mater.*, 2016, **26**, 3154-3163.

[233] T. Rodenas, I. Luz, G. Prieto, B. Seoane, H. Miro, A. Corma, F. Kapteijn, F. X. Llabrés i Xamena, J. Gascon, *Nat Mater*, 2015, **14**, 48-55.

[234] F. Y. H. Lin, D. Li, A. W. Neumann, *J. Colloid Interface Sci.*, 1993, **159**, 86-95.

[235] S. Shahid, K. Nijmeijer, *J. Membr. Sci.*, 2014, **459**, 33-44.

[236] S. Shahid, K. Nijmeijer, *J. Membr. Sci.*, 2014, **470**, 166-177.

[237] C. Zhang, L. Yang, Y. Bai, J. Gu, Y. Sun, *Sep. Purif. Technol.*, 2012, **85**, 8-16.

[238] J. Gu, X. Zhang, Y. Bai, L. Yang, C. Zhang, Y. Sun, *Int. J. Poly. Sci.*, 2013, **2013**, 1-10.

[239] J. Yao, D. Dong, D. Li, L. He, G. Xu, H. Wang, *Chem. Commun.*, 2011, **47**, 2559-2561.

[240] E. Barankova, N. Pradeep, K.-V. Peinemann, *Chem. Commun.*, 2013, **49**, 9419-9421.

[241] J. Yao, H. Wang, *Chem. Soc. Rev.*, 2014, **43**, 4470-4493.

[242] X. Dong, Y. S. Lin, *Chem. Commun.*, 2013, **49**, 1196-1198.

[243] P. Marchetti, M. F. Jimenez Solomon, G. Szekely, A. G. Livingston, *Chemical Reviews*, 2014, **114**, 10735-10806.

[244] M. G. Buonomenna, J. Bae, *Sep. Purif. Rev.*, 2015, **44**, 157-182.

[245] P. Vandezande, L. E. M. Gevers, I. F. J. Vankelecom, *Chem. Soc. Rev.*, 2008, **37**, 365-405.

[246] L. S. White, *J. Membr. Sci.*, 2006, **286**, 26-35.

[247] B. Van der Bruggen, J. Schaep, D. Wilms, C. Vandecasteele, *J. Membr. Sci.*, 1999, **156**, 29-41.

[248] K. Boussu, B. Van der Bruggen, A. Volodin, C. Van Haesendonck, J. A. Delcour, P. Van der Meeren, C. Vandecasteele, *Desalination*, 2006, **191**, 245-253.

[249] L. S. White, *J. Membr. Sci.*, 2002, **205**, 191-202.

[250] X. Li, F. Monsuur, B. Denoulet, A. Dobrak, P. Vandezande, I. F. J. Vankelecom, *Anal. Chem.*, 2009, **81**, 1801-1809.

[251] S. M. Dutczak, M. W. J. Luiten-Olieman, H. J. Zwijnenberg, L. A. M. Bolhuis-Versteeg, L. Winnubst, M. A. Hempenius, N. E. Benes, M. Wessling, D. Stamatialis, *J. Membr. Sci.*, 2011, **372**, 182-190.

[252] H. J. Zwijnenberg, S. M. Dutczak, M. E. Boerrigter, M. A. Hempenius, M. W. J. Luiten-Olieman, N. E. Benes, M. Wessling, D. Stamatialis, *J. Membr. Sci.*, 2012, **390–391**, 211-217.

[253] K. Boussu, Y. Zhang, J. Cocquyt, P. Van der Meeren, A. Volodin, C. Van Haesendonck, J. A. Martens, B. Van der Bruggen, *J. Membr. Sci.*, 2006, **278**, 418-427.

[254] D. Bhanushali, S. Kloos, D. Bhattacharyya, *J. Membr. Sci.*, 2002, **208**, 343-359.

[255] E. S. Tarleton, J. P. Robinson, C. R. Millington, A. Nijmeijer, *J. Membr. Sci.*, 2005, **252**, 123-131.

[256] J. Kwiatkowski, M. Cheryan, *Sep. Sci. Technol.*, 2005, **40**, 2651-2662.

[257] T. Tsuru, T. Sudoh, T. Yoshioka, M. Asaeda, *J. Membr. Sci.*, 2001, **185**, 253-261.

[258] N. C. Megoulas, M. A. Koupparis, *Crit. Rev. Anal. Chem.*, 2005, **35**, 301-316.

[259] K. Rissler, U. Fuchslueger, H.-J. Grether, *J. Chromatogr. A*, 1993, **654**, 309-314.

[260] K.-J. Liu, J. L. Parsons, *Macromolecules*, 1969, **2**, 529-533.

[261] L. S. Sandell, D. A. I. Goring, *Macromolecules*, 1970, **3**, 54-57.

[262] L. S. Sandell, D. A. I. Goring, *Macromolecules*, 1970, **3**, 50-54.

[263] N. Stock, S. Biswas, *Chem. Rev.*, 2012, **112**, 933-969.

[264] A. R. Klapwijk, E. Simone, Z. K. Nagy, C. C. Wilson, *Cryst. Growth Des.*, 2016, **16**, 4349-4359.

[265] J. M. Chin, E. Y. Chen, A. G. Menon, H. Y. Tan, A. T. S. Hor, M. K. Schreyer, J. Xu, *CrystEngComm*, 2013, **15**, 654-657.

[266] O. Shekhah, J. Liu, R. A. Fischer, C. Woll, *Chem. Soc. Rev.*, 2011, **40**, 1081-1106.

[267] Y. Li, L. H. Wee, A. Volodin, J. A. Martens, I. F. J. Vankelecom, *Chem. Commun.*, 2015, **51**, 918-920.

[268] Y. Li, L. H. Wee, J. A. Martens, I. F. J. Vankelecom, *J. Membr. Sci.*, In Press.

[269] G. D. Mehta, *J. Membr. Sci.*, 1982, **12**, 1-26.

[270] F. Lipnizki, *Desalination*, 2010, **250**, 1067-1069.

Appendices

A.4.1. Photographs and digital microscope images of ZIF-8-MMMs

Photographs and digital microscope images are shown in Figure A-1 and Figure A-2, the ZIF-8 cannot be identified within the MMMs due to white crystals of ZIF-8 being indistinguishable from the white PVDF support layer.

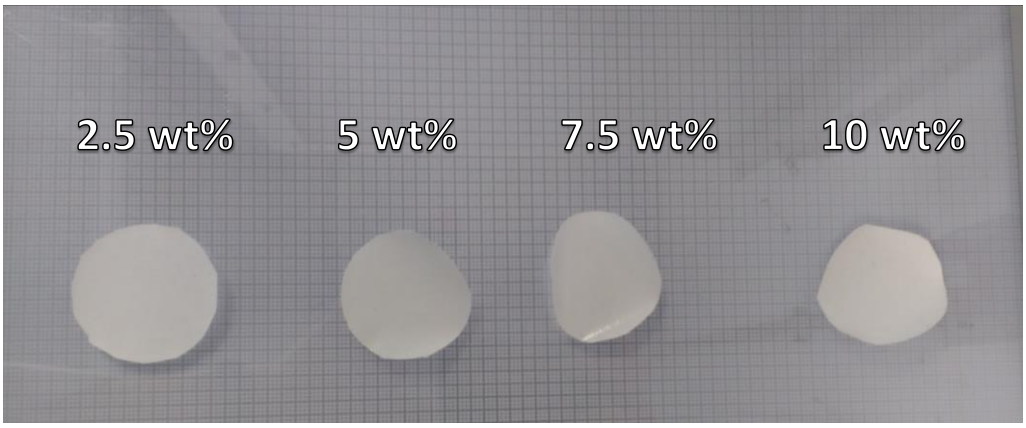

Figure A-1. Photographs of the as synthesised ZIF-8 membranes at differing wt% loading of MOF.

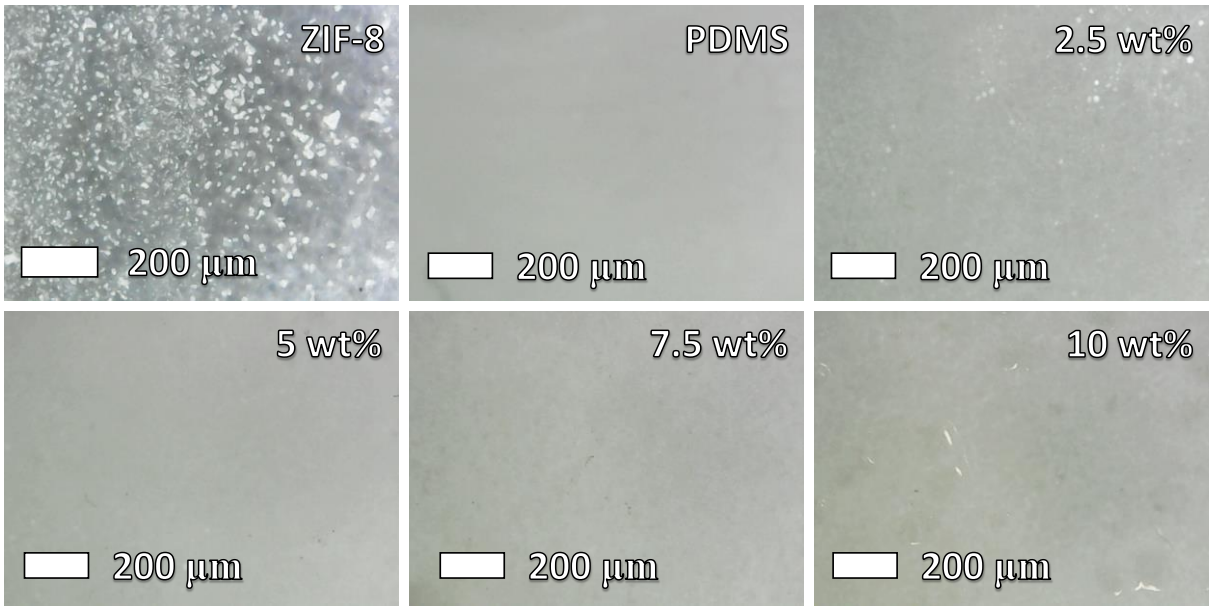

Figure A-2. Digital microscope images of the as-synthesised ZIF-8 and membranes.

A.5.1. FTIR data of Cu-MOFs and Photographs of MMMs

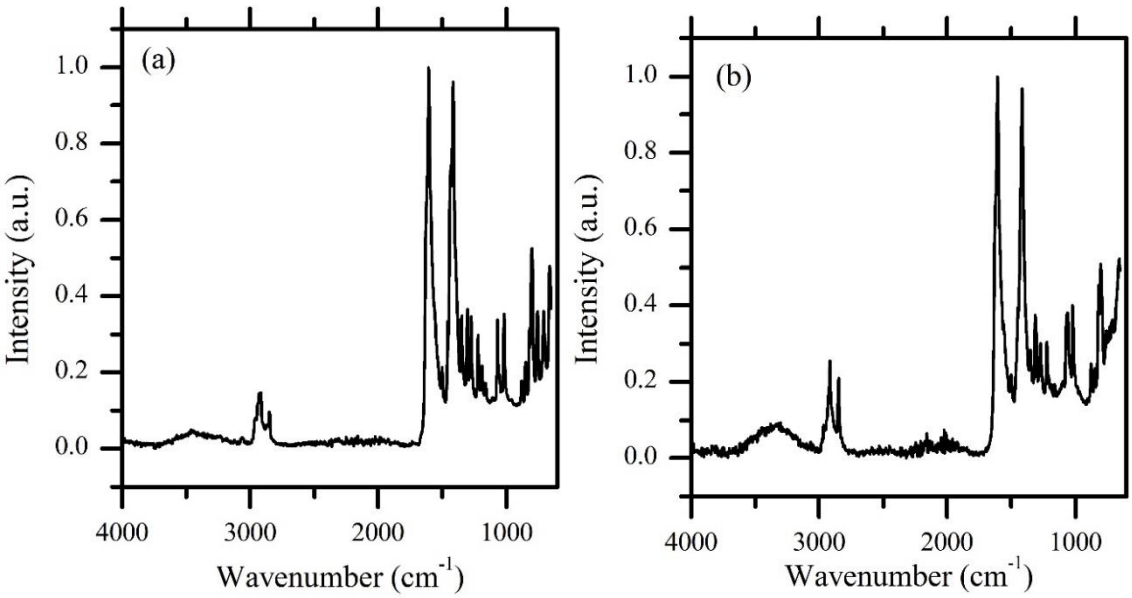

Figure A-3. FTIR for (a) CuGluBpp-Acetone and (b) CuGluBpp-MeOH.

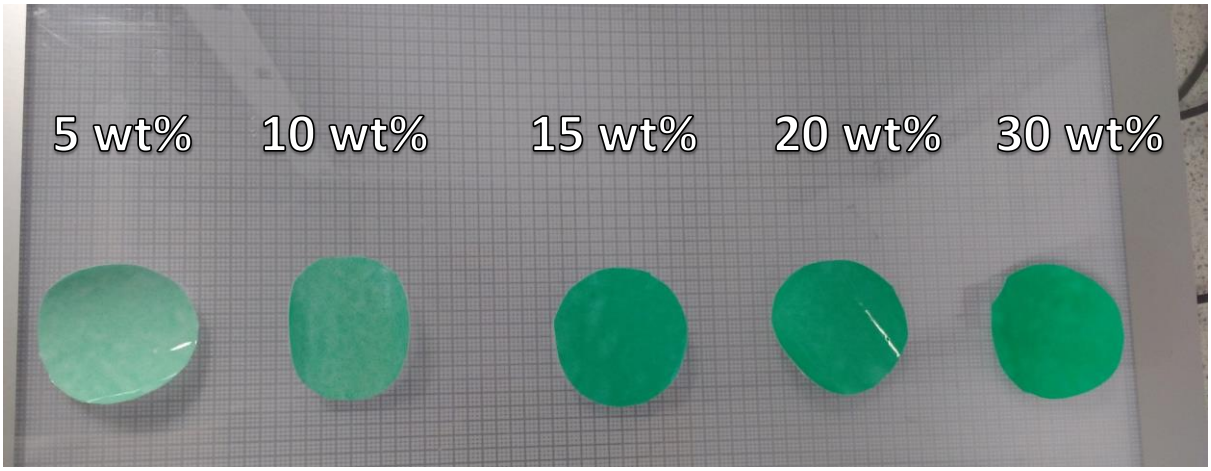

Figure A-4. Photographs of the as-synthesised CuGluBpp-Acetone-PDMS membranes with different wt% loading of MOF.

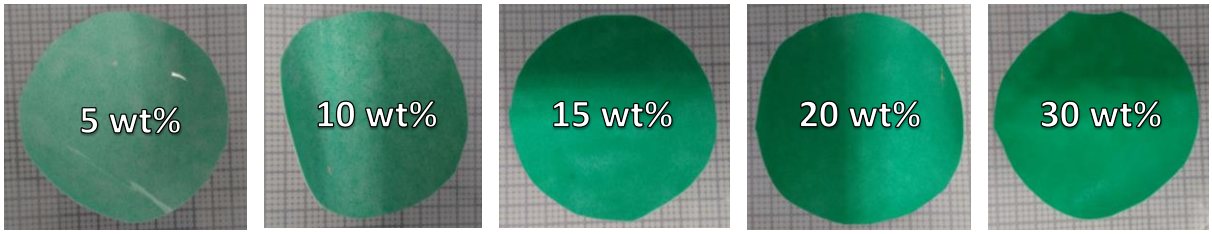

Figure A-5. Photographs of the as-synthesised CuGluBpp-Acetone-PDMS membranes with differing wt% loading of MOF.

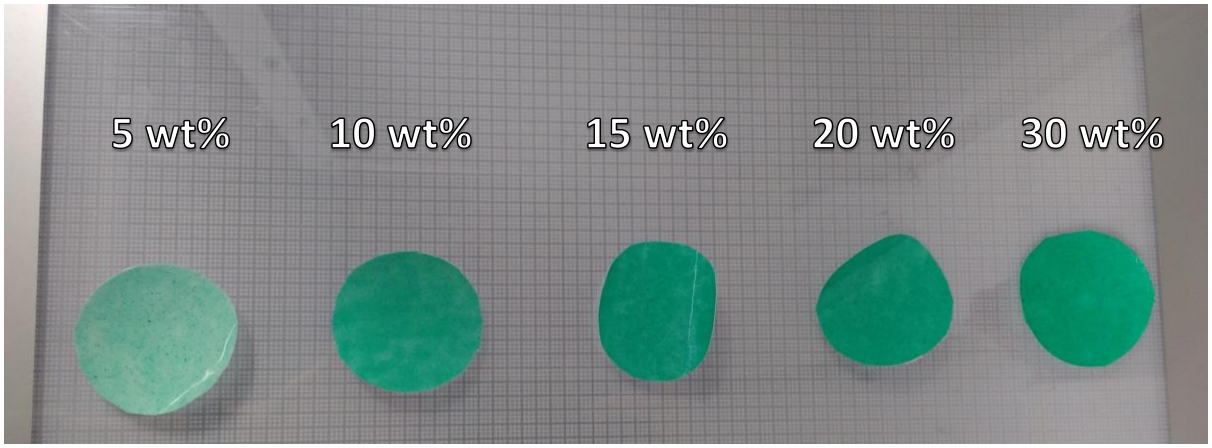

Figure A-6. Photographs of the as-synthesised CuGluBpp-MeOH-PDMS membranes with different wt% loading of MOF.

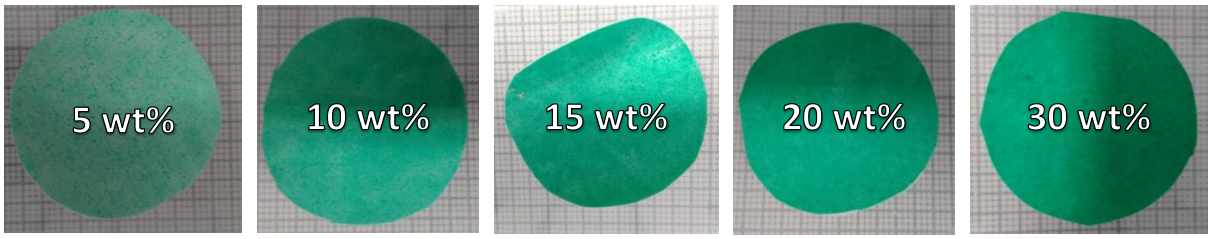

Figure A-7. Photographs of the as-synthesised CuGluBpp-MeOH-PDMS membranes with different wt% loading of MOF.

A.6.1. List of PPG Oligomers

Table A-1. Table of PPG Oligomers and presence in purchased samples and their typical retention times.

n	MW (g mol^{-1})	b.p.	Which PPG Sample	Typical retention time (min)
3	192.14	~ 273	Tri	4.58
4	250.3	-	400	5.94
5	308.4	-	400	7.13
6	366.48	-	400	8.72
7	424.56	~ 287.6	400	10.4
8	482.64	-	400	12.1
9	540.72	-	400 / 725	13.9
10	598.80	-	400 / 725	15.6
11	656.88	-	725	17.3
12	714.96	-	725 / 1000	18.9
13	773.04	-	725 / 1000	20.5
14	831.11	-	725 / 1000	22.1
15	889.19	-	725 / 1000	23.7
16	947.27	-	725/ 1000	25.3
17	1005.35	-	725 / 1000	27.0
18	1063.43	-	725 / 1000	28.6
19	1121.51	-	725 / 1000	30.3
20	1179.60	-	1000	31.9
-	>1179.6	-	1000	>32

A.6.2. Calibration Curves

A.6.2.1. Methanol Calibration Curves Poly(propylene) Glycol

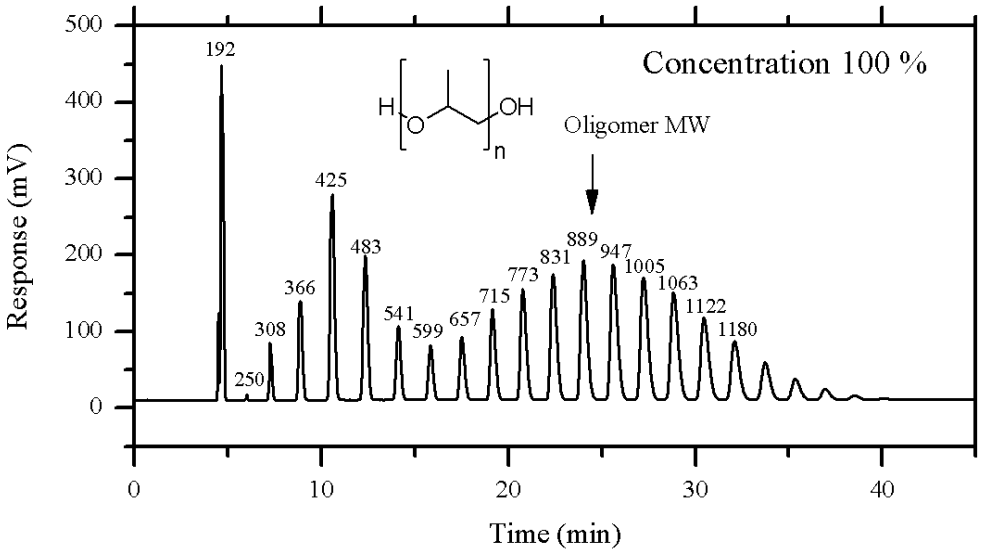

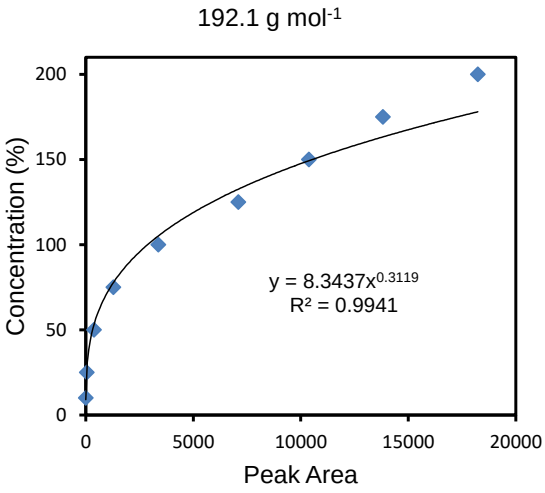

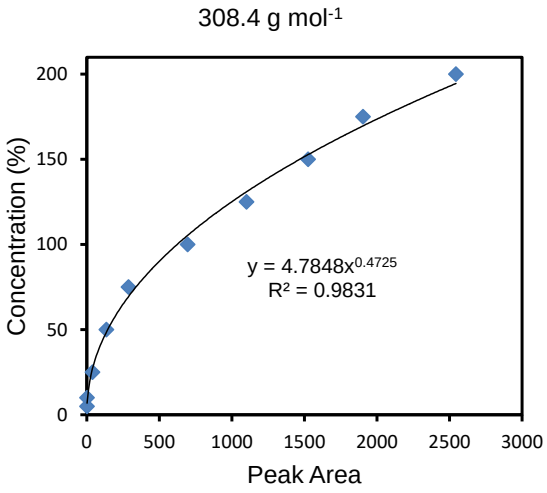

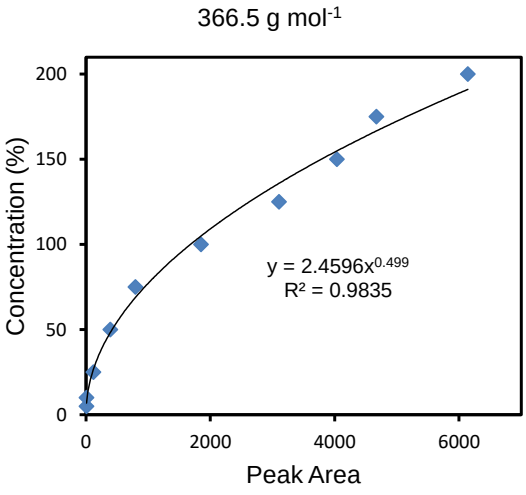

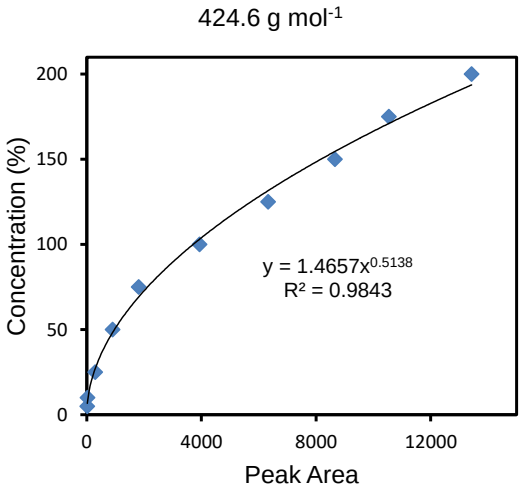

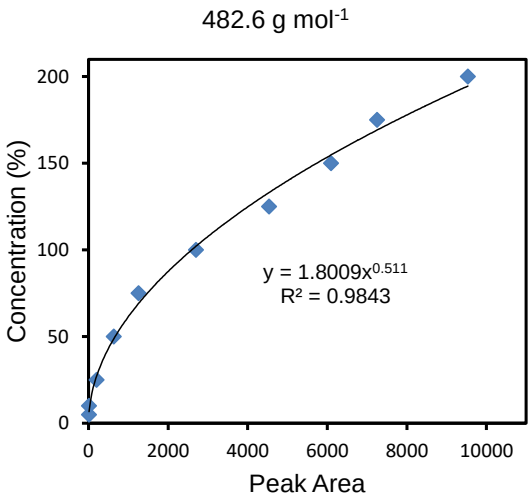
482.6 g mol-1
Concentration (%)
Peak Area
y = 1.8009x0.511
R² = 0.9843
0
50
100
150
200
0
2000
4000
6000
8000
10000

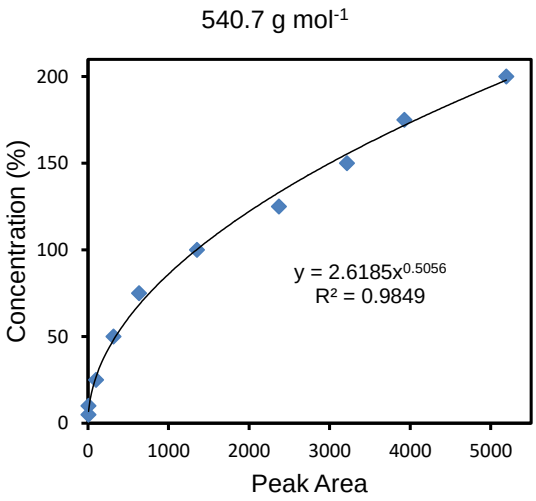
540.7 g mol-1
Concentration (%)
Peak Area
y = 2.6185x0.5056
R² = 0.9849
0
50
100
150
200
0
1000
2000
3000
4000
5000

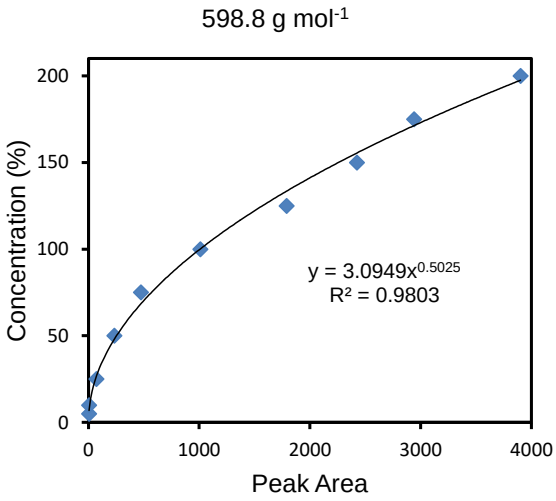
598.8 g mol-1
Concentration (%)
Peak Area
y = 3.0949x0.5025
R² = 0.9803
0
50
100
150
200
0
1000
2000
3000
4000

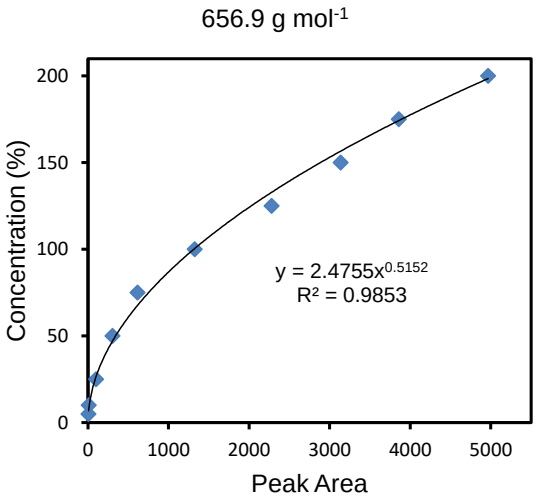
656.9 g mol-1
Concentration (%)
Peak Area
y = 2.4755x0.5152
R² = 0.9853
0
50
100
150
200
0
1000
2000
3000
4000
5000

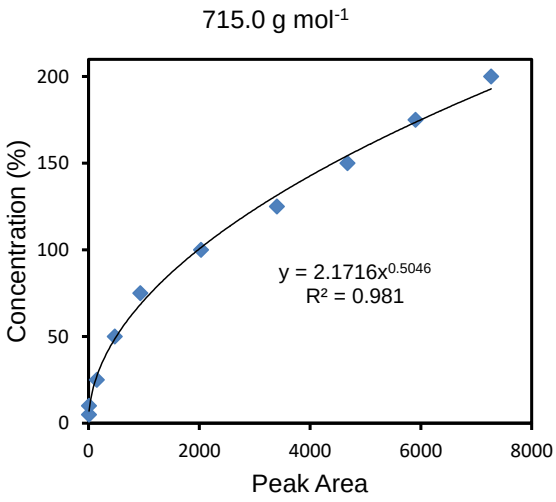
715.0 g mol-1
Concentration (%)
Peak Area
y = 2.1716x0.5046
R² = 0.981
0
50
100
150
200
0
2000
4000
6000
8000

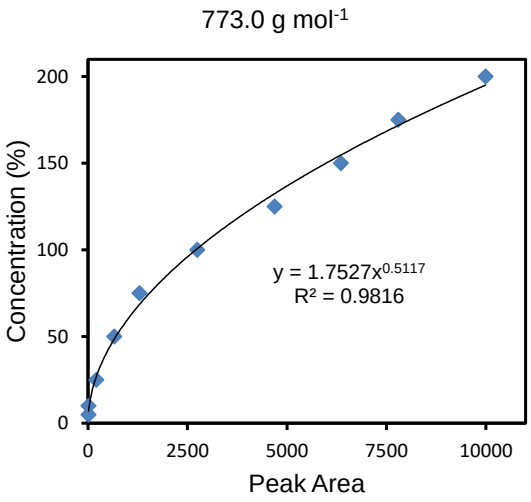
773.0 g mol-1
Concentration (%)
Peak Area
y = 1.7527x0.5117
R² = 0.9816
0
50
100
150
200
0
2500
5000
7500
10000

831.1 g mol^{-1}

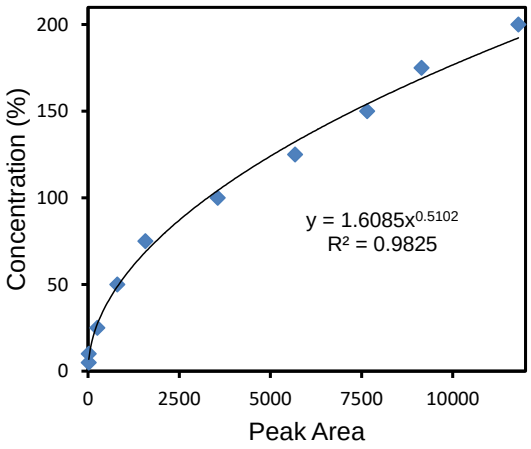

889.2 g mol^{-1}

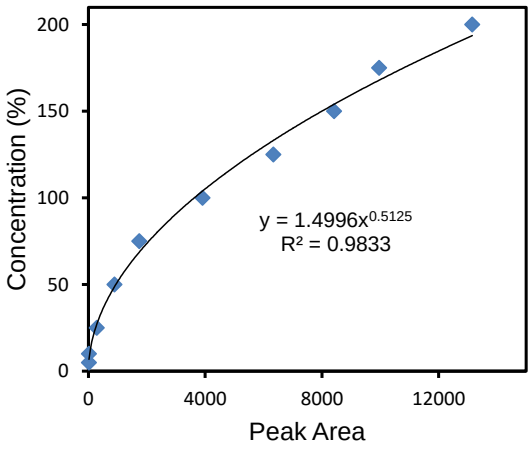

947.3 g mol^{-1}

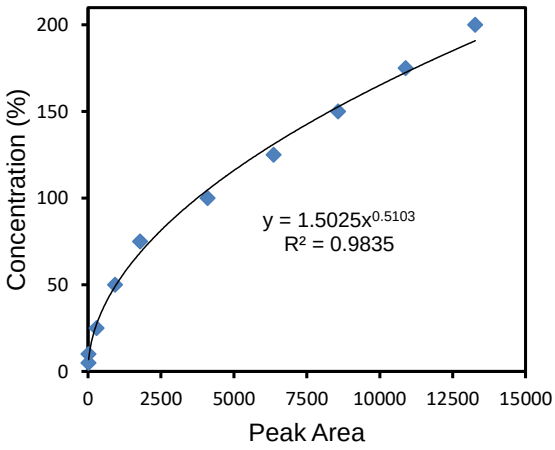

1005.4 g mol^{-1}

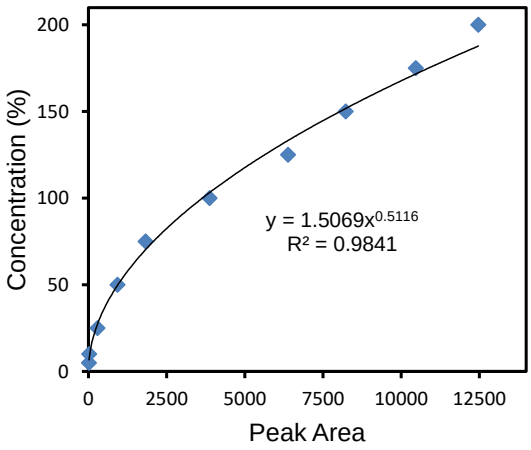

1063.4 g mol^{-1}

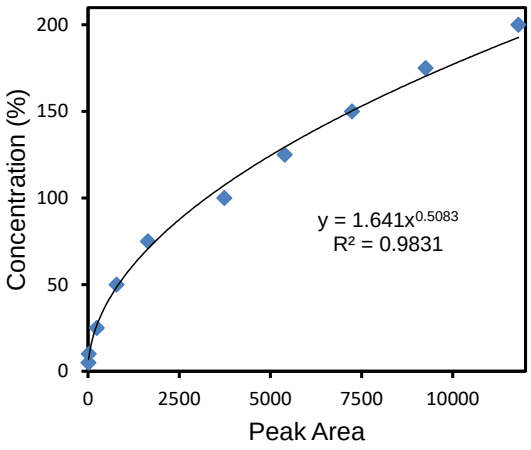

1121.5 g mol^{-1}

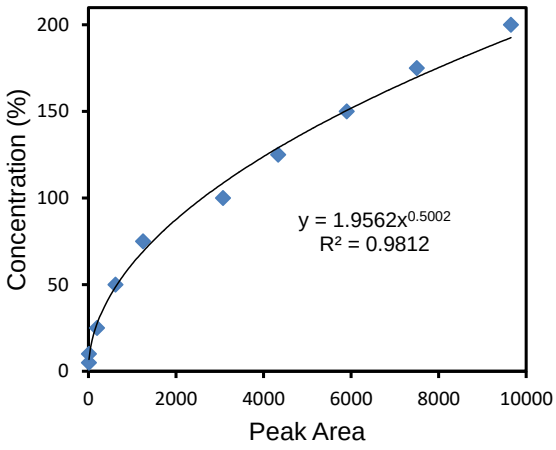

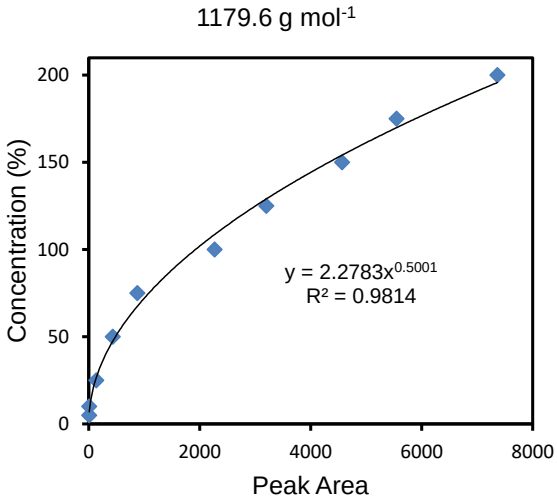
1179.6 g mol-1
Concentration (%)
Peak Area
y = 2.2783x0.5001
R² = 0.9814
0
50
100
150
200
0
2000
4000
6000
8000

A.6.2.2. Acetone Calibration Curves Poly(propylene) Glycol

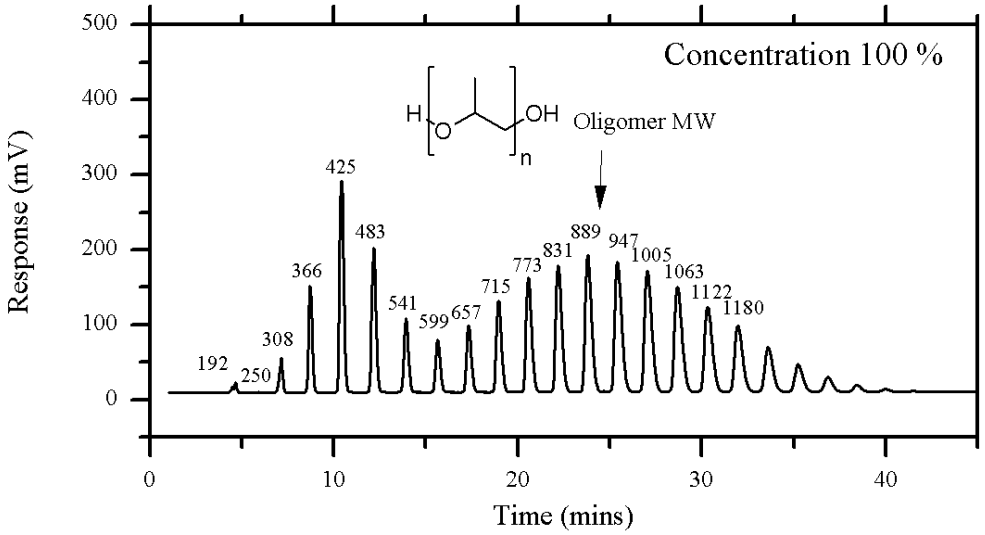

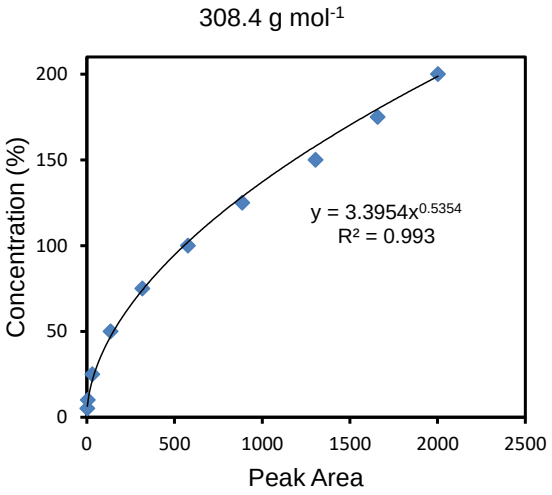

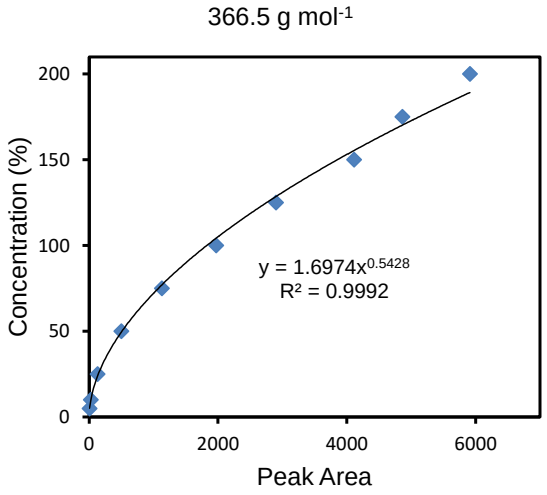

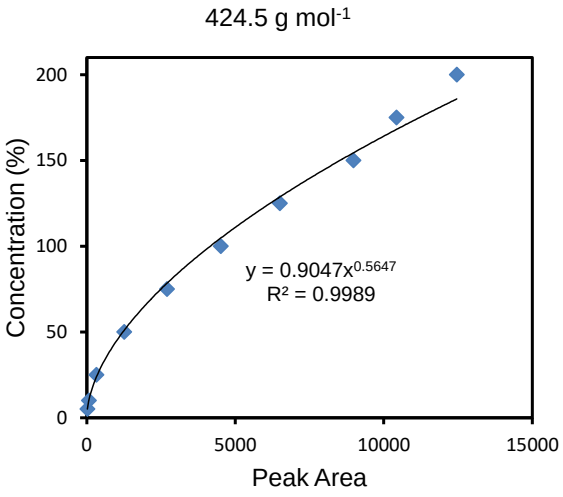

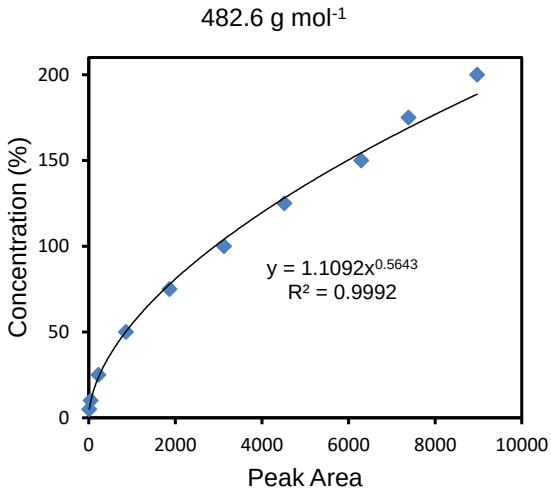

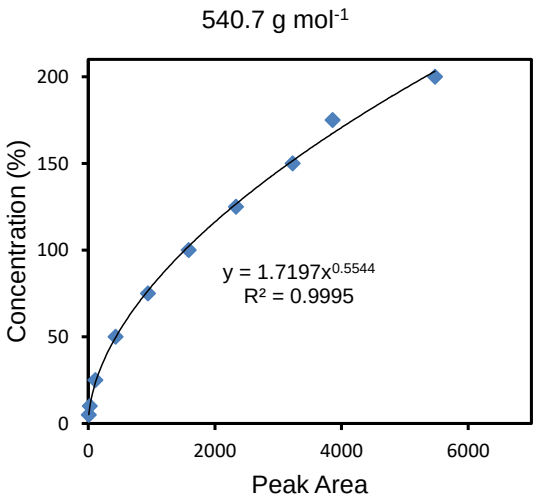
540.7 g mol-1
Concentration (%)
Peak Area
y = 1.7197x0.5544
R² = 0.9995
0
50
100
150
200
0
2000
4000
6000

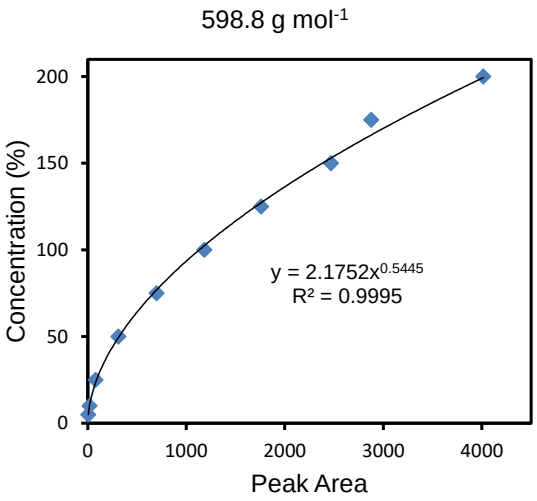
598.8 g mol-1
Concentration (%)
Peak Area
y = 2.1752x0.5445
R² = 0.9995
0
50
100
150
200
0
1000
2000
3000
4000

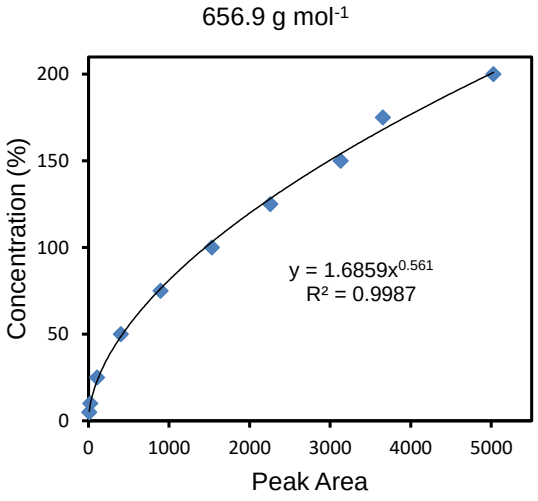
656.9 g mol-1
Concentration (%)
Peak Area
y = 1.6859x0.561
R² = 0.9987
0
50
100
150
200
0
1000
2000
3000
4000
5000

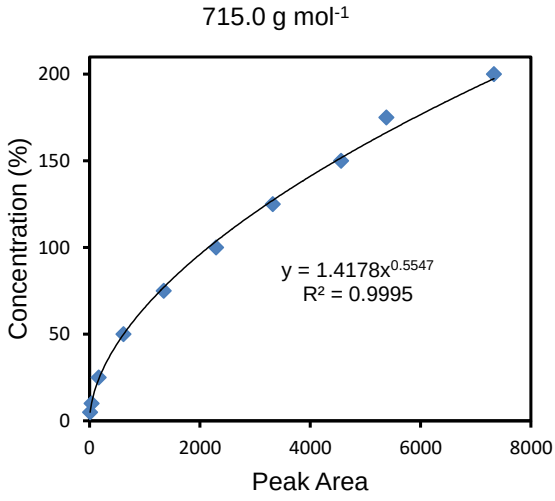
715.0 g mol-1
Concentration (%)
Peak Area
y = 1.4178x0.5547
R² = 0.9995
0
50
100
150
200
0
2000
4000
6000
8000

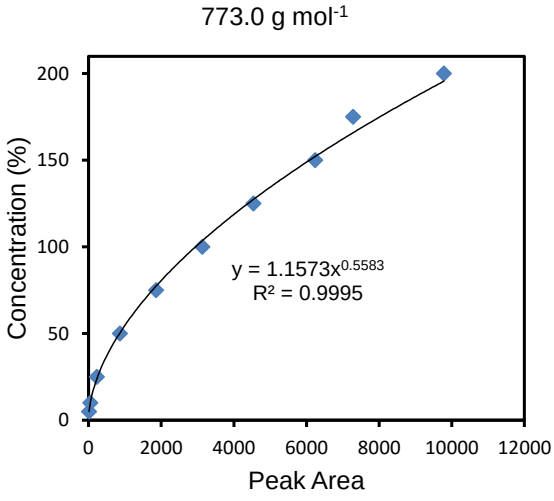
773.0 g mol-1
Concentration (%)
Peak Area
y = 1.1573x0.5583
R² = 0.9995
0
50
100
150
200
0
2000
4000
6000
8000
10000
12000

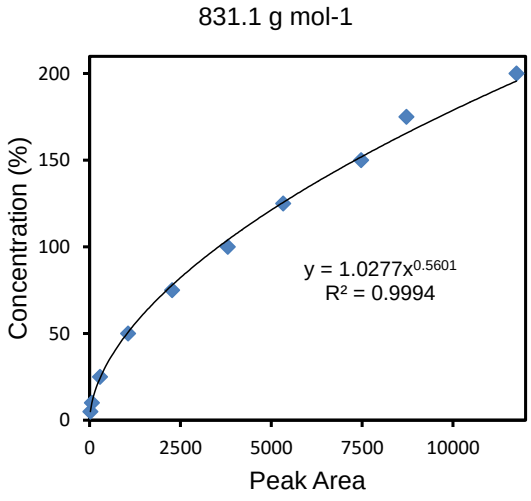
831.1 g mol-1
Concentration (%)
Peak Area
y = 1.0277x0.5601
R² = 0.9994
0
50
100
150
200
0
2500
5000
7500
10000

889.2 g mol-1

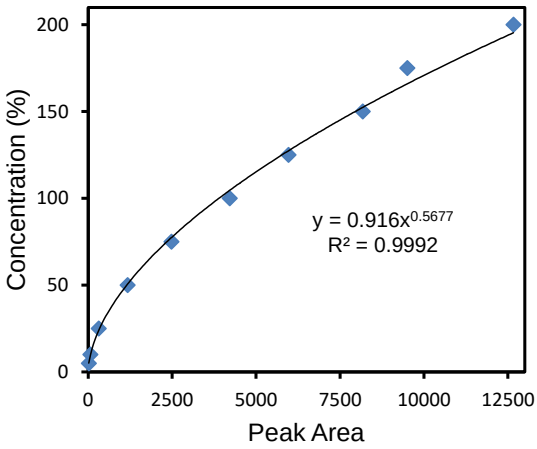

947.3 g mol^{-1}

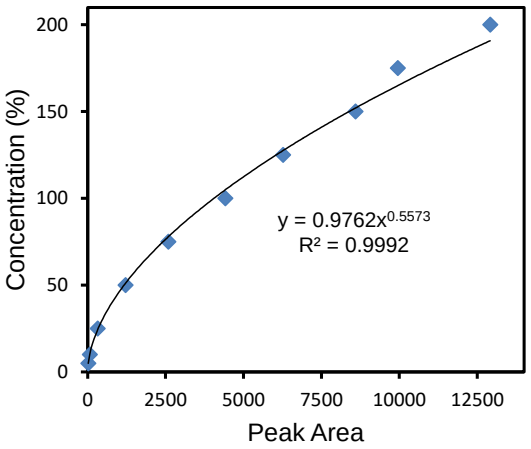

1005.4 g mol^{-1}

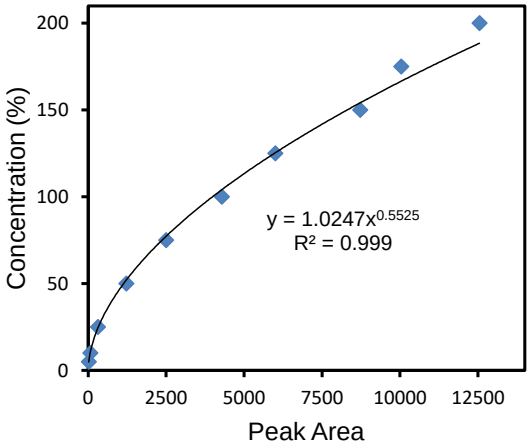

1063.4 g mol^{-1}

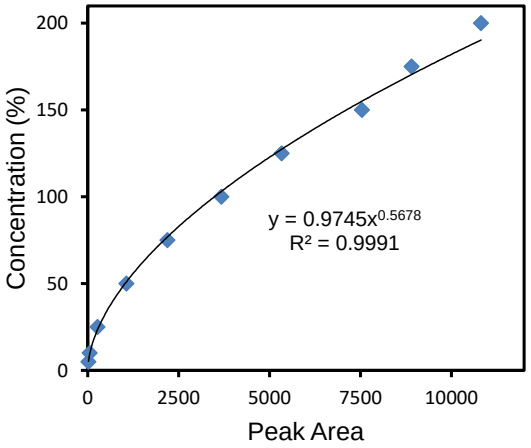

1121.5 g mol^{-1}

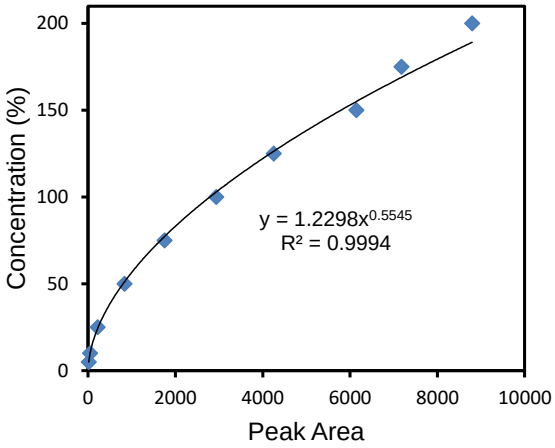

1179.6 g mol^{-1}

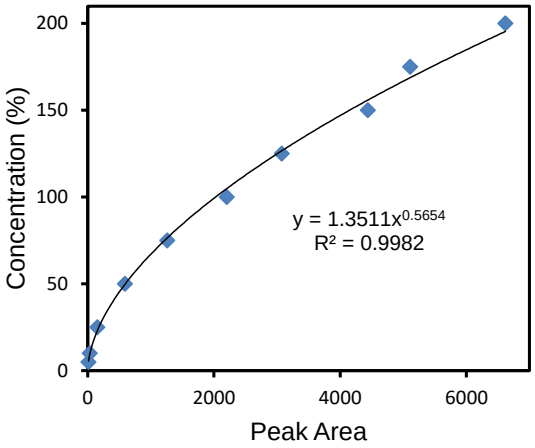

A.6.2.3. Poly(ethylene) Glycol Calibration Curves

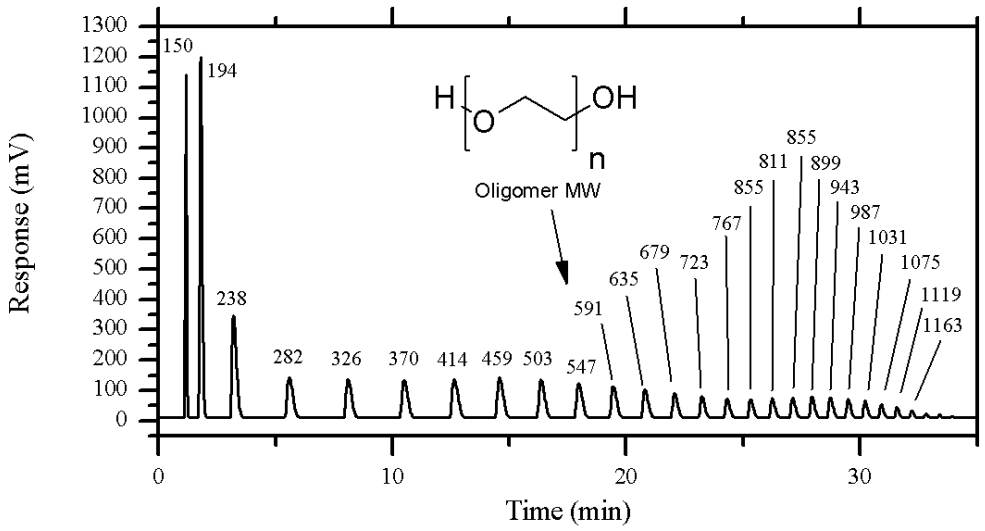

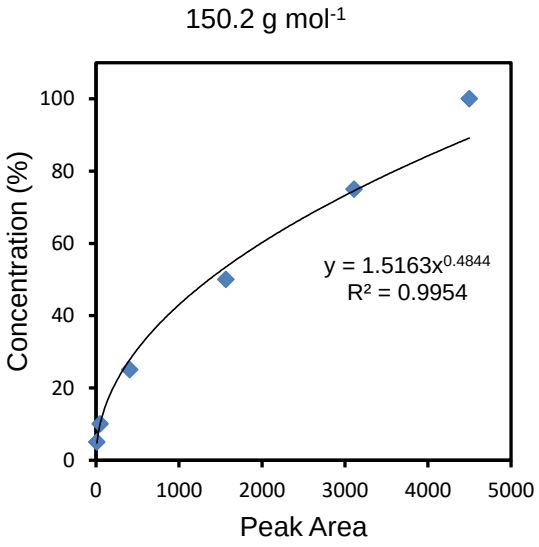

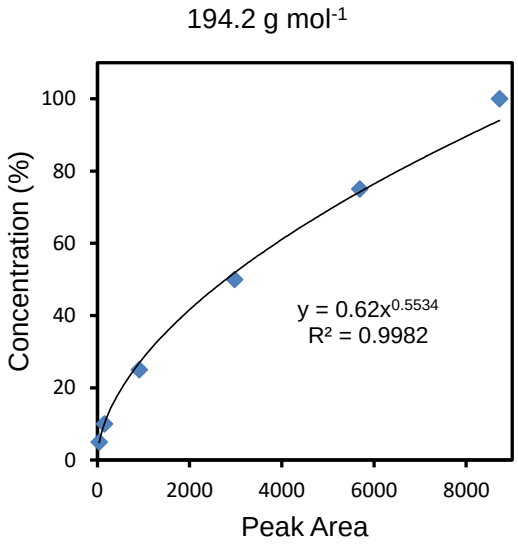

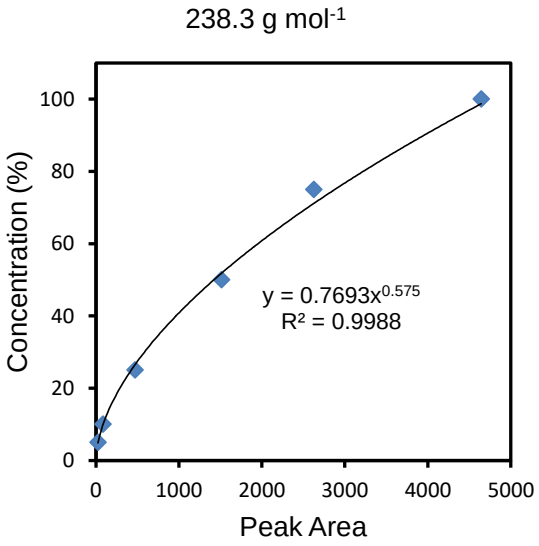

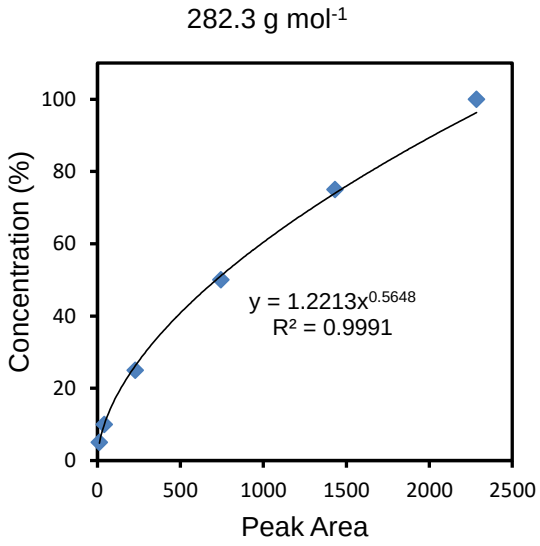

326.4 g mol^{-1}

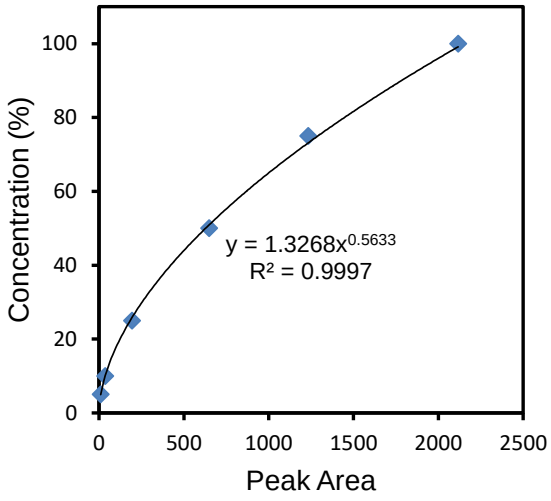

370.4 g mol^{-1}

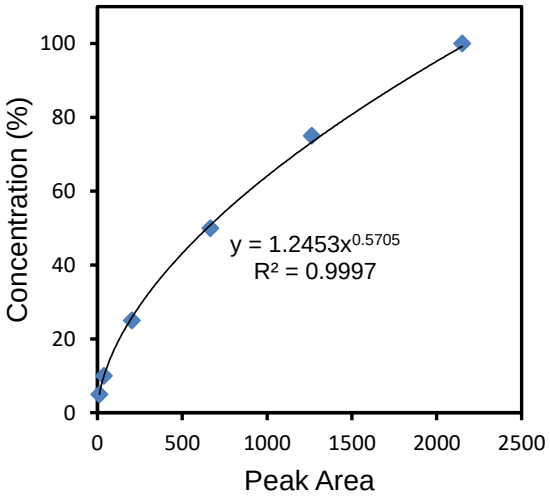

414.5 g mol^{-1}

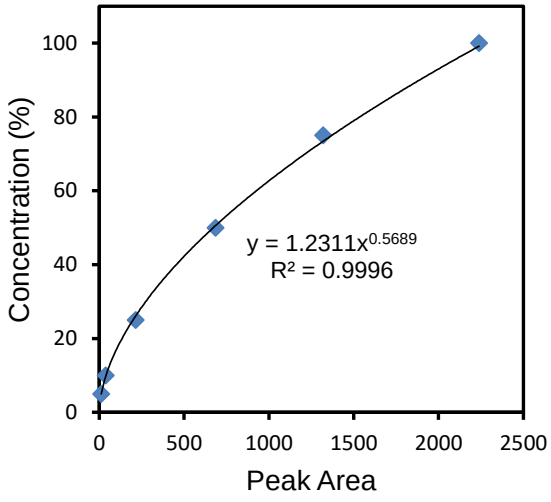

458.5 g mol^{-1}

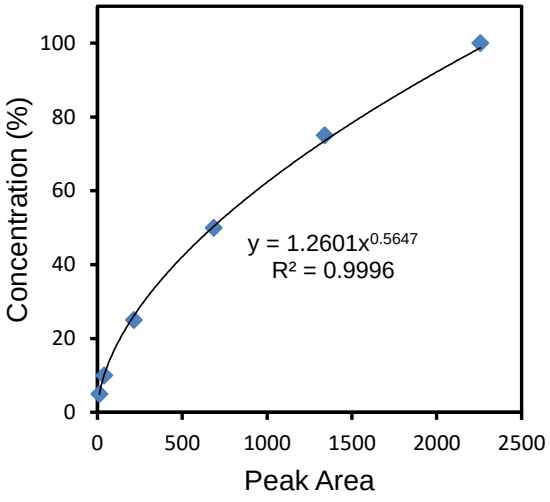

502.6 g mol^{-1}

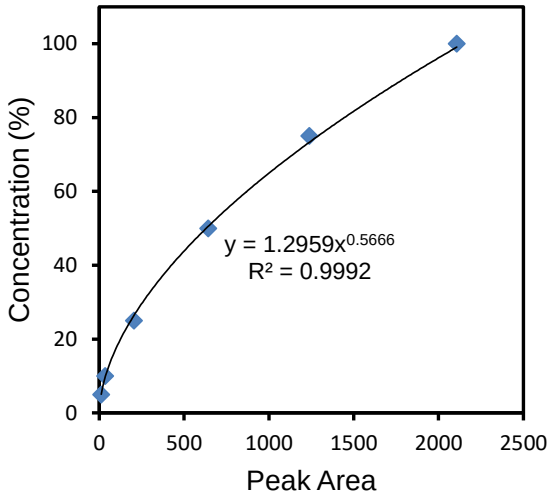

546.6 g mol^{-1}

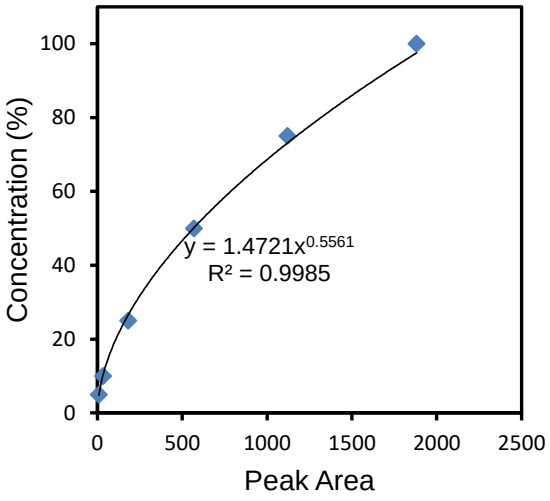

590.7 g mol^{-1}

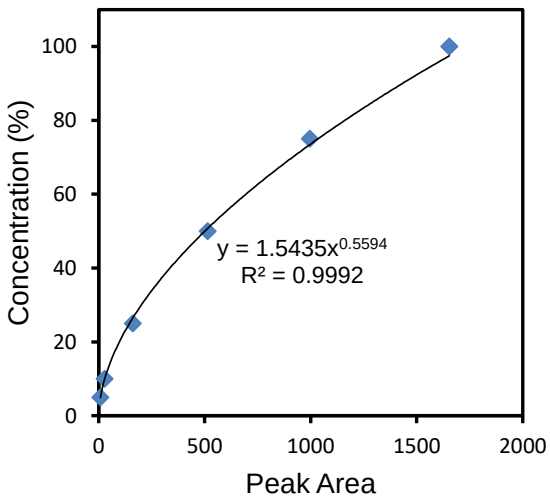

634.7 g mol^{-1}

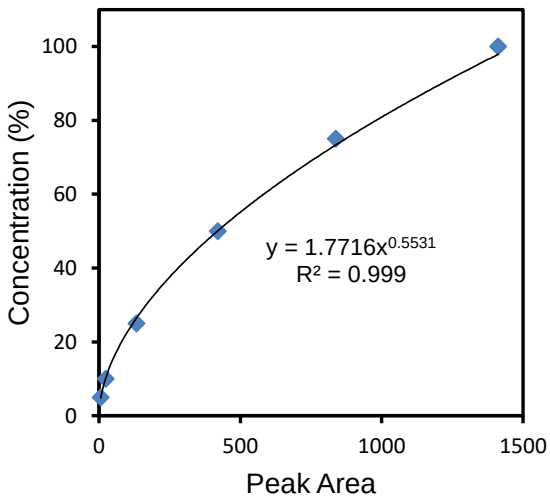

678.8 g mol^{-1}

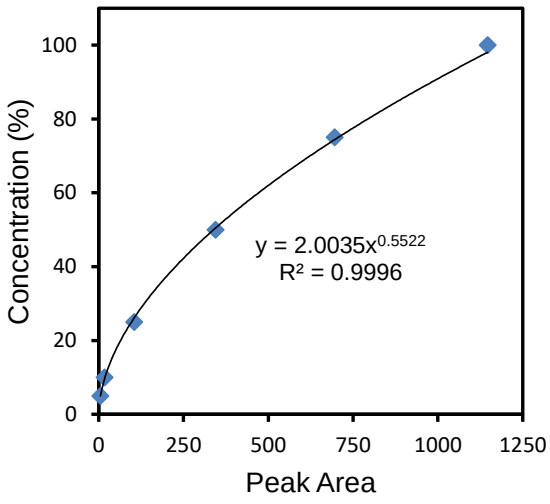

772.8 g mol^{-1}

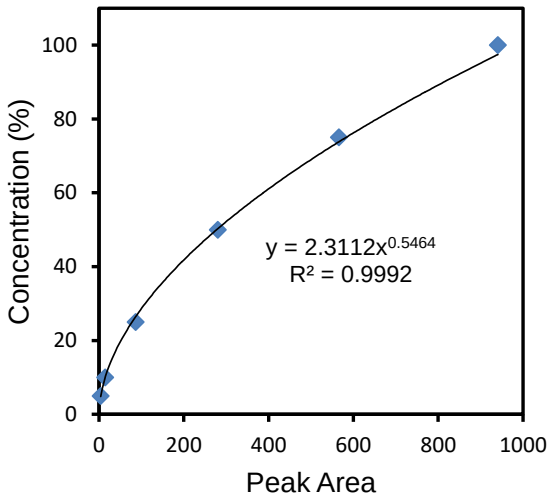

766.9 g mol^{-1}

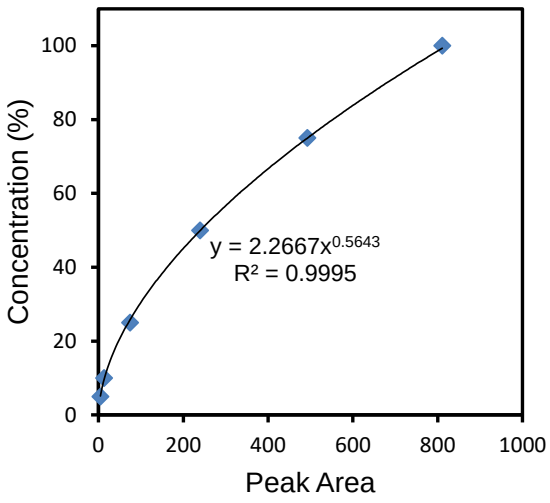

810.9 g mol^{-1}

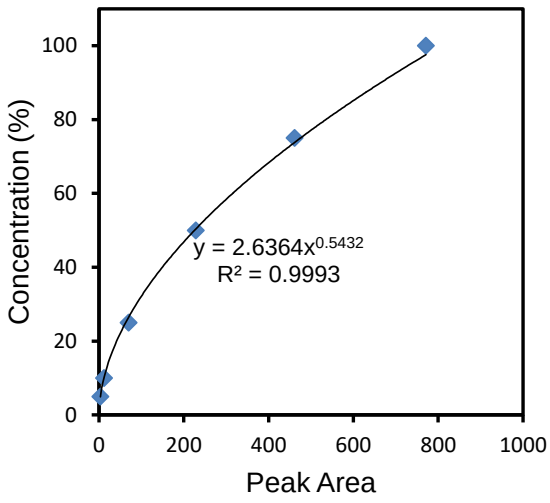

855.0 g mol^{-1}

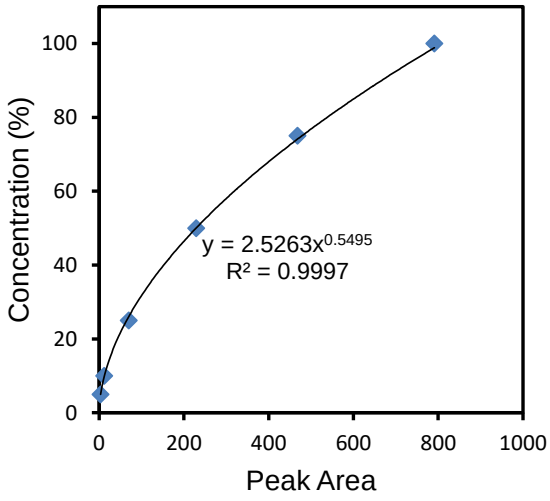

899.0 g mol^{-1}

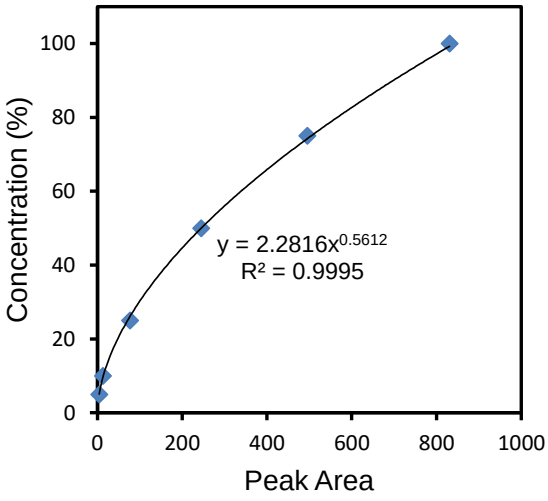

943.1 g mol^{-1}

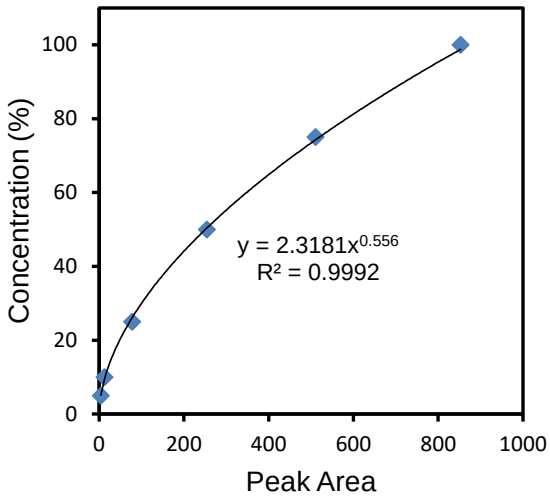

987.1 g mol^{-1}

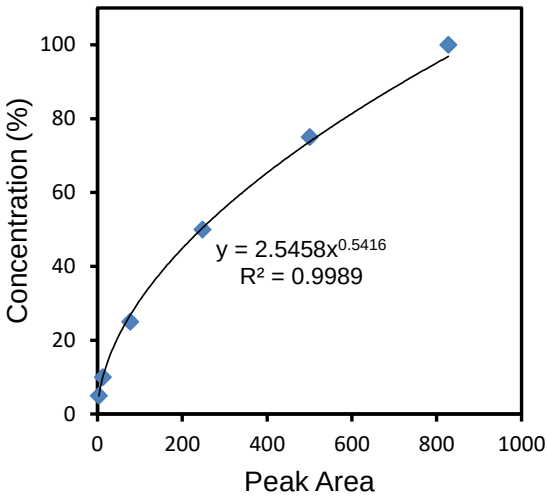

1031.2 g mol^{-1}

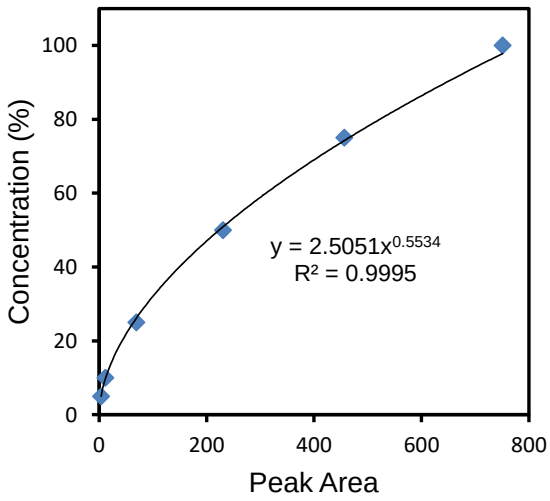

1075.2 g mol^{-1}

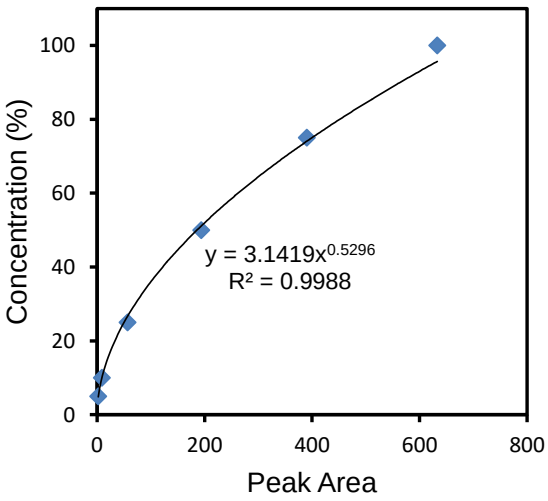

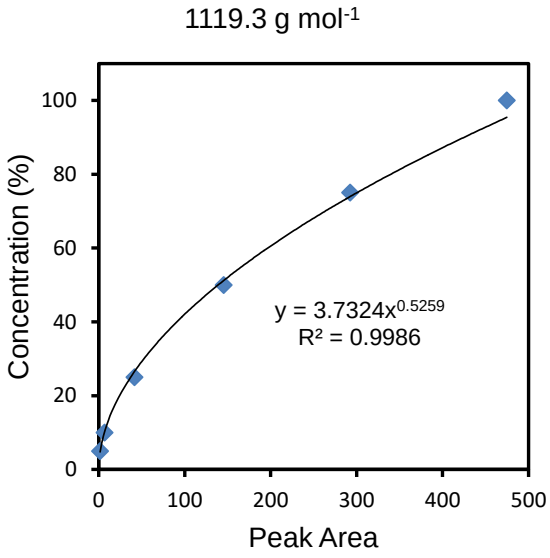
1119.3 g mol-1
Concentration (%)
Peak Area
y = 3.7324x0.5259
R² = 0.9986
0
20
40
60
80
100
0
100
200
300
400
500

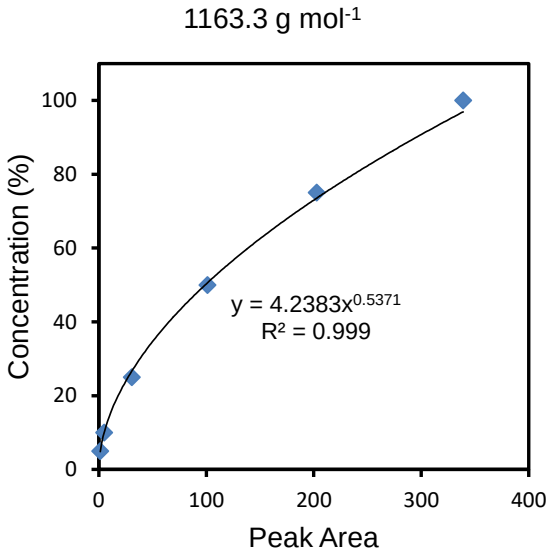
1163.3 g mol-1
Concentration (%)
Peak Area
y = 4.2383x0.5371
R² = 0.999
0
20
40
60
80
100
0
100
200
300
400